E-7107

TN-24 DRY STORAGE CASK

TOPICAL REPORT

JULY 25,1988

TRANSNUCLEAR, INC.
TWO SKYLINE DRIVE
HAWTHORNE,N.Y. 10532

REVISION LOG

Rev. No.	Date	Description
0	8/30/85	Originals as listed in Table of Contents, List of Tables and List of Figures.
1	7/25/88	All Rev 0 pages replaced.

TABLE OF CONTENTS

TABLE OF CONTENTS
(continued)

Page

TABLE OF CONTENTS
(continued)

TABLE OF CONTENTS
(continued)

TABLE OF CONTENTS
(continued)

TABLE OF CONTENTS
(continued)

TABLE OF CONTENTS
(continued)

TABLE OF CONTENTS
(continued)

TABLE OF CONTENTS
(continued)

LIST OF TABLES

LIST OF TABLES
(continued)

LIST OF TABLES
(continued)

LIST OF TABLES
(continued)

LIST OF FIGURES

LIST OF FIGURES
(continued)

LIST OF FIGURES
(continued)

LIST OF FIGURES
(continued)

1. INTRODUCTION AND GENERAL DESCRIPTION

1.1 INTRODUCTION

1.1.1 General

This topical report addresses the safety related aspects of storing spent fuel in the TN-24 dry storage cask. The format follows the guidance provided in NRC Regulatory Guide 3.48[1]. (Throughout this report, superscripted numbers in parentheses refer to reference numbers for the Section.) The report is intended for review by the NRC under 10CFR72[2]. It can be incorporated by reference into a Safety Analysis Report (SAR) submitted by an applicant for a 10CFR72 license for an Independent Spent Fuel Storage Installation (ISFSI).

The TN-24 dry storage cask provides containment, shielding, criticality control and passive heat removal independent of any other facility structures or components. It can be used either singly or as the basic storage module in an ISFSI. The site for an ISFSI could either be located at a reactor (AR) or away from reactor (AFR).

This topical report analyzes the safety related aspects of one cask and also the interactions among casks at an ISFSI. It does not deal directly with the loading and decontamination of the cask since these operations would take place before the cask is placed in storage.

Some sections of this report identify information that can only be supplied by the applicant for a site-specific license. However, where possible, typical or bounding values for installation or site-specific information are supplied in this report so that review of cask and facility interfaces is facilitated.

1. .2 Principal Design Features of Installation

1.1.2.1 Type of Dry Storage Mode

Irradiated fuel assemblies are stored in a sealed TN-24 cask fabricated mainly of forged steel. The TN-24 cask is shown in Figure 1.1-1. In the following paragraphs describing the cask, the numbers in parentheses refer to items shown in Figure 1.1-1.

The TN-24 has a forged steel body(1) for structural integrity and gamma shielding, surrounded by a layer of borated polyester resin in aluminum shells(2) for neutron shielding which is enclosed in a smooth steel outer shell(3). The cask is approximately 16.7 ft. long, 8.0 ft. in diameter and weighs approximately 113 tons on the fuel pool crane hook, filled with 24 fuel assemblies and water. The cask has a cylindrical cavity which holds a fuel basket(4) designed to accommodate 24 intact PWR fuel assemblies as specified in Sections 1.1.2.5 and 3.1.1. The basket is made of a neutron absorbing material to control criticality. The cavity atmosphere is helium at a positive pressure.

The cask is sealed with a lid(5) bolted to the body. A protective cover(6) bolted to the body provides weather protection for the lid penetrations. Two concentric metallic O-rings(7) are provided for sealing the lid to the cask body and an elastomer O-ring is used with the protective cover. The annular space between the metallic O-rings is connected to a tank(10) between the lid and the protective cover. Pressure in the tank is maintained above the pressure in the cask to prevent fission gas leakage out of, or air leakage into, the cavity. The body is provided with three pairs of removable trunnions(8) for handling and transport. A polypropylene neutron shielding disc(9) is attached to the lid when the cask is in storage. (If stored in a horizontal orientation, a neutron shielding disc must also be attached to the cask bottom.)

1.1.2.2 Description of Installation

An installation for storing spent fuel may be designed to include one or more TN-24 casks. The casks may be stored on a concrete slab in a free standing, vertical orientation, or horizontally using supports at each end.

One possible configuration for a dry storage installation with casks in a vertical orientation is shown in Figure 1.1-2. A similar configuration with casks in a horizontal orientation is shown in Figure 1.1-3.

1.1.2.3 Location of Installation

The license applicant's SAR identifies the exact location of the ISFSI.

1.1.2.4 Capacity of the Installation

The TN-24 cask is designed to store up to 24 intact PWR fuel assemblies. The ISFSI capacity will vary according to the requirements of the license applicant and the details of the specific site.

1.1.2.5 Spent Fuel Identification

The type of fuel to be stored in the TN-24 cask is LWR fuel of the PWR type. A PWR fuel assembly typically consists of zircaloy fuel rods containing uranium dioxide (UO_2) fuel pellets. The fuel rods are assembled into a square array, spaced and supported laterally by grid structures with top and bottom fittings for vertical support and handling.

Typical PWR assemblies consist of 14x14, 15x15, or 17x17 arrays of rods. Dimensions of a PWR assembly are approximately 8.4 in. square by 160 inches long. Each assembly weighs approximately 1470 lb and contains about 1014 lb (460 kg) of uranium. A detailed description of the PWR assemblies and the characteristics of the spent fuel considered for storage in the TN-24 cask are given in Section 3.1.

1.1.2.6 Waste Products

Waste products resulting from cask operation are negligible and would typically be limited to gloves and swipes that might be generated during periodic cask inspection and maintenance.

1.1.2.7 Corporate Entities

Transnuclear, Inc., (TN), provides the design, analysis, licensing support and quality assurance for the TN-24 cask. Fabrication of the cask is done by one or more qualified fabricators under TN's control.

Transnuclear, Inc., was incorporated in the state of New York in 1965 and now has offices in Hawthorne, New York and Aiken, South Carolina. Transnuclear shares are privately held by Transnucleaire, S.A. of Paris, France.

The Transnuclear Group is a world-wide organization of affiliated companies with special expertise in transportation and storage of radioactive materials. The Transnuclear Group designs, licenses, tests, owns, leases, operates and maintains special casks and containers utilized in the transportation and storage of nuclear fuel and other radioactive materials.

1.1.2.8 Time Schedules

Refer to the license applicant's SAR.

FIGURE 1.1-1

TN-24 DRY STORAGE CASK

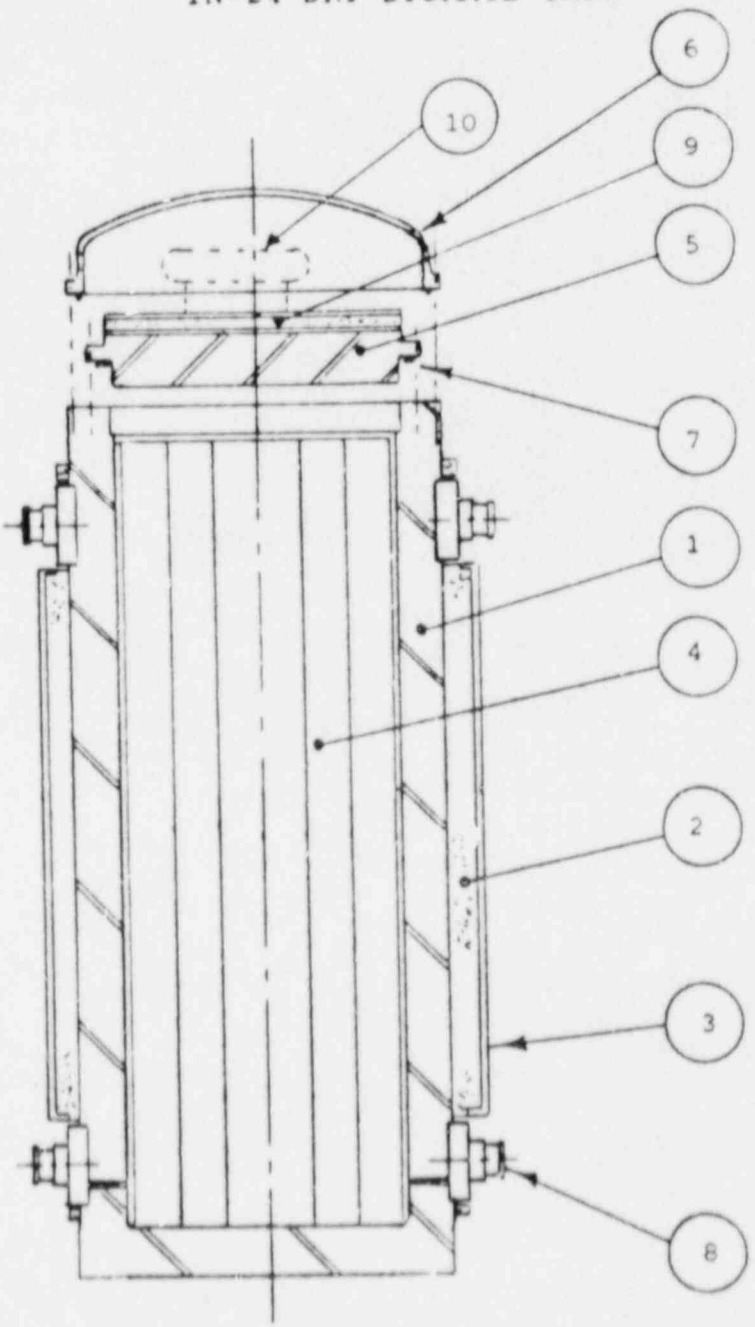

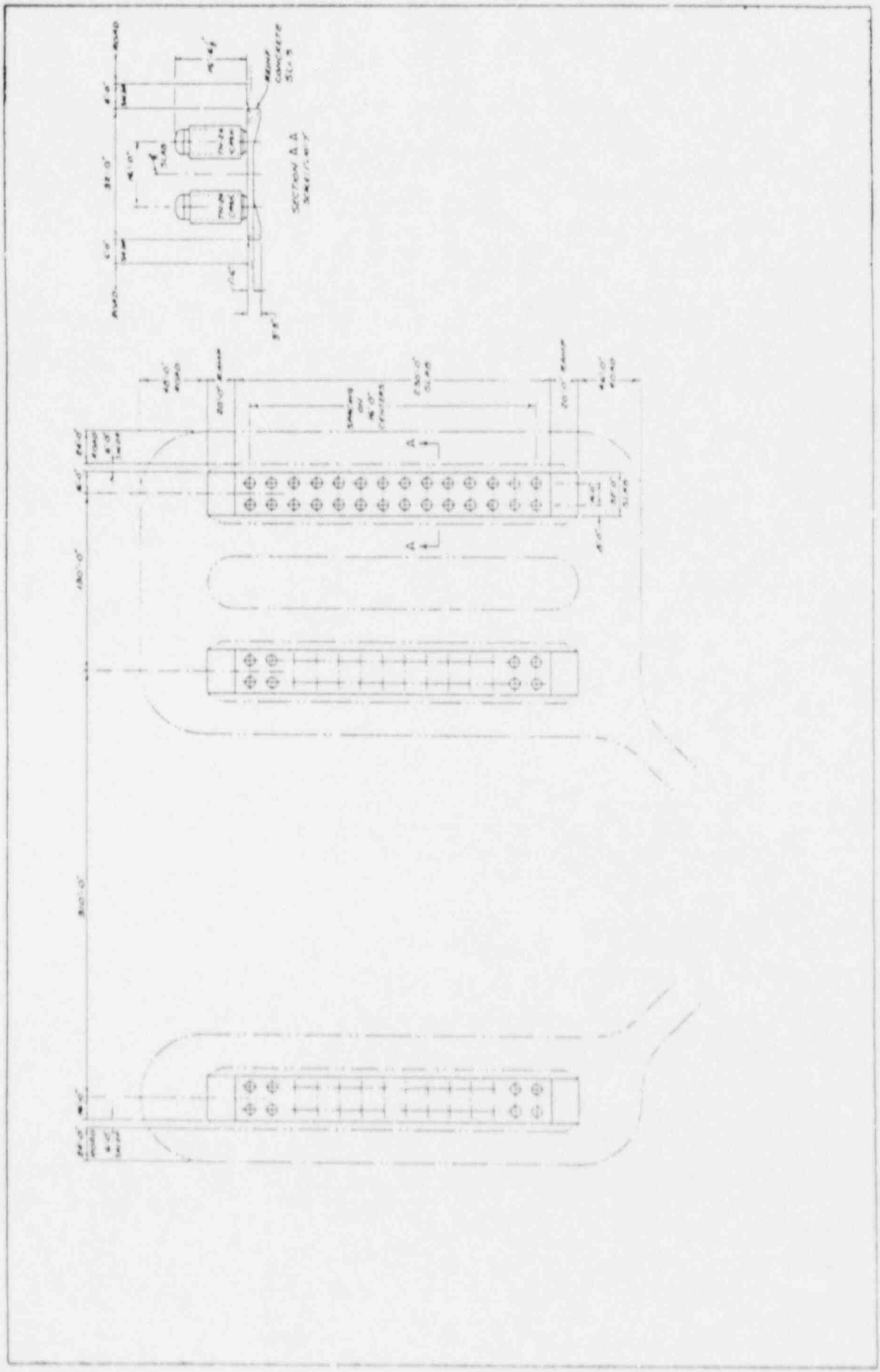

FIGURE 1.1-2
TYPICAL ISFSI VERTICAL STORAGE

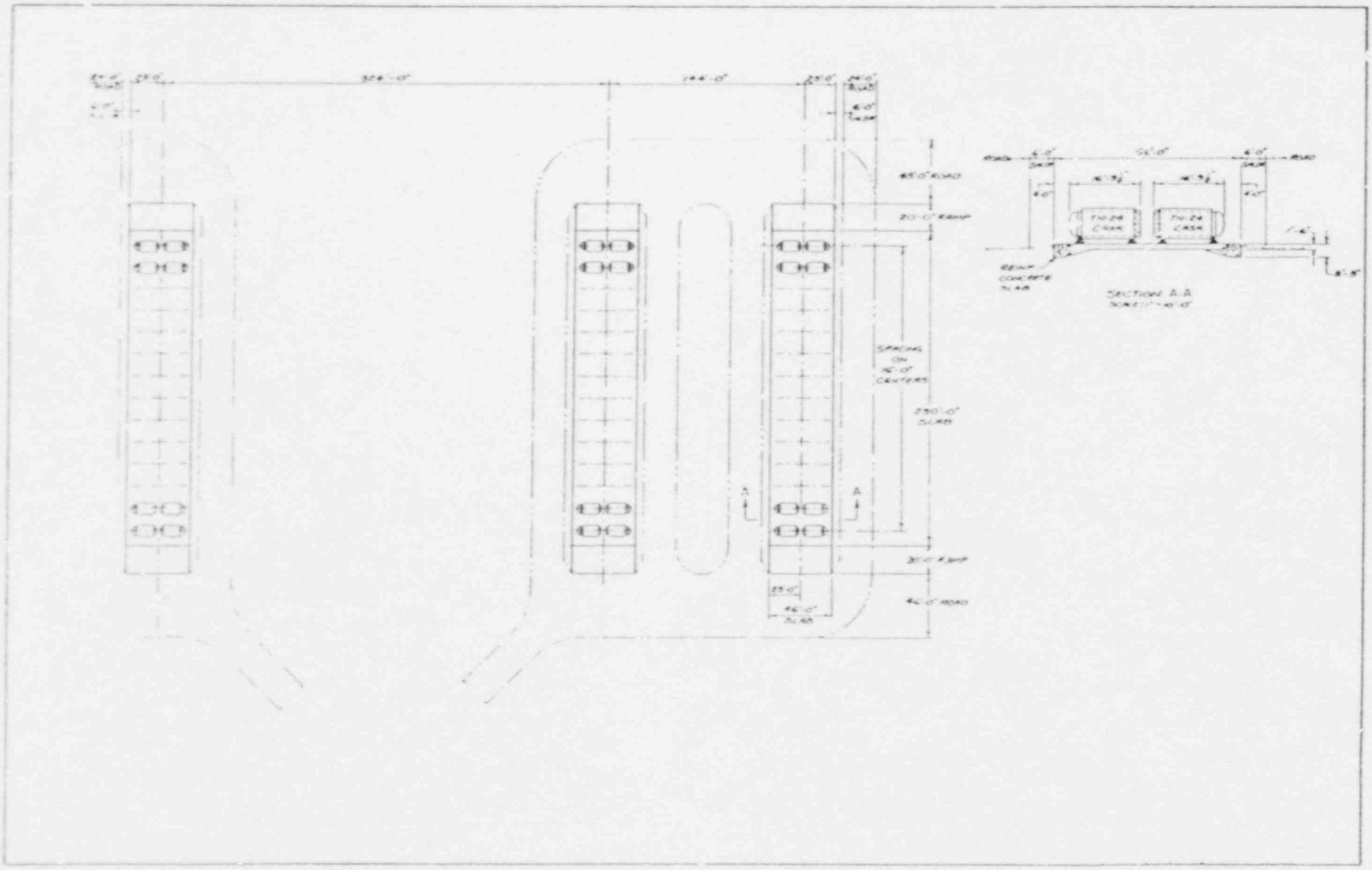

FIGURE 1.1-3
TYPICAL ISFSI HORIZONTAL STORAGE

References for Section 1.1

1. "Standard Format and Content for the Safety Analysis Report for an Independent Spent Fuel Storage Installation (Dry Storage)," Regulatory Guide 3.48, U.S. Nuclear Regulatory Commission, Washington D.C., Oct. 1981.

2. "Licensing Requirements for the Storage of Spent Fuel in an Independent Spent Fuel Storage Installation," 10CFR Part 72, Rules and Regulations, Title 10, Chapter 1, Code of Federal Regulations - Energy, U.S. Nuclear Regulatory Commission, Washington D.C., Jan. 1987.

1.2 GENERAL DESCRIPTION OF INSTALLATION

1.2.1 Principal Characteristics of the Site

Specific site characteristics are contained in the license applicant's SAR. However, the TN-24 cask design bases are chosen to include a variety of possible sites. The cask has been designed to withstand temperature extremes and forces resulting from tornados, earthquakes, floods, pressure waves, drops and fires.

1.2.2 Principal Design Criteria

The principal design bases for the TN-24 cask are presented in Table 1.2-1. The TN-24 dry storage cask is designed to store 24 intact PWR spent fuel assemblies, with a maximum assembly average burnup of 35,000 MWD/MTU and a minimum cooling time of 5 years.

The maximum total heat generation rate of the stored fuel is limited to 24 kw in order to keep the maximum fuel cladding temperature below the limit necessary to ensure cladding integrity for 40 years storage[1], considering a 115°F ambient temperature, solar load and an array of casks. The fuel cladding integrity is asssured by the limited fuel cladding temperature and maintenance of a nonoxidizing environment in the cask[2].

The containment vessel (body and lid) is designed and fabricated to the maximum practicable extent as a Class I component in accordance with the rules of the ASME Boiler and Pressure Vessel Code, Section III, Subsection NB, Articles NB-3200. The cask design, fabrication and testing are covered by a Quality Assurance Program which conforms to the criteria in Appendix B of 10CFR50[3].

The cask is designed to maintain a subcritical configuration during loading, handling, storage and accident conditions. Poison materials in the fuel basket and basket gaps between fuel assemblies are employed to maintain $k_{eff} \leq 0.95$ including statistical uncertainties. The TN-24 cask is designed to withstand the effects of severe environmental conditions and natural phenomena such as earthquakes, tornados, lightning, hurricanes and floods. Chapter 8 describes the cask behavior under these environmental conditions.

1.2.3 Operating Systems

Refer to the license applicant's SAR.

1.2.4 Fuel Handling

Refer to the license applicant's SAR.

1.2.5 Structural Features

The main components of the TN-24 cask are:

-containment vessel (body and lid)
-protective cover
-neutron shield
-outer shell
-fuel basket
-sealing system.

A set of reference drawings is presented in Appendix 1A. Dimensions and design characteristics are shown in Table 1.2-2. Table 1.2-3 is a list of components of the TN-24 cask.

The containment vessel for the TN-24 cask consists of a body which is a thick-walled, forged steel cylinder with an integrally-welded, forged steel bottom closure and a flanged and bolted forged top lid. The overall containment vessel length is 186.0 in. and the side wall thickness is 9.75 in. The cylindrical cask cavity is 163.25 in. long with a diameter of 63.0 in.

There are two penetratio s through the containment vessel, both in the lid: one for a drain opening and the other for venting. A bolted blind flange with two concentric metallic O-rings is provided for closure of each penetration. The lid is 11.5 in. thick and is fastened to the body by 48 bolts.

Double metallic O-ring seals with interspace leakage monitoring are provided for the lid closure. For additional protection from the environment, a torispherical protective cover with an elastomer O-ring is provided above the lid.

Gamma shielding is provided primarily by the thick-walled, forged steel body and neutron shielding is provided by a borated polyester resin compound surrounding the body. This resin has been used on more than 50 TN-12 transport casks in use worldwide. Tests have shown the resin to have excellent stability. Outgassing of the resin shows less than a 1% weight loss at temperatures under 300°F. The resin compound is cast into long, slender aluminum containers. The array of resin-filled containers is enclosed within a smooth outer steel shell constructed of two half cylinders. In addition to serving as resin containers, the aluminum also provides a conduction path for heat transfer from the cask body to the outer shell. A disk of polypropylene encased in a 0.25 inch steel shell is attached to the cask lid to provide neutron shielding during storage.

The fuel basket is designed to accept 24 PWR spent fuel assemblies and contains 24 compartments for the proper spacing of the assemblies. It dissipates heat to the cask body and contains

neutron absorbing material which assures that a subcritical configuration is maintained at all times. The basket is an assembly of mechanically interlocking plates made of borated stainless steel; the plates are coated with copper for improved heat transfer. The coating is applied by electroplating per ASTM B 254-79[4] and tested for adhesion per ASTM B 571-84[5] to assure that delamination will not occur.

The cavity surfaces and the outer shell have a flame sprayed Zn/Al alloy coating for corrosion protection. Additionally, the cavity is coated with Ti/Al oxide for high emissivity, and external surfaces of the cask are painted for ease of decontamination.

For corrosion prevention, a stainless steel overlay is applied to the O-ring seating surfaces on the body.

Six removable trunnions are attached to the cask body for lifting, tie-down and rotation of the storage cask.

1.2.6 Passive Decay Heat Dissipation System

During dry storage of the spent fuel, no active systems are required for the removal and dissipation of the decay heat from the fuel. The TN-24 cask is designed to transfer the decay heat from the fuel to the basket, from the basket to the cask body and ultimately to the surrounding air by radiation and natural convection. The cask is capable of removing 24 kw of decay heat without requiring the use of external fins, thus providing a smooth outer surface for ease of decontamination.

1.2.7 Radioactive Waste Treatment

Since the TN-24 dry storage casks are permanently sealed and are completely passive in operation, all radioactive materials are contained and no radioactive waste treatment is required.

Any radioactive wastes generated during loading or decontamination operations within a nuclear plant facility, prior to transfer to an ISFSI, are handled by the plant radwaste systems which are governed by a 10CFR50 license.

1.2.8 Special Features That Are Safety-Related

Some of the most important safety-related features of the TN-24 dry storage cask are:

-Passive removal of spent fuel decay heat

-Poison material and configuration to maintain subcriticality of the fuel at all times

-Radiation protection provided by sufficient gamma and neutron shielding

-Structural integrity of the containment vessel maintained during all normal and accident conditions

-Containment system as a barrier against activity release and air leakage into cavity.

A more detailed description of the safety related features of the TN-24 cask is given in Chapter 3.

TABLE 1.2-1

PRINCIPAL DESIGN BASES FOR TN-24 CASK

Design life*	20 yr
Maximum weight (loaded, flooded cask on pool crane hook)	113 U.S. tons
Number of fuel assemblies	24 - PWR (intact fuel)
Array type of fuel assemblies	14x14, 15x15, and 17x17
Spent fuel characteristics:	
a) Maximum burnup**	35,000 MWD/MTU
b) Maximum enrichment	3.7 wt% U235
c) Minimum decay time	5 yr
d) Maximum heat generation	24 kw (total)
Effective multiplication factor	keff ≤ 0.95
Maximum fuel rod clad temperature***	388°C
Internal cask atmosphere	helium
Initial cavity pressure	2.2 atm
Ambient temperature	-20°F to 115°F
Insolation (max)	1475 Btu/ft^2 per 12 hr day
Maximum dose rate at surface	60 mrem/hr
Handling/storage orientation	Horizontal or vertical

* No major maintenance

** Assembly average

*** See Section 3.3.7

TABLE 1.2-2

DIMENSIONS AND WEIGHT OF THE TN-24 CASK

Overall length (with protective cover,in)	201.0
Outside diameter (in)	94.75
Cavity diameter (in)	63.00
Cavity length (in)	163.25
Body wall thickness (in)	9.75
Lid thickness (in)	11.50
Bottom thickness (in)	11.25
Resin compound thickness (in)	5.38
Outer shell thickness (in)	0.75
Cask weight:	
Loaded on storage pad (tons)	107
Loaded on pool crane hook with water (tons)	112

TABLE 1.2-3

LIST OF COMPONENTS

Item No.	No Req'd	Shown On Dwg No.*	Description	Material
1	1	971-1	Shell	SA-350, Gr LF1
2	1	971-1	Lid	SA-350, Gr LF1
3	1	971-1	Bottom	SA-350, Gr LF1
4	6	971-1	Trunnion	SA-182, Gr F6NM
5	1	971-1	Protective Cover	SA-516, Gr 55
6	1	971-1	Radial Neutron Shield	Borated polyester
7	1	971-1	Outer Shell	SA-516, Gr. 55
8	6	971-1	Neutron Shield plug	Borated polyester SA-516 Gr 55 Shell
9	1	971-1	Top Neutron Shield	Polypropylene SA-516 Gr 55 Shell
10	1	971-1	Bottom Neutron Shield	Polypropylene SA-516 Gr 55 Shell
11	72	971-1	Trunnion Bolt	SA-320, Gr L43
12	60	971-2	Radial n-Shield Box	Aluminum alloy
13	48	971-3	Lid Bolt	SA-320, Gr L43
14	48	971-3	Protective Cover Bolt	SA-193, Gr B-8
15	1	971-3	Lid Seal	Double metallic O-ring
16	1	971-3	Protective Cover Seal	Viton O-ring
17	1	971-1	Drain Port Cover	SA-240, TP 304
18	1	971-1	Vent Port Cover	SA-240, TP 304
19	2	971-1	Drain and Vent Port Cover Seal	Double metallic O-ring
20	11	971-1	Drain and Vent Port Cover Bolt	SA-193, Gr B-8
21	8	971-1	Top & Bottom Neutron Shield Bolt	SA-193, Gr B-8
22	210	971-6	Basket Plate	SS304, 1.0 wt% Boron; copper electroplated
23	12	971-6	Basket Rail	Aluminum Alloy
24	1	971-1	Over pressure Tank	SS304
25	1	971-1	Over pressure port cover	SA-240, TP304
26	4	971-1	Over pressure port cover bolts	SA-193, Gr B-8
27	1	971-1	Over pressure port cover seal	Single metallic O-ring

*See Appendix 1A

References for Section 1.2

1. Levy, et. al., "Recommended Temperature Limits for Dry Storage of Spent Light Water Reactor Zircaloy-Clad Fuel Rods in Inert Gas," Pacific Northwest Laboratory, PNL-6189 ,1987.

2. Johnson, Jr., A. B., and Gilbert, E. R., "Technical Basis for Storage of Zircaloy-Clad Spent Fuel in Inert Gases," PNL-4835, Pacific Northwest Laboratory, Richland, Wash., Sept. 1983.

3. "Domestic Licensing of Production and Utilization Facilities," 10CFR Part 50, Rules and Regulations, Title 10, Chapter 1, Code of Federal Regulations - Energy, U.S. Nuclear Regulatory Commission, Washington D.C., Jan. 1987.

4. "Practice for Preparation of and Electroplating on Stainless Steel," ASTM B 254-79, American Society for Testing and Materials.

5. "Test Methods for Adhesion of Metallic Coatings," ASTM B 571-84, American Society for Testing and Materials.

1.3 GENERAL SYSTEMS DESCRIPTION

A general description of the basic storage component (storage cask) is given in Section 1.2.

A typical storage facility is shown in Figures 1.1-2 and 1.1-3. The facility is basically only an outdoor storage area with one or more concrete slabs on which the casks are placed. The facility could be located within or close to a reactor site.

The storage casks may be loaded dry and then decontaminated or they may be loaded in a reactor spent fuel pool, drained, dried and decontaminated. After leak testing, the cavity and over pressure tank are pressurized. The casks are then transported to the storage facility where they are placed on a concrete slab by a mobile lifting rig. The casks can be stored in either a vertical or a horizontal position.

The cask is a totally passive system and the storage facility would require only visual inspection and monitoring of the over pressure system.

If the visual inspection indicates deterioration of the painted surface, the paint can be touched up. The pressure monitoring system should be periodically calibrated. These procedures would be the responsibility of the license applicant. No other maintenance is necessary over the twenty year cask life under normal conditions.

1.4 IDENTIFICATION OF AGENTS AND CONTRACTORS

The only organizations outside of the Transnuclear Group which have been involved in the TN-24 cask design as described in this report are the following:

-Constantino, Miller and Associates - Assistance in performance of structural analyses.

-Becker, Block and Harris, Inc. - Assistance in performance of criticality and shielding analyses.

1.5 MATERIAL INCORPORATED BY REFERENCE

This topical report makes no references to any other topical reports.

2. SITE CHARACTERISTICS

2.0 GENERAL

A complete description of specific site characteristics is the responsibility of the applicant for an ISFSI license. This information will be included in the applicant's SAR. The design of the TN-24 dry storage cask is based on selected site characteristics which are judged to be sufficiently extreme to bound the majority of potential ISFSI sites.

2.1 GEOGRAPHY AND DEMOGRAPHY OF SITE SELECTED

Information on site geography and demography is the responsibility of the license applicant. Information to be provided by the applicant in his SAR will include details of site location, site description, population distribution and trends, and uses of nearby land and waters.

The license applicant will be responsible for establishing the controlled area for the ISFSI. Location of the storage casks within this controlled area must comply with the requirements of paragraphs 72.67 and 72.68 of 10CFR72.[1] Paragraph 72.68 states that the minimum distance from the spent fuel handling and storage facilities to the nearest boundary of the controlled area shall be at least 100 meters (328 ft). Analyses presented in Section 7.4 of this Topical Report provide the basis for the license applicant to determine the necessary boundary distance to meet the dose rate limit at the boundary.

References for Section 2.1

1. "Licensing Requirements for the Storage of Spent Fuel in an Independent Spent Fuel Storage Installation," 10CFR Part 72, Rules and Regulations, Title 10, Chapter 1, Code of Federal Regulations - Energy, U.S. Nuclear Regulatory Commission, Washington D.C., Jan. 1987.

2.2 NEARBY INDUSTRIAL, TRANSPORTATION, AND MILITARY FACILITIES

Information on nearby industrial, transportation and military facilities is site-specific and must be supplied by the license applicant. Analysis of the hazards presented by such facilities to the ISFSI is also the responsibility of the license applicant.

2.3 METEROLOGY

Specific meterological conditions are site dependent and must be supplied by the license applicant.

The TN-24 dry storage cask has been designed to operate safely under extreme meteorological conditions without the protection of any additional structures or facilities. In particular it is designed for an ambient temperature range of -20 to 115°F, a maximum insolation of 1475 Btu/ft^2 per 12 hr day, and ambient humidity of 0-100%.

Precipitation of any type or rate will not affect the safety of the TN-24 dry storage cask. The cask will also not be affected by lightning strikes.

The cask is designed to resist loadings resulting from tornados with characteristics defined in NRC Regulatory Guide 1.76[1] for the most tornado prone regions of the United States. Section 3.2 of this Topical Report addresses loads due to tornado winds of 360 mph and tornado missiles.

Chapter 8 provides an estimate of the dose resulting from sudden release of the entire radioactive gas inventory under stable (Pasquill condition F) atmosphere conditions and low (1 meter/s) wind speed.

References for Section 2.3

1. "Design Basis Tornado for Nuclear Power Plants," Regulatory Guide 1.76, U.S. Atomic Energy Commission, Washington D.C., April 1974.

2.4 SURFACE HYDROLOGY

Surface hydrology conditions are site dependent and must be supplied by the license applicant.

The cask can withstand flooding to a water depth of at least 56 ft and a water flow rate of 18 ft/sec without any impairment of its safety functions as shown in Section 3.2 of this Topical Report.

2.5 SUBSURFACE HYDROLOGY

Subsurface hydrology is site dependent and information on this must be provided by the license applicant.

2.6 GEOLOGY AND SEISMOLOGY

For an ISFSI based on storage casks, 10CFR72 calls for a site-specific investigation of geological and seismological characteristics to establish site suitability[1]. Responsibility for this investigation rests with the license applicant.

The design earthquake for an ISFSI will be site dependent. For sites east of the Rocky Mountain Front that are not in areas of known seismic activity, 10CFR72 suggests that the design earthquake can be described by an appropriate response spectrum anchored at 0.25 g[1]. Therefore, the safety of the TN-24 dry storage cask subject to an earthquake with a peak horizontal acceleration of 0.25g is demonstrated in Section 3.2 of this Topical Report. The value of 0.25 g is not a strict limit since the cask can endure higher accelerations without sliding or tipping over.

References for Section 2.6

1. "Licensing Requirements for the Storage of Spent Fuel in an Independent Spent Fuel Storage Installation," 10CFR Part 72, Rules and Regulations, Title 10, Chapter 1, Code of Federal Regulations - Energy, U.S. Nuclear Regulatory Commission, Washington D.C., Jan. 1987.

2.7 SUMMARY OF SITE CONDITIONS AFFECTING CONSTRUCTION AND OPERATIONS REQUIREMENTS

A summary of the bounding site characteristics discussed in this chapter is given in Table 2.7-1. The characteristics listed in this table should allow siting of an ISFSI using TN-24 dry storage casks at the majority of potential sites in the United States. In some cases a more detailed analysis using site-specific data would allow siting outside of the envelope in Table 2.7-1.

A complete summary of site conditions affecting construction and operating requirements must be provided by the license applicant for an ISFSI.

TABLE 2.7-1

SUMMARY OF BOUNDING
SITE CHARACTERISTICS

Cask to boundary distance (m)	100
Ambient temperature (°F)	-20 to 115
Ambient humidity (%)	0 to 100
Insolation (Btu/ft^2 per 12 hr day)	1475
Maximum tornado winds (mph)	360
Tornado winds (mph, rotational)	290
Tornado winds (mph, translational)	70
Tornado pressure drop (psi)	3
Flood maximum depth (ft)	56
Flood maximum velocity (ft/sec)	19.7
Earthquake peak horizontal acceleration (g)	0.25
Dispersion conditions (short term)	Pasquill F 1 m/s wind speed

3. PRINCIPAL DESIGN CRITERIA

3.1 PURPOSES OF INSTALLATION

The purpose of the installation is the interim storage of spent fuel. The TN-24 cask is designed to provide for the interim dry storage of spent fuel assemblies in a modular form at an Independent Spent Fuel Storage Installation.

3.1.1 Materials To Be Stored

The TN-24 cask is designed to store up to 24 intact PWR fuel assemblies. The physical characteristics of Westinghouse PWR fuel assemblies are given in Table 3.1-1. The design basis fuel for the TN-24 cask is the Westinghouse 17x17 PWR assembly.

The thermal and radiological characteristics for the PWR spent fuel were generated using the ORIGEN2 computer code[1]. These characteristics for the Westinghouse 17x17 assembly are shown in Table 3.1-2. For the thermal and radiological characteristics, the 17x17 assembly with an enrichment of 3.2 w/o U-235 was assumed. For criticality considerations, the 17x17 OFA assembly with an enrichment of 3.7 w/o U-235 was selected. For the containment analyses, the 15 x 15 assembly was conservatively used. (See Section 3.3.2.2).

Fuel with various combinations of burnup, specific power, enrichment and cooling time can be stored in the TN-24 cask as long as values for decay heat and gamma and neutron sources, including spectra, fall within the design limits specified in Table 3.1-2. For reference, Figure 3.1-1 shows the relationship between burnup, cooling time and decay heat for a typical PWR fuel assembly.[2] Figures 3.1-2 and 3.1-3 show the total photon and neutron sources respectively as a function of cooling time for the design basis 17x17 PWR assembly.

Specific gamma and neutron source spectra and fission product gas inventory is given in Section 7.2.

Specific fuel assembly data will be submitted by the applicant for a site-specific ISFSI. Although analyses in this topical report are performed only for the design basis fuel, any other intact PWR fuel which falls within the geometric, thermal and nuclear limits established for the design basis fuel could be stored in the TN-24 cask.

3.1.2 General Operating Functions

The TN-24 dry storage cask is a totally passive system. Information on the general operating functions of an ISFSI using TN-24 casks will be supplied by the license applicant.

TABLE 3.1-1

PHYSICAL CHARACTERISTICS OF WESTINGHOUSE FUEL ASSEMBLIES

Parameter	14x14	15x15	17x17
Number of Rods	179	204	264
Cross Section (in.)	7.763x7.763	8.426x8.426	8.426x8.426
Length (in.)	160	160	160
Fuel Rod Pitch (in.)	0.556	0.563	0.496
Fuel Rod O.D. (in.)	0.422	0.422	0.374(a)
Clad Material	Zircaloy	Zircaloy	Zircaloy
Clad Thickness (in.)	0.0243	0.0243	0.0225
Pellet O.D. (in.)	0.367	0.366	0.322(b)
U235 Enrichment (w/o)	3.7	3.7	3.7
Theoretical Density (%)	95	95	95
Active Fuel Length (in.)	144	144	144
U Content (kg)	382	459	461(c)
Assembly Weight (lb)	1300	1439	1467(d)

NOTES:
a. W17x17 OFA - 0.360 in.
b. W17x17 OFA - 0.309 in.
c. W17x17 OFA - 423 kg
d. W17x17 OFA - 1380 lb

TABLE 3.1-2

THERMAL, GAMMA AND NEUTRON SOURCES FOR
THE DESIGN BASIS 17x17 PWR FUEL ASSEMBLY

U235 Enrichment (w/o)	3.7 for criticality 3.2 for thermal/radiological*
Burnup (MWD/MTU)	35,000
Specific Power (MW/MTU)	37.5
Cooling Time (yr)	5
Decay Heat (kw/assembly)	1.0
Gamma Source (photons/sec)	8.17E+15*
Neutron Source (n/sec)	2.9E+8*

* For a given specific power and burn-up, a lower enrichment will give slightly higher thermal and radiological sources.

DECAY HEAT
PWR Assemblies

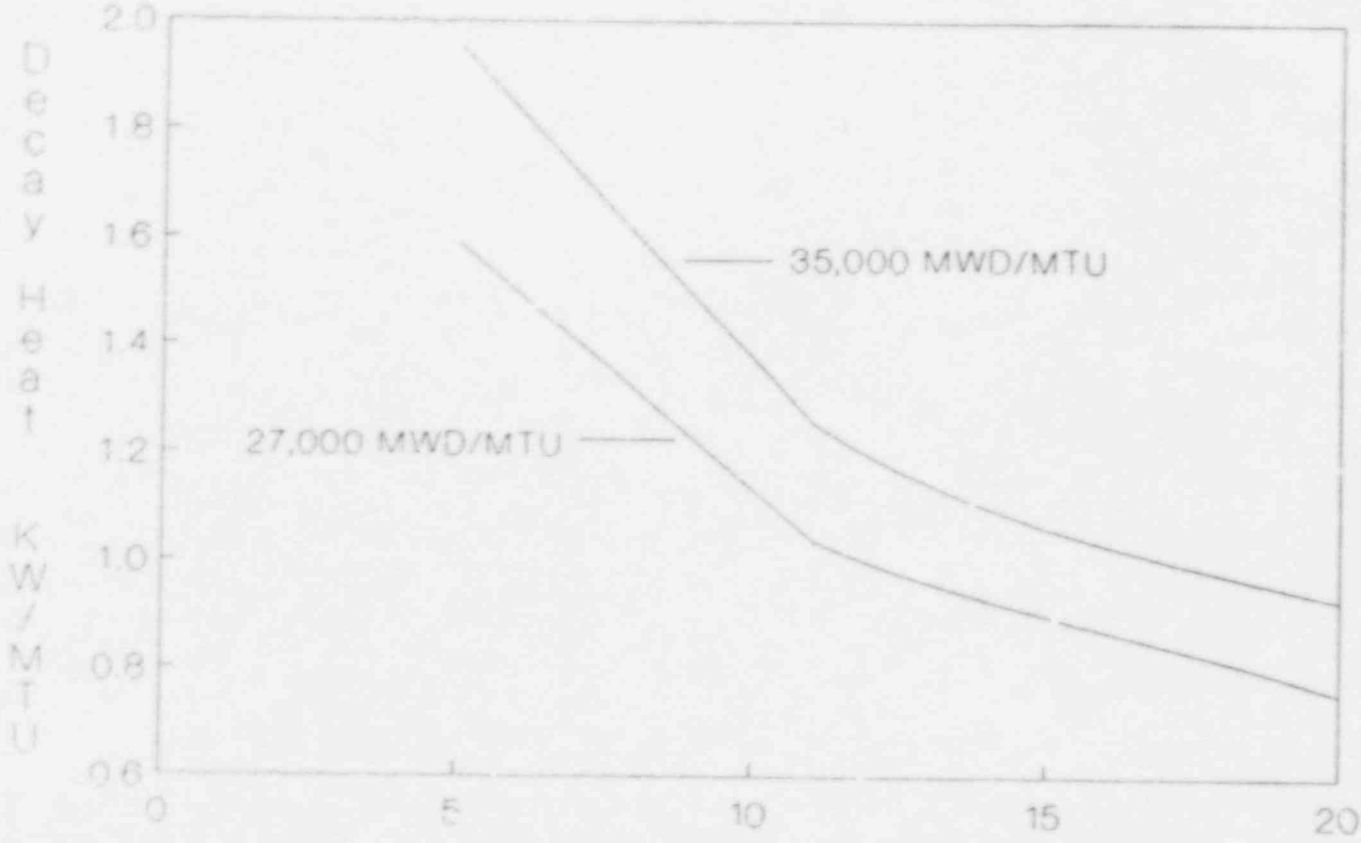

Figure 3.1-1

GAMMA SOURCE
Design Basis PWR Assembly

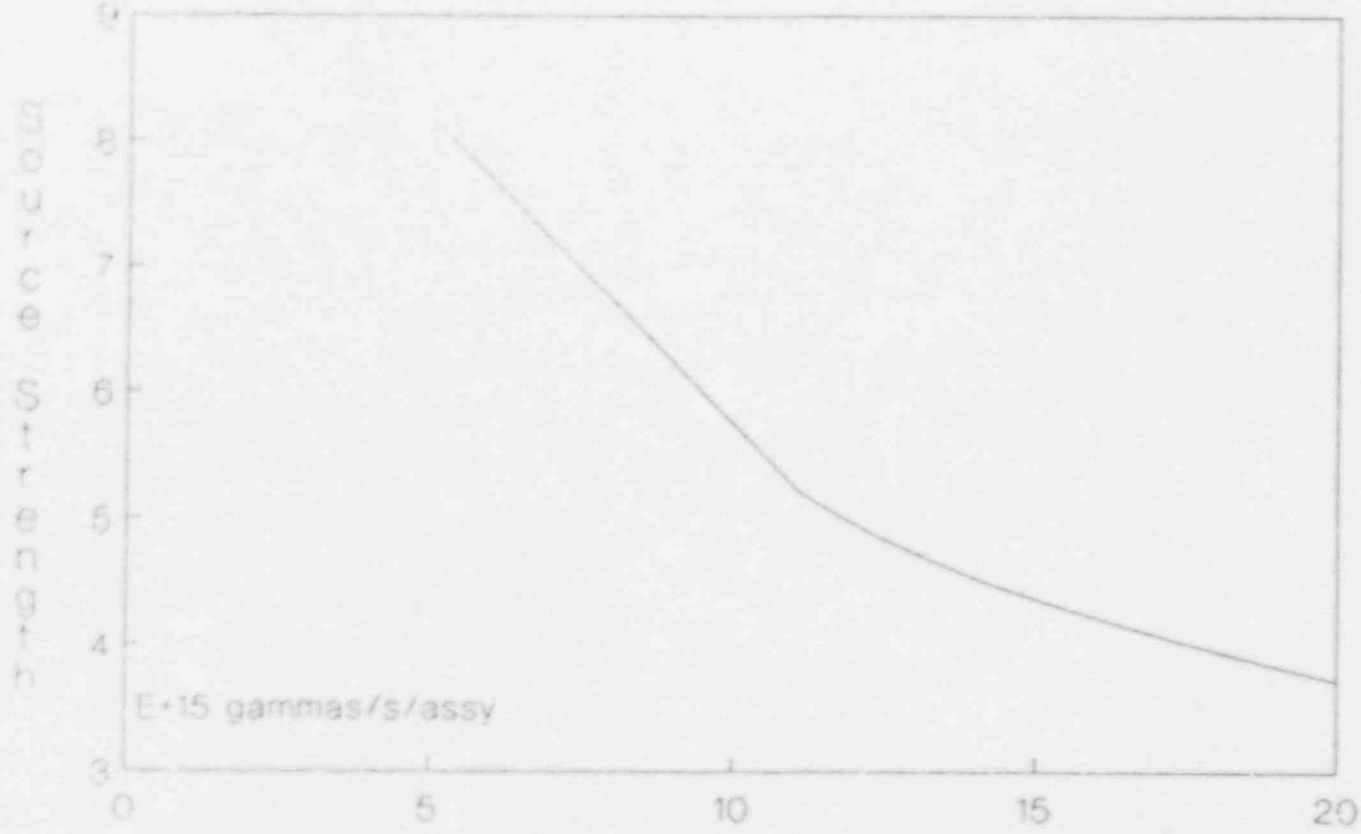

Figure 3.1-2

NEUTRON SOURCE
Design Basis PWR Assembly

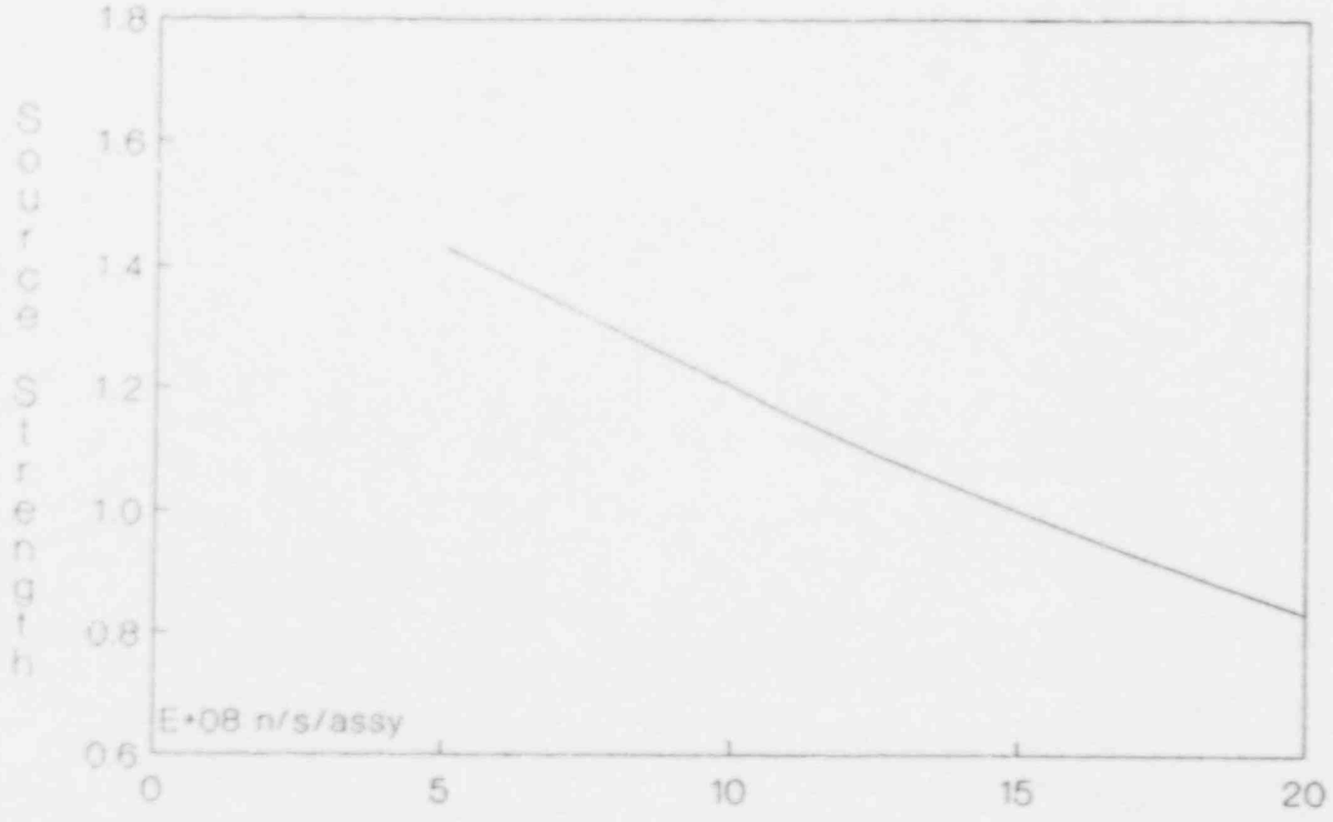

Figure 3.1-3

References for Section 3.1

1. "ORIGEN2, Isotope Generation and Depletion Code." Oak Ridge National Laboratory, CCC-371, Jan. 1987

2. "Spent Fuel Heat Generation in an Independent Spent Fuel Storage Installation," Regulatory Guide 3.54, U. S. Nuclear Regulatory Commission, Washington D.C., Sept. 1984.

3.2 STRUCTURAL AND MECHANICAL SAFETY CRITERIA

The structural and mechanical safety criteria used for design and evaluation of the TN-24 storage cask are identified in this section. These criteria satisfy the requirements of 10 CFR Part 72[1]. They consider the effects of normal operation, natural phenomena and postulated man-made accidents. The criteria are defined in terms of loading conditions imposed on the storage cask. The loading conditions are evaluated to determine the type and magnitude of loads induced on the storage cask. The combination of these loading conditions is then established based on the rules for a Class 1 nuclear component found in Section III, Subsection NB, of the ASME Boiler and Pressure Vessel Code.[2]

Since the storage cask is designed as an independent self-contained storage structure, it is the only structure important to safety which is addressed in this report.

3.2.1 Tornado and Wind Loadings

The TN-24 storage cask is designed to resist tornado loadings resulting from those in the most tornado prone regions of the United States as defined in NRC Regulatory Guide 1.76[3]. An analysis of impact on the cask by tornado missiles in accord with NUREG-0800,[4] Section 3.5.1.4 is presented in this Topical Report. Wind loading is not significant in comparison to that due to tornados; therefore, the wind loading is conservatively taken to be the same as the tornado loading.

3.2.1.1 Applicable Design Parameters

The design basis tornado wind velocity and external pressure drop based on NRC Regulatory Guide 1.76 are taken to be 360 mph and 3 psi respectively. The external pressure drop of 3 psi associated with passing of the tornado is small and, when combined with the other

internal pressure loads is far exceeded by the design internal pressure (250 psi) for the cask. Its effect is included in the effects of the other internal pressure loadings listed in Table 3.2-1.

3.2.1.2 Determination of Forces on Structures

The 360 mph tornado wind loading is converted to a dynamic pressure (psf) acting on the cask by multiplying the square of the wind velocity (in mph) by a coefficient (0.002558 at ambient sea level condition) dependent on the air density. The result is a pressure of 332 psf. This is based on data presented in a paper by T.W. Singell.[5] The net force acting on the cask is obtained by multiplying this pressure by the product of the area of the cask projected onto a plane normal to the direction of wind times a drag coefficient. A drag coefficient of 1 is used based on the geometric proportions of the cask (i.e. length to diameter ratio of approximately 2) and the conservative assumption that the cask surface is rough.

This results in a distributed load, w lb/in, acting on the cask in a vertical orientation over the length of 200.5 in. as shown in Figure. 3.2-1a. The load is calculated as follows:

$$w = \frac{332}{144} \times \text{outer shell diameter}$$

$$= \frac{332}{144} \times 94.75$$

$$= 218.5 \text{ lb/in}$$

The distributed loads acting on the cask in the horizontal orientation, as shown in Figure 3.2-1b, would be equivalent. This load and other distributed loads are listed in Table 3.2-2.

An additional type of load on the structure, listed in Table 3.2-13, is that created by the impact of tornado missiles on the cask. These impacts are analyzed for 3 types of missiles:

- Missile A: high energy deformable type missile (1800 kg automobile) impacting the cask horizontally at normal incidence at 35% of the design basis tornado horizontal wind speed.

- Missile B: rigid missile (125 kg. 8" diameter armor piercing artillery shell) impacting the cask:

  ° horizontally at normal incidence at 35% of the design basis tornado horizontal wind speed.

  ° vertically at normal incidence at 70% of the horizontal component (i.e. 24.5% of the design basis tornado horizontal wind speed).

- Missile C: small rigid steel sphere 1" in diameter impinging upon the barrier openings in the most damaging directions at 35% of the design basis tornado horizontal wind speed.

3.2.1.2a Stability of the Cask in the Vertical Position Under Wind Loading

The cask rests in an upright position on a concrete pad. The coefficient of friction between the steel cask and the concrete may be taken as 0.25 for dry concrete. This is based on data in Mark's Handbook[6] which gives a value of 0.29 for steel on sandstone. Steel on concrete would be similar. A wind velocity of 398 mph would then be required to cause the cask to slide.

This value is calculated below.

$$q = 0.002558\ V^2$$

$$\text{and } q = \frac{F}{A}$$

where F = force to overcome friction force, F_f

A = projected area of cask length, ft^2

$$\text{and } F = F_f = \text{cask weight} \times 0.25$$

$$= 214{,}000 \times 0.25$$

$$= 53{,}500 \text{ lb.}$$

$$A = 200.5 \times 94.75/144$$

$$= 132 \text{ ft}^2$$

$$\text{Therefore } 0.002558\ V^2 = \frac{53{,}500}{132} \text{ ; } V = 398 \text{ mph}$$

If the cask does not slide, a constant wind velocity of 511 mph would be required to tip the cask which is calculated as follows:

The tipping moment about the bottom edge of the cask is:

$$M_c = \frac{82.5}{2} W - w \times \frac{(200.5)^2}{2}$$

where W = cask weight = 214,000 lb

w = distributed load to tip cask, lb/in

Therefore

$$w = 82.5W/2 \times 2/(200.5)^2 = 439 \text{ lb/in.}$$

The corresponding pressure load, q, is:

$$q = \frac{439}{94.75} \times 144 = 667 \text{ psf}$$

The corresponding wind speed, V, is:

$$V = \sqrt{\frac{667}{0.002558}}$$

$$= 511 \text{ mph}$$

3.2.1.2b Stability of the Cask in the Vertical Position Under Missile Impact

It is assumed that both Missile A and Missile B impact inelastically on the cask as shown in Figure 3.2-1c. Missile A (the automobile) is assumed to crush and Missile B (the rigid shell) is assumed to partially penetrate the cask wall. The cask will tend to slide if the missile strikes it below the CG (unless it is blocked in position) or tilt if the missile strikes it above the CG. Conservation of momentum is assumed for both sliding and tipping with a coefficient of restitution of zero. The energy transferred to the cask is dissipated by friction in the sliding case or transformed into potential energy as the cask CG lifts in the tipping case. When a missile strikes the side of the cask at an elevation near the CG:

In the sliding case:

$$V = \frac{m\, v_o}{M + m}$$

In the tipping case:

$$\omega_p = \frac{m\, d_{CG}\, v_o}{m(d_{CG})^2 + I_p}$$

Where:

V = cask translational velocity after impact
v_0 = missile initial velocity
ω_p = cask angular velocity about P after impact
m = mass of Missile A
M = cask mass
d_{CG} = distance from CG to pivot point P
I_p = moment of inertia of cask about pivot point P

When the appropriate substitutions are performed for Missile A (automobile) impact, the cask velocity after impact, V, in the sliding case is found to be 3.48 ft/sec. The rotational velocity about P, ω_p, is found to be .26 rad/sec for impact at the CG elevation and .53 rad/sec for impact at the top. Missile B impact produces lower cask translational and rotational velocities because of its lower initial momentum. Vertical impact of Missile B has no effect on cask stability.

If the cask slides on the concrete pad, the cask kinetic energy after impact is absorbed by friction. The friction work can be equated to the kinetic energy. Assuming a coefficient of friction of .25:

$$E_{friction} = \mu g(M + m) l$$
$$= 1/2 (M + m) V^2$$

Where:

$E_{friction}$ = energy absorbed in friction
μ = coefficient of friction
g = acceleration of gravity
l = distance cask slides on concrete pad

When a solution is performed to determine l, the sliding distance is determined to be 1.8 ft. This is acceptable since it is less than the 8 foot spacing between casks.

When the cask tips or pivots about point P after impact, the kinetic energy is transformed into potential energy as the CG rises:

$$E_{tipping} = \text{Increase in Potential Energy} = \text{Kinetic Energy}$$
$$E_{tipping} = Mg\, d_{CG}\, [\cos(\beta+\alpha-\tfrac{\pi}{2})-\cos\beta] = \tfrac{1}{2}\, I_p\, \omega_p^{\,2}$$

Where:

$E_{tipping}$ is the increase in potential energy of the cask since the CG rises as the cask pivots about the corner.

β, α are indicated in Figure 3.2-1c.

The angle α is determined to be 82.2 degrees for impact at the top of the cask (the cask tilts 7.8 degrees and the CG lifts about 5 in.). The cask is stable and will not tip over since it will return to the vertical position as long as α is greater than about 62 degrees.

Even at this 82.2 degree angle wind will not tip over the cask (if the wind force occurs simultaneously with Missile A impact). At an 82 degree angle the tipping moment about Point P due to the 360 mph wind is less than 70% of the restoring moment due to the weight. Therefore the cask is stable in the vertical orientation under simultaneous tornado wind and tornado missile loading.

The impact forces applied to the cask as it is struck by the missiles are determined as follows:

- Missile A - (automobile) ic assumed to crush 3 feet under a constant force during the impact. The loss of kinetic energy is assumed to be dissipated by crushing of the missile.

$$F_a \times 3 \text{ ft} = \tfrac{1}{2}\, [m_a\, v_o^{\,2} - (M + m_a)\, V^2]$$

The frontal area of the automobile is assumed to be 3 ft. x 6 ft.

$$p_a = F_a/18 \text{ ft.}^2$$

where:

F_a = Impact force on cask by Missile A
P_a = Impact pressure on cask by Missile A

The impact force, F_a, is determined to be 683,000 lb, and the crush pressure on the frontal area of the automobile, p_a, is 266 psi.

- Missile B - (rigid missile) does not deform under impact. The loss in kinetic energy is assumed to be dissipated as the missile partially penetrates the cask wall. The penetration force is assumed to be equal to the yield strength of the cask body material multiplied by the frontal area of the 8 in. diameter missile.

$$F_b = S_y \times \frac{\pi}{4} (8)^2$$

The impact force, F_b, is determined to be 1.38×10^6 lb. assuming a cask body yield stress, S_y, of 27,300 psi. This force is higher than that developed by Missile A, but the impact time duration is much smaller so that a smaller impulse is applied to the cask producing less cask movement than Missile A. Missile C (1 in. diameter sphere) impact has no effect on cask stability.

The above forces, F_A and F_B, are used in the stress analysis of the cask body; they also apply when the cask is stored horizontally (see below).

3.2.1.2c Stability of the Cask in the Horizontal Position Under Wind Loading

The cask rests on two concrete saddles as shown in Figure 3.2-1d. For stability:

$$F R \cos\theta < W R \sin\theta$$

or

$$F < W \tan\theta$$

Where:

F = drag force due to wind speed, lb.

W = cask weight, 214,000 lb.

For $\theta = 60°$, Tan $\theta = 1.732$ and

Drag force = 43,709 lb. < 1.732 x 214,000 = 369,600 lb.

A wind velocity of 1048 mph is required to roll the cask over.

3.2.1.2d Stability of the Cask in the Horizontal Position Under Missile Impact

The transfer of momentum during missile impact is determined similarly to that described in 3.2.1.2b, above. If the missile strikes the side of the cask and tips it about pivot point P as shown in Figure 3.2-1d:

$$\omega_p = \frac{m R v_o}{m(R)^2 + I_p}$$

(actually assumes missile strikes at a height Rcosθ above pivot point)

ω_p, m, v_o are as defined above in 3.2.1.2b.

R = outside cask radius

I_p = moment of inertia of cask (horizontal in this case) about Pivot Point P.

The energy required to tip the cask about point P to an angle of α is:

$$E_{tip} = (m + M) R (\cos\alpha - \cos\theta)$$

α and θ are defined in Figure 3.2-1d

If θ is initially 60 degrees, the cask will stay in the cradle until α becomes 0 degrees. If we substitute values in the above equations α_a is found to be 57 degrees for Missile A (displaced 3 degrees-very stable) and α_b is 59.9 degrees for Missile B, (almost no displacement).

Therefore, the cask is stable and will not roll out of the cradle due to missile impact. When the cask is displaced to a_a the weight recovery moment exceeds the wind drag moment even under the 360 mph wind and the cask returns to its equilibrium position.

The forces acting on the cask during the impact are the same forces as defined in 3.2.1.2b, above.

3.2.1.3 Local Effect on Containment of Missile Impact

3.2.1.3a Missile A

Missile A (automobile) deforms and is crushed during the impact. The local pressure on the cask structure is between 1 and 2% of the body yield strength, therefore, no local penetration occurs.

3.2.1.3b Missile B

Missile B (rigid) partially penetrates the cask wall. The loss in kinetic energy is dissipated as strain energy in the cask wall. The force developed as the 8 in. diameter missile penetrates the cask body is:

$$F_b = S_y \times \frac{\pi}{4} (8)^2 = 1.38 \times 10^6 \text{ lb.}$$

From conservation of energy:

$$F_b \, dx = \frac{1}{2} m_b v_o^2$$

Or for constant puncture force:

$$x = \frac{m_b v_o^2}{2 F_b}$$

Where x is the penetration distance.

The penetration distance is found to be 1.26 in. for perpendicular impact of the blunt missile and about 2.56 in. for the worst angular impact.

When the impact angle is not 90 degrees, the missile will rotate during impact (conservatively neglected), limiting the energy available for penetration since part of the energy will be transformed into rotary kinetic energy. When hitting the weather protective cover, Missile B deforms the dished head before penetration begins (see Figure 3.2-1c, bottom). This will decrease the penetration distance from the above values.

In the worst case (cask horizontal with Missile B impacting at 35% of tornado wind), the following results are obtained for impact in the center of the protective cover:

43% of the kinetic energy is absorbed by weather protective cover deformation (see Fig. 3.2.1d)

57% of the energy is absorbed in punching through the cover and the lid.

Depth of penetration into the lid: 0.35 in.

The cask lid is penetrated only .35 in. which is much less than its minimum thickness of 3.5 in.

3.2.1.3c Missile C (steel sphere 1" diameter)

The impact of the steel sphere can result in a local dent by penetrating into the cask surface at the yield strength S_y for a penetration depth, d. The contact area on the cask surface is:

$$A = \pi (2Rd - d^2)$$

Where:

R is the radius of the sphere
d is the penetration depth

The kinetic energy of the steel sphere is dissipated by displacing the cask surface material:

$$\frac{1}{2} m_c v_o^2 = S_y \int_0^d \pi (2Rd - d^2)\, dd$$

Where:

m_c = sphere mass

hence:

d = 0.

A maximum impact force of 11,746 lb. will be developed. It can be concluded that only local denting of the cask will result.

If the impact point is at the center of the protective cover (dished head) the deformation will be largely elastic with no possibility of penetrating the cover.

3.2.1.4 Ability of Structures to Perform Despite Failure of Structures not Designed for Tornado Loads

The TN-24 cask itself can withstand the tornado loading. Generally the casks will be stored outside on a flat concrete slab. Therefore, there will be no structures that could collapse about the storage cask. If such structures were present at an ISFSI, further analysis would be required.

3.2.2 Water Level (Floods, Hurricanes, Tsunami and Seiches) Design

It is anticipated that the storage casks will be located on flood-dry sites. However, the storage cask is designed for an external pressure of 25 psi which would be equivalent to a static head of water of approximately 56 ft. This is greater than would be anticipated due to floods, tsunami and seiches regardless of the site.

Using a friction coefficient of 0.25, a drag force greater than 40,630 lb. is required to move the cask when the cask is in an upright position (after taking into account the bouyant force on the cask). This force is equivalent to a stream of water flowing past the cask at 18 ft/sec.

The water velocity was calculated using the following formula:

$$F = C_D A \rho \frac{V^2}{2g}$$

where F = Drag force, 40,630 lb
C_D = 1.0
A = Projected area, 132 ft^2
ρ = 62.4 lb/ft^3
V = water velocity ft/sec

Therefore $V = \sqrt{\frac{2 F g}{C_D A \rho}}$

$= 18$ ft/sec

For a lower friction coefficient, the drag force is less and the water velocity to move the cask is less. Since this is a site specific event, no attempt was made to establish a fixed requirement.

The effect of this force, which is very small, is equivalent to a uniformly distributed load along the cask outer surface of 203 lb/in.

If the cask is in a horizontal storage position, the force required to roll the cask over is much greater as shown in Section 3.2.1.2d, thus requiring a water velocity greater than 18 ft/sec.

The storage cask is designed for an internal pressure of 250 psi. The maximum cavity operating pressure is 32 psi (2.2 atm). At this pressure it is demonstrated in Section 3.3.2.2 that the leakage rate past the seals will not result in dose levels exceeding regulatory requirements. The seals are equally efficient against in-leakage due to external pressure. Therefore, there would be no leakage of water into the cask. However, even if the cask did become filled with water there would be no criticality problem since the cask is designed with sufficient poison to remain subcritical with the fuel submerged.

Therefore, the cask is evaluated for a water level of 56 ft and a water drag force of 40,630 lbs due to floods, hurricanes, tsunami and seiches. It is demonstrated that the cask is acceptable for these conditions. If a specific site would have conditions exceeding these values, further analysis would be required

3.2.3 Seismic (Earthquake) Design

Seismic design criteria are dependent on the specific site location. These criteria are established based on the general requirements stated in 10CFR Part 72.

3.2.3.1 Input Criteria

The storage cask is a stiff structure having high natural frequencies of vibration. When the cask is stored in a horizontal position supported from the four trunnions, it has a fundamental

frequency of 165 cps. If the cask rests vertically on the ground it will have a "cantilever" frequency of 41 cps. Both of these frequencies are above the minimum required (33 cps) to treat a structure as a rigid body and to ignore amplification of free field seismic motion.

As a result the cask is designed for equivalent static seismic loadings equal to the weight of the cask times the free field peak acceleration. As such there is no need to specify a design response spectrum or its associated time history. For areas east of the Rocky Mountain Front, 10CFR Part 72 suggests that the peak horizontal acceleration can be taken to be 0.25 g's. The peak vertical acceleration is taken to be 2/3 of the horizontal (0.17 g). These loads are assumed to be distributed over the cask length and cask bottom areas as shown in Figure 3.2-1 and listed in Table 3.2-2. The seismic load distribution for the cask supported in the horizontal orientation (Figure 3.2-1b), would be the same.

3.2.3.2 Seismic-System Analysis

The only significant effects of seismic loading would be sliding and tipping or overturning of the cask.

The cask will not tip over due to a seismic event with a horizontal acceleration of 0.25 g's and a vertical acceleration of 0.17 g's (i.e., $\frac{2}{3}$ of the horizontal acceleration). For a circular cask the horizontal g value necessary to tip the cask is calculated below:

$$M_{tip} = g \times W \times l_v + \frac{2}{3} g \times W \times l_r$$

Where:

M_{tip} = Moment necessary to tip the cask, in lbs
g = Acceleration value necessary to tip the cask
W = Weight of cask on pad
= 214,000 lb

l_v = vertical distance to CG
= 93 in
l_r = radial distance to CG
= 41.25 in

$$M_{stab} = W \times l_r$$

Where:

M_{stab} = stabilizing moment on cask, in lbs
W = 214,000 lb
l_r = 41.25 in.

Therefore the G value necessary to tip the cask is found by equating M_{tip} to M_{stab}

$$(g \times W \times l_v) + (\frac{2}{3} \times W \times l_r) = W\, l_r$$

$$g = \frac{41.25}{93 + 0.66 + 41.25} = 0.34$$

Reg. Guide 1.92[7] states that the maximum values of the structural responses to each of the three components of earthquake motion should be combined by taking the square root of the sum of the squares of the maximum values of the codirectional responses (caused by each of the three earthquake components) at a particular point of the structure.

Therefore the combined horizontal acceleration acting on the cask is

$\sqrt{2(0.707 \times .25)^2}$ or 0.25 g.

Since the applied horizontal acceleration of 0.25 g is less than the 0.34 g required to tip the cask, the cask will not tip over.

If the cask is to slide due to seismic loading, the horizontal component of the seismic load must overcome the normal force acting at the cask/ground interface multiplied by the coefficient of friction. The vertical seismic force is applied upward so as to decrease the normal forces and hence the sliding resistance force. When this is done it is found that a coefficient of friction between the cask and ground of 0.3 is required to prevent sliding. However, even if the cask slides without tipping over, contact with other casks is unlikely since they are spaced at 16 ft. intervals. If in the extreme event contact occurred, the cask velocity would be very low and any impact between casks would be much less severe than the accidents described in Sections 3.2.11 and 3.2.12.

3.2.4 Snow and Ice Loadings

The decay heat of the contained fuel will maintain the storage cask outer surface temperature above 32°F throughout its service life, including the end of life, with an ambient temperature of -20°F. Therefore, snow or ice would melt when it comes in contact with the cask so that snow and ice loadings need not be considered for the storage cask.

The temperature of the protective cover attached to the top of the cask above the lid under certain conditions could fall below 32°F and a layer of snow or ice might build up. A 1 ft layer of snow or a 1 in. layer of ice might form. These are equivalent to 0.056 psi and 0.034 psi, respectively, external pressures acting on the cover. These loads are insignificant since the cover is a 0.38 in. thick dished head. Therefore, the cover will maintain its intended protective function under these snow or ice loading conditions.

Another possible influence is a thermal shock when the warm outer shell is suddenly cooled by cold rain at 32°F. A number of such cycles is considered in the thermal fatigue analysis.

3.2.5 Dead (Weight) Loads

The only dead loads (hereafter referred to as weight loads) on the cask are the cask weight including the contents. The calculated weights of the individual components of the cask and the total weights are given in Table 3.2-3.

3.2.6 Handling Loads

Handling loads are those which occur during lifting, tilting between vertical and horizontal positions, and on-site transfer to the storage pad. The cask is provided with four trunnions at the top spaced 90 degrees apart for redundant lifting. Two trunnions are provided at the bottom 180 degrees apart. (See Drawings 971-1 and -2 in Chapter 1.)

The handling conditions result in loads applied directly to trunnions used during all handling operations. The trunnions then transmit the handling loads onto the cask body.

The trunnions are evaluated for g levels equivalent to 3 times and 5 times the weight of the cask. These values are based on ANSI 14.6,[8] Section 4.2 which requires that lifting devices be capable of lifting 3 times and 5 times the cask weight without exceeding the yield and ultimate strengths of the material. The loads acting on the trunnions for the handling conditions are described further in Section 3.2.13.3 .

The cask body is evaluated for a vertical lift load of 3 g (i.e., 3 times the weight of the cask). This load is transmitted to the cask body by each trunnion involved in the handling operation.

The loads per trunnion for vertical and horizontal cask orientations are shown in Figures 3.2-2 through 3.2-5 in terms of g levels. The loads acting on the trunnions during tilting are based on a 1.5 g vertical load on the lifting device. The rear trunnions on which the cask rests during tilting support one-half of the cask weight or 1.5 g. The longitudinal and vertical components at the trunnions depend on the angle of tilt.

The maximum axial and vertical components are 0.75 g at each trunnion as shown in Figure 3.2-4 for any angle of tilt.

The load used for transfer is 2 g in any direction with the cask horizontal. This value should be sufficient since it is expected that the on-site transfer is over a short distance at a very slow rate of speed. The loads acting on the trunnions during transfer are shown in Figure 3.2-5.

The statically applied inertia loads acting on the cask during these operations are listed in Table 3.2-4. This table shows the loads acting on the cask center of gravity and the trunnions. The loads are presented in terms of g levels and in kips acting on each trunnion for each handling condition. The weight of the cask used for the analysis is the loaded weight (including water), of 225,000 lb (i.e. rounded up from 224,285 lb).

These handling loading conditions result in loads being applied to the cask in three ways.

First, loads are applied to the cask body due to handling through the trunnion attachments. The TN-24 cask is provided with six trunnions for handling the cask. These trunnions are bolted to the cask body. The trunnions have two shoulders, an inner shoulder used for tilting and transfer and an outer shoulder used for lifting. The handling loads are transmitted to the cask body through the twelve 1-1/2 in. bolts which are provided for each trunnion.

Figure 3.2-7 shows the location at which the handling loads are applied to the trunnions. The lifting load, F_L, is applied at the midlength of the outer shoulder and the transfer load, F_T, is applied at the midlength of the inner shoulder. The transfer lateral load, P_T, acts on the trunnion flange. The tilting loads at the top end of the cask are applied to the outer shoulder and at the bottom end of the cask to the inner shoulder.

The attachment loads are then calculated in terms of forces and moments acting locally on the cask body. The maximum values considered to be acting during handling operations are given in Table 3.2-5.

Secondly, the cask and/or cask component weight acts as a uniformly distributed load either over the cask length, its cross-sectional area or the area the weight contacts. Two distributed loads will be used to represent all possible distributed loading conditions during handling. These are shown in Figure 3.2-6 and are the maximum values which would be expected.

The third manner in which handling operations result in applied loads is through the g loads of the contents (i.e. basket and fuel) and the lid. These loads are applied to the lid and lid bolts at the top of the cask. The lid bolts then induce forces and moments on the top end of the cask body shell. Applied bolt loads are described further in Section 3.2-9. For a g load in the other direction the contents act on the bottom plate. The contents are assumed to act as a uniformly distributed load on the lid or the bottom as shown in
Figure 3.2-6

3.2.7 Internal Pressure

The cavity pressures are calculated in Section 3.3.2.2. The pressure inside the cavity of the storage cask results from several sources. Initially the cavity will be pressurized with a gas such that the cavity pressure will be 2.2 atm at thermal equilibrium. The purpose of pressurizing the cavity above atmospheric pressure is to prevent in-leakage of air. The initial pressure is determined on the basis that a 1.1 atm pressure must exist in the cavity on the coldest day at the end of life. Pressure variations due to daily and seasonal changes in ambient temperature conditions will be small due to the large thermal capacity of the cask.

Fuel clad failure results in the release of fission gas which increases cavity pressure. Under normal storage conditions a 10% fission gas release is assumed due to fuel clad failure. This results in an increase in cavity pressure of 1.9 psi.

Another condition when internal pressure could increase is the cooldown prior to unloading. This could occur at the beginning or end of life. Unloading of fuel at the beginning of life would only be necessary due to excessive leakage past the lid seals or a severe accident, e.g. cask drop. The cask cavity wall temperature at the beginning of life is just below 320°F. Therefore, before returning the cask into a pool, cold water would be pumped into the cavity to reduce the temperature. When the water hits the cavity surface, steam would be produced and the resulting pressure inside the cavity would reach the saturated steam pressure of 75 psi (5.16 atm) corresponding to the cavity wall temperature of 320°F.

Another condition which could cause an increase of cavity internal pressure is a fire. Fires can be considered minor and major, as discussed and defined in Section 5.1.3.6. The increase in cavity pressure due to a minor fire is negligible. The major fire (which is the transport fire defined in 10CFR71[3] results in maximum cavity pressure of 53 psia. Table 3.2-1 presents a summary of internal pressures for the conditions identified. A pressure of 250 psi was chosen as the design internal pressure, since this value exceeds the cumulative effects of all conditions producing an internal pressure.

3.2.8 External Pressure

There are several conditions which can result in external pressure on the cask. The external pressure due to floods is assumed to be equal to or less than 25 psi which is equivalent to a 56 ft head of water as discussed in Section 3.2.2.

During fuel loading or unloading the cask is at the bottom of a spent fuel pool which may be 40 to 50 ft deep. This results in an external hydrostatic pressure of approximately 20 psi.

An earth pressure loading would occur if the cask were to be buried under dirt. This is similar to a hydrostatic pressure head of water. The density of loose dirt or earth is approximately 100 lb/ft^3 compared to 62.4 lb/ft^3 for that of water. Therefore 36 ft of earth is equivalent to a 56 ft head of water and an external pressure of 25 psi.

The cask is designed and evaluated for an external pressure of 25 psi. This value was selected because it exceeds the maximum external pressure which would be anticipated for the loading conditions considered above.

3.2.9 Bolt Loads

Bolt loads are induced by several loading conditions including internal pressure, handling, thermal expansion and accidents. Internal pressure loads include cavity pressurization, fission gas release, minor fire and major fire. The bolts will be preloaded so that the internal pressure loads and handling will not result in a bolt load which exceeds the preload. The handling conditions result in statically applied inertia g loads from the contents and lid.

Under thermal loading conditions there is differential thermal expansion between the lid flange and lid bolts. This results in a slight increase in bolt load. This occurs for all the thermal loading conditions except for lightning and explosions. Explosions would cause an external pressure and ,therefore, would not induce a tensile load in the bolts. Since the cask can be grounded and provides such a large thermal inertia due to its mass, lightning will not result in a significant thermal loading (see Section 3.2-10). Therefore, no effect on the bolts from these two sources is considered.

Bolt loads are also induced due to accident conditions which include cask drop, cask tipping and a major fire. The bolt loads due to the cask drops and tipping are a result of the inertia g loadings applied upon impact with the target surface by the contents and the lid. The major fire will result in differential thermal expansion between the lid flange and bolts and an increase in cavity pressure. For these accident conditions the bolt preload can be exceeded but the criteria presented in Section 4.2 cannot be exceeded. These accident loads are additive to the other loads described above.

A summary of bolt loads due to the conditions described above is given in Table 3.2-6. The method and calculations which show how these loads are obtained are given in Sections 4A.5.4 and 4A.5.7.2B

3.2.10 Thermal Loads

Thermal loads are induced by the following thermal loading conditions:

- Fuel loading
- Decay heat
- Insolation
- Beginning of life unloading
- Ambient variations
- Lightning
- Minor Fire
- Major Fire

The thermal loads which are of concern structurally are the temperature gradients in the cask and the differential thermal expansions of interfacing cask components. The magnitude of these values will be established below.

Fuel Loading

The cask is loaded in a spent fuel pool under 30-40 ft of water. The cask will be in the pool for a short time and is cooled by pool water; therefore, the thermal gradients established during fuel loading will be negligible.

Decay Heat/Solar Load

After the cask is loaded and removed from a pool, the body temperature will gradually reach steady state conditions. Since the mass of the cask is large, the time to reach equilibrium will be approximately 4 to 5 days. The temperature gradients in the cask body have an insignificant effect on the structural integrity of the body.

Several thermal analysis calculations were made for different ambient conditions. The methods used to obtain these results are discussed in Section 5.1.3.6. The maximum temperature gradients resulting from the thermal analyses were used for the structural analysis. The temperature gradients for the cask body and cask components are listed in Table 3.2-7.

Beginning of Life Unloading

This condition would occur if it were necessary to place the cask back in the pool at the beginning of life after it had been loaded and reached thermal equilibrium. Prior to placing the cask in the pool, the cask and fuel would have to be cooled by circulating water through the cask. Therefore, cold water would contact the hotter cask inside surfaces. This condition has been evaluated and is described in detail in Section 5.1.3.6. This evaluation showed that the thermal gradients in the cask body are small and would have an insignificant effect on the cask body.

Ambient Variations

Because the cask thermal inertia is large, the cask temperature response to changes in atmospheric conditions will be relatively slow. Ambient temperature variations due to changes in atmospheric conditions i.e. sun, ice, snow, rain and wind will not affect the performance of the cask. Snow or ice will melt as it contacts the cask because the outer surface will be above 32°F for ambient temperatures above -20°F. The cyclical variation of insolation during a day will also create insignificant thermal gradients. One condition which is evaluated structurally is cold rain or a hot cask. This evaluation is presented in Section 4A.5.5.6I. The assumption is made that the outer surface of the cask is restrained from contracting by the mass of the cask.

The thermal effects due to ambient variations and conditions are discussed in further detail in Section 5.1.3.6.

Lightning

Lightning will not cause a significant thermal effect. The cask can be grounded, and if struck by lightning on the lid, the electrical charge will be conducted by paths provided by the lid bolts to the body.

The lid metallic O-ring seals can withstand temperatures of up to 700°F without loss of sealing capability. It is not anticipated that lightning could result in the seals reaching temperatures above these values.

Minor and Major Fires

There are two fire conditions evaluated for the cask - a minor fire and a major fire. The latter is equivalent to the 10CFR Part 71[9] hypothetical fire accident. This major fire condition would result in maximum outside and inside cask body surface temperatures of 850°F and 300°F respectively and a maximum gradient from outside to inside surfaces of 550°F. This would produce a thermal strain of approximately 0.4 in./in.

This is slightly above the yield strain for the cask body material; however, it is well below the rupture elongation of 25%. Also this effect is a surface effect and the effect through the thickness is much less. Under the fire conditions, the maximum temperature of the seal is 479°F, which will not affect the sealing capabilities of the metal O-rings and the lid-shell joint.

Since a protective cover is placed over the closures in the lid, the temperatures will be less than those given above and the thermal loads will also be less severe.

A minor fire is defined as one which could occur from a gasoline truck catching fire in the vicinity of the cask storage area but not immediately adjacent to the cask. One of the effects would be to increase the air temperature around the cask by several degrees. Some heat from the fire would be radiated to part of the cask outer surface area facing the fire. This generally has a negligible effect on the cask in terms of structural considerations. Minor fires at specific sites can be evaluated to assure their effect is negligible.

Buried Cask

An evaluation was made to determine the increase in cask temperature with time assuming the cask was completely buried by dirt and debris with very low thermal conductivity. The details of this analysis is given in Section 5.1.3.6. The containment integrity of the cask will not be endangered if all the fuel fails. The cask body would experience less thermal strain at this temperature than during normal storage. The basket would still have sufficient structural rigidity to maintain its integrity. The analysis further shows that the cask will maintain its containment integrity up to a maximum burial period of 80 hr.

3.2.11 Cask Drops

The TN-24 cask can be transported from the spent fuel pool to its storage location in either a vertical or a horizontal position. Vertical transporters carry the cask with the bottom only about one foot off the ground. A cask drop from this height will be much less severe than the drop from a horizontal transporter as described below.

The cask will be supported on four trunnions during horizontal transport; it will be rotated to vertical about the lower trunnions, lifted off the transporter and placed on the concrete slab.

Two potential accidents during this load/unload operation are considered, and these are illustrated in Figure 3.2-8. Each is based on the assumption that the trunnion support location on the transporter will be no more than 8 ft off the foundation of the facility. The first drop accident is postulated to occur when the cask is vertically oriented. Since the trunnion is located two feet from the end of the cask, this accident would result in a six foot drop (from the bottom of the cask to the foundation) if it begins with the trunnion located at its initial eight foot height. An eight foot drop height is used assuming that the cask is lifted two feet off of the trunnion support. The cask may be vertical or orientated so that the center of gravity is directly above the (corner of the cask) so that no energy is diverted into rotational motion.

The second postulated accident is based on the cask falling off of the transporter in the unlikely event of a failure in the trunnion supports. In this case, the accident would actually be initiated with the lowest point of the cask about 5 feet above the foundation surface (8 feet to the trunnion support minus the cask radius). A drop height of seven feet is conservatively used for this accident assuming that the cask could be raised two feet off the trunnion supports. The cask is assumed to be oriented with its axis parallel to the foundation or at a shallow angle relative to the foundation.

For each of these accident conditions, the cask is assumed to fall onto a surface which consists of a concrete slab resting on a soil foundation.

The energy associated with the drop conditions must be absorbed by either deformation of the cask or deformation of the concrete slab/soil foundation system. Since there are no impact limiters on the storage cask, the cask surface will be rigid in comparison with the foundation target materials. An evaluation of the crushing strength of typical foundations is discussed in Section 3.2.11.1 below.

Results of the analysis in terms of peak decelerations acting on the cask are given in Section 3.2.11.2. These decelerations are used to determine cask loadings and stresses in Appendix 4A.

3.2.11.1 Crushing Strength of Foundation

The foundation is assumed to be a concrete slab resting on soil. The model used to describe the response of the concrete slab/soil system is described below.

The slab/soil system is an infinite disk (slab) on an elastic foundation (soil) that absorbs energy by elastic deformation. The concrete simultaneously absorbs energy by being crushed if the contact stress between cask and concrete exceeds the concrete crushing strength. As the slab/soil system is deformed during cask impact, the total deflection is then the elastic deflection of the disk on elastic foundation plus the depth of penetration into the concrete.

The total energy absorbed in the foundation is:

$$E = E_c \text{ (Crushing of Concrete)} + E_s \text{ (Deflecting Slab/Soil)}$$

$$E = \int_0^{\Delta} F d\Delta + \int_0^{\Delta_s} F d\Delta_s$$

Where:

E is the total energy absorbed
F is the impact force
Δ is the depth of cask penetration into the concrete
Δ_s is the slab/soil system elastic deflection

The impact force is equal to both the concrete crushing force and the elastic force on the slab/soil system

$$F = \sigma_c S_\Delta = K \Delta_s$$

$$\text{and } \Delta_s = \frac{F}{K}$$

Where:

σ_c is the concrete crushing stress, 1,000 psi, in this report.

S_Δ is the crushed concrete surface area projected normal to the cask at a given penetration.

$$E = \int_0^{\Delta} \sigma_c S_\Delta \, d\Delta + \int_0^{\Delta_s} K\Delta_s \, d\Delta_s$$

$$E = \sigma_c \int_0^{\Delta} S_\Delta \, d\Delta + \frac{1}{2} K(\sigma_c S_\Delta)^2$$

The change in potential energy of the cask between the initial state and at the end of the impact is:

$$E_p = W \text{ (Elevation Change of CG)}$$

The change in potential energy is then equated to the absorbed energy and solved for the various cases of interest. Note that the concrete crush area, S_Δ, varies with penetration distance, Δ, in a different manner for different cask orientations. When the solution is obtained the maximum impact force, F, and moment about the CG, M_{CG}, (based on force F and centroid of concrete crush area), are determined. Then the inertia loads become:

$$G = \frac{F}{W} \text{ for cask translation}$$
$$\Phi'' = \frac{M_{CG}}{I_{CG}} \text{ for cask rotation}$$

Where:

W is the cask weight

M is the moment of the impact force about the CG or other pivot point

I_{CG} is the cask moment of inertia about its CG or other pivot point

The solution for K, the slab/soil stiffness, is obtained from Timoshenko, "Theory of Plates and Shells"[10].

$$K = 8 \sqrt{\frac{k E T_s^3}{12(1-\nu^2)}}$$

Where:

k = Soil foundation modulus

E = Concrete Young's Modulus (3500 ksi)

ν = Concrete Poisson's Ratio (0.15)

T_s = slab thickness (36 in.)

Analyses were performed for a range of soil (k) stiffnesses. A value of 380 psi per in.[11] was selected as a conservative (high) value for final analysis.

3.2.11.2 Analysis of Cask Impact

End Impact

In this case, the slab deforms slightly until the concrete crushing stress is reached. At that point, the crush area is constant, and hence the force on and acceleration of the cask are constant also.

$S_\Delta = \pi R^2$ where R is the end radius of the cask

$F = \sigma_c S_\Delta$

$G = \frac{\sigma_c S_\Delta}{W} = 100$ g

Although some energy is absorbed elastically by the soil/slab system, crushing eventually begins and at that point the elastic slab deflection remains constant:

Slab Deflection, $\Delta_s = 1.2$ in.

Concrete Penetration, $\Delta_c = 0.4$ in.

Crush Area, $S_\Delta = 37$ ft^2

Corner Impact

The corner impact orientation (Figure 3.2.9) is a "near vertical" drop with the center of gravity directly above the impact point.

The concrete crush area is:

$$S_D = \frac{R^2}{\sin \alpha}\left[\cos^{-1}\left(1 - \frac{\Delta}{R \cos \alpha}\right) - \left(\frac{1}{2}\sin\left(2\cos^{-1}\left(1 - \frac{\Delta}{R \cos \alpha}\right)\right)\right)\right]$$

Integrating to find the energy absorbed in concrete crushing:

$$E_c = \int_0^{\Delta} \sigma_c S_\Delta d\Delta$$

$$E_s = \frac{1}{2}K(\sigma_c S_\Delta)^2$$

$$E_p = W(H') = W(H+\Delta+\Delta_s) = E_c + E_s$$

These equations are solved iteratively for a drop height, H of 8 ft yielding:

$$G = 27g$$

$$\Delta = 8.85 \text{ in.}$$

$$\Delta_s = 0.3 \text{ in.}$$

$$S_\Delta = 10.1 \text{ sq. ft.}$$

Horizontal Impact

In this case crush area increases with cask penetration into the concrete (see Figure 3.2.10)

$$\Delta = R\ (1 - \cos \theta)$$

$$S_\Delta = 2L\ R \sin\theta$$

$$E_c = \int_0^\theta \sigma_c\ S_\Delta\ d\Delta = [\theta/2 - 1/2 \cos\theta \sin\theta]\ 2Lr^2\sigma_c$$

$$E_s = \frac{1}{2}\ K(\sigma_c\ S_\Delta)^2$$

$$E_p = WH' = E_c + E_s$$

H', the total elevation change of the CG, equals the drop height, H, plus the penetration into the concrete, Δ, plus the slab/soil deflection, Δ_s. An iterative solution is performed until $E_p = E_c + E_s$ and $H' = H+\Delta_c+\Delta_s$.

For a drop height, H, of 7 ft:

$G = 65\ g$

$\Delta = 1.36$ in.

$\Delta_s = 0.84$ in.

Crush area, S_Δ, = 24 sq. ft.

Impact On a Trunnion

If a trunnion hits the foundation first, it will penetrate the concrete since it protrudes approximately two inches beyond the outer surface (outer shell) of the cask. The area of crushed concrete is 26.2 $in.^2$ and the force generated on the cask is:

$F = \sigma_c\ (26.2) = 104{,}600$ lb.

As the trunnion penetrates the concrete, the cask will rotate about its center of gravity through an angle, Φ, such that:

$$I_{CG}\,\Phi'' = \text{moment of F about the cask CG}$$

Where:

I_{CG} is the moment of inertia of the cask about its CG

Integration of this equation shows that:

$$\Phi = 130\ t^2$$

Since the cask body impacts .0073 seconds after the trunnion, Φ = .0071 degrees. Therefore, the effect of trunnion impact is negligible.

Shallow Angle Slapdown

If the cask is not quite horizontal at impact, one end will contact first and then the cask will rotate about this point that first embeds itself in the concrete (point P in Figure 3.2-10). The cask will then slapdown against the other end. It is assumed that the first impact is perfectly inelastic (coefficient of restitution = 0) and that the impact applies an impulsive loading to the cask that initiates rotation. Then:

Initial System Momentum + External Impulse = Final System Momentum

Translation

$$MV_1 - \int F\,dt = MV_2$$ (Since the impulsive loading decreases the initial velocity)

Rotation

$$\int F \text{ (distance, a, to CG)} dt = I_{CG}\omega \quad \text{(The impulsive loading initiates rotation)}$$

Where

M is the mass of the cask
V_1 is initial cask velocity (at CG)
V_2 is CG velocity after first impact
ω is rotational velocity about pivot point P after first impact
I_{CG} is moment of inertia of cask about CG

We can solve the translational and rotational equations for the impulse, $\int Fdt$, and equate:

$$\int Fdt = M(V_1 - V_2) = \frac{I_{CG}\,\omega}{a}$$

After the initial contact, the velocity at the contact point is assumed to be zero. The cask is then rotating so that:

$$\omega = V_2/a$$

If we substitute for ω in the impulse equation, we find that:

$$V_2 = \frac{M}{M + I_{CG}/a^2} V_1$$

and

$$\omega = \frac{1}{a} \frac{M}{M + I_{CG}/a^2} V_1$$

We can then determine the energy absorbed by the initial impact:

$$\Delta E = \frac{1}{2} MV_1^2 - [\frac{1}{2} MV_2^2 + \frac{1}{2} I_{CG}\omega^2]$$

When the computation is performed, it is found that 30% of the initial kinetic energy is absorbed in this first contact and 70% of the energy remains to be absorbed in the second impact.

Section 3.2.12, below, provides a complete discussion of rotating or tipping impact. Slapdown after a shallow angle, near horizontal drop is similar to the case of the cask tipping about its base. See and compare Figures 3.2-9 and 3.2-12. The slapdown analysis is performed using the approach of Section 3.2.12 assuming that 70% of the potential energy is absorbed during the secondary impact. The results obtained are:

Δ = 2.08 in.
Δ_s = 0.62 in.
S_Δ = 19.9 sq. ft.
Φ'' = 175 rad/sec.^{2}
$G_{\text{cask tip}}$ = 69.8 g

3.2.12 Cask Tipping

Two tipping accidents are considered (see Figures 3.2.11 and 3.2.12). The first would occur if the cask were accidently released while being rotated about one set of trunnions to bring it from the horizontal position to the vertical position (or vertical to horizontal position). If released, the cask could then rotate about the trunnions, which are 8 ft. above the foundation, and impact on the foundation. The second accident considered occurs if the cask tips over from its normal upright position on the concrete storage pad.

As discussed in Section 3.2.11, the cask is conservatively assumed to be rigid and all deformation occurs in the foundation. The concrete crushing and slab/soil deformation assumptions are discussed in Section 3.2.11.1 and apply to the tipping accidents as well as the drop accidents.

The tipping accidents differ from the drop accidents in that the cask rotates about a fixed point as it deforms the foundation in the tipping accidents while it translates in a fixed orientation during the drop accidents (3.2.11).

3.2.12.1 Analysis of Tipping Accidents

Two types of tipping accidents are considered. The first involves rotating about the trunnions when the trunnions are positioned 8 feet above the concrete foundation. The second involves tipping over when the cask is standing upright on its foundation.

a. Tipping About Trunnions

The case considered is shown in Figure 3.2-11. The total potential energy to be absorbed is:

$$E_p = WH' = W\ (1 + \sin \alpha)\ \overline{OCG}$$

The vertical distance that the cask center of gravity drops during this accident is the sum of two components (80 in.+80 in.sin α). The 80 in. figure is a conservative estimate of the distance from the pivot point (i.e., trunnion centerline) to the cask center of gravity. The greater the distance assumed, the more conservative the calculation; the actual value with the fuel centered in the cavity is 75.75 in. The second component (80 in. sin α) is the drop distance due to the rotation of the cask below the pivot point. This value is shown on Figure 3.2.11 and is greater than it would be using 75.75 in. Therefore, the total energy to be absorbed, from which the deceleration loads are determined, is conservative.

The change in potential energy is absorbed by crushing of the concrete and elastic deflection of the slab/soil system. The crushed and displaced concrete is shown cross hatched on Figure 3.2-11. If the tip of the cask penetrates into the concrete by an amount Δ, then the portion of the cask shown cross hatched is embedded in the concrete. The force developed on the cask is the crushing strength of the concrete slab material multiplied by the projected area of this cross hatched zone of material on the cask. The energy absorbed by concrete crushing is the integral of the force versus displacement through the concrete.

The energy absorbed by the elastic slab/soil system is small compared to that absorbed by concrete crushing and is calculated in the same manner as in the cask drop cases described in Section 3.2.11. Equating the energy absorbed by the concrete crushing plus slab/soil deflection to the change in potential energy during the accident allows an iterative solution for the deformation ,Δ. Once Δ is known, the projected area, and therefore the total force can be calculated. Then the translational and rotational decelerations are determined.

The following is a development of the analysis described above. Consider the slice of crushed material, dz, located z in. from the corner as shown in Figure 3.2-11. The force exerted on the cask by the crushing of this slice of concrete is dF and is given by:

$$dF = 2\,\sigma_c\,X_c\,dz \qquad (1)$$

where

$$X_c = [2R\delta\cos\alpha - \delta^2\cos^2\alpha]^{\frac{1}{2}}$$

$$\delta = (\Delta - z\mathrm{Tan}\,\alpha)$$

The deformation across the slice varies from Δ at the center to 0 at the ends and follows an elliptic profile in between. The increment of energy absorbed in crushing this slice of concrete is:

$$\Delta E_c = 2\int_0^{X_c} \sigma_c \left[\delta - \frac{R}{\cos\alpha}\left(1-\sqrt{1-\left(\frac{X}{R}\right)^2}\right)\right] dx \qquad (2)$$

The equations are evaluated numerically by dividing the crushed region into 10 segments (see Figure 3.2-11). The solution is obtained by assuming a deformation, Δ, and then using Equations (1) and (2) to to calculate the energy increment in each of the ten segments. These are then summed to obtain the crushing energy to which is added the slab/soil energy. The total absorbed energy is then compared with the change in potential energy and the Δ required to absorb the potential energy is found iteratively. The maximum force on the cask occurs when Δ is maximum. Hence $F = S_\Delta \times \sigma_c$ where S_Δ is the projected area of the crushed concrete shown in Figure 3.2-11. Force F exerts a moment, M_t, about the trunnion equal to F multiplied by the moment arm from the centroid of S_Δ to the trunnion pivot point O. The angular deceleration of the cask is then:

$$\Phi'' = M_t / I_o$$

I_o = the moment of inertia of the cask about pivot O.

Solving the above equations results in:

$\Delta = 11.6$ in.

$\Delta_s = .26$ in.

$S_\Delta = 8.28$ sq. ft.

$\Phi'' = 135$ rad/sec^2

$G_{\text{cask tip}} = 57$ g

The linear deceleration at any point on the cask is then this angular deceleration multiplied by the distance between the trunnion and the point of interest.

b. Tipping About Base of Cask

This problem involves tipping of the cask about its base (falling over) as shown in Figure 3.2-12. The analysis is identical to the above except that concrete crushing occurs along the entire length of the cask. The same type of analysis is performed and the following results are determined:

Δ = 1.64 in.

Δ_g = 0.55 in.

S_Δ = 17.6 sq. ft.

ϕ'' = 155 rad/sec^2

$G_{r\ sk\ tip}$ = 67 g

3.2.13 Combined Loading Criteria for Containment Vessel

The storage loading conditions are listed in Table 3.2-8. These loading conditions include those described in 10CFR Part 72, which are categorized as normal, man-made and natural phenomena. The applied loads acting on the different cask components due to these loading conditions have been determined and are discussed in the preceding Sections 3.2.1 through 3.2.12. This section describes the bases which are used to combine the loads for each cask component and the criteria against which each load combination will be compared.

3.2.13.1 Containment Vessel

The storage loading conditions for the containment vessel are categorized based on the rules of the ASME Boiler and pressure Vessel Code Section III, Subsection NB, for a Class 1 nuclear component.

These storage loading conditions translate into five service loading conditions in terms of the ASME code. They include Primary Service and Levels A, B, C and D Service Loadings. The Primary Service Loadings are basically equivalent to the Design Loadings as defined by Section III of the ASME Boiler and Pressure Vessel Code.

For each of the service loading conditions there are several applied loads acting on the containment vessel. The Primary Service loads are listed in Table 3.2-9. They include internal and external pressure; lid bolt preload including the effect of the gasket reactions; distributed loads due to weight, wind, [illegible] and handling; a design earthquake; and attachment loads applied by the trunnion to the cask body.

The inertia g loads are statically applied loads which are multiples of the weight of the cask and/or contents. The magnitude of the Primary Service Loads envelops the maximum Level A, B and C Service Loads. Thermal effects are excluded, except for their influence on the preload of the lid bolts because the ASME Code does not consider these as design (i.e. primary service) loads.

The Level A Service loads are listed in Table 3.2-10 and are basically the same as the Primary Service Loadings except the Level B and C loads have been excluded and the thermal loads acting on the containment vessel are included. The thermal loads consist of temperature differences and differential thermal expansion due to decay heat, solar insolation, ambient temperature variations and ambient conditions, e.g. ice, snow, wind, sun.

The loads due to the Level B and C Service Loading Conditions are listed in Tables 3.2-11 and 3.2-12; they include natural phenomena and minor accidents respectively. These conditions occur less frequently and therefore higher stress values are allowed.

The loads due to Level D Service Loading Conditions, which are accident conditions, are listed in Table 3.2-13.

Loading combinations for Primary Service and Level A, B, C and D Service Loadings which are evaluated are given in Table 3.2-14. The loads are listed across the top of the table and the Load Combinations are designated in the first column of the table. There are three Primary Service Load combinations listed, three level A combinations, two Level B and C combinations and seven Level D combinations. The loads which are acting simultaneously for each of these combinations are denoted by an "X" under the load column heading. As an example, for Primary Service Load Combination P2, internal pressure due to cavity pressurization, fission gas release and minor fire, distributed weight, wind or water and seismic loads, and lid bolt preload are acting simultaneously.

The stresses due to each of the loads acting on the containment vessel are calculated in Appendix 4A. The maximum stresses due to the worst combination of service loading conditions were determined and compared with the ASME Code allowable stress intensity limits. The limits and the results of the comparison are summarized in Section 4.2.1.1, Subsection E and listed in Table 4.2-8 through 4.2-10.

3.2.13.2 Basket

The loadings acting on the basket are categorized as handling loads due to lifting, tilting and transfer; thermal loads due to thermal gradients and temperature differences; and storage accident conditions.

The handling loads, i.e. inertia g loads, which are listed in Table 3.2-4 are limited by the yield strength. Therefore, they would produce no permanent deformation of the material. The thermal loads in combination with the normal handling loads are limited to two times the yield strength.

This allows some local yielding of the basket structure. However, since thermal stresses are self-relieving the deformation would be insignificant. This represents a one time deformation since there is no cycling. In addition, the thermal stress will decrease with time as the decay heat load decreases.

The storage accident conditions are considered separately. The thermal stresses are self-relieving and cannot cause failure of a structure from a one-time occurrence. Therefore, they are not combined with the inertia g loads due to the storage accidents. The accident loads are allowed to result in local plastic deformation. The criteria allows a plastic hinge to form at the support, i.e. at intersecting plates, and yield stress to be exceeded at the surface of the plates at the center between supports.

The thermal analysis of the basket is given in Section 5.1.3.6. The structural analysis of the basket is in Section 4A.6 of Appendix 4A including the material properties on which the analysis is based. A summary of the results and comparison with design criteria are given in Section 4.2.1.2.

The specification to which the basket material would be procured is given in Appendix 4B.

3.2.13.3 Trunnions

The trunnions are evaluated for the combined effect of inertia g loads during handling operations of lifting, tilting, and transfer. During lifting, the trunnions are evaluated for a vertical lift on the outer shoulders equivalent to three times and five times the weight of a fully loaded (including water) cask. For a load three times the weight, the maximum tensile stresses shall not exceed the minimum yield strength of the trunnion material. For a load five times the weight, the maximum tensile stresses shall not exceed the minimum ultimate tensile strength of the trunnion material.

For tilting, the trunnions are evaluated for a 3 g load on the inner shoulder. The stresses are limited to the minimum specified yield strength of the trunnion material.

For transfer the trunnions are evaluated for the combined inertia g loads of 2 g vertical, 2 g longitudinal and 1 g lateral. The stresses are limited to the minimum specified yield strength of the trunnion material.

The loads acting on the trunnions are given in Table 3.2-4 in terms of g levels and in terms of force (kips). The structural analysis of the trunnions is presented in Section 4A.7 of Appendix 4A. A summary of the results and comparison with allowable design criteria are given in Section 4.2.1.3.

3.2.13.4 Outer Shell

The outer shell is evaluated for the combined effects of inertia g loads due to handling operations of lifting, tilting and transfer, and internal pressure. The inertia g loads which are multiples of the weights acting on the outer shell are listed in Table 3.2-4.

Outgassing from the resin between the cask body and outer shell may cause a slight pressure on the inside of the outer shell. A pressure relief valve is provided in the outer shell to assure any pressure build-up is small. The design is based on several years operating experience with this type of resin neutron shield. An internal pressure of 3 psi will occur due to the reduced external pressure during a tornado. However, since the cask is designed for an external pressure of 25 psi, an internal pressure of 25 psi is used to evaluate the outer shell for conservatism. The outer shell is supported by the resin shield material under an external pressure.

The structural analysis of the outer shell is presented in Section 4A.8 of Appendix A. A summary of results and comparison with design criteria are given in Section 4.2 1.4.

The combined effect of the inertia g loads and pressure is limited to the minimum yield strength of the outer shell material.

TABLE 3.2-1

SUMMARY OF INTERNAL AND EXTERNAL PRESSURE LOADS

Loading Condition	Maximum Pressure, psi
Internal:	
(a) Initial cavity pressurization	32
(b) With 10% fuel failure	35
(c) In a minor fire	32
(d) In a major fire (100% fuel failure)	53
(e) Beginning of life unloading	120
(f) Tornado	3*
External Pressure:	
(a) Flood	25
(b) Fuel Loading & Unloading	20
(c) Earth	25

* This is due to a reduced external pressure

TABLE 3.2-2

SUMMARY OF DISTRIBUTED LOADS ACTING ON CASK

Loading Condition	Magnitude
Wind or water	218.5 lb/in.
Tornado Driven Missile (5)	1.38×10^6 lb. (max)
Weight	Note (3)
Seismic	
Vertical(1)	17 lb/in.^{2}
Lateral	297 lb/in.
Handling(2)(3)	
Cask Weight(4)	225,000 lb
Cask Vertical	290 lb/in.^{2}
Cask Horizontal	3670 lb/in.
Contents	
Cask Vertical	81 lb/in.^{2}
Cask Horizontal	1230 lb/in.

(1) Value based on area of cask in contact with concrete pad.

(2) Values based on 3 g static inertia load.

(3) Distributed loads due to weight (i.e. 1 g dead weight) are 1/3 of handling load values listed.

(4) Dry weight used in calculations (weight including water used for trunnion calculations)

(5) Several values are used in the analysis.

TABLE 3.2-3

SUMMARY OF WEIGHTS

COMPONENT	WEIGHT, lb
Body	105,758
Bottom	17,010
Lid	11,624
Aluminum Boxes	2,186
Resin	10,484
Outer Shell	10,344
Trunnions	1,453
Protective Cover	1,413
Basket and rails	17,372
Fuel Assemblies	36,000
Water in Voids	12,054
	225,698 (calculated)

Weight Loaded (including water and w/o protective cover	224,285
Weight Unloaded (w/o water and w/o protective cover)	176,231
Weight on Crane Hook (w/o lift beam)	224,285
Weight on Storage Pad (dry with protective cover)	213,644

TABLE 3.2-4

SUMMARY OF INERTIA G LOADS DUE TO HANDLING OPERATIONS

Handling Condition	Load in g's at Cask CG		
	Vertical	Longitudinal	Lateral
Lifting - Cask Vertical	3	0	0
Cask Horizontal	3	0	0
Tilting[a]	3	0	0
Transfer	2	2	1
	Load in g's at each Trunnion		
Lifting - Cask Vertical	1.5	0	0
Cask Horizontal	0.75	1.30	0
Tilting[b]	0.75	0.75	0
Transfer	0.5	0.5	1
	Load in Kips at Each Trunnion[c]		
Lifting - Cask Vertical	337.5	0	0
Cask Horizontal	168.75	292.5	0
Tilting	168.75	168.75	0
Transfer	112.5	112.5	225

a - Load evenly split between one set of front and rear trunnions.

b - Maximum value from horizontal to vertical orientation.

c - Based on a cask weight of 225,000 lbs.

TABLE 3.2-5

ATTACHMENT LOADS ON CASK BODY APPLIED BY TRUNNIONS

Handling Operation	LOAD: Shear Force, Longitudinal $V_L=F_L$ (lb)	Shear Force, Circumferent. $V_C=F_T$ (lb)	Radial Force $P=P_t$ (lb)	Moments, Longitudinal M_L (in.-lb)	Moments, Circumferent. M_C (in.-lb)
Lifting:					
Cask Vertical	3.375E5	0	0	2.6E6	0
Cask Horizontal	2.925E5	1.69E5	0	2.25E6	1.3E6
Tilting	1.69E5	1.69E5	0	1.3E6	1.3E6
Transfer	1.125E5	1.125E5	2.25E5	5.54E5	5.54E5

Attachment loads acting on cask body are obtained as follows:

Radial Force: $P = P_T$

Circumferential Moment, M_C

$M_C = F_T (4.13 + 3.54) = 7.67F_T$ (Lifting/Tilting Front Trunnions)

$M_C = F_T (1.38 + 3.54) = 4.92F_T$ (Transfer/Tilting Rear Trunnions)

Longitudinal Moment, M_L

$M_L = 7.67F_L$ (Lifting/Tilting Front Trunnions)

or

$M_L = 4.92F_T$ (Transfer/Tilting Rear Trunnions)

Note: The maximum values in the table are used for the trunnions and the local effects on the cask body shell.

TABLE 3.2-6

BOLT LOADS

Loading	Total Bolt Load ($\times 10^6$ lb)
Cavity Pressurization	0.110
Fission Gas Release (100% major fire)	0.182
Gasket Seating	0.929
Handling	0.278
Differential Thermal Expansion (normal)	0.194
Subtotal	1.693

Preload = 1.79×10^6 lb > 1.693×10^6 lb; therefore the criteria is met.

	Max Load Per Bolt (lb)
Cask Drop - Tipping	19,640
Major Fire	10,640

TABLE 3.2-7

TEMPERATURE GRADIENTS IN THE CASK BODY USED FOR THE STRUCTURAL ANALYSIS

	LOCATION	MAX ΔT
1.	At junction between cylinder and bottom plate	25°F
2.	Axial gradient in cylinder	.5°F/in.
3.	Radial gradient across cylinder wall	27°F
4.	Radial gradient in bottom plate	10°F
5.	Gradient across thickness of bottom plate	25°F
6.	Gradient through thickness of inner portion of lid	15°F
7.	Gradient through thickness of outer portion of lid (lid flange)	10°F
8.	Radial gradient in lid	
	Center inner portion	6.5°F
	Outer portion (flange)	3.5°F

TABLE 3.2-8

STORAGE LOADING CONDITIONS

Normal

Pressure
Weight
Handling
Thermal variations (e.g. insolation, heat decay, rain, snow, ice, ambient)

Man-Made

Fuel cladding failure
Fire
Explosion
Cask drop
Cask tipping

Natural Phenomena

Earthquakes
Tornados
Hurricane
Flood
Tsunami
Seiches
Lightning

TABLE 3.2-9

PRIMARY SERVICE LOADS

Applied Load	Loading Condition
Internal Pressure	(1) and (2)
External Pressure	(3)
Distributed Loads	Weight Cask Body Contents Live Snow Ice Wind Flood (Includes Tsunami & Seiches) Seismic Handling Lifting Tilting Transfer
Attachment Loads	Handling Lifting Tilting Transfer
Bolt Loads	Preload for 250 psi Handling

(1) Cask designed for 250 psi internal pressure which envelopes all internal pressure effects.

(2) For normal conditions, the fission gas release should be less than 10%, however, for analysis purposes 100% release is assumed.

(3) Cask designed for 25 psi external pressure which envelopes all external pressure effects.

TABLE 3.2-10

LEVEL A SERVICE LOADS

Applied Load	Loading Condition
Internal Pressure	(1) and (2)
External Pressure	(3)
Distributed Loads	Weight Cask Body Contents Live Snow Ice Wind Handling Lifting Tilting Transfer
Bolt Loads	Preload for 250 psi Handling Thermal Effects
Attachment Loads	Handling Lifting Transfer Tilting
Thermal Loads	Decay Heat Solar Insolation Cold Rain on Hot Cask

(1) Cask designed for 250 psi internal pressure which envelopes all internal pressure effects.

(2) For normal conditions, the fission gas release should be less than 10%, however, for analysis purposes 100% release is assumed.

(3) Cask designed for 25 psi external pressure which envelopes all external pressure effects.

TABLE 3.2-11

LEVEL B SERVICE LOADS

Load	Loading Condition
Internal Pressure	(1) and (2)
Distributed Loads	Weight Live Handling
Thermal	Decay Heat Solar Insolation
Bolt Load	Preload for 250 psi Handling Thermal Effects
Attachment Loads	Handling Lifting Tilting Transfer

(1) Cask designed for 250 psi internal pressure which envelopes all internal pressure effects.

(2) For normal conditions, the fission gas release should be less than 10%, however, for analysis purposes 100% release is assumed.

TABLE 3.2-12

LEVEL C SERVICE LOADS

Load	Loading Condition
Internal Pressure	(1) and (2)
External Pressure	(3)
Distributed Loads	Wind (Tornado) Weight
Bolt Loads	Preload for 250 psi Thermal Effect
Thermal Loads	Minor Fire Decay Heat Solar Insolation

(1) Cask designed for 250 psi internal pressure which envelopes all internal pressure effects.

(2) For normal conditions, the fission gas release should be less than 10%, however, for analysis purposes 100% release is assumed.

(3) Cask designed for 25 psi external pressure which envelopes all external pressure effects.

TABLE 3.2-13
LEVEL D SERVICE LOADS

Load	Cause
Internal Pressure	(1) and (2)
External Pressure	(3)
Inertia g Loads	Cask Drop Cask Tipping
Bolt Loads	Preload for 250 psi Differential Thermal Expansion due to Fire Drop/Tipping Accidents
Local Loads	Tornado Wind Driven Missiles
Thermal Loads	Fire Beginning of Life Unloading
Distributed Loads	Weight Tornado Seismic

(1) Cask designed for 250 psi internal pressure which envelopes all internal pressure effects.

(2) For normal conditions, the fission gas release should be less than 10%, however, for analysis purposes 100% release is assumed.

(3) Cask designed for 25 psi external pressure which envelopes all external pressure effects.

(4) Explosions close to the cask are unexpected. Explosions at a significant distance from the cask would have a negligible effect and certainly be less than the equivalent external pressure which acts during drop and tipping accidents.

TABLE 3.2-14

LOAD COMBINATIONS ON VESSEL

Loading Combination Designation \ Applied Load	Pressure (1) Internal (2) Cavity Press.	Fission Gas Release	Minor Fire	Major Fire	Beginning of ... Unloading	Explosion	Pressure External: Fuel Loading or Unloading	Inland Tsunami Seiches		Distributed Load: Weight	Wind or Water	Seismic	(4) Handling	Static Inertial Loads: Tornado Missiles	Cask Drop	Cask Tipping
Primary Service																
P1	-	-	-	-	-	-	*	*		*	*	*	* -			
P2	*	-	-		-		-	-		*	*	*	* *			
P3	*	*	*	*	*		-	-		*	*	*	- -			
Level A																
A1	*	-	-	-						*	*		* *			
A2	*	*	*	*			-	-		*		-	- -			
A3	-	-	-	-	-		*	*		*		-	* *			
Level B																
B1	*	*	-	-	-	-	-	-		*	*	*	* *			
B2	*	*	-	-	-	-	-	-		*	*	*	- -			
Level C																
C1	*	*	-	*	*	-	-	-		*	*	-	- -			
C2	*	*	-	-	-	-	*	*		*	*	-	- -			
Level D																
D1	-	*	*	*	*	-	-	-		*	-	-		-	-	-
D2	*	*	*	*	*	-	-	-		-	-	*		-	-	-
D3	*	*	*	*	*	-	-	-		-	-	-			*	-
D4	*	*	*	*	*	-	-	-		-	-	-			-	*
D5	*	*	*	*	*	-	-	*		-	-	-			-	-
D6	*	*	*	*	*	*	-	-		*	-	-			-	-
D7	*	*	*	*	*	-	-	-		*	*	-		*	-	-

TABLE 3.2-14
(continued)

Applied Loading Load Combination Designation	THERMAL (5)										
	Decay Heat	Solar Load	Fuel Loading	Beginning of Life Unloading	Ambient Temperature Variations	Snow, Ice Wind, Solar	Buried Cask	Minor Fire	Major Fire	Explosion	Earthquake
Primary Service											
P1											
P2											
P3											
Level A											
A1	x	x				x					
A2	x	x				-					
A3	-	-				-					
Level B											
B1	x	x									
B2	x	x									
Level C											
C1	x	x						x			
C2	x	x						-			
Level D											
D1							-		x	-	-
D2							-		-	-	x
D3							-		-	-	-
D4							-		-	-	-
D5							x		-	-	-
D6							-		-	x	-
D7							-		-	-	-

TABLE 3.2-14
(continued)

Notes:

(1) Bolt preload acts simultaneously with internal or external pressure.

(2) All internal pressure effects are covered because the cask is evaluated for an internal pressure of 250 psi. It should be noted that the handling loads do not act at the same time that the internal pressure is at its maximum value or at the rated value of 250 psi. The handling loads would act with initial cavity pressurization but this is a less critical combination.

(3) This column also includes the condition of a buried cask.

(4) Handling results in both distributed loads on the entire cask body and local loads at the trunnion attachments. herefore, there are two columns for x's for some load combinations.

(5) The thermal effects of fuel loading through minor fire are negligible compared to the effects of decay heat and solar load. One exception is the case of a cold rain on a hot cask which is evaluated.

FIGURE 3.2-1a
DISTRIBUTED LOADS DUE TO
EARTHQUAKE, WIND & WATER.
CASK IN VERTICAL STORAGE POSITION

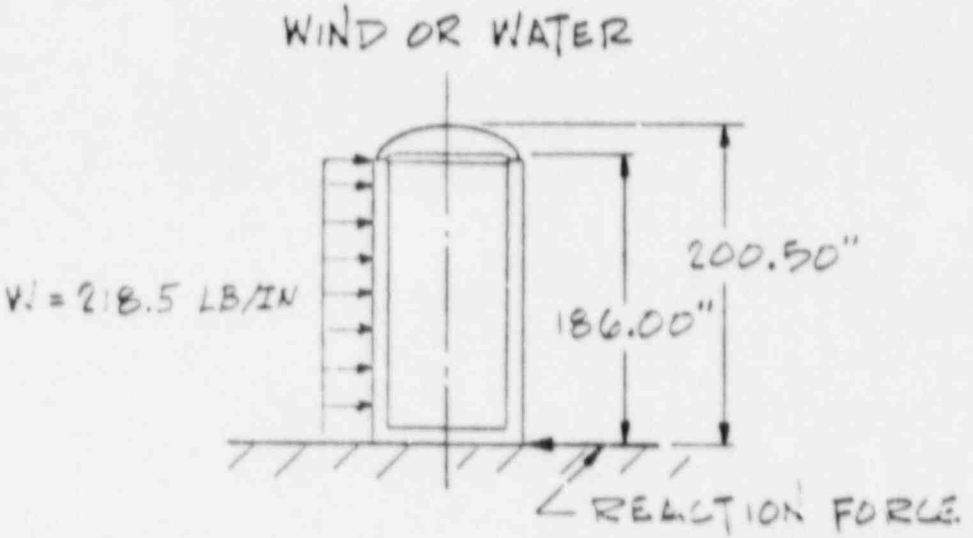

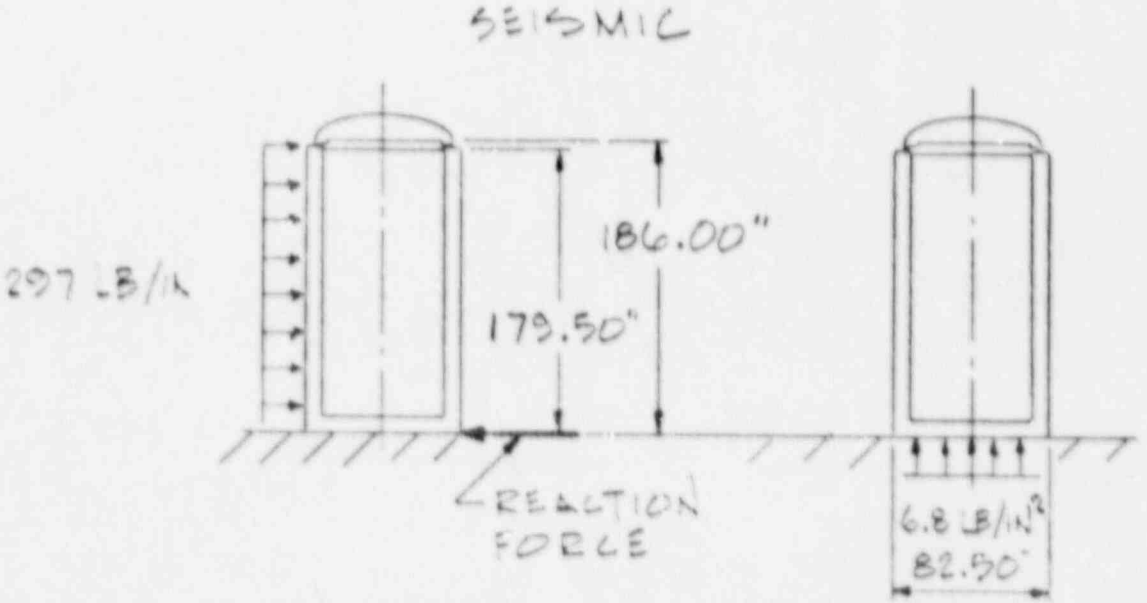

FIGURE 3.2-16
DISTRIBUTED LOADS DUE TO
EARTHQUAKE, WIND & WATER
CASK IN HORIZONTAL STORAGE POSITION

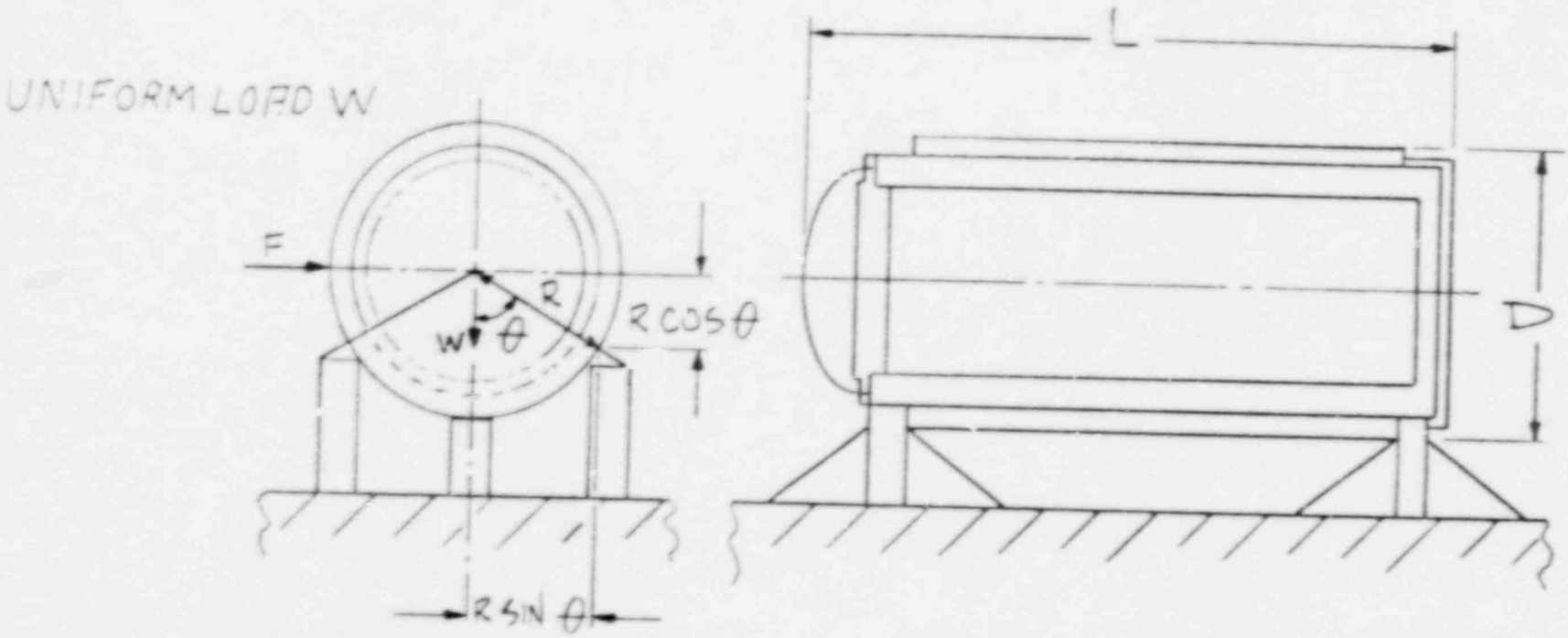

FOR STABILITY: FR COS θ < WR SIN θ WHERE
F = DRAG FORCE, W = 214000 LBS (WEIGHT OF CASK)

FIGURE 3.2-1C

TORNADO MISSILE IMPACT ON CASK IN VERTICAL ORIENTATION

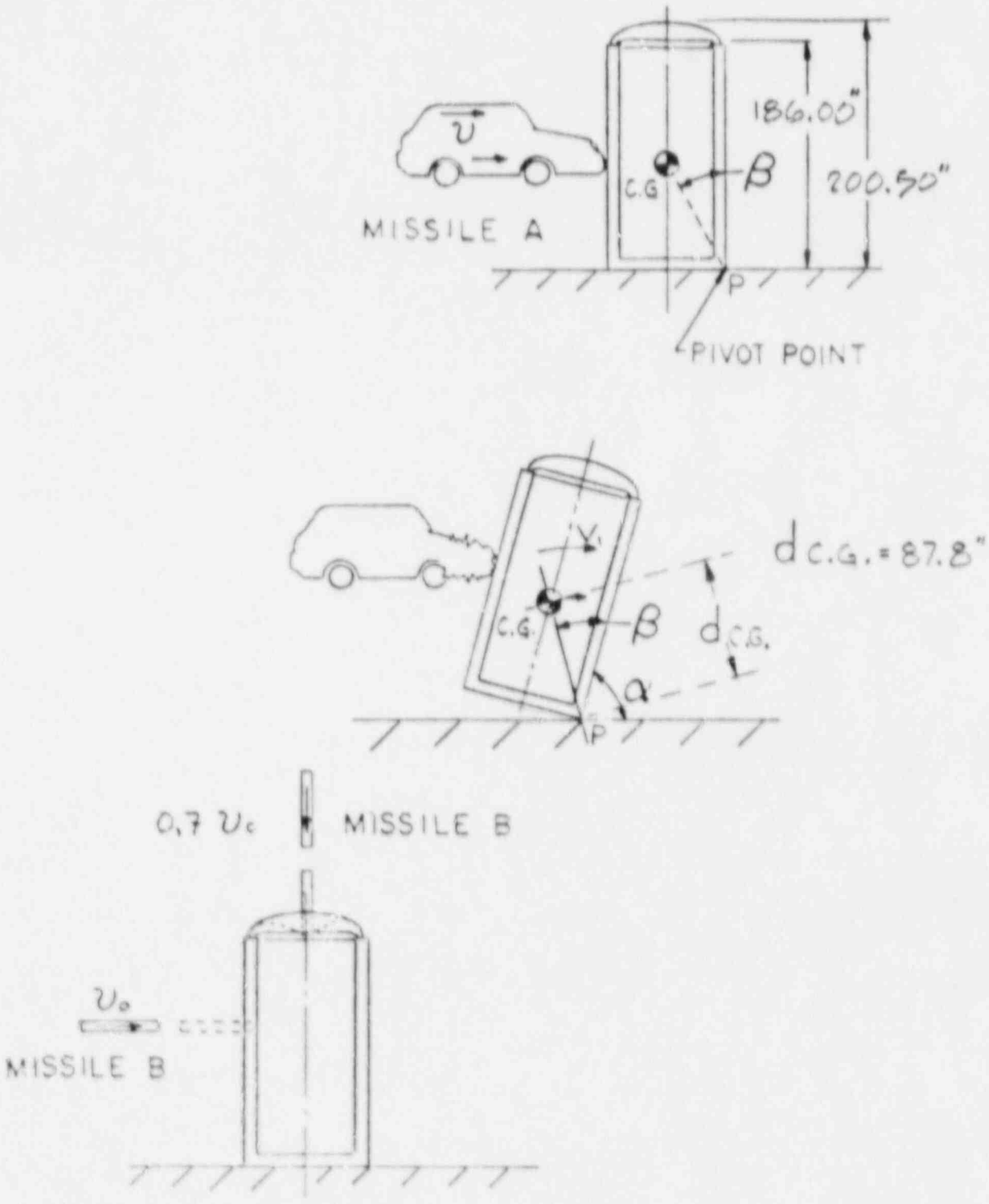

FIGURE 3.2-1d

TORNADO MISSILE IMPACT ON CASK IN HORIZONTAL POSITION

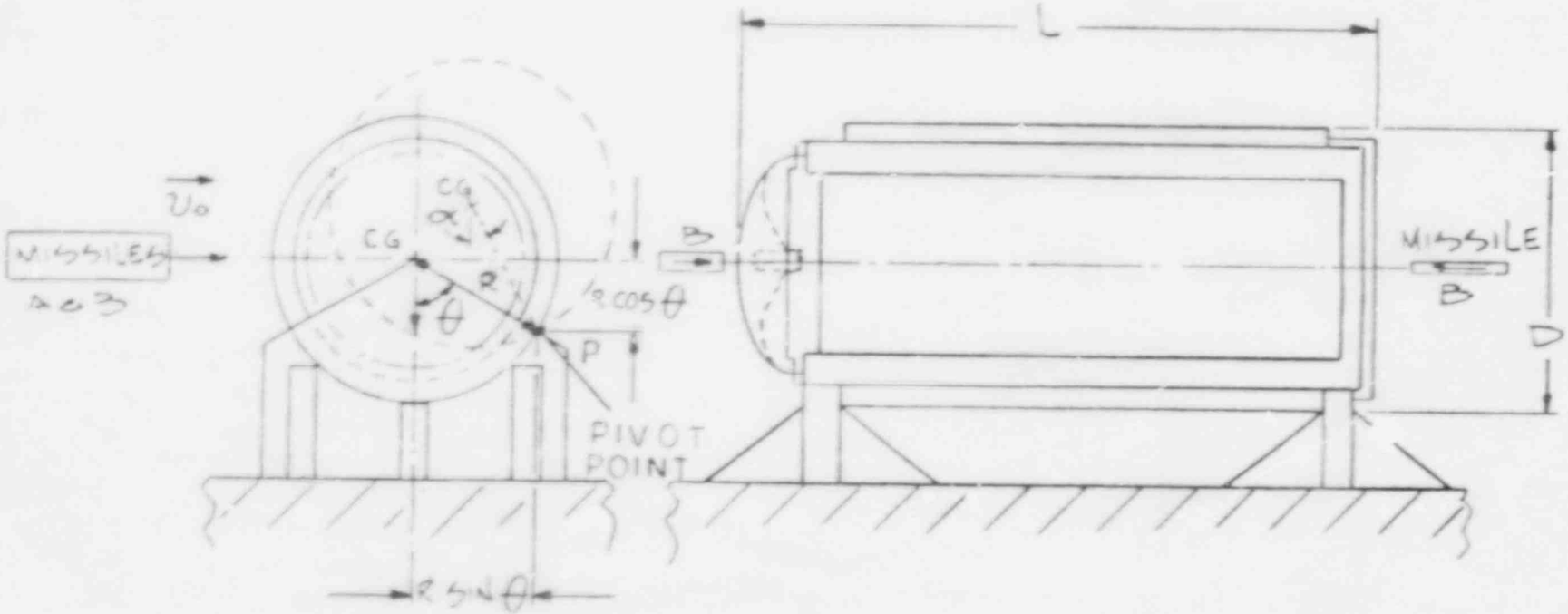

FOR STABILITY: $FR\cos\theta < WR\sin\theta$.

3.2-63

FIGURE 3.2-2

HANDLING LOADS APPLIED TO TRUNNIONS FOR A VERTICAL LIFT-CASK VERTICAL

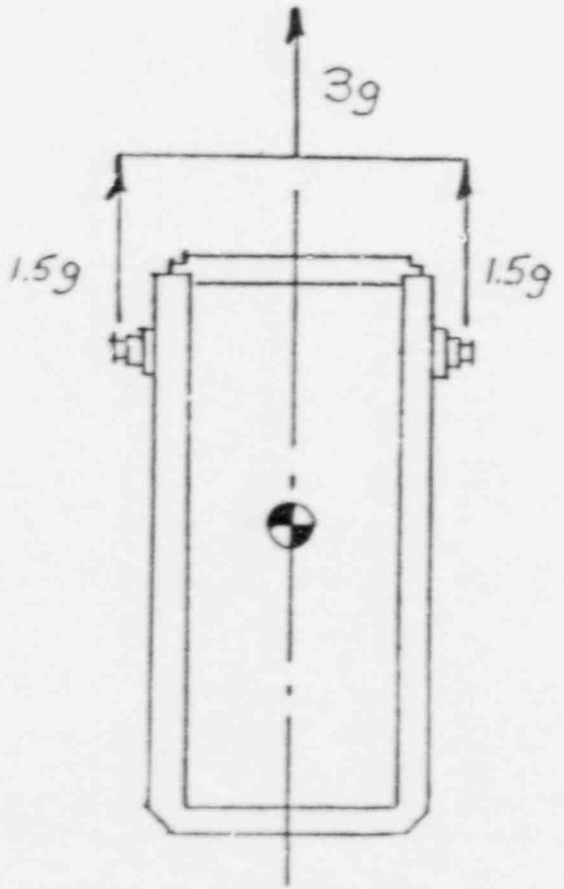

3g LOAD APPLIED TO OUTER SHOULDER AT ONE SET OF TRUNNIONS. LOAD PER TRUNNION IS 1.5g. THIS CAUSES A LONGITUDINAL (ie AXIAL) MOMENT ON THE CASK BODY

FIGURE 3.2-3

HANDLING LOADS APPLIED TO TRUNNIONS FOR A VERTICAL LIFT - CASK HORIZONTAL

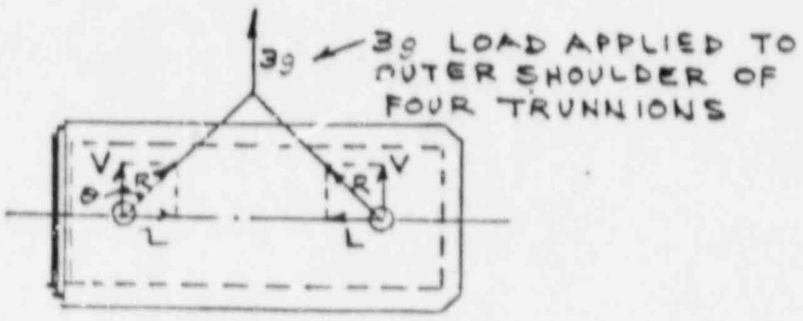

MAXIMUM VERTICAL LOAD PER TRUNNION	V = 0.75 g
FOR θ = 30°	R = 0.87 g
	L = 0.43 g
FOR θ = 45°	R = 1.06 g
	L = 0.75 g
FOR θ = 60°	R = 1.50 g
	L = 1.30 g

MAXIMUM ANGLE θ LIMITED TO 60°

MAXIMUM LONGITUDINAL LOAD PER TRUNNION IS 1.3g WHICH CAUSES A LONGITUDINAL MOMENT ON THE CASK BODY.

MAXIMUM VERTICAL LOAD PER TRUNNION IS 0.75g WHICH CAUSES A CIRCUMFERENTIAL MOMENT ON THE CASK BODY

FIGURE 3.2-4

HANDLING LOADS APPLIED TO TRUNNIONS
FOR TILTING OPERATION

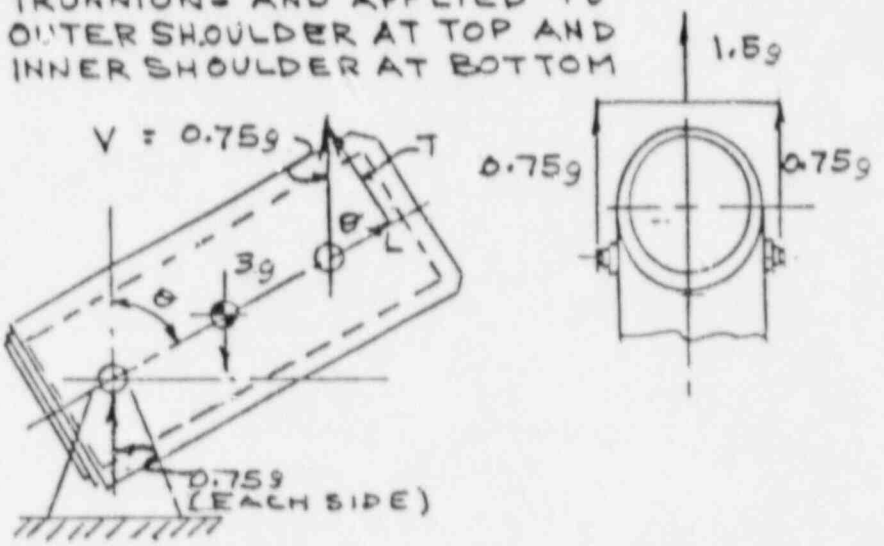

VERTICAL LOAD (ALSO RESULTANT)	V = 0.75g
FOR θ = 60°,	T = 0.65g
	L = 0.38g
FOR θ = 45°,	T = 0.50g
	L = 0.50g
FOR θ = 30°,	T = 0.38g
	L = 0.65g
FOR θ = 0°,	T = 0
	L = 0.75g

MAXIMUM LONGITUDINAL LOAD PER TRUNNION IS 0.75g (i.e. JUST WHEN CASK IS VERTICAL) WHICH CAUSES A LONGITUDINAL MOMENT ON CASK BODY. MAXIMUM TANGENTIAL LOAD PER TRUNNION IS 0.75g (i.e. WHEN CASK IS HORIZONTAL) WHICH CAUSES A CIRCUMFERENTIAL MOMENT ON CASK BODY.

FIGURE 3.2-5

HANDLING LOADS APPLIED TO TRUNNIONS
DUE TO TRANSFER OPERATIONS

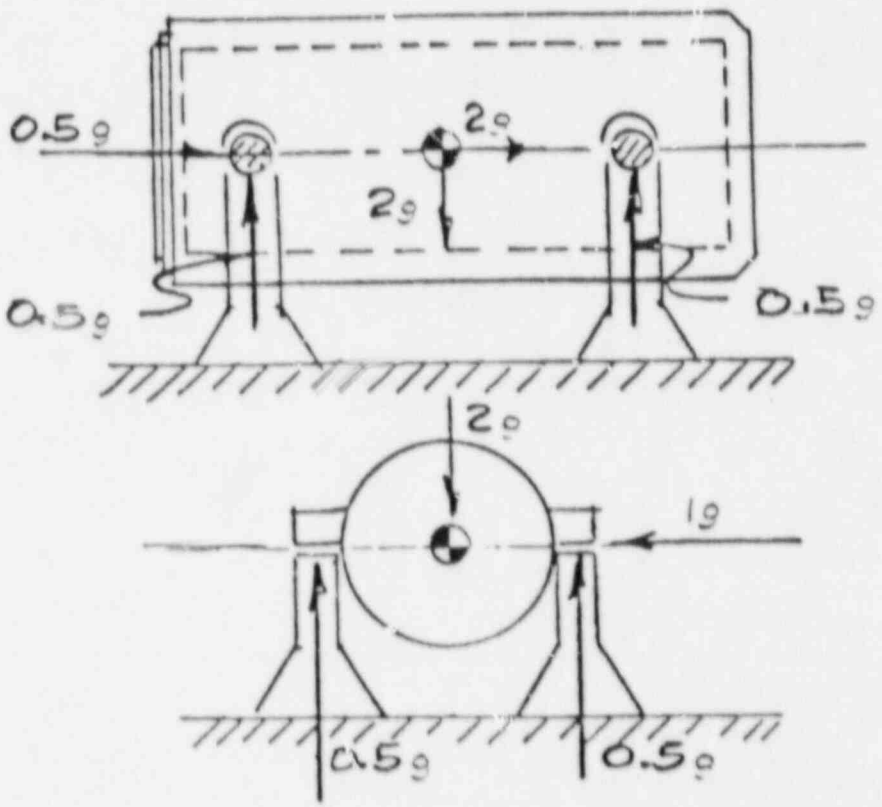

2 g VERTICAL LOAD DISTRIBUTED ON FOUR TRUNNIONS (i.e. 0.5 g PER TRUNNION) AND APPLIED TO INNER SHOULDER. THIS CAUSES A CIRCUMFERENTIAL MOMENT ON CASK BODY.

2 g LONGITUDINAL LOAD DISTRIBUTED ON FOUR TRUNNIONS (i.e. 0.5 g PER TRUNNION) APPLIED TO INNER SHOULDER. THIS CAUSES A LONGITUDINAL MOMENT ON CASK BODY.

2 g LATERAL LOAD DISTRIBUTED ON TWO TRUNNIONS (i.e. 1.0 g PER TRUNNION). THIS CAUSES A RADIAL LOAD ON CASK BODY.

FIGURE 3.2-6
APPLICATION OF DISTRIBUTED LOADS ON CASK DUE TO
HANDLING OPERATIONS

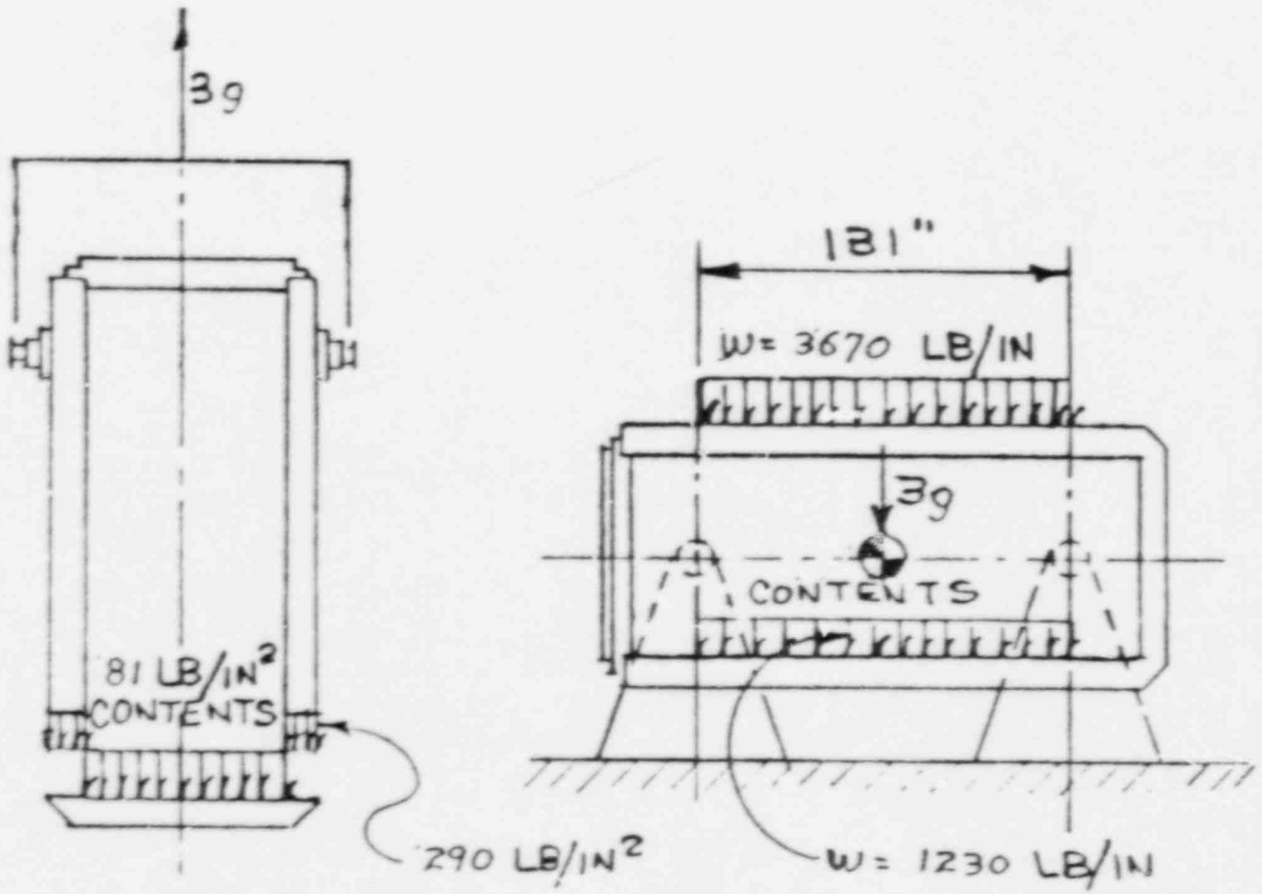

FIGURE 3.2-7
HANDLING LOADS APPLIED TO TRUNNIONS

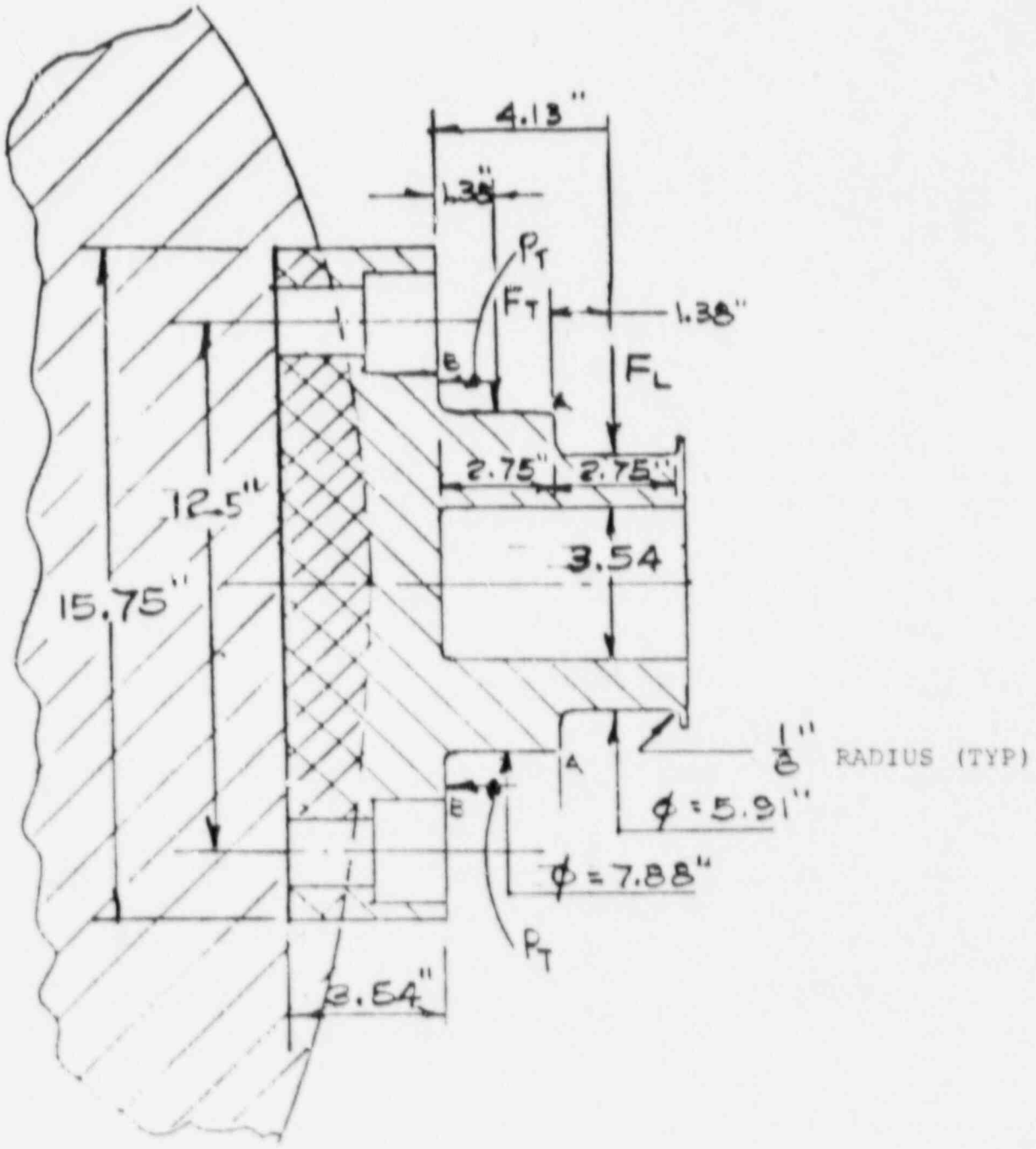

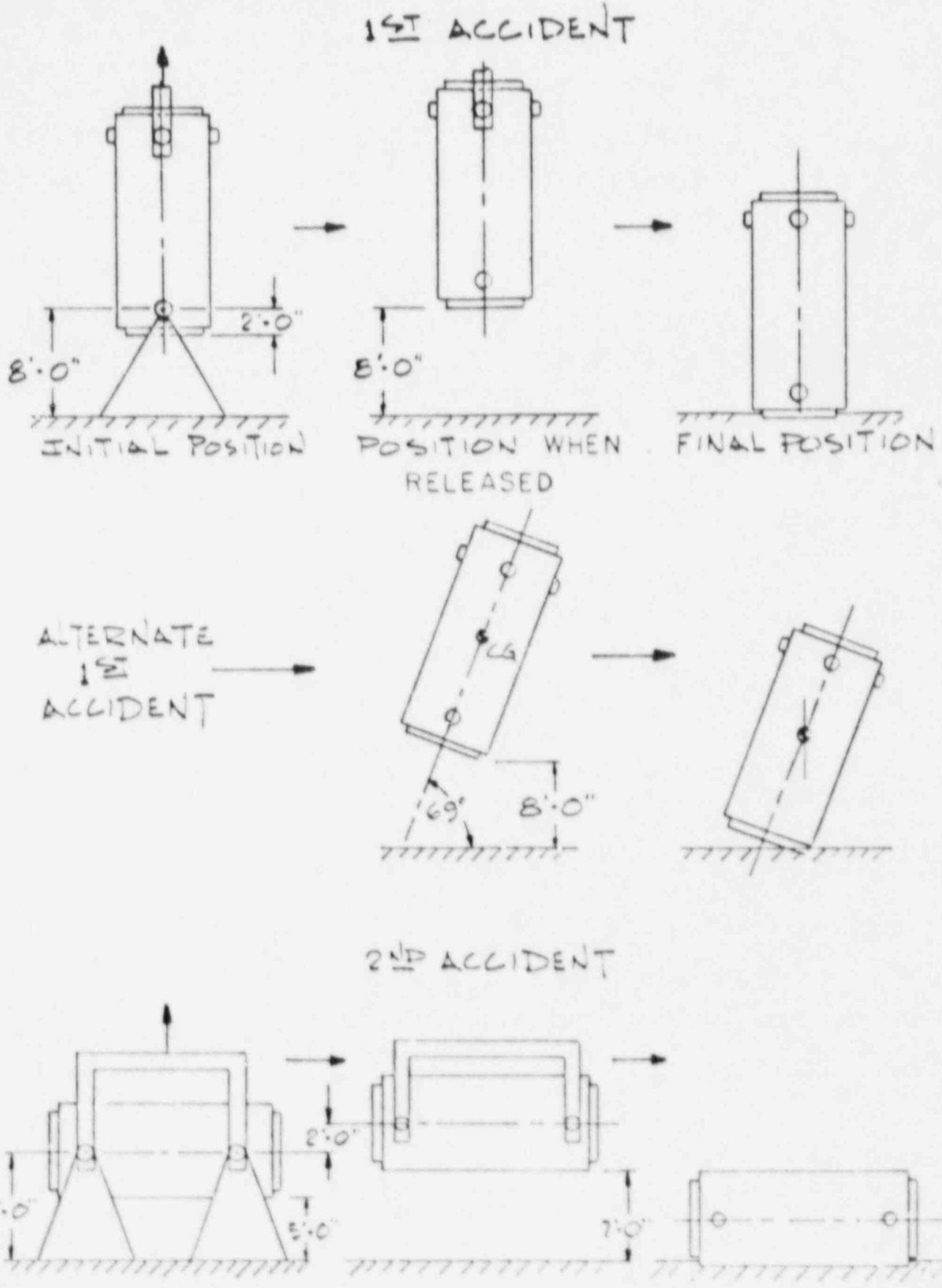

FIGURE 3.2-8
CASK DROP ACCIDENTS CONSIDERED

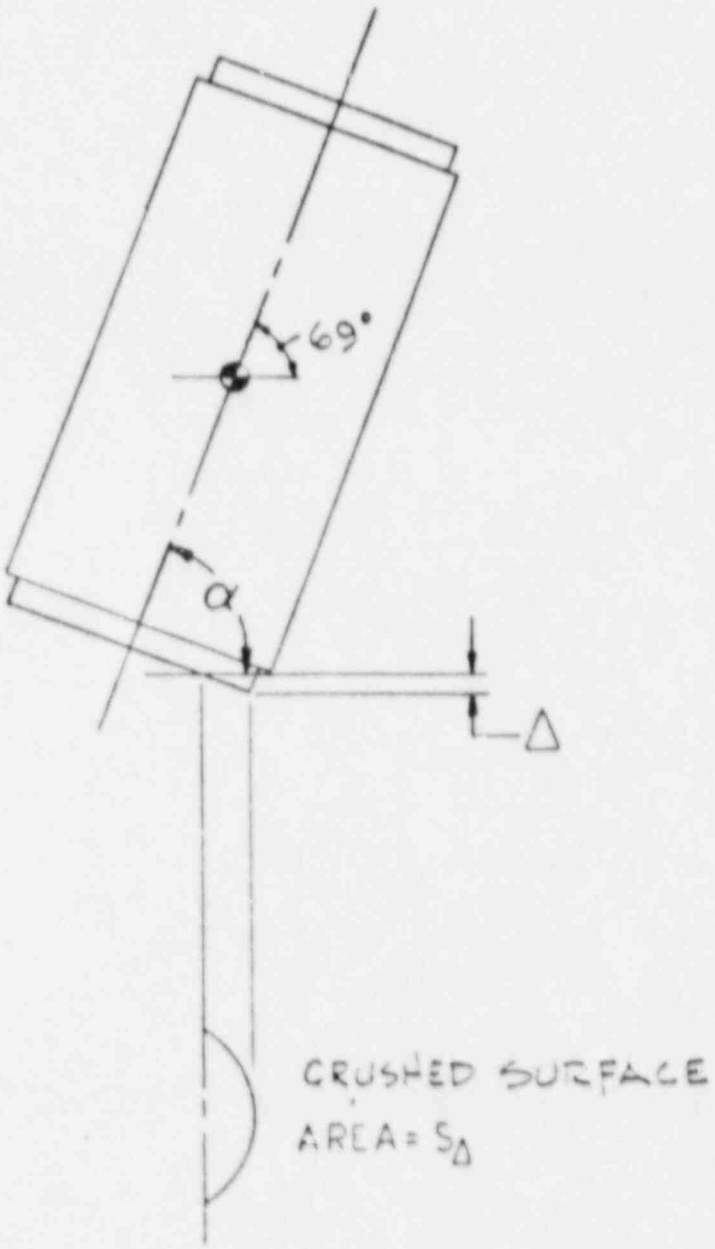

FIGURE 3.2-9
CORNER IMPACT

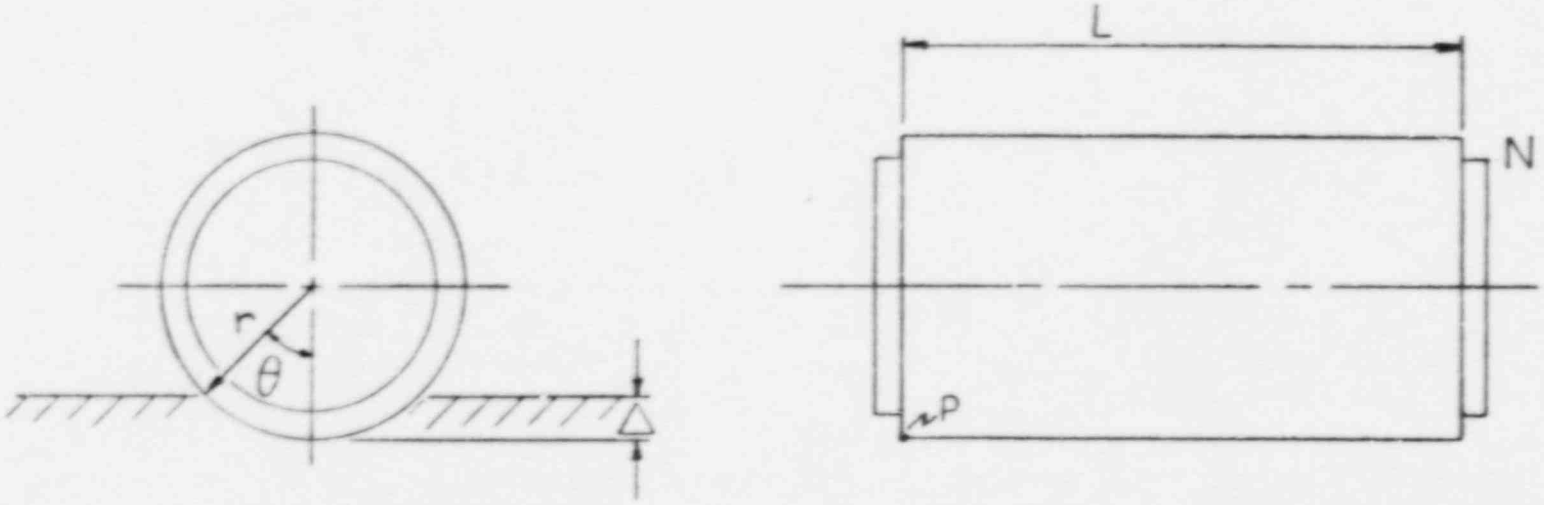

FIGURE 3.2-10
HORIZONTAL IMPACT

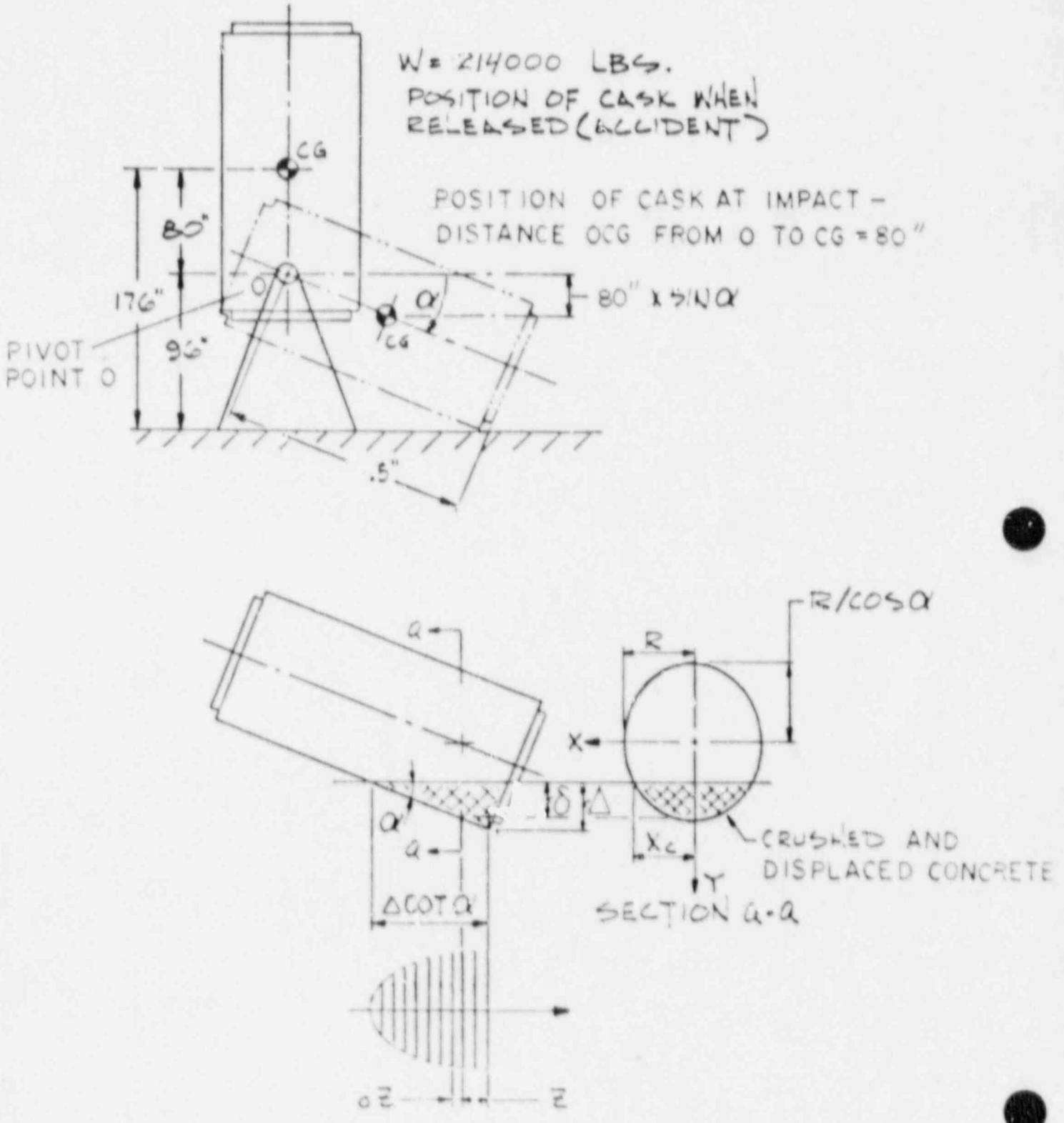

FIGURE 3.2-11

CASK TIPPING ACCIDENT - ROTATION ABOUT TRUNNIONS

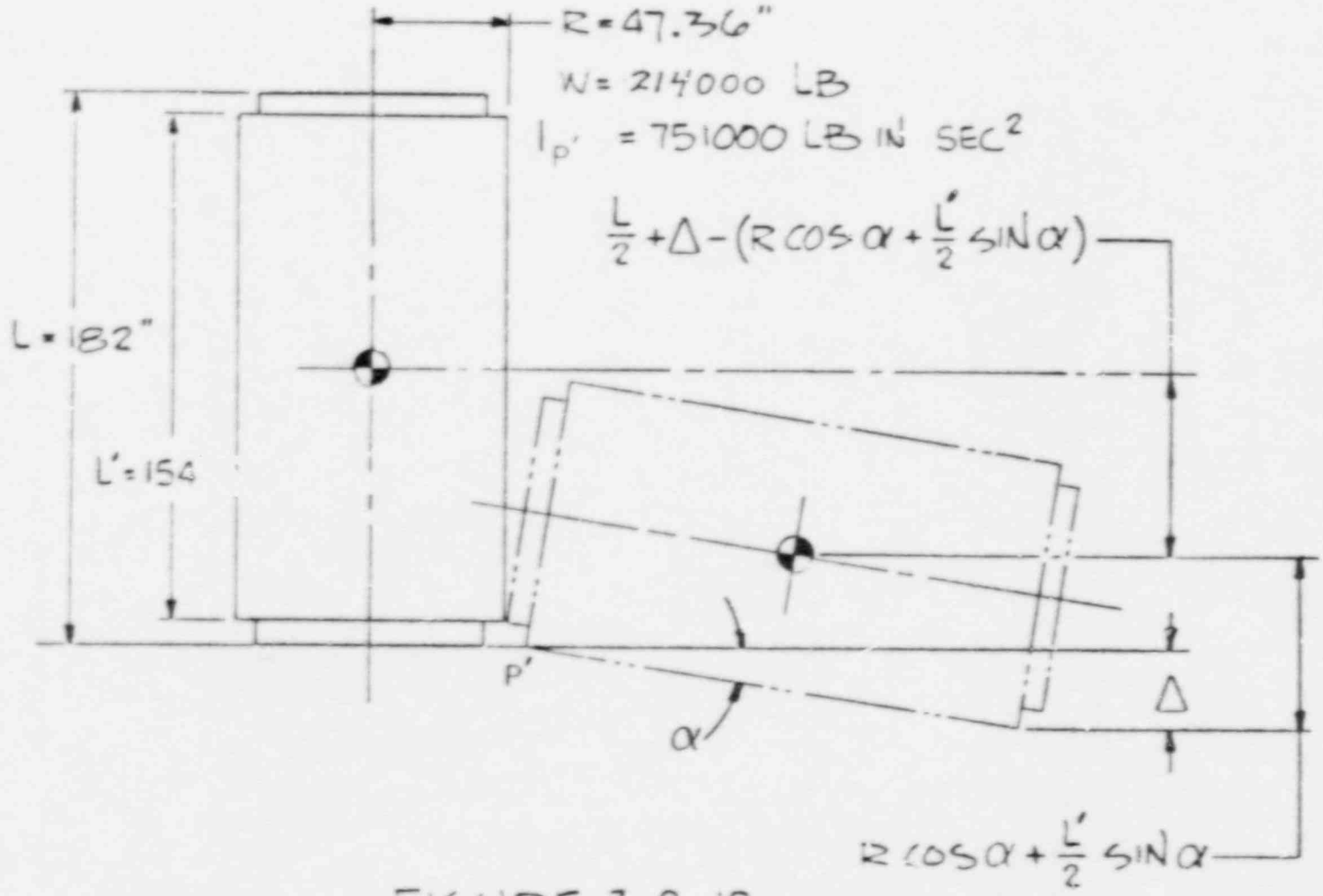

FIGURE 3.2-12

CASK TIPPING ACCIDENT - ROTATION ABOUT BASE

References For Section 3.2

1. "Licensing Requirements for the Storage of Spent Fuel in an Independent Spent Fuel Storage Installation," 10CFR Part 72, Rules and Regulations, Title 10, Chapter 1, Code of Federal Regulations - Energy, U.S. Nuclear Regulatory Commission, Washington D.C., Sept. 1982.

2. "Rules For Construction Of Nuclear Power Plant Components," ASME Boiler And Pressure Vessel Code, Section III, Division 1 - Subsection NB, The American Society of Mechanical Engineers, New York.

3. "Design Basis Tornado For Nuclear Power Plants," Regulatory Guide 1.76, U.S. Atomic Energy Commission, Washington D.C., April 1974.

4. "Standard Review Plan, Missiles Generated by Natural Phenomena", Section 3.5.1.4, NRC NUREG-0800, Rev 2, July 1981.

5. "Wind Forces on Structures: Forces on Enclosed Structures.", T. W. Singell, ASCE Structural Journal, July 1958.

6. Burmeister and Marks, Standard Handbook for Mechanical Engineers, Seventh Edition.

7. "Combining Modal Responses and Spatial Components in Seismic Response Analysis", Regulatory Guide 1.92, U.S. Nuclear Regulatory Commission, Feb 1976.

8. "American National Standard for Special Lifting Devices for Shipping Containers Weighing 10,000 Pounds (4500 kg) or More for Nuclear Materials.", ANSI N14.6, American National Standards Institute, New York.

9. "Packaging And Transportation Of Radioactive Material," 10CFR Part 71, Rules and Regulations, Title 10, Chapter 1, Code of Federal Regulations - Energy, U.S. Nuclear Regulatory Commission, Washington D.C., Jan 1987.

10. Timoshenko, S., and Woinowsky-Kreiger, S., Theory of Plates and Shells, McGraw Hill Book Co., New York, 1959.

11. Zeevaert, L., Foundation Engineering, Van Nostrand Reinhold, 1983.

3.3 SAFETY PROTECTION SYSTEMS

3.3.1 General

The TN-24 dry storage cask is designed to provide storage of spent fuel for at least twenty years. The cask cavity pressure is always above ambient during the storage period as a precaution against the in-leakage of air which might be harmful to the fuel. Since the containment vessel consists of a thick-walled forged steel cylinder with an integrally-welded forged bottom closure, the cavity gas can escape only through the lid closure system. In order to ensure cask leak tightness, two safety systems are employed. A double barrier system for all potential lid leakage paths consisting of covers with multiple seals is utilized. Additionally, pressurization of monitored seal interspaces provides a continuous positive inward and outward pressure gradient which guards against a release of the cavity gas to the environment and the admission of air to the cavity.

3.3.2 Protection By Multiple Confinement Barriers and Systems

3.3.2.1 Confinement Barriers and Systems

A combined cover-seal pressure monitoring system (Figure 3.3-1) always meets or exceeds the requirement of a double barrier closure which guarantees tight, permanent containment. There are two lid penetrations, one for a drain pipe and one for venting and pressurization. When the cask is placed in storage, a pressure greater than that of the cavity is set up in the gaps (interspaces) between the double metallic seals of the lid and the lid penetrations. A decrease in the pressure of the monitoring system to below 3 atm would be signalled by pressure transducers located in the overpressure tank which is located on top of the cask lid (Figure 3.3-1). Three transducers are provided to ensure measurement redundancy. The system is pressurized through a fill valve mounted on the overpressure tank.

Connections to the overpressure tank are welded or Cajon VCR fittings.[1] A quick connect Hansen coupling with a NUPRO diaphragm valve is used to fill the tank.

The Helicoflex metallic face seals of the lid and lid penetrations possess long-term stability and have high corrosion resistance over the entire storage period. These high performance seals are comprised of two metal linings formed around a helically-wound spring. The sealing principle is based on plastically deforming the seal's outer lining. Permanent contact of the lining against the sealing surface is ensured by the outward force exerted by the helically-wound spring. Additionally, all metallic seal seating areas are stainless steel overlay for improved surface control. The overlay technique has been used for Transnuclear's transport casks.

For protection against the environment, a torispherical protective cover equipped with an elastomer seal is provided above the lid. In the unlikely event that unacceptable leakage was detected in the monitoring system, a containment cover (described in Section 4.5) could replace the protective cover. The space between this containment cover and the lid could be used as a pressure-monitored gas barrier. The option to weld the containment cover to the cask body is also available, if necessary.

The lid and cover seals described above are contained in grooves. A high level of sealing over the storage period is assured by utilizing seals in a deformation-controlled design. The deformation of the seals is constant since bolt loads assure that the mating surfaces remain in contact. The seal deformation is set by its original diameter and the depth of the groove.

Cajon VCR fittings, NUPRO diaphram valves and Helicoflex metallic seals are all capable of limiting leak rates to less than 1×10^{-7} atm-cc/sec of helium.

3.3.2.2 Analysis of Cask Pressures and Leakage Rates

The cask cavity's maximum operating pressure is 2.2 atm. This pressure will assure an end of storage (20 years) pressure of 1.1 atm based on a decay heat load of 0.3 kw/assembly and a minimum ambient temperature of -20°F. The maximum operating pressure of 2.2 atm corresponds to the maximum decay heat load of 1 kw/assy, insolation, a 115°F ambient temperature and the storage of the casks in a 2 x 10 array.

During normal storage, pressure variations due to changing ambient conditions will be small. However, fuel clad failure could result in an increase in cavity pressure due to free gas release of the fuel rods. Based on data from Ref. 2, the Westinghouse 15x15 assembly contains the most free gas, 3.72 m^3 at STP. The TN-24 cask has a cavity free volume of 5.49 m^3. A 10% release of fission gas would cause an increase in cavity pressure of about 1.9 psi at an average cavity gas temperature of 480°F (Table 5.1-3).

The pressure during a major fire is calculated assuming a 100% fuel failure. In Section 5.1.3.6, the maximum cavity gas temperature is calculated to be no more than 518°F for a cask stored in an array. This results in a maximum cavity pressure of 3.6 atm (53 psia).

The monitoring system's initial operating pressure is set at 5.8 atm. Over the storage period, the monitoring system's pressure decreases as a result of leakage from the system and as a result of temperature reduction of the gas in the system. Since the level of permeation through the containment vessel is negligible and leakage past the higher pressure of the monitoring system is physically impossible, a decrease in cavity pressure during the storage period occurs only as a result of a reduction in the cavity gas temperature with time. As long as the cavity pressure is greater than ambient pressure and the pressure in the monitoring system is greater than that of the cavity, no in-leakage of air nor out-leakage of cavity gas is possible.

The calculations which follow define the monitoring system helium test leakage rate which ensures that no cavity gas can be released to the environment nor air admitted to the casks for the twenty-year storage period. All seals are considered collectively in the analysis as the monitoring system pressure boundary.

The instantaneous leakage L from the monitoring system is equal to the leakage rate L_x during an infinitely small time period dt and L is also equal to the system volume V times the change in system pressure dp.

$$L = L_x dt = V dp$$
$$dt = V dp / L_x$$

From ANSI N14.5[3]:

$$L_x = L_y N_y (Pu^2 - Pd^2) x / [N_x (Pu^2 - Pd^2) y]$$

L_x = actual leakage rate of helium at the monitoring system temperature (atm-cc/sec)

L_y = measured leakage rate of helium test gas at 77°F (atm cc/sec)

N_x = fluid viscosity of helium at the monitoring system temperature (cp)

N_y = fluid viscosity of helium at 77°F = 0.0223 cp

Pu_x = actual upstream pressure (atm)

Pd_x = actual downstream pressure = 1.0 atm

Pu_y = test upstream pressure = 1.0 atm

Pd_y = test downstream pressure = 0.0 atm

Therefore,

$$dt = Vdp \Big/ \frac{L_y N_y (Pu^2 - Pd^2) x}{N_x (Pu^2 - Pd^2) y}$$

and

$$t = \int_{PE}^{PB} Vdp \Big/ \frac{L_y N_y (Pu^2 - Pd^2) x}{N_x (Pu^2 - Pd^2) y}$$

PB = monitoring system pressure at the beginning of the storage period = 5.8 atm

PE = monitoring system pressure at the end of the storage period (atm)

V = monitoring system volume (cc)

The integration of this equation accounts for the change in the monitoring system leakage rate which occurs during the storage period because of the change in the monitoring system pressure. Although the cask cavity pressure is initially 2.2 atm and remains above ambient during the storage period, it is conservatively assumed in this analysis that both the inner and outer seals of the monitoring system are subject to a constant 1.0 atm downstream pressure.

Since V, L_y, N_y, N_x, Pd_x, and $(Pu^2 - Pd^2)y$ are constant,

$$t = A \int_{PE}^{PB} dp/(Pu^2 - Pd^2)_x$$

where $A = V N_x(Pu^2 - Pd^2)y/(L_y N_y)$

Performing the integration yields:

$$t = [A/2Pdx)]\ln [(Pu - Pd)_x/(Pu + Pd)_x] \Big|_{P_E}^{P_B}$$

Expressing P_E as a function of t by rearranging and simplifying the above equation,

$$P_E = Pd_x [B/\exp (2t\ Pd_x/A) + 1]/[1 - B/\exp(2t\ Pd_x/A)]$$

where $B = (P_B - Pd_x)/(P_B + Pd_x)$

Since this equation only accounts for the monitoring system pressure loss due to leakage, a correction of pressure based on a decrease in system gas temperature was employed at the end of each three month time step at which the relation was evaluated. In order to ensure that the monitoring system pressure is simultaneously greater than the ambient and the cavity gas pressures, both the monitoring system gas and the cavity gas temperatures were established as a function of time. The cavity gas and the monitoring system gas temperatures were calculated for both the beginning and end of storage conditions and they were assumed to decrease linearly during the storage period. The end of storage condition for this calculation was conservatively assumed to be 0.3 kw/assembly and an ambient temperature of 115°F. It was determined that the cavity pressure would decrease from an initial value of 2.2 atm to 1.68 atm in 20 years due to an average gas temperature reduction. The viscosity of the monitoring system gas was also corrected for temperature change for each successive time increment evaluated.

The determination of the maximum allowable helium test leakage rate is graphically depicted in Figure 3.3-2. According to this figure, the cavity pressure of 1.68 atm after twenty years is equivalent to the

monitoring system pressure after twenty years when the helium test leakage rate is 1.1×10^{-5} atm cc/sec. In Figure 3.3-3, the change in both the monitoring system gas and the cavity gas pressures are shown as a function of time.

3.3.3 Protection by Equipment and Instrumentation

3.3.3.1 Equipment

The metallic seals utilized in the Safety Protection System are desribed in Section 3.3.2.1.

3.3.3.2 Instrumentation

The only safety-related instrumentation that is part of the cask are the pressure transducers which provide a continuous monitoring signal of the pressure in the seal interspaces. Since the pressure is higher in these interspaces than in the cask cavity, the transducers would provide an indication of seal failure before any release occurs. Three pressure tranducers are provided for redundancy.

3.3.4 Nuclear Criticality Safety

3.3.4.1 Control Methods for Prevention of Criticality

The design criterion for criticality is that the effective neutron multiplication factor, k_{eff}, including statistical uncertainties, shall be less than 0.95 for all postulated arrangements of fuel within the cask under all conditions.

The control methods used to prevent criticality are:

(1) Incorporation of neutron absorbing material (boron) in the basket material

(2) Incorporation of gaps in the basket to separate assemblies and to act as neutron traps when the cask is filled with water, as it may be at the time of loading.

The amount of boron in the basket and the gap width are selected to assure an ample margin of safety against criticality under the condition of cask flooding. The methods of criticality control are in keeping with the requirements of 10CFR72.73[11].

Criticality analysis is performed using the KENO-V.a[4] Monte Carlo code along with data prepared using the NITAWL[5] code and the SCALE 27-group cross section library. These codes and cross section library are part of the SCALE[6] system prepared by Oak Ridge National Laboratory for the U.S. Nuclear Regulatory Commission Office of Nuclear Regulatory Research. They are widely used for criticality analysis of shipping casks, fuel storage pools and storage casks. Benchmark problems are run to verify the codes, methodology and cross section library.

In the criticality calculation, fuel assembly, basket, and cask wall geometries are modeled explicitly. Within each assembly, each fuel pin and each guide tube is represented. Materials are not homogenized. The fuel assembly analyzed is the Westinghouse 17x17 OFA (optimized fuel assembly) with 3.7% enriched fuel. This fuel assembly design is conservative (yields higher k_{eff}) with respect to similar analyses using a 14x14 or a 15x15 design[2]. The analysis uses fresh fuel composition and a fuel length of 2000 cm (compared to the typical active length of 366 cm).

Subcriticality is established for the case of a cask fully flooded with water and surrounded by a water reflector. The geometric model used is shown in Figure 3.3-4, and the material compositions used in the model are listed in Table 3.3-1. The gap in the eight outside compartments was not explicitly modeled. However, the boron stainless steel plate thickness was reduced by 0.1 cm and the outside layer of copper neglected. Varying the water density in calculations for similar casks has verified that optimum moderation (maximum k_{eff}) occurs with full density water. Calculations have also verified that surrounding the model with a neutron reflector to simulate an infinite array of casks does not change k_{eff}.

The result of the calculation is k_{eff} = 0.9206 ± 0.0044. Including the bias determined from bench mark calculations and 2 sigma yields k_{eff} = 0.941, which satisfies the criterion.

Therefore, the TN-24 storage cask is safe with respect to criticality for the specified fuel designs and enrichment.

3.3.4.2 Error Contingency Criteria

Provision for error contingency is built into the criterion used in Section 3.3.4.1. above. The criterion, used in conjunction with the KENO-V.a and NITAWL codes, is common practice for licensing submittals. Because conservative assumptions are made in modeling, it is not necessary to introduce additional contingency for error.

3.3.4.3 Verification Analysis-Benchmarking

Five critical experiments by Pacific Northwest Laboratory[7][8] (PNL) are used to validate the criticality analysis. The PNL experiments were designed to simulate conditions associated with both fuel element shipping packages and with fuel storage pools. The experiments selected are associated with critical separation between water flooded subcritical clusters of fuel rods with and without poison plates between clusters. Run A contained Boral plates, Run B borated stainless steel plates, Run C SS304L plates and Run D no poison plates. All four experiments have steel reflecting walls. The fifth experiment (E) contains no poison plates and no reflecting walls.

The NITAWL code is used to perform resonance calculations and to prepare the working library from the SCALIAS 27 group cross section library for input to KENO-V.a.

Fuel rods and dimensions are illustrated in Figure 3.3-5. The experimental geometry is shown in Figure 3.3-6. The poison plates, when present, are positioned at the outer cell boundary of the center fuel cluster. Dimensions are shown in Table 3.3-2.

The KENO-V.a geometric representation includes the explicit model of each fuel rod and poison plate. The NITAWL and KENO-V.a inputs for Run A are shown in the Appendix.

The results of the calculations are shown in Table 3.3-3. The results show a non-conservative average bias of 1.2%. Thus the criticality result for the TN-24 is increased by a factor of 1.012.

3.3.5 Radiological Protection

3.3.5.1 Access Control

The storage casks will be located in a restricted area on a site to which access is controlled. In keeping with the terminology of 10CFR72[11], the terms restricted and unrestricted area refer only to areas within the controlled area. The controlled area and the site are taken to be the same. The term restricted area is defined in 10CFR20.3[12]. The specific procedures for controlling access to the site and to the restricted area within the site are to be addressed by the license applicant's Safety Analysis Report.

3.3.5.2 Shielding

Shielding has the objective of assuring that radiation dose rates at key locations are at acceptable levels for those locations. Three locations are of particular interest:

(1) Immediate Vicinity of the Cask
(2) Restricted Area Boundary
(3) Controlled Area (Site) Boundary

Dose rates in the immediate vicinity of the cask are important in consideration of occupational exposure. The design criterion for shielding is 60 mrem/hr at the cask surface. Because of the passive nature of storage with this cask, occupational tasks related to the cask are infrequent and short. A list of expected tasks is provided

in Table 3.3-4. The dose rates are based on those calculated in Chapter 7. Time required to perform the operation is based on Transnuclear's experience with transport casks. Maintenance type activities are listed in Table 7.4-1. Most of the exposures listed in this table will occur before the cask is placed in storage at an ISFSI.

Dose rates at the restricted area boundary should be such that people outside the restricted area need not have their radiation exposures monitored. Dose rates at the site boundary should be in accordance with applicable regulatory guides. The estimated occupational doses for personnel comply with the requirements of 10CFR20.101.

Detailed discussion of shielding is provided in Chapter 7, Radiation Protection.

3.3.5.3 Radiological Alarm System

No radiologigcal alarm system is provided with the TN-24 storage cask. Such a system can be provided by the license applicant if deemed necessary.

3.3.6 Fire and Explosion Protection

There are no combustible or explosive materials associated with the operation of the TN-24 dry storage cask. In general no such materials would be stored within the ISFSI controlled area.

Even though the occurrence of a fire or explosion is highly unlikely, these events have been analyzed:

a) Minor Fire This is categorized as a Level C Service Loading Condition. It might be caused by an event such as the accidental release and ignition of fuel oil from a storage facility located outside of the controlled area. Such a fire would raise the ambient temperature of the cask outer surface by only a few degrees.

b) Major Fire This is categorized as a Level D Service Loading condition. It assumes exposure of 1475°F for a period of 30 minutes under the conditions specified in 10CFR71[13]. It is shown in Section 5.1.3.6 that the integrity of the cask is maintained and that the dose rate limits of 10CFR72 for accident conditions are not exceeded.

c) Explosion (external) This is categorized as a Level D Service Loading condition. Since the cask is designed for an external pressure of 25 psia (as a Level A Service Loading condition), the cask will withstand external pressures of several psi due to a chemical explosion. The structural calculations for external pressure are presented in Chapter 4.

3.3.7 Material Handling and Storage

3.3.7.1 Spent Fuel Handling and Storage

The handling and storage of spent fuel within a nuclear power station is addressed as part of the facility license under 10CFR50[14]. This includes loading the spent fuel into the cask and handling of the cask prior to transfer to the ISFSI. No actual fuel handling occurs at the ISFSI since the casks are sealed and decontaminated prior to the arrival at the ISFSI.

No increase in surface contamination levels will occur during storage at the ISFSI because all sources of potential contamination are sealed within the cask. The exterior surfaces of the cask are metal spray coated and/or painted for corrosion protection and ease of decontamination.

The design criteria for the TN-24 dry storage cask require that the maximum fuel cladding temperature of the hottest fuel rod in the cask shall not exceed the temperature limit calculated according to PNL-6189[10]. This temperature limit, has been calculated as a function of fuel age to account for the effect of fuel age on creep deformation and fuel cladding rupture. As the age of fuel

increases, its cooling rate rapidly decreases. If the initial fuel temperature is too high at loading, significant creep deformation can occur as a result of the decreasing cooling rates with fuel age. The Commercial Spent Fuel Management Program (CSFM)[10] used the TN-24P packaging as one of its models for developing generic fuel cladding temperature limit curves for 40 year dry storage. Since the TN-24 and TN-24P are similar cask designs, the CSFM generic curves are used to establish fuel cladding temperature limits for 5-, 6-, 7-, 10- and 15- year fuel ages. The TN-24 has a storage life of 20 years and it is conservative to use the CSFM curves developed for 40 year storage.

From Ref. 10, the midwall hoop-stress is given by the equation,

$$S_{mhoop,\ T_2} = (PD_{mid}/2t)(a)(T_2/T_1)$$

where

$S_{mhoop,\ T_2}$ = the midwall hoop-stress (psi) at temperature of interest T_2 (°K)

P = the internal pressure (psi) at the hot-volume average temperature, T_1 (°K)

D_{mid} = the midwall diameter (in.) accounting for cladding corrosion

t = the cladding thickness (in.)

a = 0.95 for PWR fuel assemblies

Using fuel data provided in Ref. 2, a W 15 x 15 assembly (rod dia. = 0.422 in., cladding thickness = 0.0243 in.) with a burnup of 35 GWD/MTU has a lead fuel rod pressure of 835 psia at 100°C. The corresponding pressure for a W 17 x 17 assembly (rod dia. = 0.374 in., cladding thickness = 0.0225 in.) is 818 psia.

Substituting values and simplifying,

$S_{mhoop}, T_2 = 17.4\ T_2$ psi/K for W 15 x 15 assemblies and
$S_{mhoop}, T_2 = 16.3\ T_2$ psi/K for W 17 x 17 assemblies.

For conservatism, the W 15 x 15 fuel assembly equation is used to determine the fuel rod temperature limits. The temperature limits are determined graphically by plotting the midwall hoop-stress equation on the CSFM generic limit curves of Ref. 10. Table 3.3-5 lists the fuel cladding temperature limits.

Using the ORIGEN2 code, decay heat and source terms have are generated for a W 17 x 17 fuel assembly cooled for 5, 6, 8, 10, 12 and 15 years. The corresponding decay heats are listed in Table 3.3-6.

In Section 5.1.3.6, an ANSYS finite element model of the packaging cross section was developed for the normal storage analysis. Computer runs are made with decay heat loads corresponding to 5-, 6-, 8-, 10-, 12- and 15-year cooled fuel. The maximum fuel cladding temperature is calculated for each run and is reported in Table 3.3-6. The maximum fuel cladding temperature is plotted as a function of fuel age in Figure 3.3-7 along with the fuel cladding temperature limits.

The design criteria for the TN-24 dry storage cask require that nuclear criticality safety be assured under all operating and accident conditions by maintaining an effective neutron multiplication factor (k_{eff}) of less than 0.95. The nuclear analysis demonstrating that this is achieved, even with a loading of fresh fuel and the cavity filled with water, is presented in Section 3.3.4.

Subcriticality is maintained by means of borated stainless steel basket plates and gaps (flux traps) which are part of the basket assembly structure. Structural calculations, presented in Section 4.4.6, demonstrate that the basket structure will perform its criticality control function under all operating and accident conditions.

The design criteria for nuclear criticality safety discussed above permit an infinite array of casks to be stored at the ISFSI with no limitation on cask-to-cask spacing.

However, because of radiation heat transfer considerations, in order not to exceed the cladding temperature limit of the cask array configuration will be double rows of casks with a minimum cask-to-cask centerline spacing of 16 ft.

3.3.7.2 Radioactive Waste Treatment

Since the TN-24 dry storage casks are permanently sealed and are completely passive in operation, all radioactive materials are contained and no radioactive waste treatment is required.

Any radioactive wastes generated during loading or decontamination operations within the nuclear plant facility, prior to transfer to the ISFSI, are handled by the plant radwaste systems which are part of the 10CFR50 licensed activities.

3.3.7.3 Waste Storage Facilities

No waste storage facilities are required for ISFSI operation with the TN-24 casks.

3.3.8 Industrial and Chemical Safety

Fire and explosion hazards are covered in Section 3.3.6.

Since no hazardous chemicals are used in connection with the storage of TN-24 casks at an ISFSI, personnel or plant safety are not impaired due to potentially dangerous chemical reactions.

Transfer of the storage cask from the nuclear plant to the ISFSI will require lifting, rotating, and lowering operations which are important to plant personnel safety. Adherence to the ISFSI procedures covering these operations will ensure that the risks incurred are minimized.

TABLE 3.3-1

MATERIAL COMPOSITION FOR KENO MODEL

MIXTURE	DENSITY g/cm^3	NUCLIDE/ ELEMENT	LIBRARY NUMBER	DENSITY Atoms/b.cm
UO_2 Fuel	10.41	U235	92235	8.7014E-4
3.7 wt% U235		U238	92238	2.2361E-2
		O	8016	4.6462E-2
Zircaloy	6.44	*	40302	4.2518E-2
Water	0.998	H	1001	6.6759E-2
		O	8016	3.3380E-2
Borated (1.0 wt%)				
Stainless Steel	7.8	B10	5010	8.5866E-4
		B11	5011	3.4859E-3
		Cr	24304	1.6994E-2
		Mn	25055	1.6930E-3
		Fe	26304	5.7875E-2
		Ni	28304	7.5252E-3
Copper	8.96	Cu	29000	8.4918E-2
Carbon Steel	7.82	C	6012	3.9217E-3
		Fe	26000	8.3500E-2

*40302 is a composite cross section for 97.91 wt% Zr, 1.59% Sn, 0.5% Fe

TABLE 3.3-2

BNL BENCHMARK EXPERIMENTS

Case No.	Length x Width (fuel rods)	Poison Plates (mm)	Fuel Cluster Separation (mm)
A*	(1) 25 x 18 (2) 20 x 18	Borated SS (2.98)	48.0
B*	(2) 20 x 18	Boral (2.92)	26.9
C*	(2) 20 x 18	SS304L (3.02)	82.8
D*	(1) 25 x 18 (2) 20 x 18	None	95.1
E*	20 x 15	None	63.9

* 17.85 cm thick steel walls placed at 1.32 cm from fuel clusters

TABLE 3.3-3

KENO-V.a BENCHMARK RESULTS

Experiment No.	Keff	Sigma
A	0.9900	0.004
B	0.9909	0.004
C	0.9865	0.005
D	0.9885	0.004
E	0.9856	0.004

Avg = 0.9883

TABLE 3.3-4

OCCUPATIONAL EXPOSURES FOR CASK LOADING, TRANSPORT, AND EMPLACEMENT

(One Time Exposure)

Task	Time Required (hr)	No. of Persons	Dose Rate (rem/hr)	Man-Rem
Placement in pool and Loading process	6	3	0.005	.09
Removal from pool	1	3	0.030*	.09
Processing of cask	10	3	0.030*	.90
Leak testing	2	2	0.030*	.12
Decontamination and inspection	3	3	0.030*	.27
Preparation for transport	2	3	0.030*	.18
Transfer of cask to ISFSI	1	3	0.020**	.06
Emplacement of cask	2	3	0.030*	.18
Monitoring system connection and trunnion removal	2	2	0.030*	.12
Total				2.01

* Based on effective distance of 1 meter from cask surface.

** Based on effective distance of 2 meters from cask surface.

TABLE 3.3-5

FUEL CLADDING TEMPERATURE LIMITS

Initial Fuel Age	Temperature Limit
5 years	730°F (388°C)
6 years	707°F (375°C)
7 years	666°F (352°C)
10 years	655°F (346°C)
15 years	642°F (339°C)

TABLE 3.3-6

DECAY HEAT AND MAXIMUM FUEL CLADDING TEMPERATURE
AS A FUNCTION OF FUEL AGE

Fuel Age	Decay Heat Per Assembly	Maximum Fuel Cladding Temperature
5 years	1.000 kw	642°F (339°C)
6 years	0.821 kw	575°F (302°C)
8 years	0.680 kw	518°F (270°C)
10 years	0.616 kw	490°F (254°C)
12 years	0.572 kw	471°F (244°C)
15 years	0.518 kw	446°F (230°C)

FIGURE 3.3-1

SEAL AND PRESSURE MONITORING SYSTEM

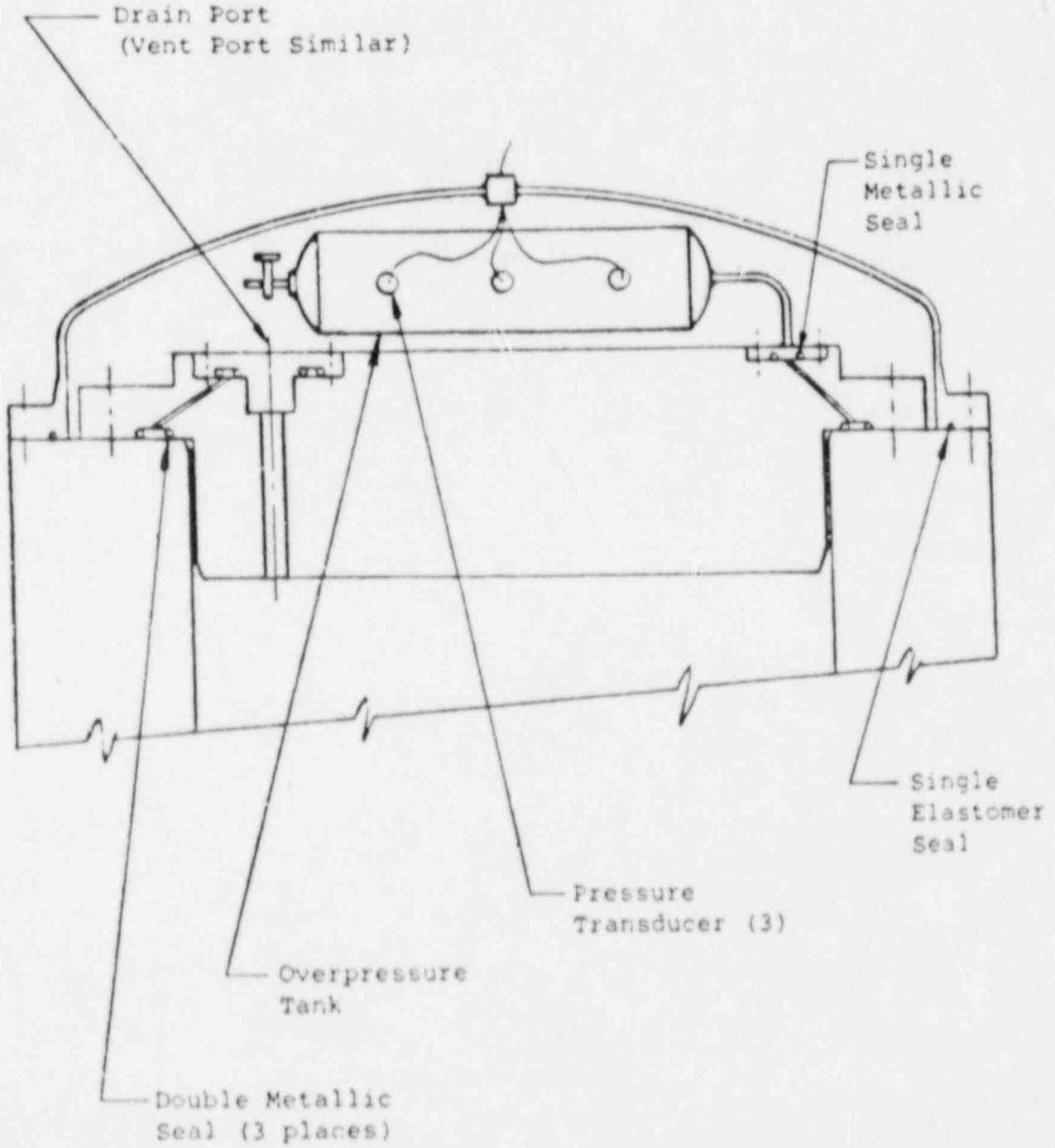

FIGURE 3.3-2

DETERMINATION OF MAXIMUM ALLOWABLE

HELIUM TEST LEAKAGE RATE

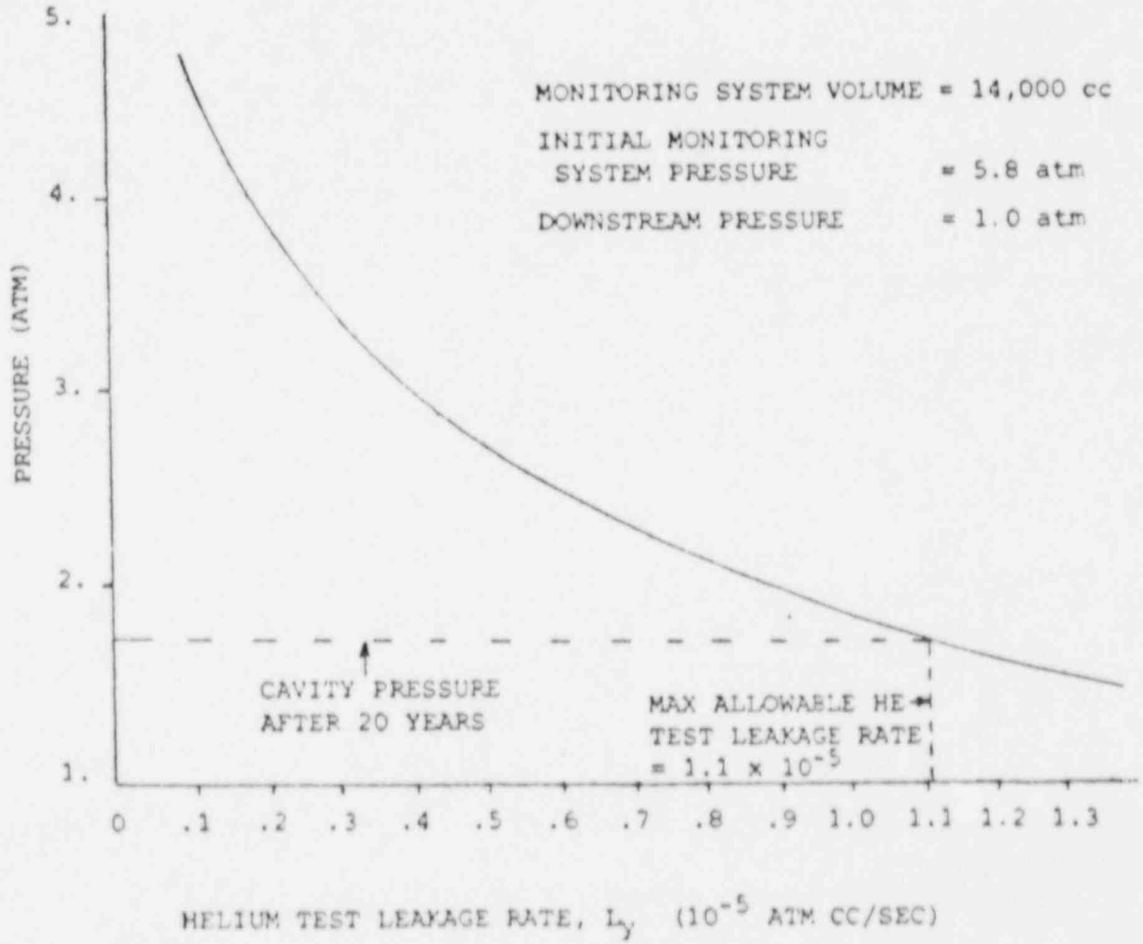

FIGURE 3.3-3

CHANGE IN MONITORING SYSTEM
AND CAVITY PRESSURE DURING STORAGE

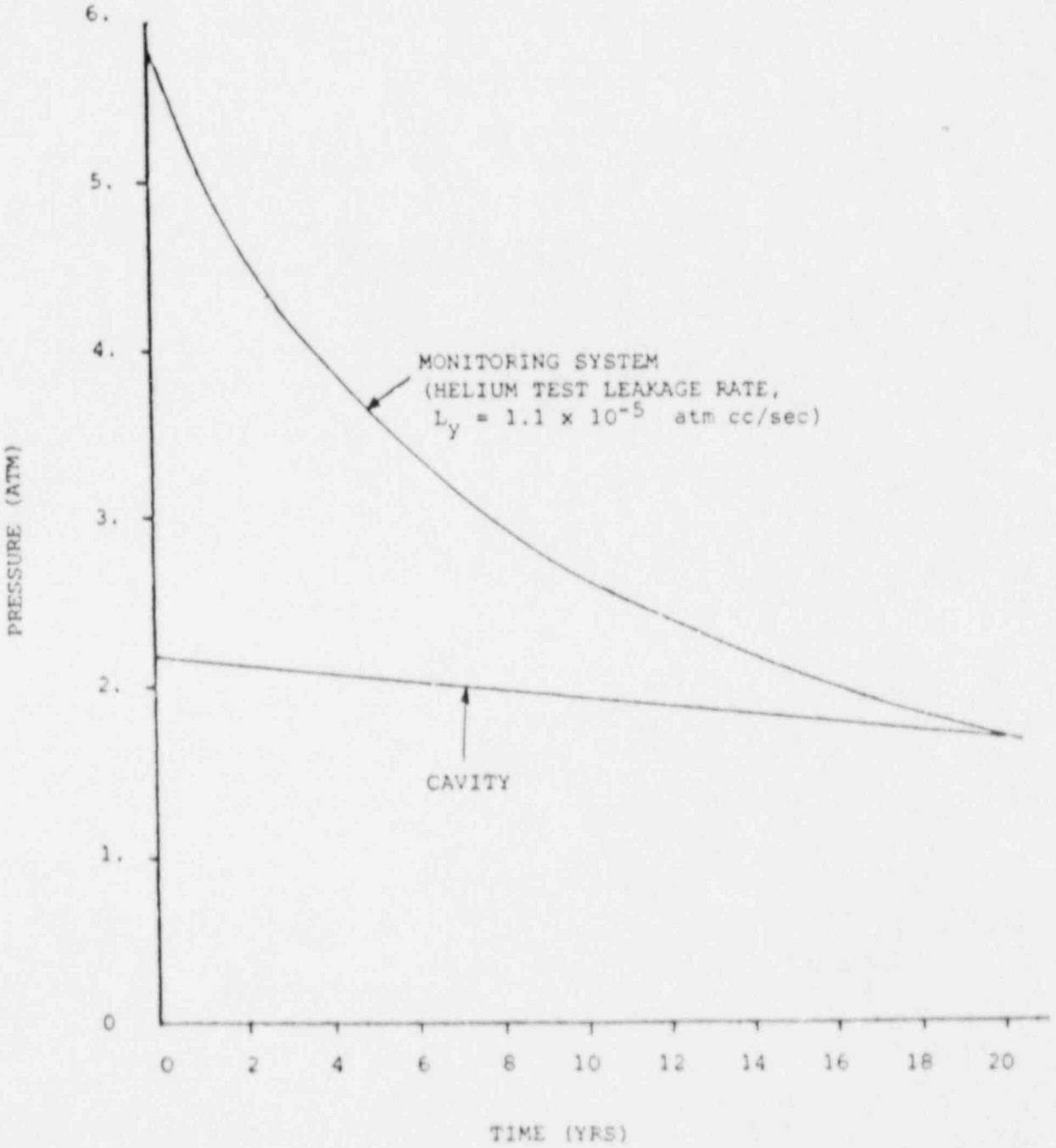

FIGURE 3.3-4

TN-24 KENO-V.a GEOMETRY

Axial length of model = 2000 cm plus 30 cm water top and bottom

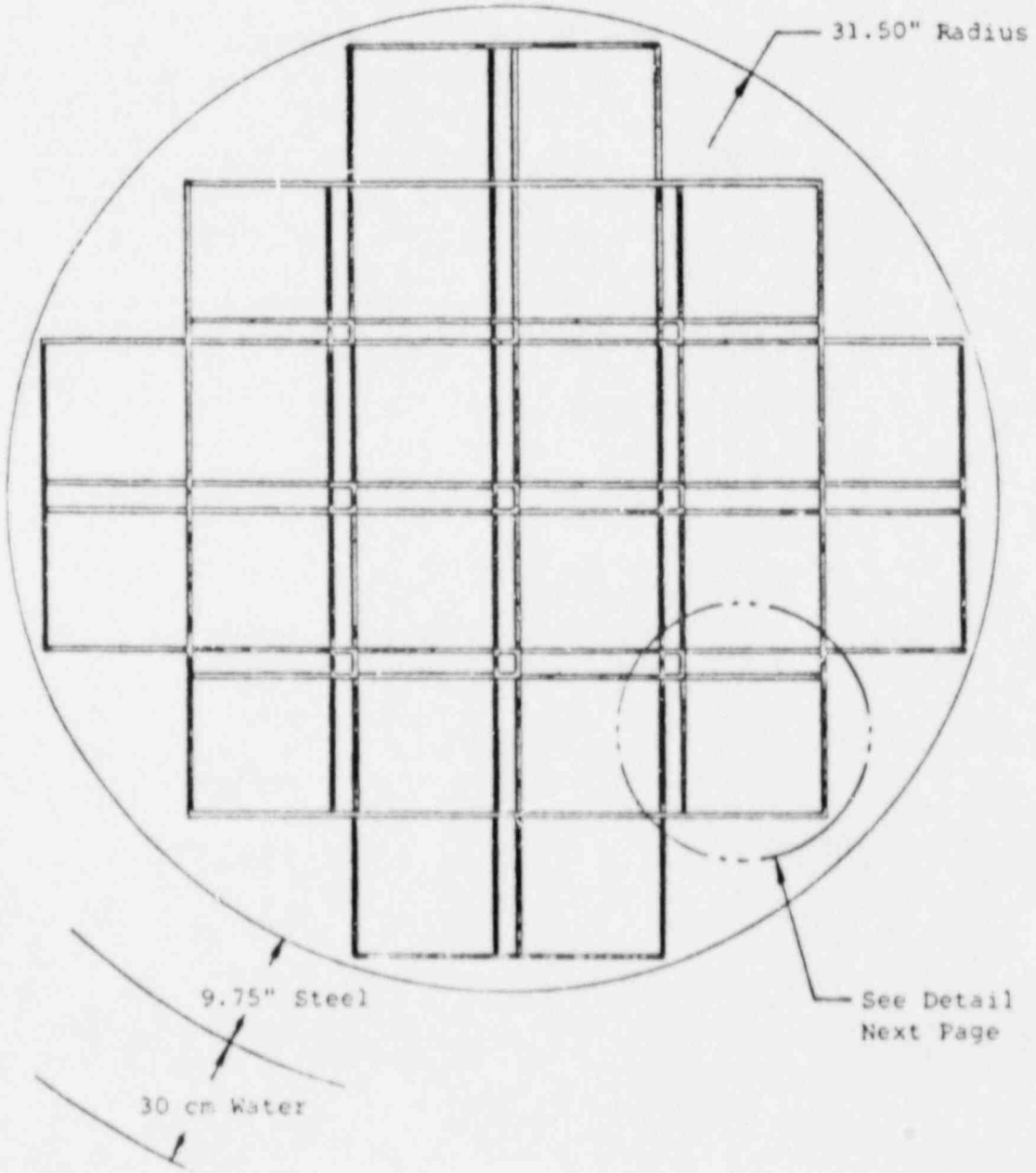

FIGURE 3.3-4 cont'd

TN-24 KENO-V.a GEOMETRY (DETAIL)

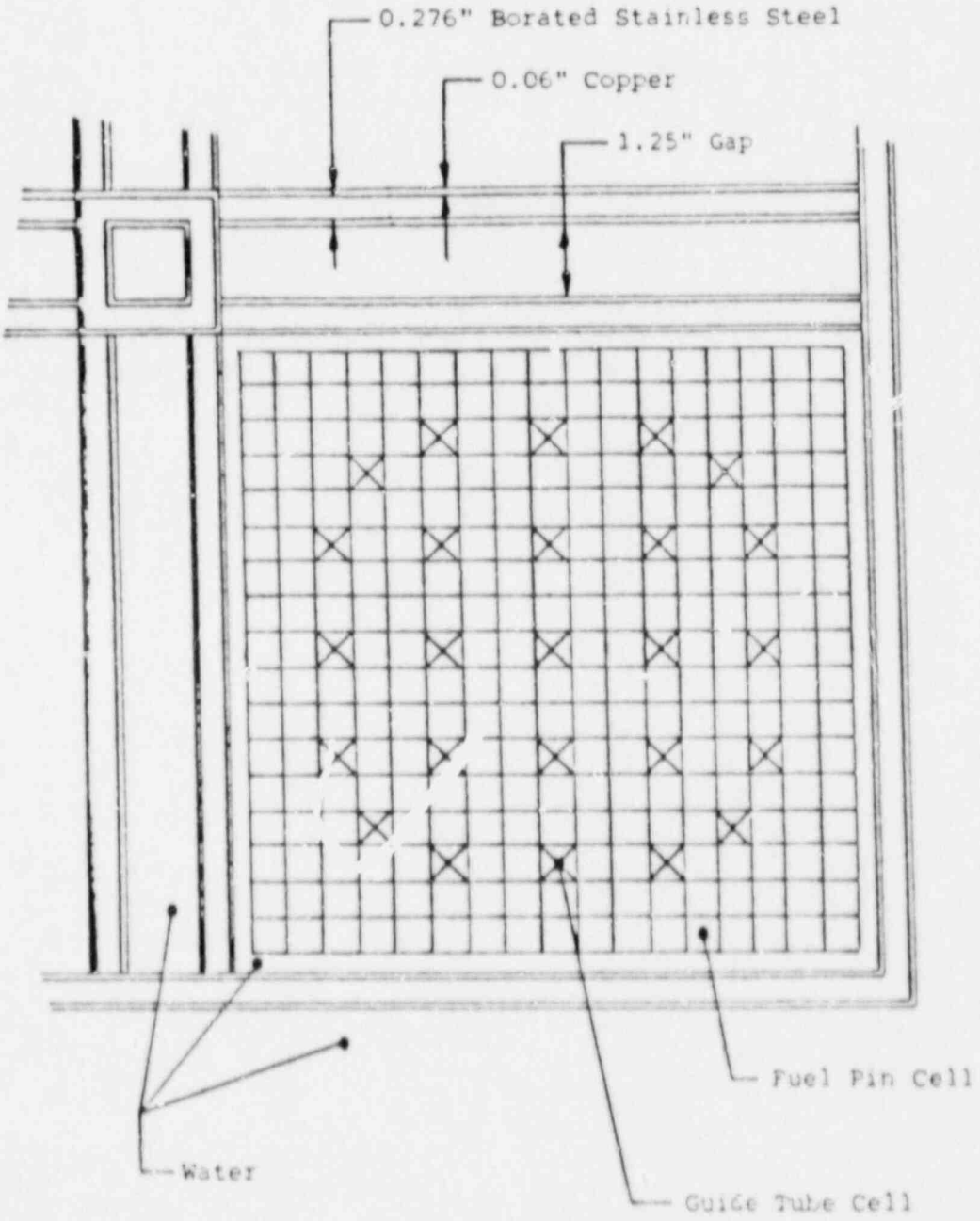

FIGURE 3.3-5

PNL BENCHMARK EXPERIMENT FUEL RODS

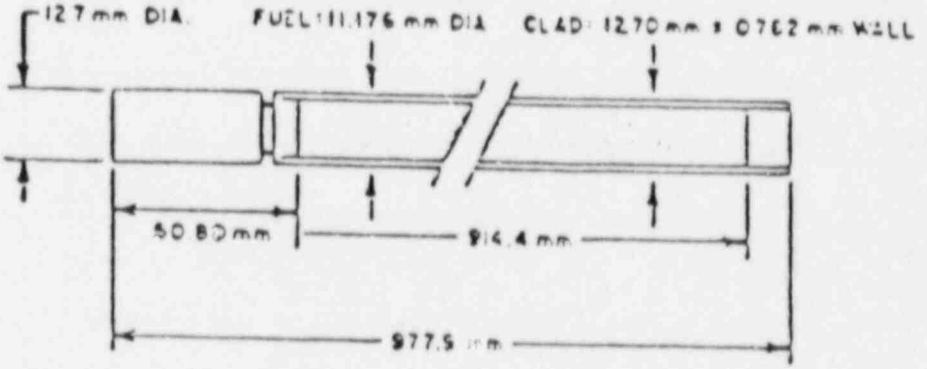

CLADDING: 6061 ALUMINUM TUBING SEAL WELDED WITH LOWER END PLUG OF 5052-H32 ALUMINUM AND A TOP PLUG OF 1100 ALUMINUM.

TOTAL WEIGHT OF LOADED FUEL RODS: 917 gm (AVERAGE)

LOADING: 825 gm OF UO_2 POWDER/ROD, 726 gm OF U/ROD, 17.08 gm OF U-235/ROD

ENRICHMENT: 2.35 ± 005 w/o U-235

FUEL DENSITY: 9.20 mg/m.m^3 (84% THEORETICAL DENSITY)

FIGURE 3.3-6

TYPICAL PNL BENCHMARK EXPERIMENT

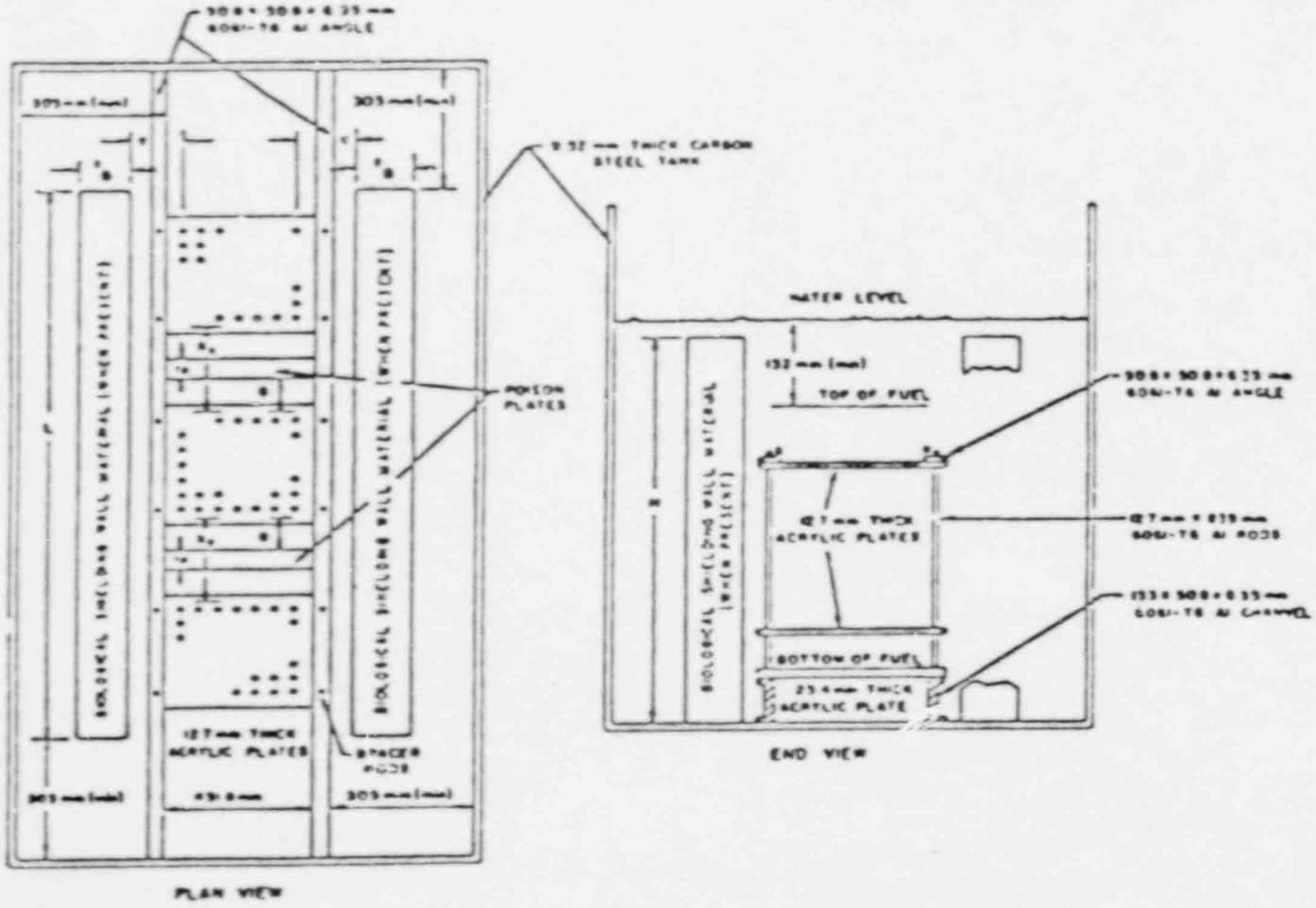

MAXIMUM AND ALLOWABLE
FUEL ROD TEMPERATURES

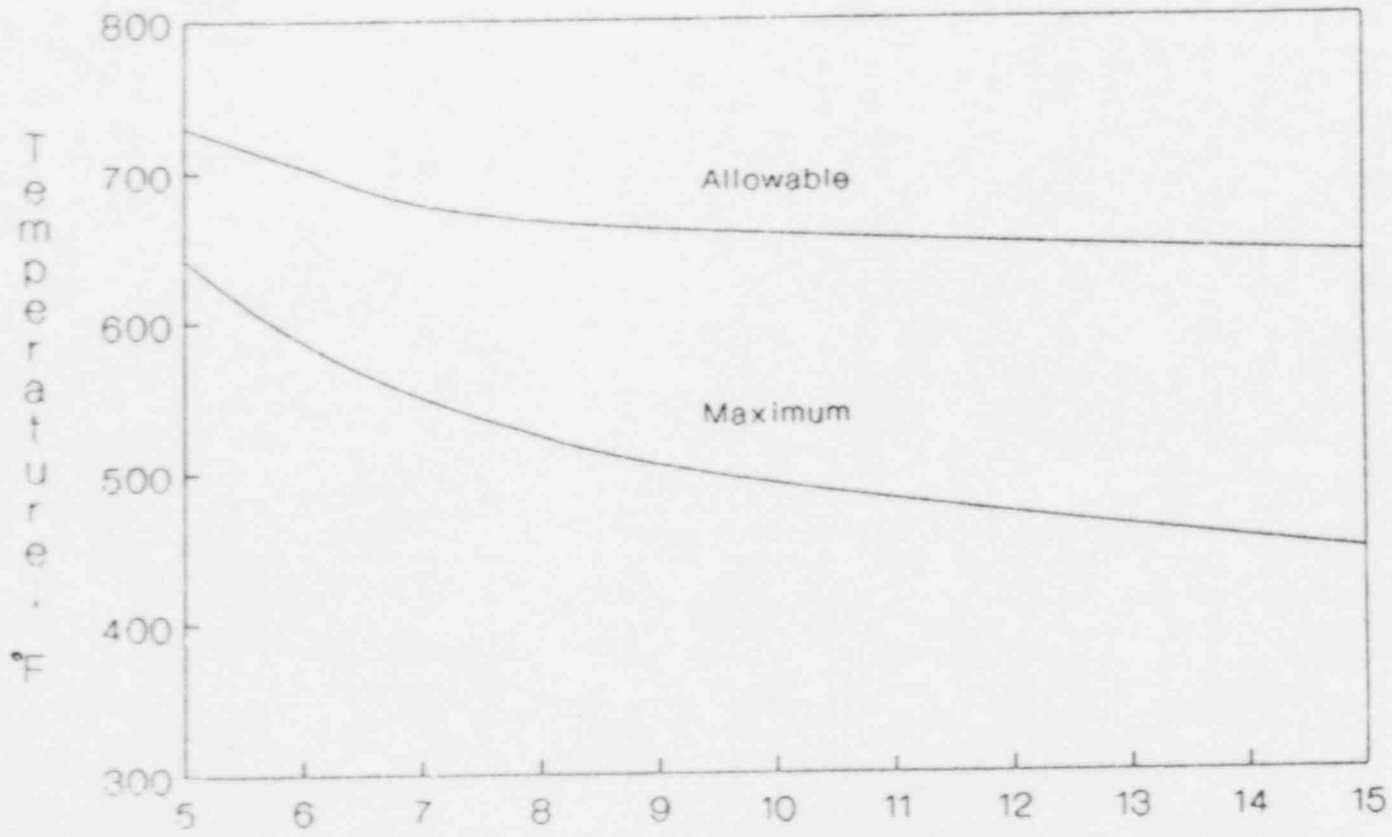

Figure 3.3-7

References for Section 3.3

1. "VCR Metal Gasket Face Seal Fitting", Technical Catalog Ca-887, July, 1987, Cajon Company, Macedonia, OH.

2. "Extended Fuel Burnup Demonstration Program Topical Report: Transport Considerations for Transnuclear Casks," DOE/ET 34014-11 Transnuclear, Inc., White Plains, N.Y., Dec. 1983.

3. "National Standard for Leakage Tests on Packages for Shipment of Radioactive Materials", ANSI N14.5-1977, American National Standards Institute, New York, Oct. 1977.

4. Petrie, L.M. and Landers, N. F., "KENO-V.a, An Improved Monte Carlo Criticality Program with Supergrouping," NUREG/CR-0200, Oak Ridge Laboratory, December, 1984.

5. Greene, N. M., et.al., "NITAWL-S: Scale System Module for Performing Resonance Shielding and Working Library Production," NUREG/CR-0200, Oak Ridge National Laboratory, October, 1981.

6. "SCALE: A Modular Code System for Performing Standardized Computer Analysis for Licensing Evaluation," Revision 3 , ORNL/NUREG/CR-0200, U.S. Nuclear Regulatory Commission, Revision 3., December 1984.

7. Bierman, S. R. et. al., "Critical Separation Between Subcritical Clusters of 2.35 wt% U235 Enriched UO2 Rods in Water with Fixed Neutron Poisons," PNL-2438, Pacific Northwest Laboratory, October 1979.

8. Bierman, S. R. and Clayton, E. D., "Criticality Experiments with Subcritical Clusters of 2.35 wt% and 4.31 wt% U235 Enriched UO2 Rods in Water with Steel Reflecting Walls," NUREG/CR-1784, PNL-3602, Pacific Northwest Laboratory, January 1981.

9. "Regulations for the Safe Transport of Radioactive Materials," IAEA Safety Standards, Safety Series No. 6, Revised Edition, International Atomic Energy Agency, Vienna, 1973.

10. Levy, et. al., "Recommended Temperature Limits for Dry Storage of Spent Light Water Reactor Zircaloy - Clad Fuel Rods in Inert Gas," Pacific Northwest Laboratory, PNL-6189, 1987.

11. "Licensing Requirements for the Storage of Spent Fuel in an Independent Spent Fuel Storage Installation," 10CFR Part 72, Rules and Regulations, Title 10, Chapter 1, Code of Federal Regulations - Energy, U.S. Nuclear Regulatory Commission, Washington D.C., Jan. 1987.

12. "Standards for Protection Against Radiation", 10CFR Part 20, Rules and Regulations, Title 10, Chapter 1, Code of Federal Regulations - Energy, U.S. Nuclear Regulatory Commission, Washington, D.C., Jan 1987.

13. "Packaging and Transportation of Radioactive Material", 10CFR Part 71, Rules and Regulations, Title 10, Chapter 1, Code of Federal Regulations - Energy, U.S. Nuclear Regulatory Commission, Washington, D.C., Jan 1987.

14. "Domestic Licensing of Production and Utilization Facilities", 10CFR Part 50, Rules and Regulations, Title 10, Chapter 1, Code of Federal Regulations - Energy, U.S. Nuclear Regulatory Commission, Washington, D.C. Jan 1987.

3.4 CLASSIFICATION OF STRUCTURES, COMPONENTS, AND SYSTEMS

The structures, components and systems of the TN-24 Dry Storage Cask may be classified as "Important to Safety" and "Not Important to Safety." A tabulation of the structures, components, systems by their classification is shown in Table 3.4-1.

The criteria for selecting the classification for particular structures, components, or systems, are based on the definitions given in 10CFR72[1], Subpart A.

All items, regardless of their classification, are designed in accordance with the requirements of the TN-24 Design Criteria which ensure that the General Design Criteria of 10CFR72, Subpart F, are satisfied. Those items which are classified as important to safety are designed, fabricated, inspected and tested, to the maximum practicable extent, in accordance with the ASME Boiler and Pressure Vessel Code, Section III, Subsection NB, Article NB-3200. The seismic design considerations of 10CFR72, and the quality assurance requirements of Appendix B to 10CFR50[2] are applied.

Those items which are classified as not important to safety are designed in accordance with design rules which are indicated in the structural analysis of those items in Section 4.2.

The classification of structures, components, and systems which are part of the ISFSI, but not part of the cask, is included in the Safety Analysis Report submitted by the applicant for a license under 10CFR72.

TABLE 3.4-1

CLASSIFICATION OF STRUCTURES, COMPONENTS, AND SYSTEMS

Important to Safety	Not Important to Safety
Containment Vessel	Protective Cover
Cask Body Shell	Overpressure System
Cask Body Bottom	
Lid	
Lid Bolts	
Lid Gaskets	
Lid Penetration Covers, Bolts, Gaskets	
Basket Assembly	
Port Covers	
Bolts	
Gaskets	
Trunnions	
Trunnion Bolts	
Neutron Shield	

References for Section 3.4

1. "Licensing Requirements for the Storage of Spent Fuel in an Independent Spent Fuel Storage Installation", 10CFR Part 72, Rules and Regulations, Title 10, Chapter 1, Code of Federal Regulations - Energy, U.S. Nuclear Regulatory Commission, Washington, D.C. Jan 1987.

2. "Domestic Licensing of Production and Utilization Facilities", 10CFR Part 50, Rules and Regulations, Title 10, Chapter 1, Code of Federal Regulations - Energy, U.S. Nuclear Regulatory Commission, Washington D.C. Jan 1987.

3.5 DECOMMISSIONING CONSIDERATIONS

The TN-24 storage cask is designed for dry storage and will require no decontamination of any liquids or associated liquid handling systems. The cask has smooth interior and exterior surfaces to facilitate decontamination after unloading of the fuel assemblies. The inside of the cask can be flushed with water and/or chemical decontamination agents to remove particulate materials.

Another consideration for decommissioning is the slight activation of the cask from the neutron flux present. Activation calculations are performed to address this subject. The following assumptions were made:

1. The cask contains 24 reference PWR assemblies.

2. The neutron flux is assumed constant for 20 years.

3. The neutron spectrum is the same as in a PWR reactor.

The activation calculation is performed using the computer code ORIGEN2[1] with the total neutron fluxes taken from the radial shielding calculation performed with the XSDRN-PM code (See Chapter 7). The fluxes at the cask centerline, the cavity wall, the inside radius of the neutron shield, and the inside radius of the outer shell are used to irradiate the basket, the body lid, the neutron shield, and the outer shell and protective cover, respectively. The fluxes, material compositions, and masses of irradiated material are listed in Table 3.5-1. The ORIGEN2 cross section library for PWR's at a burnup of 33000 MWD/MTU is used.

The results listed in Table 3.5-2 indicate that after 20 years irradiation and 30 days decay (to eliminate very short lived radionuclides), the total activity is less than 0.06 Ci.

To evaluate the TN-24 cask and basket for disposal, the specific activity of the isotypes listed in Tables 1 and 2 of 10CFR61.55[2] is determined and compared with the limits for Class A wastes in those tables.

The actual material volumes of the cask components are used to evaluate their specific activity, rather than diluting the activity over the envelope of the entire cask.

The results of the calculation, shown in Table 3.5-3, show that the TN-24 will be far below the specific activity limits for both long and short lived nuclides for Class A waste.

TABLE 3.5-1

DATA FOR TN-24 ACTIVATION ANALYSIS

ZONE	FLUX $n/cm^3/s$	MATERIAL	MASS kg	COMPOSITION wt%
Basket	3.1E5	Borated SS	5140	Mn 1.3
				Cr 19.2
				Ni 12.8
				Cr 0.04
				Cu 0.16
				Mo 0.07
				Fe 64.89
				B 1.0
				C 0.04
				Si 0.5
		Copper	2503	Cu 100
Body, Lid, Basket Rails	1.9E5	Carbon Stl	60947	Fe 98.5
				Mn 1.0
				C 0.2
				Si 0.3
		Aluminum	237	Si 0.6
				Mg 1.0
				Cr 0.2
				Cu 0.3
				A 97.9
Neutron Shield	2.3E4	Resin	4755	H 5.05
				B 1.05
				C 35.13
				O 41.73
				Al 14.93
				Zn 2.11
		Aluminum	992	(See above)
Shell, Cover	6.1E2	Carbon Stl	5333	(See above)

TABLE 3.5-2

RESULTS OF ORIGEN2 ACTIVATION CALCULATION

NUCLIDE	ACTIVITY (Ci)				
	Basket	Body	N-Shield	Shell	TOTAL
H3			3.49E-10		3.49E-10
C14	2.43E-12	8.83E-11	8.45E-10	2.48E-14	9.36E-10
Cr51	2.90E-3	8.35E-5			2.98E-3
Mn54	3.32E-4	3.66E-3			3.99E-3
Fe55	3.65E-3	3.97E-2		1.12E-5	4.34E-2
Fe59	6.73E-5	7.42E-4			8.10E-4
Co58	6.03E-4				6.03E-4
Co60	3.17E-3				3.17E-3
Ni63	4.26E-4				4.26E-4
Ni59	3.25E-6				1.98E-5
Nb94	3.06E-12				3.06E-12
Tc99	8.55E-11				8.85E-11
Zn65			1.98E-5		1.98E-5
TOTAL					5.56E-2

Note: Only nuclides with activity greater than 10^{-5} curie and those nuclides listed in 10CFR61.55 are reported here.

TABLE 3.5-3

COMPARISON OF TN-24 ACTIVITY WITH
CLASS A WASTE LIMITS

Long Lived Isotopes, 10CFR61.55, Table 1

Zone	Volume m^3	Nuclide	Specific Activity Ci/m^3	Limit Ci/m^3
Basket	0.941	C14	2.58E-12	80
		Ni59	3.46E-6	220
		Nb94	3.25E-12	0.2
		Tc99	9.40E-11	3
Body	7.78	C14	1.14E-11	80
N-Shield	3.71	C14	2.28E-10	8
Shell	0.69	C14	3.59E-14	80

Short Lived Isotopes, 10CFR61.55, Table 2, Column 1

Zone	Nuclide	Specific Activity	Limit
Basket	Co60	3.36E-3	700
	Ni63	4.53E-4	35
	T5*	8.03E-3	700
Body	T5*	5.68E-3	700
N-Shield	H3	9.42E-11	40
	T5*	5.33E-5	700
Shell	T5*	1.64E-5	700

*Nuclides with half life less than 5 years:
Cr51, Mn54, Fe55, Fe59, Co58, Zn65

References for Section 3.5

1. "ORIGEN2, Isotope Generation and Depletion Code," Oak Ridge National Laboratory, CCC-371, Jan 1987.

2. "Licensing Requirements for Land Disposal of Radioactive Waste", 10CFR Part 61, Rules and Regulations, Title 10, Chapter 1, Code of Federal Regulations - Energy, U.S. Nuclear Regulatory Commission, Washington, D.C. Jan 1987.

4. INSTALLATION DESIGN

4.1 SUMMARY DESCRIPTION

Two possible configurations for an ISFSI using TN-24 dry storage casks are shown in Figure 1.1-2 and 1.1-3. One arrangement is for vertical cask storage while the other is for horizontal cask storage. In both arrangements, the casks would be stored on reinforced concrete slabs, in double rows, spaced on 16 ft centers.

A complete summary description of an ISFSI using TN-24 casks will be provided in the Safety Analysis Report submitted as part of the license application under 10CFR Part 72.

4.2 STORAGE STRUCTURES

4.2.1 Structural Specifications

This section summarizes the structural analysis of the TN-24 storage cask. For purposes of structural analysis, the cask has been divided into four basic components: the containment vessel, the trunnions, the outer shell, and the basket. For each of these components, the following information is provided: a brief description of the components; the design bases and criteria; the method of analysis used; a summary of stresses for the most critical or highest stressed locations; a comparison with the allowable stress criteria; and a review of the applicable codes and standards for materials, fabrication, and examination.

4.2.1.1 Containment Vessel

A. Description

The containment vessel is the primary boundary for containment of the stored radioactive material. It consists of the cask body, the lid and lid bolts, the seals, the port closures and their bolts and seals. The containment vessel is shown in Figure 4.2-1. Details are shown on drawings 971-1, -2, -3 and -4 in Appendix 1A.

B. Design Bases and Criteria

The design bases specific for the containment vessel are listed in Table 4.2-1. These design bases are consistent with the general design bases for the storage cask as described in Chapter 1.

The stress limits for the containment vessel are those of the ASME Boiler and Pressure Vessel Code, Section III, Subsection NB[1], except the limits for Design Loadings are applied to the Primary Service Loadings.

Stress limits for Primary Service and Levels A, B, C, and D service loading conditions are given in Tables 4.2-2a and 2b. The allowable stress limits used for Level D load-induced stresses, determined on an elastic basis, are based on the entire structure resisting the accident load. Local yielding at the point of contact with the applied load is allowed. The allowable elastic stress limits of Appendix F[2] of Section III are used.

The allowable stress intensity value, S_m, as defined by the Code may be taken at the temperature calculated for each service load condition or at the design temperature.

The deviations from the rules of Subsection NB are as follows:

(1) The Design Loads have been designated as Primary Service Loads which are basically equivalent. However, the maximum primary service load does not necessarily act concurrently with the maximum primary service temperature although for this analysis they are evaluated coincidentally.

(2) The design pressure and temperature have been replaced by rated pressure and temperature, respectively. The difference is that the rated pressure does not necessarily act coincidentally with the rated temperature.

C Method of Analysis

The stresses induced in the containment vessel due to the applied loads are calculated using the methods described in Sections 4A.5.1, 4A.5.2, 4A.5.3, 4A.5.4, 4A.5.5, 4A.5.6, 4A.5.7 and 4A.5.8.

For purposes of analysis, the containment vessel is divided into four areas: the bottom plate and its connection with the cylindrical shell, the lid and its connection with the cylindrical shell, the lid bolts, and the cylindrical shell. The analyses of

these areas for the Primary Service, Level A, Level B, and Level C loads are given in Appendix 4A, Section 4A.5.2, 4A.5.3, 4A.5.4 and 4A.5.5, respectively. The analyses of the connections of the lid and bottom plate with the shell are performed using discontinuity methods equivalent to the ASME code methods. The local stresses in the shell at the trunnions are calculated separately using Bijlaard's method and then combined with the results of the other calculations. The details of the analysis are given in Section 4A.5.1.

The analyses of the containment vessel for the accident loads, i.e. Level D, are given in Sections 4A.5.6, 4A.5.7 and 4A.5.8 of Appendix 4A.

D. Loads Acting on the Containment Vessel

The magnitude of the loads acting on the containment vessel for each service loading combination is listed in Tables 4.2-3 through 4.2-7.

In each table the type of load is listed in the left hand column and the magnitude of the load for each combination of each loading condition, i.e. Primary, Level A, Level B, Level C, and Level D, is given on the right side of the table. The loads are established and discussed in Sections 3.2.1 through 3.2.12. The load combinations which are listed are taken from Section 3.2.13 and Table 3.2-14.

E. Summary of Stresses

Stresses which were calculated at various locations in the primary containment vessel for the applied loads are given in Appendix 4A. These results were reviewed to determine the maximum stresses and their location and the stresses at other locations of interest. For locations which were expected to have the lowest margin of safety, stresses were combined for each load combination. A summary of the maximum stresses at critical locations in the containment vessel for

the most severe load combinations is presented in Table 4.2-8a, 8b, 8c and 8d. The first column identifies the load combination for which stress summaries are presented. The next column identifies the ASME code stress categories. The surface on which the stress acts is indicated in the next column.

The first set of stresses listed are the maximum combined stress components, i.e. tangential (circumferential) σ_t, longitudinal σ_l, radial σ_r, and shear τ. These are listed for each stress category for which an allowable limit must be determined. The stress intensity limits are identified for the service loading in Tables 4.2-2a and 2b. Using the three stress components and the shear stress, the principal stresses were calculated and are listed in the three columns adjacent to the stress components. Table 4.2-8a, 8b, 8c and 8d show that either longitudinal stress, σ_l, in the lid flange and bottom or the radial stresses, σ_r, in the shell are most frequently zero or of very small magnitude and, therefore, the stress state can be considered as one of plane stress. Negligible error is introduced by not using the cubic equation for triaxial stress states because the longitudinal or radial stresses are small compared to the other stress components.

For the plane stress state, when a shear stress is acting, the maximum and minimum principal stress are obtained from Mohr's equations for plane stress. If the shear stress is zero, the principal stresses are the same as the stress components. The maximum shear stress theory, i.e. the difference between the maximum and minimum principle stresses, is used to obtain the actual stress intensity, S for comparison to the allowable stress intensity limit, S_m. The values of S_m are obtained from the Section III Appendices for the particular material at the temperature and location considered. The S_m value for Primary Service Limits is based on the rated temperature. The Level A, B, C, and D Service Limits are based on the actual temperature which exists at the location for the service loads acting for each combination.

The most highly stressed locations in the containment vessel are in the lid flange at the gasket location, at the junction of the shell with the bottom plate, in the shell at the trunnions, and in the lid bolts. The stresses in the shell at the trunnions are of interest because of the local stresses due to the attachment loads transmitted by the trunnions.

The maximum stresses due to the accident loads do not always act at the same location as the maximum stresses due to the other loads. However, in the load combination they are conservatively added to the maximum stresses due to the other loads.

The load combinations for which the maximum stresses occur are presented and discussed below. The effects of distributed loads due to weight, wind, water and seismic effects are negligible.

The Primary Service Load combination P3 is presented in Table 4.2-8a, 8b, 8c, and 8d for comparison of calculated versus allowable stresses. The internal pressure P3 is 250 psi compared to a 25 psi external pressure for combination P1. The stresses due to the internal pressure are approximately 10 times larger than those due to external pressure, therefore P3 is the more severe load combination. The handling loads due to lifting, transfer and tilting do not act with the maximum internal pressure of 250 psi. The handling loads would act with an internal pressure of 32 psi which corresponds to initial pressurization. Further the internal pressure should never exceed one-half the value of 250 psi used. Therefore, the stresses presented are significantly higher than those which would actually occur. However, load combination P3 is evaluted for the stresses acting in the shell at the connection with the bottom plate due to the attachment loads acting on the trunnions. For Primary Service Loads thermal loads do not have to be considered.

The Level A2 load combination is also presented in Tables 4.2-8a, 8b, 8c, and 8d for comparison. Again this load combination includes

internal pressure and is more severe than the load combination A3 which includes external rather than internal pressure. The solar load in combination with the decay heat load results in the maximum temperatures, thermal gradients and differential thermal expansions. Therefore, these effects are combined in load case A2. This load combination also includes the effects of the attachment loads acting on the trunnions.

Level B2 combination is presented for comparison in Tables 4.2-8a, 8b, 8c and 8d. As it turned out, load combination B2 is the same as load combination A2.

Level C load combinations are less severe than Level A and B combinations, therefore, results are not presented.

Comparison of stresses for Level D service load combination D3 (cask drop), D4 (cask tipping) and D7 (tornado missiles) are presented in Tables 4.2-8a, 8b, 8c, and 8d. These combinations consider that an internal pressure of 250 psi and bolt preload are acting during these accidents. No other loadings are acting. Thermal stresses are considered secondary and do not have to be evaluated in combinations with these accidents. Accident conditions D2, D5, and D6 are less severe than D3, D4, and D7.

As shown in Chapter 3.0, the seismic g loads due to an earthquake are low, i.e. 0.25 vertical and 0.17 horizontal. These are insignificant compared to the g loads for the drop and tipping accident.

The effects of the major fire are discussed in Section 3.2.10. The maximum temperatures and thermal gradients are considerably higher than for other thermal loads, however the ASME code does not require analysis of thermally induced stresses due to accident conditions. These stresses are self-limiting and cannot induce failure. The material will deform to accommodate the temperature variation, by an

amount which is approximately 0.4 percent strain. Therefore, this one time event would not cause failure of the primary containment boundary.

Load combination D5 considers the effect of a cask burial due to some accident event, e.g. an earthquake. The discussion in Section 3.2.10 shows that, the cask would have to be uncovered in 80 hours, based on the assumption of no heat dissipation through the earth in order to prevent high temperatures. Since thermal stresses need not be evaluated per the ASME code, no comparison is presented in Tables 4.2-8a, 8b, 8c, and 8d.

An explosion near the cask is unlikely. However, it is not anticipated that an explosion could produce an equivalent pressure load equal to that for which the cask was evaluated. The vertical drop equivalent pressure load is 2260 psi. Therefore is not necessary to evaluate the explosion as a separate condition.

The maximum stress intensities for the loading combination from Tables 4.2-8a, 8b, 8c, and 8d are listed in Table 4.2-8e and comared with the ASME code allowable stress intensities. The margins of safety for each service condition are also calculated. As shown, the calculated stress intensities are lower than the allowable limits and the margins of safety positive. The maximum bolt stress intensities for each service condition are listed in Table 4.2-8f. These stresses are compared to the allowable stress intensities and margins of safety determined. As shown, the calculated stress intensities are less than the allowable stress limits and the margins of safety are positive. Therefore the containment vessel meets the ASME code stress criteria.

Also, the maximum bolt stresses, even for the storage accident conditions, are less than the yield strength of the bolt material. Therefore, the bolts will restore the sealing load on the gaskets after the accident has occurred.

4.2.1.2 Basket

A. Description

The basket of the TN-24 dry storage cask is shown in drawings 971-005 and 006 in Appendix 1A.

It is fabricated of borated stainless steel plates, 0.276 in. thick by 16.18 in. high. The plates are electroplated with a 0.060 in. layer of copper on each side. The plates are slotted at intervals of approximately 9 in. along the sides, as shown in drawing 971-005. When assembled, they interlock to form an egg crate structure with compartments having a cross section of 8.7 in. by 8.7 in. as shown on drawing 971-006. Brackets and channels are used at the cavity wall to provide restraint against bending and bucklings of the plates at the ends.

B. Design Bases and Criteria

The basket for the TN-24 dry storage cask contains 24 compartments for the proper spacing of the intact spent fuel assemblies. The basket plates transfers heat to the cask body wall, and provides neutron absorbing material which assures that he nuclear criticality safety requirements are met. The compartment size is based on the design basis fuel assembly dimensions with a nominal gap of 1/8 in.

Differential thermal expansion between the basket and the cask body, and between the basket plates themselves is considered. The specific design bases for the structural design and analysis of the basket are given in Table 4.2-9.

The maximum tensile stress at any location in the basket due to the application of the handling loads is not to exceed the minimum yield strength of the basket material.

The basket may plastically deform locally without gross deformation when subjected to the cask drop and tipping accidents. The plastic deformation is expected to occur at the slotted intersection of the basket plates. If a plastic hinge forms at a slotted plate region, the local strain is limited and the stress at the center of the plate between slots is also limited to prevent formation of a plastic hinge in this area.

C. Method of Analysis

The basket assembly is analyzed using the ANSYS finite element computer program. A frame model of the egg crate structure is constructed by representing the plates as beam elements. The depth of the beam is the height of one plate, 16.18 in. The frame model is used to determine the response of the basket structure and obtain load distributions, deformations, and stresses for normal handling and storage accident conditions. The results of the analysis are compared with the allowable stresses and deformations to assure that the design criteria are met.

D. Loads Acting on Basket

The loads acting on the basket are a result of handling operations, thermal load, and storage accidents.

The inertia g loads due to the handling operations are listed in Table 3.2-4. The inertia loads on the basket plates applied by the fuel assemblies and the load due to the weight of the plates themselves are represented by distributed loads on the compartment walls.

The decay heat load of the fuel produces differential thermal expansion between the basket and the cask body. There is ample gap between the end of the plates and the cavity wall for differential thermal expansion. Radial temperature differences occur with the

maximum temperatures at the center. The slots interrupt the heat transfer path, but the resulting axial gradient in the plate is negligible.

The maximum inertia g load due to the cask drop and tipping accident conditions is less than 75 g. (See Sections 3.2.11 and 3.2.12). This value (75 g) is used for analysis purposes.

E. Summary of Results

The calculated stresses and deformations due to the applied loadings are listed in Table 4.2-10. It can be seen that the maximum stresses due to handling and accident loads do not exceed the allowable stress values. Plastic hinges do not form at the slot or center of the plates.

4.2.1.3 Trunnions

A. Description

Six removable trunnions are bolted to the cask body, four near the top and two near the bottom. The trunnions consist of an outer shoulder (small diameter), an inner shoulder (large diameter), and a trunnion flange which is bolted to the cask body by twelve 1.5 in. diameter bolts. The outer shoulder is used for lifting. The inner shoulder is used for rotation of the cask between horizontal and vertical and for support during transfer. The trunnions are shown in Fig. 3.2-7 and on drawing 971-002 in Appendix 1A.

B. Design Bases and Criteria

The trunnions are designed in accord with the design requirements of ANSI 14.6[3] in addition to the requirements herein. The trunnions are constructed to the requirements of ASME material specification SA-5641 Type 630. The bolt material conforms to ASME

material specification SA-320, Gr.L43. The temperature at which the mechanical properties are obtained is 300°F.

Each pair of trunnions is evaluated for a vertical lift, on the outer shoulders of the trunnions, equivalent to three and five times the weight of the fully-loaded cask (inertia g loads of 3g and 5g statically applied). For three times the weight, the maximum tensile stresses shall not exceed the minimum yield strength of the trunnion materials. For five times the weight, the minimum ultimate strength of the trunnion materials shall not be exceeded.

The trunnions are also evaluated for the loads due to tilting and transfer from the pool area to a storage pad. These loads shall not result in maximum tensile stresses exceeding the minimum yield strength of the material.

C. Method of Analysis

The trunnion shoulders, flange, and bolts are analyzed for the worst load which is the lifting load acting on the outer shoulder.

The trunnion shoulders are analyzed assuming they are cantilevered from the flange. The bending and shear stresses, and stress intensities due to the applied loads are calculated at the base of each shoulder and the results are compared to the allowable stress criteria.

The trunnion flange is analyzed using a conservative approach. The applied bending moment is assumed to be simply reacted by the tension of the bolts and the bearing pressure (contact force) at the flange cask body interface.

The trunnion bolts are also analyzed in a conservative manner by disregarding the bolt preload contribution, and by equating the applied moment to the moments of the bolt loads about a pivot point on the vector of the resultant bearing force.

D. Loads Acting on Trunnions

The load acting on the trunnions are a result of the handling operations due to lifting, tilting, and transfer. The inertia g loads due to these handling operations are listed in Table 3.2-4. The maximum loads on the trunnion outer shoulder are the 3g and 5g loads due to the vertical lift. The maximum load on the trunnion inner shoulder is 0.75 g which occurs during the tilting operation.

E. Summary of Stresses

The calculated stresses on the trunnion shoulders are reported in Table 4.2-11. The maximum stress intensities occur at the base of the outer (Section A-A) and inner (Section B-B) shoulder. The stresses for a 3 g load are 46,190 psi and 34,850 psi, respectively, which are less than the minimum yield strength of 93,000 psi for the material. The stresses for a 5 g load are 77,000 psi and 58,000 psi, respectively, which are both less than the minimum ultimate strength of 133,000 psi for the trunnion material.

The calculated stresses acting on the trunnion flange and/or bolts are listed in Table 4.2-12. The maximum stress intensities in the flange and bolts due to the 3 g and 5 g loads are considerably less than the minimum yield and ultimate strengths of the flange and bolt materials. The friction force acting at the trunnion flange-cask body interface is larger than the load applied to the trunnion until the load exceeds 3.6 g. Therefore, the bolts do not carry a shear load for the 3 g case as shown in Table 4A.7-2. The bolts do carry a shear load in 5 g case; but the combined stress intensity is well below the ultimate strength.

Based on the comparison of analysis results with allowable values, it is concluded that design criteria have been met.

4.2.1.4 Outer Shell

A. Description

The outer shell (Drawing 971-001) consists of a cylindrical shell section with closure plates at each end. The closure plates are welded to the outer surface of the body. The outer shell provides an enclosure for the resin-filled aluminum containers and maintains the resin in the proper location with respect to the active length of the spent fuel assemblies in the cavity. The outer shell has no other structural function.

The outer shell is shown in Drawing 971-001 in Appendix 1A.

B. Design Bases and Criteria

The outer shell is designed for the loads due to handling operations and a pressure differential of 25 psi. The material is carbon steel which conforms to an ASTM material specification or equivalent. The maximum operating temperature is 250°F. The outer surface of the outer shell is protected by a metallic coating and paint. The thickness of the outer shell is based on dose rate requirements as well as structural requirements.

The maximum tensile stress in the outer shell due to the application of normal handling loads and pressure loads is not to exceed the minimum yield strength of the material. The resin and the aluminum containers are not considered to have load-carrying capability. The outer shell may undergo local plastic deformation due to the cask drop and tipping accidents and the neutron resin shield may be crushed. The dose rate limits for accident conditions are not to be exceeded.

C. Method of Analysis

The outer shell is analyzed using simplified conservative methods and assumptions. The cylindrical shell section is analyzed as a simple beam for handling loads and as a cylinder under internal pressure. The closure plates are analyzed as plates cantilevered from the cask body for both the handling and pressure loads.

D. Loads Acting on Outer Shell

The loads acting on the outer shell are a result of the handling operations and internal pressure. The inertia g loads due to the handling operations are listed in Table 3.2-4. The g values are multiples of the weights acting on the outer shell including its own weight.

The internal pressure is a result of outgassing in the resin material. A pressure relief value is provided in the outer shell to limit the pressure build-up. Therefore, an internal pressure of 25 psi accounts for this effect and for the reduced external pressure of 3 psi.

E. Summary of Stresses

The combined stress intensities in the outer shell and closure plates are reported in Table 4.2-13. The maximum stress intensity occurs in the closure plate at the junction between the plate and the containment vessel. These stresses are lower than the allowable values therefore the design criteria are met.

4.2.2 Installation Layout

The details of installation layout for an ISFSI are site specific. Typical installations have been depicted in Figures 1.1-2 and 1.1-3.

4.2.5 Individual Unit Description

The TN-24 dry storage cask is the individual unit. It is described in Section 1.2 and 1.3. The function, components and design bases of the TN-24 cask are also been described in Sections 1.2 and 1.3.

The safety-related components of the cask are listed in Table 3.4-1. The cask components are designed and fabricated under a quality assurance program which meets the requirements of 10CFR50 Appendix B.

TABLE 4.2-1

DESIGN BASES FOR CONTAINMENT VESSEL

Code Classification:	ASME Section III, Subsection NB
Rated Pressure (1):	250 psi
Rated Temperature:	350°F
Internal Atmosphere:	Helium
Closures:	
Lid	Flanged & bolted; double metallic O-rings
Lid Penetrations	Bolted, metallic O-rings
Instrumentation Access Openings:	To be determined
Material:	
Cask body	SA-350, Gr.LF1
Lid	SA-350, Gr.LF1
Bolts	SA-320, Gr.L43
Surface protection:	
a) Interior containment vessel vessel surfaces	Metallic Coating
b) Exterior exposed surfaces	Metallic Coating and Paint
c) Sealing surfaces	Stainless Steel Overlay

Containment Vessel Dimensions:

a) I.D. and cavity length to be minimum consistent with the requirement of the cask capacity.

b) Thicknesses (radial, top and bottom) shall be based on lowest dose rates consistent with weight limitations and neutron shield thickness requirements.

Note (1) This value is intended to exceed any pressure resulting from the combination of loading conditions and is a Primary Service Loading Condition.

TABLE 4.2-2a

STRESS LIMITS (1)

Primary Service

Classification	Stress Intensity Limit
P_m	S_m
P_L	$1.5\ S_m$
P_m (or P_L) + P_b	$1.5\ S_m$

Level A

Classification	Stress Intensity Limit
P_m (or P_L) + P_b + Q	$3S_m$
P_m (or P_L) + P_b + Q + F	S_a

Level D (2)

Classification	Stress Intensity Limit
P_m	Smaller of $2.4\ S_m$ or $0.7\ S_u$
P_L	Smaller of $3.6\ S_m$ or S_u
P_m (or P_L) + P_b	Smaller of $3.6\ S_m$ or S_u

NOTES: (1) Terms are as defined in ASME B&PV Code, Section III, Article NB-3200 and Appendix XIII.

(2) Limits are in accordance with ASME B&PV Code, Section III, Appendix F.

TABLE 4.2-2b

ASME CODE STRESS LIMITS FOR BOLTS (1)

Primary Service

Classification	Stress Intensity Limit
P_m (Tensile)	S_m

Level A and Level B

Classification	Stress Intensity Limit
P_m (Tensile)	$2S_m$
$P_L + P_b$ (Tensile + Bending)	$3S_m$
Combined	$3S_m$

Level D (2)

Classification	Stress Intensity Limit
P_m (Tensile)	Smaller of S_y or $0.7\ S_u$
$P_L + P_b$ (Tensile + Bending)	S_u
Shear	Smaller of $0.42\ S_u$ or $0.6\ S_y$
Combined Shear & Tension	$\frac{(f_t)^2}{(F_{tb})^2} + \frac{(f_v)^2}{(F_{vb})^2} \leq 1$

NOTES: (1) Terms are defined in ASME B&PV Code, Section III, Article NB-3200.

(2) Limits are in accordance with ASME B&PV Code, Section III, Appendix F.

TABLE 4.2-3

MAGNITUDE OF LOADS ACTING ON CONTAINMENT VESSEL
FOR PRIMARY SERVICE LOADS

Load	Primary Service Load Combinations		
	P1	P2	P3
Pressure (psi)			
Internal	-	32	250
External	25	-	-
Distributed (1) (lb/in. and lb/in.^{2})			
Weight Wind/Water Seismic Handling	4900/290	4900/290	-
Attachment Loads			
Handling			
Radial Force (lb)	-	-	0.225×10^6
Longitudinal Moment (in.-lb.)	-	-	2.6×10^6
Circumferential Moment (in.-lb.)	-	-	1.3×10^6
Bolt Loads (lb)			
Preload	1.79×10^6	1.79×10^6	1.79×10^6

(1) Values listed are maximum values for distributed load effects.

TABLE 4.2-4

MAGNITUDE OF LOADS ACTING ON CONTAINMENT VESSEL
FOR LEVEL A SERVICE LOADS

Load	Level A Service Load Combinations		
	A1	A2	A3
Pressure (psi)			
Internal	32	250	-
External	-	-	25
Distributed (1) (lb/in. and lb/in.^{2}) Weight, Wind/Water, Seismic, Handling	4900/290	-	4900/290
Attachment Loads			
Handling			
Radial Force (lb)	0.225×10^6	0.225×10^6	0.225×10^6
Longitudinal Moment (in.-lb.)	2.6×10^6	2.6×10^6	2.6×10^6
Circumferential Moment (in.-lb.)	1.3×10^6	1.3×10^6	1.3×10^6
Bolt Loads (lb)(2)			
Preload	1.79×10^6	1.79×10^6	1.79×10^6
Thermal			
Decay Heat + Solar Load	[See Table 3.2-7]		-
Rain	Cold Rain on Hot Cask		-

(1) Values listed are maximum values for distributed load effects.

TABLE 4. 2-5

MAGNITUDE OF LOADS ACTING ON CONTAINMENT VESSEL

FOR LEVEL B SERVICE LOADS

Load	Level B Service Load Combinations	
	B1	B2
Pressure (psi)		
Internal	32	250
External	-	-
Distributed (1) (lB/in. and lb/in.^{2})		
Weight		
Wind/Water		
Seismic	4900/290	-
Handling		
Attachment Loads		
Handling		
Radial Force (lb)	0.225×10^6	0.225×10^6
Longitudinal Moment (in.-lb)	2.6×10^6	2.6×10^6
Circumferential Moment (in.-lb)	1.36×10^6	1.36×10^6
Bolt Loads (lb)		
Preload	1.79×10^6	1.79×10^6
Thermal		
Decay Heat + Solar Load	(See Table 3.2-7)	

(1) Values listed are maximum values for distributed load effects.

TABLE 4.2-6

MAGNITUDE OF LOADS ACTING ON CONTAINMENT VESSEL

FOR LEVEL C SERVICE LOADS

Load	Level C Service Load Combinations	
	C1	C2
Pressure (psi)		
Internal	250	-
External	-	25
Distributed [1] (lb/in. and lb/in^2)		
Weight	4900/290	4900/290
Wind/Water		
Bolt Loads (lb)		
Preload	1.79×10^6	1.79×10^6
Thermal		
Decay Heat + Solar Load	[See Table 3.2-7]	
Minor Fire	(2)	

(1) Values listed are maximum values for distributed load effects

(2) Negligible effect

TABLE 4.2-7

MAGNITUDE OF LOADS ACTING ON CONTAINMENT VESSEL

FOR LEVEL D SERVICE LOADS

Level D Service Load Combinations

Load	D1	D2	D3	D4	D5	D6	D7
Pressure (psi)							
Internal	250	250	250	250	250	-	250
External	-	-	-	-	-	25	-
Distributed (1)							
(lb/in and lb/in.^{2}	4900/290		-	-	-	4900/290	
Weight							
Wind							
Seismic							
Handling (lb)(2)	-	-	-	-	-	-	-
Bolt Loads (lb)							
Preload (total)	1.79×10^6	1.79×10^6	1.79×10^6	1.79×10^6	1.79×10^6	1.79×10^6	1.79×10^6
Thermal (3)	-	-	-	-	-	-	-
Inertia Loads (g)							
Cask Drop	-	-		-	-	-	-
Vertical			100				
Horizontal			69				
Corner-over C.G.			27				
Cask Tippling	-	-			-	-	-
About Trunnions				55			
About Base				62			
Tornado Missiles (Max)							
Missile A (lb)							0.68×10^6
Missile B (lb)							1.38×10^6

(1) Maximum values of distributed loads, are listed

(2) Handling loads i.e. attachment loads at trunnions are not acting during accidents

(3) Thermal loads which induced secondary stresses, do not have to be considered in combination with other accident conditions. The major fire is evaluated separately.

TABLE 4.2-8a
COMPARISION OF ACTUAL WITH ALLOWABLE STRESS
INTENSITY IN THE CONTAINMENT VESSEL
LID FLANGE AT SEAL

LOADING COMBINATION	STRESS CATEGORY	SURFACE	MAXIMUM COMBINED STRESS COMPONENTS t	l	r	PRINCIPAL STRESSES (PSI) 1	2	3	STRESS INTENSITY (PSI)	ALLOWABLE STRESS INTENSITY (PSI)
PRIMARY SERVICE P3	P_m			N O T	A P P L I C A B L E					
	P_L+P_b	INNER	-20950	-250	-20950	3935	-17015	-24885	-250	24535	1.5 S_m =
		OUTER	20950	0	20950	3935	24905	16995	0	24905	26175
	P_m			N O T	A P P L I C A B L E					
LEVEL A A2	P_L+P_b	INNER	-20950	-250	-20950	3935	-17015	-24885	-250	24635	1.5 S_m =
		OUTER	20950	0	20950	3935	24905	16995	0	24905	26175
	P_L+P_b+Q	INNER	-31880	-250	-31880	5825	-26055	-37705	-250	37455	3 S_m =
		OUTER	31600	0	31600	5825	37425	25775	0	37425	52350
	P_m			N O T	A P P L I C A B L E					
LEVELS B&C B2	P_L+P_b	INNER	-20950	-250	-20950	3935	-17015	-24885	-250	24635	1.5 S_m =
		OUTER	20950	0	20950	3935	24905	16995	0	24905	26175
	P_L+P_b+Q	INNER	-31880	-250	-31880	5825	-26055	-37705	-250	37455	3 S_m =
		OUTER	31600	0	31600	5825	37425	25775	0	37425	52350
LEVEL D D4	P_L+P_b+Q (D4)	INNER	-36480	-250	-36480	9165	-27315	-45645	-250	45395	3.6 S_m or S_u
		OUTER	36480	0	36480	9165	45645	27315	0	45645	= 60000

TABLE 4.2-8b

COMPARISION OF ACTUAL WITH ALLOWABLE STRESS INTENSITY IN THE CONTAINMENT VESSEL SHELL AWAY FROM ENDS

LOADING COMBINATION	STRESS CATEGORY	SURFACE	MAXIMUM COMBINED STRESS COMPONENTS t	l	r		PRINCIPAL STRESSES (PSI) 1	2	3	STRESS INTENSITY (PSI)	ALLOWABLE STRESS INTENSITY (PSI)
	P_m	INNER	1040	640	-250	0	1040	640	-250	1290	S_m =
PRIMARY		OUTER	790	640	0	0	790	640	0	790	17450
SERVICE	P_L+P_b	INNER	-1000	-750	0	3600	2730	-4480	0	7200	1.5 S_m =
		OUTER	-1000	-750	0	3600	2730	-4480	0	7200	26175
LEVEL A	P_m	INNER	1040	640	-250	0	1040	640	-250	1290	S_m =
		OUTER	790	640	0	0	790	640	0	790	17450
A2	P_L+P_b	INNER	-1000	750	0	3600	2730	-4480	0	7200	1.5 S_m =
		OUTER	-1000	750	0	3600	2730	-4480	0	7200	26175
	P_L+P_b+Q	INNER	-6000	-6890	-250	3600	-2820	-10070	-250	9822	3 S_m =
		OUTER	-4000	5390	0	3600	6610	-5220	0	11834	52350
	P_m	INNER	1040	640	-250	0	1040	640	-250	1290	S_m =.
		OUTER	790	640	0	0	790	640	0	790	17450
LEVELS B&C	P_L+P_b+Q	INNER	-1000	-750	0	3600	2730	-4480	0	7200	1.5 S_m =
B2		OUTER	-1000	-750	0	3600	2730	-4480	0	7200	26175
	P_L+P_b+Q	INNER	-6000	-6890	-250	3600	-2820	-10072	-250	9820	3 S_m =
		OUTER	-4000	5390	0	3600	6610	-5221	0	11830	52350
LEVEL D	P_L+P_b	INNER	40530	12490	-250	0	40530	12490	-250	40780	3.6 S_m or S_u
D3 & D7	(D3)	OUTER	-38700	-11210	0	0	-38700	-11210	0	38700	= 60000
	P_L+P_b	INNER	24160	7580	-250	6485	26395	5340	-250	26645	3.6 S_m or S_u
	(D&7)	OUTER	19810	6350	-27300	6485	20685	-28170	6350	34530	= 60000

TABLE 4.2-8c
COMPARISION OF ACTUAL WITH ALLOWABLE STRESS
INTENSITY IN THE CONTAINMENT VESSEL
SHELL AT JUNCTION WITH BOTTOM PLATE

LOADING COMBINATION	STRESS CATEGORY	SURFACE	MAXIMUM COMBINED STRESS COMPONENTS				PRINCIPAL STRESSES (PSI)			STRESS INTENSITY (PSI)	ALLOWABLE STRESS INTENSITY (PSI)
			t	l	r		1	2	3		
	P_m	INNER	950	350	-250	0	950	350	-250	1200	S_m =
PRIMARY		OUTER	700	350	0	0	700	350	0	700	17450
SERVICE	P_L+P_b	INNER	-1460	1580	-250	2150	2690	-25730	-250	2940	1.5 S_m =
P3		OUTER	-1580	-2880	0	2150	0	-4480	0	4490	26175
LEVEL A	P_m	INNER	950	350	-250	0	950	350	-250	1200	S_m =
		OUTER	700	350	0	0	700	350	0	700	17450
A2	P_L+P_b	INNER	-1450	1580	-250	2150	2690	-2570	-250	5270	1.5 S_m =
		OUTER	-1580	-2880	0	2150	0	-4480	0	4490	26175
	P_L+P_b+Q	INNER	-12540	-7665	-250	5030	-4510	-15690	-250	15440	3 S_m =
		OUTER	-10350	6365	0	5030	7760	-11750	0	19510	52350
LEVELS B&C	P_m	INNER	950	350	-250	0	950	350	-250	1200	S_m =
B2		OUTER	700	350	0	0	700	350	0	700	17450
	P_L+P_b	INNER	-1460	1580	-250	2150	2690	-2573	-250	5270	1.5 S_m =
		OUTER	-1580	2880	0	2150	0	-4480	0	4490	26275
	P_L+P_b+Q	INNER	-12540	-7665	-250	5030	-4510	-15690	-250	15440	3 S_m =
		OUTER	-10350	6365	0	5030	7760	-11750	0	19510	52350
LEVEL D	P_L+P_b	INNER	-6825	25840	-250	4510	26450	-7440	-250	33890	3.6 S_m or S_u
:D31		OUTER	-8060	13660	0	4510	14560	-8960	0	23520	= 60000

TABLE 4.2-8d
COMPARISION OF ACTUAL WITH ALLOWABLE STRESS
INTENSITY IN THE CONTAINMENT VESSEL
BOTTOM PLATE AT CENTER

LOADING COMBINATION	STRESS CATEGORY	SURFACE	MAXIMUM COMBINED STRESS COMPONENTS t	l	r		PRINCIPAL STRESSES (PSI) 1	2	3	STRESS INTENSITY (PSI)	ALLOWABLE STRESS INTENSITY (PSI)
PRIMARY SERVICE P3	P_m		N O T			A P P L I C A B L E					
	P_L+P_b	INNER	-2305	-250	-2305	0	-2305	-2305	-250	2055	1.5 S_m = 26175
		OUTER	-1610	0	-1610	0	-1610	-1610	0	1610	
LEVEL A	P_m		N O T			A P P L I C A B L E					
	P_L+P_b	INNER	-2305	-250	-2305	0	-2305	-2305	-250	2055	1.5 S_m = 26175
		OUTER	-1610	0	-1610	0	-1610	-1610	0	1610	
	P_L+P_b+Q	INNER	-2120	-250	-2120	0	-2120	-2120	-250	1870	3 S_m = 52350
		OUTER	1760	C	1760	0	1760	1760	0	1760	
LEVELS B&C B2	P_m		N O T			A P P L I C A B L E					
	P_L+P_b	INNER	-2305	-250	-2305	0	-2305	-2305	-250	2055	1.5 S_u = 26175
		OUTER	-1610	0	-1610	0	-1610	-1610	0	1610	
	P_L+P_b+Q	INNER	-2120	-250	-2120	0	-2120	-2120	-250	1870	3 S_m = 52350
		OUTER	1760	0	1760	0	1760	1760	0	1760	
LEVEL D D3 & D7	P_L+P_b (D3)	INNER	-35190	-1990	-35190	0	-35190	-35190	-1990	33200	3.6 S_m or S_u = 60000
		OUTER	35100	4000	35100	0	35100	35100	-4000	39100	
	P_L+P_L (D7)	INNER	13725	-250	13725	6485	21210	7240	-250	20460	3.6 S_m or S_u = 60000
		OUTER	-17640	27300	17640	6485	-15010	-30720	-17640	15710	

TABLE 4.2-8c

SUMMARY OF MAXIMUM STRESS INTENSITITES AND
ALLOWABLE STRESS LIMITS FOR THE CONTAINMENT VESSEL

SERVICE CONDITION	LOCATION	MAXIMUM STRESS INTENSITY (psi)	ALLOWABLE (psi)	MARGIN OF SAFETY
PRIMARY	IN THE SHELL	P_m = 1,240	S_m = 17,450	12.5
LEVELS A B and C	IN THE LID AT THE SEAL LOCATION	P_L+P_b = 24,905	1.5 S_m = 26,175	0.05 (1)
		P_L+P_b+Q = 37,455	3 S_m = 52,350	0.4
LEVEL D	IN THE LID AT THE SEAL LOCATION	P_L+P_b = 45,645	3.6 S_m or S_u = 60,000	0.3

(1) It should be noted that the stresses and margin of safety is based on an internal pressure of 250 psi. It is not anticipated that the pressure would even reach one-half this value. Therefore, actual stresses would be much lower and margins of safety higher.

TABLE 4.2-8f

SUMMARY OF MAXIMUM STRESS INTENSITY AND ALLOWABLE STRESS LIMITS FOR LID BOLTS

Service Condition	STRESS CATEGORY				ALLOWABLE STRESS INTENSITY (PSI)				Margin of Safety
	Tensile	Tensile + Bending	Shear	Combined	Tensile	Tensile + Bending	Stress Shear	Combined	
Primary Service	25000	-	-	-	S_m=31200	-	-	-	0.25
Levels A, B and C	25000	-	-	-	$2S_m$=62400	-	-	-	1.5
	-	47200	-	-	-	$3S_m$=93600	-	-	0.98
	-		10880	51980	-	-	$3S_m$=93600	-	0.8
Level D	38200	-	-	-	$0.7S_u$=78050	-	-	-	
	-	60400	-	-	-	S_u=111500	-	-	
	-	-	10880	-	-	-	-	0.42 S_u or 0.6S_y = 46830	

$$\frac{(f_t)^2}{(f_{tb})^2} + \frac{(f_v)^2}{(f_{tu})^2} = \frac{(60400)^2}{(111500)^2} + \frac{(10880)^2}{(46830)^2} = 0.29 + 0.06 = 0.35 \leq 1.0$$

TABLE 4.2-9

DESIGN BASIS FOR BASKET

Number and Type of Fuel Assemblies	24 - W PWR (intact fuel)
Fuel Assembly Dimensions (after irradiation)	8.426" x 8.426" x 160.46"
Active Fuel Length	144 in.
Maximum Fuel Assembly Weight	1500 lb.
Basket Material	Borated Stainless Steel* (1.0% Boron)
Maximum Operating Temperature	650°F

* All plates are coated with copper

TABLE 4.2-10

COMPARISON OF ACTUAL WITH ALLOWABLE
STRESS AND DEFORMATIONS IN BASKET

LOADING	MAXIMUM STRESS/STRAIN (psi)	ALLOWABLE STRESS/STRAIN (psi)	MAXIMUM DEFLECTION (in.)
HANDLING, 3 g	4,380	25,840	0.0052
ACCIDENT CONDITION (1)	47,700	67,310	1,219
HORIZONTAL DROP	0.0927 in/in.	0.100	

(1) The design criteria for the accident load is not based on a single comparison of stress values. It is based on the condition that plastic hinges do not form, that strain levels are maintained and that the basket compartment walls maintain separation of adjacent fuel assemblies (See Appendix 4A, Section 4A.6.3.

TABLE 4.2-13

COMPARISON OF MAXIMUM STRESS INTENSITY
WITH ALLOWABLES IN OUTER SHELL

LOAD	MAXIMUM STRESS INTENSITY (psi)		ALLOWABLE STRESS (psi)
	OUTER SHOULDER	INNER SHOULDER	
INTERNAL PRESSURE PLUS 3 g HANDLING INERTIA LOAD	1,820	13,770	σ_y = 26,600

FIGURE 4.2-1

TN-24 CONTAINMENT VESSEL

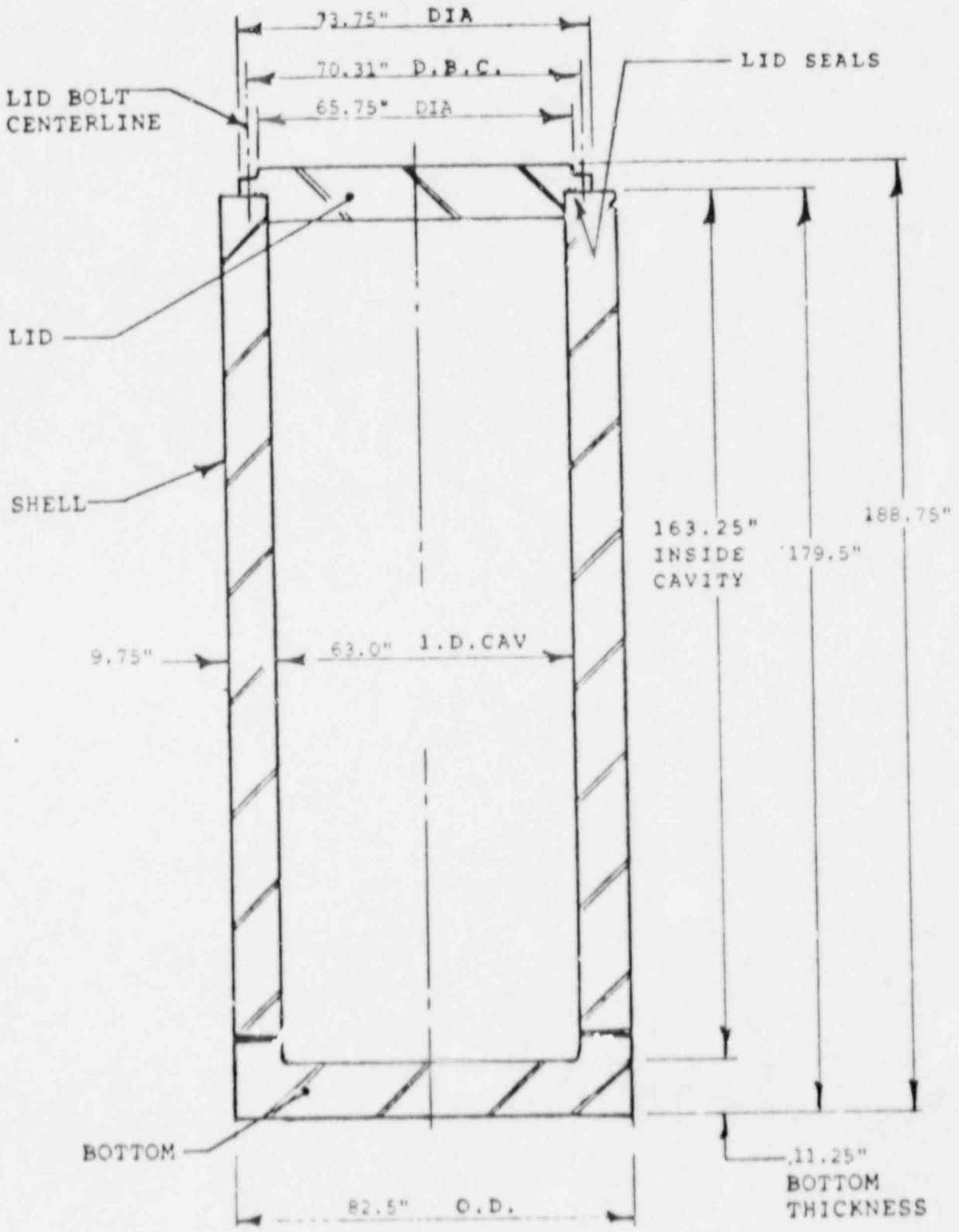

References for Section 4.2

1. "Rules for the Construction of Nuclear Power Plant Components," ASME Boiler and Pressure Vessel Code, Section III, Division 1 - Subsection NB, The American Society of Mechanical Engineers, New York.

2. "Rules for the Construction of Nuclear Power Plant Components," ASME Boiler and Pressure Vessel Code, Section III, Division 1 - Appendices, The American Society of Mechanical Engineers, New York.

3. "American National Standard for Special Lifting Devices for Shipping Containers Weighing 10,000 Pounds (4500 kg) or More for Nuclear Materials," ANSI N14.6, American National Standards Institute, New York, February 1978.

4.3 AUXILIARY SYSTEMS

The TN-24 dry storage cask is a totally passive system and requires no auxiliary systems for its operation. Information on the auxiliary systems of an ISFSI using TN-24 casks will be supplied by the license applicant.

4.4 DECONTAMINATION SYSTEMS

Systems for decontamination of equipment and personnel are site specific and will be addressed by the applicant for a site specific license under 10CFR Part 72.

4.5 SHIPPING CASK REPAIR AND MAINTENANCE

After the TN-24 casks have been loaded, decontaminated, and placed into storage at an ISFSI, no repair operations are anticipated which would require moving casks from their permanent storage location. Periodic maintenance procedures will consist of:

a. Washdown of exterior surfaces
b. Inspection and touchup on exterior surface protective coating
c. Annual calibration of leak detection instrumentation.

The cask sealing system, which is described in Section 3.3.2, may require maintenance if the leak rate through the lid seal or the penetration cover seals exceeds operational limits. The maintenance procedures would involve tightening of lid bolts and penetration cover bolts. If the leak rate does not decrease sufficiently, the cask could be transfered back to the fuel pool area where new seals would be installed or the protective cover could be replaced by a containment cover at the ISFSI site. The containment cover is essentially the same as the protective cover except that it contains double metallic seals and is thicker. The containment cover is bolted onto the cask, replacing the protective cover, and it becomes part of the containment boundary. The volume under the protective cover is backfilled with helium and a pressure transducer installed to monitor the "cavity" pressure. If desired, the containment cover could also be seal welded to the cask.

All the above maintenance procedures can be performed within the ISFSI area, without the need for cask transfer. Estimates of personnel exposure during these operations are presented in Section 7.4.

4.6 CATHODIC PROTECTION

Surface protection is provided for the TN-24 cask, both on the interior and exterior surfaces, by a metallic flame-sprayed coating. In addition, the exterior surfaces will be covered by a sealer which acts to protect the metal spray coating and provide a smooth surface for decontamination. Coating systems of this type have been developed to provide long-term service under the operating conditions anticipated for the TN-24 cask. The specific materials which will be used for the coating system will be selected based on a test program which is currently in progress. All seal seating surfaces will be stainless steel clad by weld overlay.

Although cathodic protection, as such, is not required because the inert gas internal atmosphere and the surrounding air atmosphere are poor electrolytes, many of the metal spray coatings do provide cathodic protection for the base metal. However, the principal purpose of the surface coatings is protection against other types of corrosion.

4.7 FUEL HANDLING OPERATING SYSTEMS

Fuel handling operation systems are site specific and will be addressed by the applicant for a site specific license under 10CFR Part 72.

APPENDIX 4A

STRUCTURAL ANALYSES OF TN-24 STORAGE CASK

4A.1 INTRODUCTION

This appendix contains the details of the structural analysis of the TN-24 storage cask which consists of the cask body, trunnions, outer shell and basket. The cask body consists of the cylindrical shell section, the integrally-welded bottom closure and the bolted on lid. The cask body, lid bolts and gaskets, and the port closures, constitute the primary pressure boundary which is hereafter referred to as the containment vessel. The detailed calculations for the containment vessel are given in Section 4A.5 below. The detailed calculations for the basket, trunnions, and outer shell, are presented in Sections 4A.6, 4A.7, and 4A.8, respectively.

The design basis and criteria for the containment vessel are in accordance with the ASME Boiler and Pressure Vessel Code, Section III, Subsection NB[1]. The stress criteria is also in accord with Subsection NB, Class 1 components. The allowable stress intensity value, Sm, is obtained from Table I-1.1[2]. The criteria are discussed in detail in Section 4.2.1.1.

The design criteria for the basket, trunnions, and outer shell, are described in Sections 4.2.1.2, 4.2.1.3 and 4.2.1.4, respectively.

4A.2 DESCRIPTION

A description of the storage cask is presented in Chapter 1. The individual descriptions of the cask body and components which were analyzed, are presented in each of the appropriate sections.

4A.3 LOADING CONDITIONS AND STRESSES

The loading conditions and the loads they produced on the containment vessel or components are identified and described in Section 3.2. The loads which are acting on the containment vessel or component are identified in each appropriate section herein. The effects of the accident loads on the containment vessel are addressed separately in Sections 4A.5.6 and 4A.5.7.

Stresses in the containment vessel due to each load are calculated and tabulated according to the appropriate stress categories and presented in the tables at the end of Section 4A.5. These stresses are summarized and compared with the allowable stress values in Section 4.2.1.1 for each loading combination identified in Section 3.2.13.

Stresses in the basket, trunnions and outer shell due to each load are calculated and tabulated in Sections 4A.6, 4A.7 and 4A.8, respectively. These stresses are summarized and compared with the appropriate allowable stress values in Sections 4.2.1.2, 4.2.1.3 and 4.2.1.4.

4A.4 MATERIALS PROPERTIES DATA

Physical and mechanical material property data for the containment vessel are obtained from the ASME Boiler and Pressure Vessel Code, Section III, Appendices[2], when available. Other sources which are used are identified separately.

The material property data used for the other components are given in the appropriate section. The materials property data used for the borated stainless basket material are based on the procurement specification in Appendix 4B.

4A.5 STRUCTURAL ANALYSIS OF THE CONTAINMENT VESSEL

The structural analysis of the containment vessel for all loads is presented herein. For purpose of analysis, the containment vessel is divided into separate areas and the analysis performed for each individual load. The results are then combined by superposition as appropriate.

The different areas are as follows:

i. Containment vessel at trunnions and outer shell
ii. Containment vessel to bottom closure plate junction
iii. Containment vessel to lid junction
iv. Containment vessel cylindrical shell

4A.5.1 Local Stresses at Connections to Containment Vessel

4A.5.1.1 Local Stresses Due to Attachment Loads Applied by Trunnions

Local membrane and bending stresses are induced in the shell of the containment vessel in the area of the trunnions. The lateral forces and bending moments are applied to the shell by the trunnion flange and the 12-1.5 in. diameter bolts which attach the trunnion to the shell. The radial force is a direct tensile or compressive load applied at the shell-trunnion flange interface.

4.A.5.1.1a Method of Analysis

The local stresses induced in the shell (referred to hereafter as the cylinder) by the trunnions are calculated using Bijlaard's method[3]. The modified set of reference curves of Reference 3, which take into account the results of actual vessel tests, are used. The trunnion is approximated by an equivalent attachment so that the curves of Reference 3 can be used to obtain the coefficients necessary to calculate membrane forces and moments in the cylinder induced by the applied loads. These coefficients are plotted for the cylinder parameter down to a value of 5 only. The

parameter for the cask body cylinder is 3.731. Therefore, these curves are replotted and extrapolated so that coefficients at the parameter of 3.731 can be obtained and the value of the membrane forces and moments calculated. With the membrane forces and moments, the membrane and bending stresses are calculated for each of the applied loads, i.e., radial force P, longitudinal moment M_A, and circumferential moment M_C. The computation sheet used in this method is shown in Table 4A.5-1.

4A.5.1.1b Model, Boundary Conditions and Assumptions

The cask body cylinder is assumed to be a hollow cylinder of infinite length. Since the trunnions are located well in from the ends of the body, this assumption is acceptable because the local effects are not significantly affected by the end restraints. This is conservative since the end restraint would reduce the local bending effects. The attachment parameter, β, is obtained by using an attachment radius, r_o, based on the bolt circle diameter. This is also conservative since it results in a lower value of β which results in higher calculated stresses.

4A.5.1.1c Input Data

The only required input data for this method are the dimensions of the trunnion and the cylinder. These are obtained from drawings 971-1 and -2 in Appendix 1A. The dimensions and Bijlaard parameters are listed in Table 4A.5-2.

4A.5.1.1d Applied Loads

The loads applied to the cylinder by the attachments are based on Section 3.2. The method by which these values are obtained is given Section 3.2.6. The magnitudes of the loads are listed in Table 4A.5-3 and shown in Fig. 4A.5-13.

The maximum longitudinal load occurs during vertical lifting. The cask is lifted by two trunnions and each takes one-half the load or 337,500 lb. The load is applied to the middle of the outer

trunnion shoulder, therefore, the longitudinal moment acting at the shell is 2.6×10^6 in-lbs. During a horizontal lift, four trunnions (two front and two rear) share the load. This results in a circumferential load and moment of 168,750 lb and 1.3×10^6 in-lbs respectively. During the horizontal lift, the longitudinal load per trunnion is less (Section 3.2, Fig. 3.2-3) than the longitudinal load during the vertical lift. Therefore, the latter is used for analysis and combined with the other loads. The maximum radial load is assumed to occur during transfer of the cask to the storage pad and is 225,000 lb per trunnion. All the loads are assumed to act simultaneously and at the same location on the cask shell (i.e., cylinder).

4A.5.1.1e Results

The tangential, σ_t, longitudinal, σ_l, and shear, τ, stresses due to the applied loads are listed in Table 4A.5-4. The radial stresses, σ_r, are zero. The local membrane stresses are categorized as P_L stresses and the bending stresses are categorized as Q stresses in accordance with Subsection NB of the ASME Boiler and Pressure Vessel Code[1]. These stresses are combined and the principal stresses and stress intensities are calculated and compared with ASME Code allowable stress intensity values presented in Section 4.2, Table 4.2-2.

4A.5.1.2 Local Stresses Due to Attachment Loads Applied by the Outer Shell Connection

The loads applied to the cask body cylinder by the outer shell are less in magnitude than the attachment loads acting at the trunnions. A comparison of the loads is given in Table 4A.5-5. The magnitudes of the loads applied by the outer shell are given in Section 4A.8.8. In addition the loads are applied over a greater contact area between the outer shell and cask body as compared to the trunnion-cask body interface. Therefore, if the stresses in the cask body cylinder at the trunnions are acceptable they are also acceptable at the outer shell connection.

4A.5.2 Stress Analysis of Junction of Cask Body Cylindrical Shell with the Bottom Closure Plate

4A.5.2.1 Description

This section describes the analysis performed and results obtained for the containment vessel at the junction of the cask body cylindrical shell with the bottom closure plate. A longitudinal section of the storage cask is shown in Figure 4A.5-1; more detail is available from drawing 971-1 in Appendix 1A.

4A.5.2.2 Method of Analysis

The cylinder and the bottom closure plate (referred to as the plate) are first analyzed as free bodies. The cylinder is assumed to be free at the edges and the plate simply supported. For each loading condition, stresses, deflections and rotations are obtained.

Then for each loading condition a compatibility analysis is performed by equating the deflection and rotation at the edge of the cylinder to the corresponding deflection and rotation of the plate at the connection with the cylinder. The discontinuity stress resultants (bending moments and shears) and the discontinuity stresses are thus obtained. The discontinuity analysis method used follows that described in Article A-6000 of the Appendices[2]. Other articles of Appendix A of the Appendices are also used in this section and are referenced as appropriate. The sign convention, arbitrarily chosen for the analysis, is as indicated in Figure 4A.5-2.

The stress components for each loading condition are calculated and categorized according to the ASME code, Subsection NB[1].

4A.5.2.3 Model, Boundary Conditions and Assumptions

The model of the cylinder and plate used in the analysis is shown in Figure 4A.5-3. The boundary conditions and assumptions made for the analysis are as follows:

a) Forces and moments are calculated based upon elastic behavior of the elements.

b) The cylinder and plate are of constant thickness.

c) The upper end of the cylinder is at a distance greater than $3/\beta$ from the junction of the cylinder with the bottom end:

Where

$$\beta = \left[\frac{3(1 - \nu^2)}{R_m^2 \, t_s^2}\right]^{1/4}$$

ν = Poisson's ratio, 0.3
R_m = mean radius of cylinder, 36,375 in.
t_s = cylinder thickness, 9.75 in.

The value of $3/\beta$ is approximately 45 in. and the cylinder length is 168.25 in. tnerefore the influence of the top edge on the bottom edge is negligible (Paragraph A2251[2]) and each end can be evaluated separately.

d) The statically-applied inertia loads due to the cask contents, resulting from handling operations, are assumed to act as a uniformly distributed load and are simulated by an equivalent pressure.

4A.5.2.4 Analysis

A. Internal Pressure

A.1a Free Body Displacements

Cylinder

The radial displacement of the mid-surface of a closed-end thick cylinder under internal pressure is given by (Para. A-6230, Article 6000(2)):

$$(W_L)_{CYL} = \frac{p R_i^2}{E(R_o^2 - R_i^2) R_m}\left(R_m^2 (1 - 2\nu) + R_o^2 (1 + \nu)\right) \qquad \text{Eq. 1}$$

And the rotation is:

$$(\theta_L)_{CYL} = 0 \qquad \text{Eq. 2}$$

Where

W = displacements, in.

θ = rotations, radians

p = pressure, 250 psi

R_m = mean cylinder radius, 36.375 in.

R_o = inside cylinder radius, 41.25 in.

R_i = outside cylinder radius, 31.5 in.

E = Young's modulus

ν = Poisson's ratio, 0.3

t = thickness of cylinder, 9.75 in.

Subscript L is the location at the junction of plate and cylinder (See Fig. 4A.5-2)

$$(W_L)_{CYL} = \frac{p}{E} \frac{(31.5)^2}{(41.25^2 - 31.5^2)\ 36.375} \times [36.375^2(1-2 \times 0.3) + 41.25^2(1 + 0.3)]$$

$$= 105.4 \frac{p}{E}$$

Plate

The radial displacement and the rotation at point L, Figure 4A.5-2, due to internal pressure is given by (A-5223, Article 5000[2]):

$$(W_L)_{PL} = - (t/2)(\theta_L)_{PL} \qquad \text{Eq. 3}$$

$$(\theta_L)_{PL} = P \frac{F_1}{E(t/R)^3} \qquad \text{Eq. 4}$$

Where

t = thickness of plate, 11.25
R = outer radius of plate, 41.25 in.
F_1 = geometry constant as defined in Para. A-5240 of Article A-5000[2])
= 1.01

Therefore

$$(\theta_L)_{PL} = +49.68 \frac{P}{E}$$

And

$$(W_L)_{PL} = -279.43 \frac{P}{E}$$

A.1b Free Body Stresses due to Internal Pressure

Cylinder

The stresses are (Para. A-2212, Article 2000[2]):

$$\sigma_t = p(1 + Z^2)/(Y^2 - 1) \qquad \text{Eq. 5}$$
$$\sigma_l = p/(Y^2 - 1) \qquad \text{Eq. 6}$$
$$\sigma_r = p(1 - Z^2)/(Y^2 - 1) \qquad \text{Eq. 7}$$

Where

σ_t = tangential stress
σ_l = longitudinal stress
σ_r = radial stress
$Y = R_o/R_i = 1.31$
$Z = R_o/R$, R being an intermediate radius between R_o and R_i where the stress is calculated

Subscript PL means bottom plate
Subscript CYL means cylinder
Subscript L is the location at the junction of plate and cylinder (See Fig. 4A.5-2)

Orientation of Stress	Inside Surface psi	Outside Surface psi
σ_t	+ 3.79 p	+ 2.79 p
σ_l	+ 1.4 p	+ 1.4 p
σ_r	- p	0

Plate

The stresses are (Para. A-5224, Article A-5000(2)):

$$\sigma_r = \frac{(x)\ p}{t(-t/R)^2}\left[(F_2) - \frac{3(3+\nu)r^2}{4R^2}\right] \qquad \text{Eq. 8}$$

$$\sigma_t = \frac{(x)\ p}{t(-t/R)^2}\left[(F_2) - \frac{3(1+3\nu)r^2}{4R^2}\right] \qquad \text{Eq. 9}$$

$$\sigma_l = (x - t/2)\left(p/t\right) \qquad \text{Eq. 10}$$

where

(x) = surface at which stress acts, in.
Note that inside surface is (-) t/2
p = internal pressure, 250 psi

t = plate thickness, 11.25 in.

R = outer radius of plate, 41.25 in.

ν = Poisson's ratio, 0.3

r = radius at which stress acts, in.

F_2 = geometry constant as defined in Para. A-5240, Article A-5000[2]

= 1.762

Therefore the stresses are:

Orientation of Stress		At Junction with Cylinder	At Center of Plate
		psi	psi
σ_r:	inside	- 2.14 p	- 11.84 p
	outside	+ 2.14 p	+ 11.84 p
σ_t:	inside	- 6.26 p	- 11.84 p
	outside	+ 6.26 p	+ 11.84 p
σ_l:	inside	- p	- p
	outside	0 p	0

A.2 Discontinuity Analysis for Internal Pressure

The calculated values of the deflection and rotation for the free cylinder and plate at point L, caused by the internal pressure, are different. To maintain continuity at point L, it is therefore necessary to apply uniform moments and shears at the cylinder edge and at the plate, to make those deflections coincide.

The expressions for the displacements due to discontinuity loads in the cylinder are (Para. A-2243 Article A-2000[2]).

$$\left.\begin{aligned} (W_L)_{CYL} &= \frac{1}{2\beta^3 D} Q_L + \frac{1}{2\beta^2 D} M_L \\ (\theta_L)_{CYL} &= \frac{1}{2\beta^2 D} Q_L + \frac{1}{\beta D} M_L \end{aligned}\right\} \quad \text{Eq. 11}$$

Where

Q_L = distributed discontinuity force at junction L, lb/in.
M_L = distributed discontinuity moment at junction L, in-lb/in.
$D = E\ t^3_{CYL}/12(1-\nu^2) = 84.8\ E$
t_{CYL} = thickness of cylinder, 9.75 in.
$\beta = 0.064\ in.^{-1}$

For this calculation β was based on the outer radius of the shell, 41.25 in rather than the inner shell rasius of 36.375 in. This results in slightly higher stresses.

Therefore

$$(W_L)_{CYL} = (23\ \theta_L + 1.43\ M_L)1/E$$

$$(\theta_L)_{CYL} = (1.43\ Q_L + 0.184\ M_L)1/E$$

The expression for the discontinuity loads in the plate are (Para. A-5223.2, Article A-5000(2):

$$(W_L)_{PL} = \frac{-2F3}{3E(t/R)}\ Q_L - \frac{F3}{ER(t/R)^2}\ M_L$$

Eq. 12

$$(\theta_L)_{PL} = \frac{F3}{ER(t/R)^2}\ Q_L - \frac{2F3}{ER^2(t/R)^3}\ M_L$$

Where

F_3 = geometry constant as defined in A-5240 of Article A-5000(2)
= 3.42
t = plate thickness, 11.25 in.
R = radius of outer edge of plate, 41.25 in.

Therefore

$$(W_L)_{PL} = (-8.36\ Q_L + 1.11\ M_L)1/E$$

$$(\theta_L)_{PL} = (1.11\ Q_L - 0.2\ M_L)1/E$$

Adding to these displacements those due to the pressure, yields the expressions for the total displacements for the cylinder and plate respectively as follows:

For the cylinder

$$(W_L)_{CYL} = (23\ Q_L/E + 1.43\ M_L/E + 105.4\ p/E) \quad \text{Eq. 11a}$$
OUTWARD DISPLACEMENT +

$$(\theta_L)_{CYL} = (1.43\ Q_L/E + 0.184\ M_L/E + 0) \quad \text{Eq. 11b}$$
COUNTER CLOCKWISE ROTATION +

For the plate

$$(W_L)_{PL} = (-8.36\ Q_L/E + 1.11\ M_L/E - 279.43p/E) \quad \text{Eq. 12a}$$
OUTWARD DISPLACEMENT +

$$(\theta_L)_{PL} = (1.11\ Q_L/E - 0.2\ M_L/E + 49.68\ p/E) \quad \text{Eq. 12b}$$
COUNTER CLOCKWISE ROTATION +

By imposing the condition that the total displacements of the cylinder and the plate must be compatible, i.e.

$$W_{\text{Total cylinder}} = W_{\text{Total plate}}$$

$$\theta_{\text{Total cylinder}} = \theta_{\text{Total plate}}$$

This provides two equations relating the discontinuity forces. These are:

$$31.36\ Q_L + 0.32\ M_L = -384.83p$$

$$0.32\ Q_L + 0.384\ M_L = 49.68p$$

or in matrix form

$$\{K_\delta\} \times \{F\} = \{\Delta\} \qquad \text{Eq. 13}$$

where

$$\{K_\delta\} = \begin{Bmatrix} 31.36 & 0.32 \\ 0.32 & 0.382 \end{Bmatrix} \times 1/E$$

$$\{F\} = \begin{Bmatrix} Q_L \\ M_L \end{Bmatrix} \; ; \; \{\Delta\} = \begin{Bmatrix} -384.83 \\ 49.68 \end{Bmatrix} \times p/E \qquad \text{Eq. 13a}$$

Multiplying both members of Eq. 13 by $[K_\delta]^{-1}$ yields

$$\{F\} = \{K_\delta\}^{-1} \{\Delta\} \qquad \text{Eq. 14}$$

where

$$\{K_\delta\}^{-1} = \begin{Bmatrix} 0.0318 & -0.0264 \\ -0.0264 & 2.64 \end{Bmatrix} E \qquad \text{Eq. 14a}$$

is the inverse of $[K_\delta]$.

The final expression for the discontinuity forces caused by the internal pressure is:

$$\begin{Bmatrix} Q_L \\ M_L \end{Bmatrix} = \begin{Bmatrix} -13.54 \\ 141.29 \end{Bmatrix} \times p \qquad \text{Eq. 14a}$$

Eq. 14a gives the values of the discontinuity moment and shear as a function of pressure. When these values are substituted back into Equations 11 and 12, the displacements resulting from discontinuity loads are obtained. Only the displacements for the cylinder which are required to calculate the discontinuity stresses are given here:

$$\begin{Bmatrix} W_{L\ CYL} \\ \theta_{L\ CYL} \end{Bmatrix} = \begin{Bmatrix} -8.985 \\ 6.635 \end{Bmatrix} \times p/E \qquad \text{Eq. 14b}$$

Now that the discontinuity resultant forces and displacements are obtained, the discontinuity stresses in the cylinder and plate can be calculated using the following general expressions:

For the cylinder

$$\left.\begin{aligned} \sigma_t &= \frac{N_t}{t_{CYL}} \pm \frac{6(\upsilon M_L)}{(t_{CYL})^2} \\ \sigma_l &= \frac{6M_L}{(t_{CYL})^2} \end{aligned}\right\} \qquad \text{Eq. 15}$$

Where N_t = resultant tangential force per unit length, lb/in.

$$N_t = \frac{E\, t_{CYL}\ (W_L)_{CYL}}{R_m} \qquad \text{Eq. 16}$$

and t_{CYL} = cylinder thickness, 9.75 in.
ν = Poisson's ratio, 0.3
M_L = discontinuity moment, in.-lbs./in.
$(W_L)_{CYL}$ = displacement in cylinder at L, in.
R_m = mean radius of cylinder, 36.375 in.

For the plate

$$\sigma_r = \sigma_t = \frac{F_4}{t}\left(1 - 6(x)\right) Q_L - \frac{12F_4\ (x)\ M_L}{t^3} \qquad \text{Eq. 17}$$

Where F_4 = geometry constant as defined in Para. A-5240, Article 5000(2).
= 0.922
t = plate thickness, 11.25 in.
(x) = surface at which stress acts
Note that inside surface is (-) t/2
Q_L = discontinuity shear force, lbs/in.
M_L = discontinuity moment, in-lbs/in.

Direction of action of Q_L and M_L

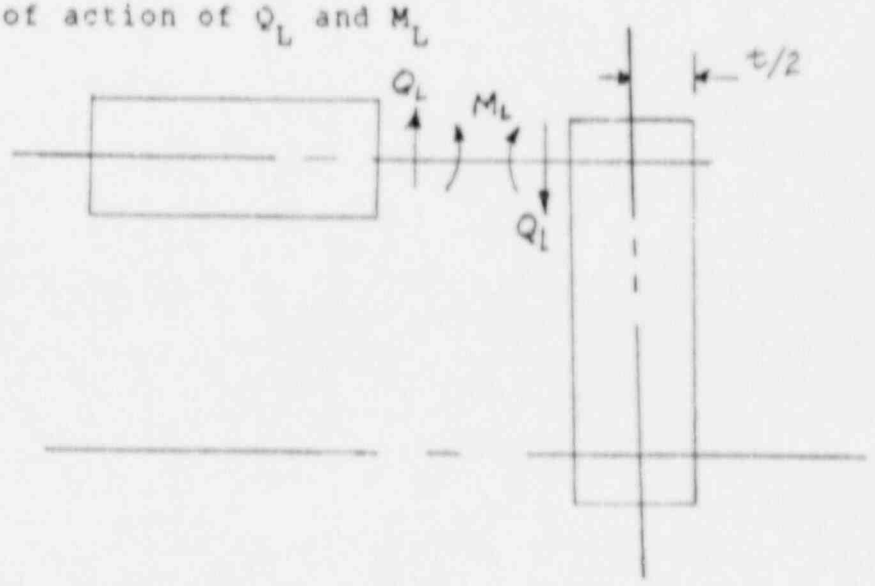

These stresses are summarized below:

Orientation of Stress		Cylinder psi	Plate at Junction and Center psi
σ_t:	inside	(0.25 + 2.68) p	1.74 p
	outside	(0.25 - 2.68) p	- 3.96 p
σ_l:	inside	+ 8.94 p	0
	outside	- 8.94 p	0
σ_r:	inside	0	1.74 p
	outside	0	- 3.96 p

This completes the analysis for the internal pressure.

B. Loads Due to Handling Operations

The loads which occur on the cask during handling are described in Section 3.2.6. The maximum load which occurs during handling is a 3 g or 3 times the weight of the cask on the crane hook. The orientation of the cask is vertical when this maximum load occurs. For the analysis of the junction of the cylinder to bottom plate, the loads on the bottom plate are the weights of the fuel, basket, contained water and the bottom plate itself. This is assumed to be a statically applied load.

The total load is calculated as follow:

$$W_T = W_{fuel} + W_{basket} + W_{water} + W_{plate}$$

$$= 36,000 + 17,372 + 12,054 + 17,010$$

$$= 82,436 \text{ lb.}$$

The weight of the water and bottom plate are uniformly distributed (i.e. equivalent pressure) loads. The fuel assemblies apply 24

point loads at the center of the basket compartments. The basket plates apply line loads at the contact surfaces with the bottom plate. Since the fuel assemblies and basket plates are uniformly spaced across the bottom plate these loads are also assumed to be uniformly distributed as an equivalent pressure. The total equivalent pressure, P_E is calculated as follows:

$$P_E = \frac{3\ W_T}{\pi R^2}$$

Where

W_T = total weight acting on plate, 82,436 lb.
R = inside radius of cylinder at plate junction, 31.5 in.

Therefore

$$P_E = \frac{3 \times 82,436}{\pi \times 31.5^2} = 79.4 \text{ psi (Use 81 psi)}$$

The free body displacement of the cylinder due to the equivalent pressure on the plate is zero. Also, as before, the free body rotation of the cylinder is zero.

The free body displacement and rotation of the plate due to the equivalent pressure are determined using Equations 3 and 4.

The discontinuity analysis due to the equivalent pressure is evaluated using Equations 11 and 12.

Using the same approach as for an internal pressure, we obtain

$$\begin{Bmatrix} Q_L \\ M_L \end{Bmatrix} = \begin{Bmatrix} -10.19 \\ 138.51 \end{Bmatrix} \times P_E \qquad \text{Eq. 18}$$

The values of the deflection and rotation imposed on the cylinder as a result of the comparibility condition are under an equivalent pressure on the bottom plate are:

$$\begin{Bmatrix} (W_L)_{CYL} \\ (\theta_L)_{CYL} \end{Bmatrix} = \begin{Bmatrix} -14.9915 \\ 10.9 \end{Bmatrix} \times p_E/E \qquad \text{Eq. 19}$$

The stresses in the cylinder and the plate are calculated with the same equations as used for the internal pressure except for the free body stresses of the cylinder. Since the equivalent pressure does not act on the cylinder, the free body stresses are zero. All the other equations are used as shown except the equivalent pressure p_E is used instead of p.

Therefore Equations 18 and 19 are used in Equations 15, 16 and 17 to obtain stresses in terms of the equivalent pressure p_E. These are shown below:

Orientation of Stress		Cylinder psi	Plate at Junction and Center psi
σ_t:	inside	$(-1.1 + 2.62)\ p_E$	$+2.71\ p_E$
	outside	$(-1.1 - 2.62)\ p_E$	$-4.4\ p_E$
σ_l:	inside	$+ 8.74\ p_E$	0
	outside	$- 8.74\ p_E$	0
σ_r:	inside	0	$+2.71\ p_E$
	outside	0	$-4.4\ p_E$

Stresses in the bottom plate due to pressure only are given by Equations 8, 9 and 10.

C. Thermal Loading

Detailed temperature distributions in the cylinder and plate for the cask in the horizontal and vertical position and for different

ambient conditions were calculated as described in Section 5.1.3.6. These temperature data show that there exists:

a) A differential thermal expansion between cylinder and plate.
b) A thermal gradient across the cylinder wall.
c) A thermal gradient across the plate thickness.
d) An axial gradient in the cylinder.
e) A radial gradient in the plate

Each of these loads are analyzed separately and their effects superimposed.

C.a) Differential Thermal Expansion

The temperature distribution in the cylinder and plate show that the average temperature of the cylinder and that of the plate are different. The shell and plate are assumed free and grow a different amount. Also in this calculation the cylinder is assumed to be at a uniform temperature and the plate at a uniform temperature where

$\bar{T}_1$ = average temperature of cylinder near the junction
= 261°F (See Fig. 5.1-10 of Chapter 5.0)

$\bar{T}_2$ = average temperature of the plate
= 246°F (See Fig. 5.1-14 of Chapter 5.0)

$\bar{T}_b$ = Room temperature of cylinder and plate (70°F)

Therefore the maximum difference in the average temperature of the cylinder and plate is 15°F. A value of 25°F was used for analysis. It should be noted that the temperature shown for each color in the temperature distribution figures is the maximum value for that color in that region. The low temperature for the color is the value for the next lowest temperature region and associated color.

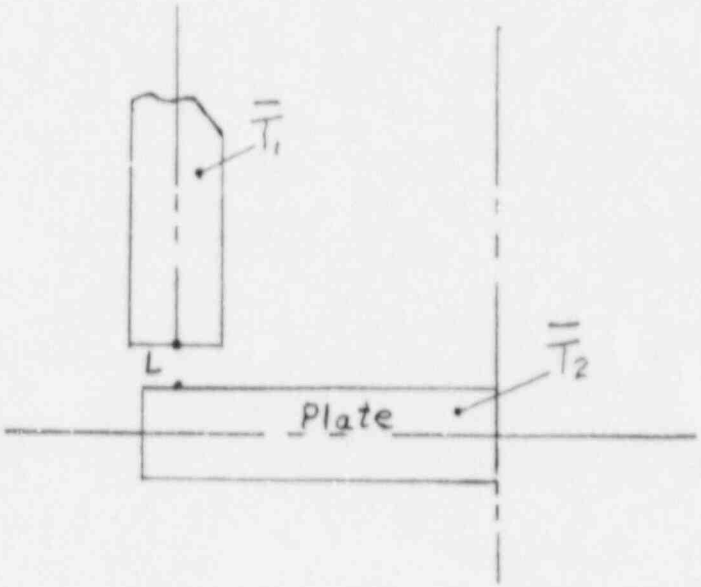

Then the free deflections of the cylinder and plate are:

$$W_{CYL} = \alpha R_m(\bar{T}_1 - T_b); \quad \theta_{CYL} = 0$$
$$W_{PL} = \alpha R_m(\bar{T}_2 - T_b); \quad \theta_{PL} = 0 \qquad \text{Eq. 20}$$

Stresses due to the differential thermal expansions of the cylinder and plate are calculated below and superimposed with the stresses due to thermal gradients calculated in succeeding sections.

To determine the discontinuity loads caused by the differential thermal expansion, use is made of Eqs. 14, and 14a, where the deflection matrix obtained from Eq. 13a is now:

$$\{\Delta\} = \begin{Bmatrix} \alpha R_m (\bar{T}_2 - \bar{T}_1) \\ 0 \end{Bmatrix}$$

Where $\alpha R_m (\bar{T}_2 - \bar{T}_1)$ is the difference in displacement between the cylinder and plate due to differential thermal expansion. There is no rotati of the plate or cylinder due to the differential thermal expansion. Eq. 14a then becomes:

$$\begin{Bmatrix} Q_L \\ M_L \end{Bmatrix} = E \begin{Bmatrix} .0318 & -0.0264 \\ -0.0264 & 2.64 \end{Bmatrix} \begin{matrix} \alpha R_m \\ 0 \end{matrix} \quad (\bar{T}_2 - \bar{T}_1)$$

or

$$\begin{Bmatrix} Q_L \\ M_L \end{Bmatrix} = \begin{Bmatrix} 1.151 \\ 0.96 \end{Bmatrix} \quad x \quad E\alpha(\bar{T}_2 - \bar{T}_1) \qquad \text{Eq. 21}$$

and the deflection of the cylinder due to the discontinuity forces is:

$$W_{CYL} = \frac{1}{E} (23.37\ Q_L + 1.43\ M_L) \qquad \text{Eq. 22}$$

or

$$W_{CYL} = 25.56\ \alpha\ (\bar{T}_2 - \bar{T}_1)$$

Equations 21 and 22 are used in Equations 15, 16 and 17 to obtain stresses in terms of $E\alpha\ (\bar{T}_2 - \bar{T}_1)$. These stresses are shown below. The values of E and α are taken from Table 4A.5-9.

STRESSES DUE TO DISCONTINUITY FORCES CAUSED BY DIFFERENTIAL THERMAL EXPANSION

STRESSES	CYLINDER	PLATE	
TANGENTIAL	(0.7054 ±0.0182) $E\alpha(\bar{T}_2-\bar{T}_1)$	+0.337 -0.148 $E\alpha(\bar{T}_2-\bar{T}_1)$	i o
LONGITUDINAL	± 0.061 $E\alpha(\bar{T}_2-\bar{T}_1)$	0	
RADIAL	0	+0.337 -0.148 $E\alpha(\bar{T}_2-\bar{T}_1)$	i o

C.b) Thermal Gradient Across Cylinder Wall

Let T_1^* and T_2^* be the uniform temperatures of the cylinder wall at the inside and outside surfaces respectively and let the temperature variation through the thickness be linear; then the stresses in the free cylinder at large distances L greater than 3ß from the ends of the cylinder are given by (Reference 4, p. 498):

$$\sigma_t = \sigma_1 = \pm \frac{E\alpha(T_1^* - T_2^*)}{2(1 - \nu)}$$

At the edge $x = L$ $(\sigma_1) = 0$

and

$$\sigma_t = \frac{E\alpha(T_1^* - T_2^*)}{2(1 - \nu)} \left(1 - \nu \pm \sqrt{1 - \frac{\nu^2}{3}} \right)$$

Where T_1 = Maximum temperature at inner surface of cylinder
= 313°F (See Fig. 5.1-14)

T_2 = Maximum temperature at outer surface of cylinder
= 286°F (See Fig. 5.1-14)

Therefore the maximum temperature differences radially in the cylinder wall would be 27°F. The more detailed temperature gradients as shown in Figs. 5.1-9 and 5.1-10 would indicate a much lower temperature differences, i.e., approximately 7°F.

At the edge of the cylinder the free deflection and rotation are (Ref. 4, p. 470):

$$(W_L)_{CYL} = \frac{1 + \nu}{2\beta^2} \times \frac{\alpha(T_1^* - T_2^*)}{t_{CYL}}$$

$$(\theta_L)_{CYL} = \frac{1 \times \nu}{\beta} \times \frac{\alpha(T_1^* - T_2^*)}{t_{CYL}}$$

and those of the plate are:

$$(W_L)_{PL} = 0; \quad (\theta_L)_{PL} = 0$$

The deflection matrix used in Eq. 13a to obtain the discontinuity forces is obtained from the above boundary conditions and is:

$$\{\Delta\} = \begin{Bmatrix} -\frac{1+\nu}{2\beta^2 t_{CYL}} \\ -\frac{1+\nu}{\beta t_{CYL}} \end{Bmatrix} \alpha (T_1^* - T_2^*) \qquad \text{Eq. 23}$$

$$= \begin{Bmatrix} -14.31 \\ -1.953 \end{Bmatrix} \alpha (T_1^* - T_2^*)$$

Substituting into Equation 13 yields

$$\begin{Bmatrix} Q_L \\ M_L \end{Bmatrix} = \begin{Bmatrix} -0.403 \\ -4.778 \end{Bmatrix} \alpha E \quad (T_1^* - T_2^*) \qquad \text{Eq. 24}$$

Substituting Eq. 24 into Eq. 11a, the deflection of the cylinder due to the compatibility forces is obtained.

$$W_{CYL} = [23.37 \times (-0.403) + 1.43 \times (-4.778)] \alpha (T_1^* - T_2^*) \qquad \text{Eq. 25}$$
$$= -16.251 \quad (T_1^* - T_2^*)$$

Equations 24 and 25 are used in Equations 15, 16 and 17 to obtain stresses in terms of $E\alpha(T_2^* - T_1^*)$. These stresses are shown below. The values of E and α are taken at 300°F from Table 4A.5-9.

DISCONTINUITY STRESS

STRESS ORIENTATION	CYLINDER	PLATE	
TANGENTIAL	$(-.447 \pm .0909\ E\ Q\ (T_1^*-T_2^*)$	-0.341 $+0.275$	$E\ Q(T_1^*-T_2^*)\ \begin{matrix} i \\ o \end{matrix}$
LONGITUDINAL	$\pm 0.302\ E\ Q(T_1^*-T_2^*)$	0	
RADIAL	0	-0.341 $+0.275$	$E\ Q(T_1^*-T_2^*)\ \begin{matrix} i \\ o \end{matrix}$

C.c) Thermal Gradient Across the Thickness of the Bottom Closure Plate

The top and bottom of the plate are assumed to be at uniform temperatures with a linear variation across the thickness.

Fig. 5.1-14 would indicate an almost uniform temperature of the bottom plate. Fig. 5.1-10 shows a small gradient at the junction with the cylinder, i.e. 237°F at the inner surface and 258°F at the outer surface. A linear gradient, ΔT, of 25°F was used as a conservative value.

This distribution causes a rotation of the plate and results in discontinuity loads since the cylinder wall resists this rotation. The boundary conditions for the discontinuity analysis are:

For the cylinder:

$$(W_L)_{CYL} = (\theta_L)_{CYL} = 0$$

For the plate

$$(W_L)_{PL} = (\theta_L)_{PL} (t_{PL}/2)$$

$$(\theta_L)_{PL} = \alpha R_m \Delta T / t_{PL}$$

The deflection matrix for use in Eq. 13a to obtain the discontinuity moment and shear is:

$$\{\Delta\} = \begin{Bmatrix} \frac{R_m}{2} \\ \frac{R_m}{t_{PL}} \end{Bmatrix} \alpha\Delta T \quad \begin{Bmatrix} 18.19 \\ -3.233 \end{Bmatrix} \quad \alpha\Delta T \qquad \text{Eq. 26}$$

and the discontinuity moment and shear from Eq. 13a and Eq. 26 are:

$$\begin{Bmatrix} Q_L \\ M_L \end{Bmatrix} = \begin{Bmatrix} 0.664 \\ -9.02 \end{Bmatrix} \quad E \quad \alpha\Delta T \qquad \text{Eq. 27}$$

The deflection in the cylinder from Eq. 27 and Eq. 11a is:

$$(W_L)_{CYL} = 2.62 \quad \alpha\Delta T \qquad \text{Eq. 28}$$

Equations 27 and 28 are used in Equations 15, 16 and 17 to obtain stresses in terms of $E\alpha\Delta T$. These stresses are shown below. The values of E and α are taken from Table 4A.5-9.

DISCONTINUITY STRESSES

STRESS	CYLINDER	PLATE
TANGENTIAL	$(.072 \mp .171)\ E\alpha(\Delta T_2)$	$\begin{matrix}-0.176\\+0.285\end{matrix}\ E\alpha(\Delta T_2)\ \begin{matrix}i\\o\end{matrix}$
LONGITUDINAL	$\mp 0.569\ E\alpha(\Delta T_2)$	0
RADIAL	0	$\begin{matrix}-0.172\\+0.285\end{matrix}\ E\alpha(\Delta T_2)\ \begin{matrix}i\\o\end{matrix}$

C.d) Linear Gradient in the Axial Direction of the Cylinder

The stress in the free cylinder a large distance from the edge is given by (Reference 4, p. 500):

$$\sigma_l = 0.353\ E\alpha\sqrt{R_m t_{CYL}}\ \frac{(\bar{T}_3 - \bar{T}_1)}{L_V}$$

$$\sigma_t = \nu\sigma_l$$

Where:

$\bar{T}_1$ = Average temperature of the cylinder at the edge location x = L

= 232°F at lid end and 259°F at bottomed (See Fig. 5.1-14)

T_3 = Maximum temperature of the cylinder at distant L_V

= 313°F (See Fig. 5.1-14)

The temperature over most of the cylinder length is 313°F as shown in Fig. 5.1-14. This is basically a uniform temperature over most of the cylinder. The maximum axial temperature gradient is calculated as follows:

$$\Delta T = \frac{(\bar{T}_3 - \bar{T}_1)}{L_V}$$

Where

L_V = cylinder length

= 168.25 in.

Therefore $\Delta T = \frac{313 - 232}{168.25}$

$= 0.48$ Use $0.5 \frac{°F}{in.}$

The axial gradient results in a rotation of the end of the cylinder which produces a discontinuity between the cylinder and plate. The boundary conditions for the discontinuity analysis are as follows:

For the cylinder:

$$(W_L)_{CYL} = 0$$

$$(\theta_L)_{CYL} = -\frac{R_m}{L_V}\,\alpha\,(\bar{T}_3 - \bar{T}_1)$$

For the plate:

$$(W_L)_{PL} \text{ and } (\theta_L)_{PL} = 0$$

The deflection matrix used in Eq. 13a to obtain the discontinuity moment and shear is:

$$\{\Delta\} = \begin{Bmatrix} 0 \\ R_m \end{Bmatrix} \alpha \frac{(\bar{T}_3 - \bar{T}_1)}{L_V} = \begin{Bmatrix} 0 \\ -33.375 \end{Bmatrix} \times \alpha \frac{(\bar{T}_3 - \bar{T}_1)}{L_V} \qquad \text{Eq. 29}$$

and the discontinuity moment and shear from Eq. 13a and 29 are

$$\begin{Bmatrix} Q_L \\ M_L \end{Bmatrix} = \begin{Bmatrix} 0.9603 \\ -96.03 \end{Bmatrix} \times \frac{E\alpha(T_3 - T_1)}{L_V} \qquad \text{Eq. 30}$$

The deflection of the cylinder from Eq. 11a and 30 is:

$$(W_L)_{CYL} = -114.88 \times \alpha \frac{(\bar{T}_3 - \bar{T}_1)}{L_V} \qquad \text{Eq. 31}$$

Equations 30 and 31 are used in Equations 15, 16 and 17 to obtain stresses in terms $E\alpha\Delta T$. These stresses are shown below. The values of E and α are taken from Table 4A.5-9.

DISCONTINUITY STRESSES

STRESS	CYLINDER	PLATE		
TANGENTIAL	$(-3.16 \mp 1.818)\frac{E\alpha(\bar{T}_3-\bar{T}_1)}{L_V}$	-3.88 +4.04	$\frac{E\alpha(T_3-T_1)}{L_V}$	i o
LONGITUDINAL	$\mp 6.061\frac{E\alpha(\bar{T}_3-\bar{T}_1)}{L_V}$	0		
RADIAL	0	-3.88 +4.04	$\frac{E\alpha(T_3-T_1)}{L_V}$	i o

C.e) Radial Gradient in the Bottom Closure Plate

For this condition the temperature in the plate, which is a function of the radius, is assumed constant across the thickness. The plate is simply supported and free to expand. The effect of a gradient through the plate is analyzed in Section C.c) above.

The stresses due to the radial gradient are (Ref. 8, p. 217):
At the center of plate:

$$\sigma_t = \sigma_r = \frac{E\alpha}{2} (\bar{T}_2 - T_c)$$

where:

$\bar{T}_2$ = Average temperature of the plate.
= (259 + 232)/2 (Fig. 5.1-14)
= 245.50°F

T_c = Temperature at the center of the plate.
= (244 + 237)/2 (Fig. 5.1-10)
= 240.5°F

At the outer edge:

$$\sigma_r = 0; \sigma_t = E\alpha (\bar{T}_2 - T_a)$$

Where:

T_a = Temperature of the plate outer edge.
= (251 + 244)/2 (Fig. 5.1-10)
= 247.5°F

These stresses are additive to the discontinuity stresses due to the other thermal effects described above. The values of E and α are taken from Table 4A.5-9.

4A.5.2.5 Analysis Results

The tangential stress, σ_t, the longitudinal stress, σ_l, the radial stress, σ_r, and the shear stress, τ, due to the applied loads, were calculated for the most critical sections and are listed in Tables 4A.5-6 through 4A.5-8. The applicable stress classification per the ASME Boiler and Pressure Vessel Code are also indicated in these tables for each load. Table 4A.5-6 presents the stresses in the cylinder at the junction between the cylinder and the bottom plate.

Tables 4A.5-7 and 4A.5-8 present the stresses in the bottom plate at the junction with the cylinder and at its center, respectively.

These stresses are combined, principal stresses and stress intensities determined, and compared to the allowable stress intensity values in Section 4.2.

4A.5.3 Stress Analysis of the Lid and the Junction of the Lid with the Cask Body Cylindrical Shell

4A.5.3.1 Description

This section describes the analysis performed and the results obtained for the containment vessel lid and the junction of the lid with the cask body cylindrical shell, referred to as the cylinder. Figure 4A.5-1 shows a longitudinal section of the storage cask. Figure 4A.5-4 shows the geometry and dimensions of the lid and the lid to cylinder junction.

4A.5.3.2 Loading Conditions

The loading conditions analyzed are listed below:

1) Internal pressure
2) Bolt preload and load required to seat the gaskets
3) Inertia loads of the internals acting on the lid during handling operations.
4) Temperature gradient across the lid thickness.
5) Temperature gradient in lid in the radial direction.
6) Differential thermal expansion between lid and cylinder.

The internal pressure used in the analysis is 250 psi at a temperature of 350°F.

4A.5.3.3 Method of Analysis

The cask lid is analyzed as a circular plate which is simply supported at the periphery by the bolts. Because of the reduced thickness of the lid at the lid flange, the lid is divided into two parts: an inner solid circular plate of thickness t_1 = 11.5 in. and an outer circular plate of thickness t_2 = 3.5 in. which represents the lid flange as shown in Figure 4A.5-5. The interaction of the junction of the two plates is considered.

Each loading condition is analyzed separately and the stress components calculated and categorized in accordance with the ASME Code, Subsection NB[(1)]. Stresses are calculated at the locations of interest, i.e. the center of the plate and the lid flange at the step and gasket location.

4A.5.3.4 Models, Boundary Conditions and Assumptions

The model of the lid and the junction of the lid and cylinder are shown in Figures 4A.5-5, -7 and -12. Figure 4A.5-6 shows the sign convention used in the analysis. The formulas used in this analysis are taken from References 7 and 2 and their validity is based on the following assumptions:

1) The lid is flat, and the inner and outer plates are of homogeneous and isotropic material. The mid surfaces of the plates are horizontal and the loads are perpendicular to the plates.

2) The inner and outer plates have the same mid surface.

3) The thicknesses of the plates are less than 1/4 of their diameters, and the deflections are small compared to the thicknesses of the plates.

4) There is no deformation in the middle plane of the plates. This plane remains neutral during bending.

5) The stresses are below the elastic limit so that Hooke's law is valid.

6) As shown in Figure 4A.5-5, a portion of the lid is omitted. This assumption is conservative since it results in higher deflections and stresses in this area than actually exist.

7) The outer plate thickness at the gasket location is reduced to account for the groove.

4A.5.3.5 Materials Used

The cask lid and the cylindrical shell are made of SA-350 Gr. LF1. The bolts connecting the lid flange to the cylinder are made of SA-320, Gr. L43.

The properties for the above materials are taken from Reference 2 and are listed in Table 4A.5-9.

4A.5.3.6 Analysis

A. Internal Pressure

The following conservative assumptions are made for this loading condition (See Figure 4A.5-8):

1) The portion of the plate outside the bolt circle is not considered for the pressure loading.

2) The outer plate is considered simply-supported at the bolt circle.

3) The pressure is assumed to act up to the middle of the gasket.

4) The pressure in the area between the periphery of the inner plate and the gasket is conservatively replaced by a resultant line load P_2 in lb/in. applied at the periphery of the inner plate as shown on Figure 4A.5-8.

The moments and forces due to the pressure are obtained by writing the expressions of the slope at r = b for Case 1, Case 2a and Case 2b (Figure 4A.5-8), and imposing the condition that the slopes at r = b for the inner and outer plates must be equal.

The expressions for the slope at r = b are (Formulas from Ref. 7, Table 24):

Case 1 (Cases 10a plus 13a, Ref. 7):

$$(\theta_b)_1 = \frac{pb^3}{8D(1+\nu)} + \frac{M_b \times b}{D(1+\nu)} \qquad \text{Eq. 1}$$

Case 2a (Case 1a, Ref. 7):

$$(\theta_b)_{2a} = \frac{W a^2}{D} \frac{L_9}{C_7} \qquad \text{Eq. 2}$$

Case 2b (Case 5a, Ref. 7):

$$(\theta_b)_{2b} = \frac{M_b a}{D} \frac{L_8}{C_7} \qquad \text{Eq. 3}$$

Where

$(\theta_b)_1$ = rotation (slope) of inner plate at junction with outer plate due to pressure load and moment M_b (See Fig. 4A.5-8)

$(\theta_b)_{2a}$ = rotation (slope) of outer plate at junction with inner plate due to line load W (See Fig. 4A.5-8)

$(\theta_b)_{2b}$ = rotation (slope) of outer plate at junction with inner plate due to moment M_b (See Fig. 4A.5-8)

p = internal pressure load, psi

W = line load due to internal pressure, lb./in.

M_b = moment at interface of outer and inner plates, in.-lb./in.

a = radial distance to bolt center line, 35.16 in.

b = radial distance to interface of inner and outer plates, 31.86, in.

ν = Poisson's Ratio, 0.3

$$D = \frac{E\ tp^3}{12(1 - \nu^2)}$$ (Note: t_p for inner plate is 11.25 in. and t_p for outer plate is 3.5 in.

$= 3.93\ E$ for the outer plate

$$L_8 = (1/2)[1 + \nu + (1 - \nu)(b/a)^2]$$

$= 0.9367$

$$L_9 = \frac{b}{a}\left(\frac{1 + \nu}{2} \ln \frac{a}{b} + \frac{1 - \nu}{4}[1 - (b/a)^2]\right)$$

$= 0.0874$

$$C_7 = (1/2)(1 - \nu^2)[(a/b) - (b/a)]$$

$= 0.0909$

(See Reference 7, Table 24 for dimensionless coefficients)

Substitution of the numerical values for a, b, D, C_7, L_8 and L_9 and of the expression for $\bar{w}$ (See Fig. 5A.5-8) as a function of p yields:

$$(\theta_b)_1 = 22.244(p/E) + 0.176\ (M_b/E) \qquad \text{Eq. 4}$$

$$(\theta_b)_2 = (\theta_b)_{2a} + (\theta_b)_{2b}$$

$$= 5196\ (p/E) - 92.275\ (M_b/E) \qquad \text{Eq. 5}$$

Equating Eq. 4 to Eq. 5 and solving for M_b yields

$$(\theta_b)_1 = (\theta_b)_2$$

$$M_b = 55.962\ p$$

The moment M_c at the center of the plate is:

$$M_C = \frac{3 + \nu}{16} pb^2 + M_b L_8 = 264.79\ p$$

Note: $L_8 = 1$, for $r = b$

The reaction at the support is:

$$Q_a = W\ (b/a) = 15.533\ p$$

The moment at the seal location M_s is conservatively taken equal to M_b, i.e.

$$M_s = M_b = 55.962\ p$$

The expressions for the stiesses are:

At the plate center $\sigma_r = \sigma_t = \frac{6M_c}{(t_{ip})^2}$ Eq. 6

At the junction of inner and outer plates,

$$\sigma_r = \sigma_t = 6M_b/(t_{op})^2;\ \tau = Q/t_{op}$$ Eq. 7

At the gasket where $t_3 = (t_{op} - 0.26)$

$$\sigma_r = \sigma_t = 6M_s/(t_3)^2;\ \tau = Q_s/t_3$$ Eq. 8

Where

$$Q_s = W\ (63.63/66/10) = 17.164\ p \times 0.964$$
$$= 16.55\ p$$

Also

σ_r = radial stress, psi

σ_t = tangential stress, psi

σ_l = longitudinal stress, psi
= 250 psi at inside surface (i.e. $\sigma_l = p$)
= 0 psi at outside surface

B. Bolt Preload and Load Required to Seat the Gasket

For this loading condition the outer plate (lid flange) is considered simply-supported at the step location. The loads acting on the lid flange are shown in Figure 4A.5-9 and are:

1) The bolt preload, which is selected on the basis of the following requirements:

a) It has to be greater than the load required to seat the metallic seals.

b) It has to be of such a magnitude that the seal between the lid and vessel is maintained under any loading condition.

A bolt preload corresponding to a bolt direct stress of Sm (i.e., 25000 psi), satisfies the above requirements. Hence the bolt preload is:

$$F_B^* = S_m \times A_B$$

Expressed as a line load acting, lb/in., at the bolt circle:

$$F_B = n F_B^*/(2 \pi R_{BC})$$

$$= n S_m A_B/(2\pi R_{BC})$$

Where:

n = number of bolts, 48
R_{BC} = radius of bolt circle, 35.16 in.
A_B = bolt area = 1.492 $in.^2$

Therefore

$$F_B = \frac{48 \times 25000 \times 1.492}{2 \times 3.14 \times 35.16}$$

$$= 8108 \text{ lb./in.}$$

2) The load, required to seat the metal gasket is

4474 lb/in. from Ref. 5.

The solution to the problem is obtained by imposing the condition that, for continuity, the slopes at r = b of the inner and outer plates are equal, and solving for the unknown moment M_b (Figure 4A.5-9).

The slope at r = b for Case 1 is (Case 13a, Ref. 7):

$$(\theta_1)\ r = b = -\frac{M_b \times b}{D(1 + \nu)} = -0.176\ M_b/E \qquad \text{Eq. 9}$$

The slope at r = b for Case 2 is the sum of the slopes of Cases 2a, 2b and 2c.

Case 2a (Ref. 4, pg. 58):

$$(\theta_b)\ r = b = \frac{bM_b}{D(a^2 - b^2)} \left(\frac{b^2}{1 + \nu} + \frac{a^2}{1 - \nu} \right) \qquad \text{Eq. 10a}$$

Where

M_b D and ν were previously defined.
a and b as defined on Fig. 4A.5-9.

Therefore

$$(\theta_b)\ r = b = \frac{31.82\ M_b}{3.93\ E\ (36.88^2 - 31.82^2)} \left(\frac{31.82^2}{(1 + 0.3)} + \frac{36.88^2}{(1 - 0.3)} \right) \qquad \text{Eq. 10a}$$

$$= 63.46\ \frac{M_b}{E}$$

Case 2b (Case 1k, Ref. 7):

$$(\theta_b)\ r = r_{o2} = -\ \frac{F_B\ a^2}{D\ C_7} \left(\frac{r_{o2}\ C_9}{b} - L_9 \right) \qquad \text{Eq. 10b}$$

$$= -192.4486\ F_B/E$$

Where

F_B = bolt preload, 8108 lb/in.
a and r_{o1} as defined on Fig. 4A.5-9

$D = 3.93\ E$

C_7 and C_9 as defined before and equal to 0.135 and 0.1214 respectively for this case.

$$L_9 = \frac{r_{o2}}{a} \left(\frac{1 + \nu}{2} \ln \frac{a}{r_{o2}} + \frac{1 - \nu}{4} \left(1 - \frac{r_{o2}^2}{a} \right) \right)$$

$$= 0.0445$$

Therefore

$$(\theta_b)\ r = r_{o2} = \frac{F_B\ (36.88)^2}{3.93E \times 0.135} \left(\frac{35.16 \times 0.1214}{31.82} - 0.0445 \right)$$

$$= 229.5\ \frac{F_B}{E}$$

Case 2c (Case 1k, Ref. 7):

$$(\theta_b)\ r = r_{o1} = \frac{F_S\ a^2}{D\ C_7}\left(\frac{r_{o1}\ C_9}{b} - L_9\right) \qquad \text{Eq. 10c}$$

Where

F_S = metal gasket seating load, 4474 lb/in.
$D = 3.93\ E$
a, b and r_{o1} are as defined in Fig. 4A.5-9
C_7 and C_9 as defined before and equal to 0.135 and 0.1214 respectively for this case
$L_9 = 0.095$ for $r = r_{o1}$

Therefore

$$(\theta_b)_{r = r_{o1}} = \frac{F_S\ (36.88)^2}{3.93E \times 0.135}\left(\frac{33.05 \times 0.1214}{31.82} - 0.095\right)$$

$$= 80.4\ \frac{F_S}{E}$$

Therefore

$$\theta_b = (\theta_b)_{r=b} + (\theta_b)_{r=r_{o2}} + (\theta_b)_{r=r_{o1}}$$

$$= 1/E\ [63.46 M_b - 229.5\ F_B + 80.43\ F_S]$$

Equating the slopes of Eq. 9 with Eqs. 10a, 10b and 10c yields

$$0.176\ \frac{M_b}{E} = \frac{1}{E}\ (63.46\ M_b - 229.5\ F_B + 80.43\ F_S)$$

Therefore

$$M_b = -(3.493\ F_B - 1.264\ F_S) \qquad \text{Eq. 11a}$$

The reaction at the support r = b as a function of F_B and F_S is:

$$Q_b = -F_S \frac{r_{o1}}{b} + F_B \frac{r_{o1}}{b}$$

$$Q_b = -1.039\ F_S + 1.105\ F_B \qquad \text{Eq. 11b}$$
$$= -1.039 \times 4474 + 1.105 \times 8108$$
$$= 4310\ \text{lb/in.}$$

and the bending moment at the center of the inner plate is the same as M_b:

$$M_c = M_b = -(3.493\ F_B - 1.264\ F_S) \qquad \text{Eq. 11c}$$
$$= -(3.493 \times 8108 - 1.264 \times 4474)$$
$$= -\ 22666\ \text{in-lb/in.}$$

The same moment M_b and reaction Q_b are conservatively used to calculate the stresses at the gasket location. Equations 6, 7 and 8 are used to calculate the stresses.

C. Inertia Loads Due to Handling Operations

The inertia load due to handling is applied by the internal components to the lid. This load is equal to the weight multiplied by a g factor of 3 and is approximated by an equivalent pressure p_E. If W is the total weight acting on the lid, then:

$$PE = \frac{3 \times W}{R_L^{\ 2}} = 81$$

Where

R_L is the inside radius of the cylinder 31.5 in.

W = 82436 (See Section 4A.5.2.4B)

The analysis for this loading condition is identical to that of the internal pressure Section 4A.5.3.6A where p is now replaced by p_E.

D. Thermal Gradients Across the Lid Thickness

The following assumptions are made for this condition:

a) The temperature variation across the thickness of the lid is linear.

b) For the inner and outer plates into which the lid is divided, the temperature, which is different in each plate, does not vary in planes parallel to the middle surface of the plates.

For this temperature distribution, stresses arise only if the plate is restrained from freely deforming to a spherical surface of curvature:

$$\frac{1}{r} = \frac{\alpha \Delta T}{t}$$

The lid is considered pinned at the bolt circle and simply supported at the point where the change in thickness occurs as shown in Figure 4A.5-10.

For continuity the slopes at r = b for the inner and outer plates must be equal. By setting the slopes equal to each other, it is possible to solve for the unknown moment M_b at r = b, and to calculate the moment at the other locations of interest.

D.1 Inner Plate

The slope at r = b in the case of a simply supported unrestrained plate is:

$$(\theta_b)_1 = \alpha_1(\bar{T}_2 - \bar{T}_1)b/t_{ip} \qquad \text{Eq. 12}$$

Where

$(\theta_b)_1$ = rotation (slope) of inner plate at b

α_1 = thermal expansion coefficient of inner plate, in/in-°F

B = radius to interface of inner and outer plates, 31.82 in.

t_{ip} = thickness of inner plate, 11.5 in.

$\bar{T}_2$ = average temperature at inner surface of inner plate, °F
= (228 + 215)/2 = 221.5°F (See Figure 5.1-9)

$\bar{T}_1$ = average temperature at outer surface of inner plate, °F
= (215 + 202)/2 = 208.5°F (See Figure 5.1-9)

Therefore

$$(\theta_b)_1 = 2.767\ \alpha_1\ (\bar{T}_2 - \bar{T}_1)$$

D.2 Outer Plate

The free rotation of the outer plate at r = b is given by the expression (Case 8c, Table 24, Ref. 7):

$$(\theta_b)_2 = \frac{-\alpha_2\ (1 + \nu)a(\bar{T}_4 - \bar{T}_3)}{t_{op}} \times \frac{C_9\ L_2 + C_3\ (1 - L_8)}{C_1\ C_9 - C_3\ C_7} \qquad \text{Eq. 13}$$

Where

$(\theta_b)_2$ = rotation (slope) of outer plate at b

α_2 = thermal expansion coefficient of outer plate, in/in - °F

a = radius to bolt centerline, 35.16 in.

$\bar{T}_4$ = average temperature of inner surface of outer plate, °F
= (228 + 215)/2 = 221.5°F (See Figure 5.1-9)

$\bar{T}_3$ = average temperature of outer surface of outer plate, °F
= (228 + 215)/2 = 221.5°F (See Figure 5.1-9)

t_{op} = thickness of outer plate, 3.5 in.

C_1, C_3, C_7, C_9, L_2 and L_8 are constant depending on geometry and are given by equations in Table 24, Ref. 7 and are

C_1 = 0.094
C_3 = 0.00014
C_7 = 0.0909
C_9 = 0.0874
L_2 = 0.0044
L_8 = 0.937

Therefore

$$(\theta_b)_2 = \frac{-\alpha_2 (1.3)\ 35.16\ (\bar{T}_4 - \bar{T}_3)}{3.5} \left(\frac{0.874 \times 0.0049 + 0.00014(1-0.937)}{0.094 \times 0.874 - 0.00014 \times 0.0908}\right)$$

$$= -0.62\ \alpha_2(\bar{T}_4 - \bar{T}_3)$$

D.3 Junction of Inner to Outer Plates

If the lid is split at the step location into two plates a discontinuity will result at the split line. To reestablish continuity at r = b a moment M_b, as shown in Figure 4A.5-10, must be added to make the slope of the inner plate equal to that of the outer plate. Therefore Equation 12 becomes:

$$\text{Eq. 12} = \frac{M_b\ b}{D\ (1 + \nu)}$$

$(\theta_b)_1$ = Eq. 13a

Where

Eq. 12 = $2.767\ \alpha_1\ (T_2 - T_1)$
M_b = moment at interface of inner and outer plate, in-lb/in.
b = 31.82 in.

$$D = \frac{E_1\ (t_{ip})^3}{12(1-\nu^2)} = \frac{(11.5)^3\ E_1}{12(1-0.3^2)}$$

$$= 139.3E_1$$

Therefore $(\theta_b)_1$ final becomes:

$$(\theta_b)_1 = \alpha_1(\bar{T}_2 - \bar{T}_1) - 0.176\, M_b/E_1 \qquad \text{Eq. 12a}$$

And

$$(\theta_b)_2 = \text{Eq. 13} - \frac{M_b\, a}{D}\left(\frac{C_3L_8 - C_9L_2}{C_1C_9 - C_3C_7}\right)$$

Where

$$\text{Eq. 13} = -0.62\, \alpha_2\, (\bar{T}_2 - \bar{T}_1)$$

M_b, a and Constants C_1, C_3, C_7, C_9, L_2 and L_8 are defined above in D.2.

Therefore

$$(\theta_b)_2 = -0.62\, \alpha_2\, (\bar{T}_2 - \bar{T}_1) + 0.278\, M_b/E_2 \qquad \text{Eq. 13a}$$

When the slopes at r = b are equated, i.e., Eq. 12a = Eq. 13a

$$2.767\, \alpha_1\, (\bar{T}_2 - \bar{T}_1) - 0.176\, M_b/E_1 = -0.62\, \alpha_2 (\bar{T}_4 - \bar{T}_3) + 0.228\, M_b/E_2$$

This yields the unknown value of M_b:

$$M_b = [6.0955\ \alpha_1\, (\bar{T}_2 - \bar{T}_1) + 1.3722\, \alpha_2\, (\bar{T}_4 - \bar{T}_3)]\, E$$

where E_1 is assumed equal to E_2. All the other required quantities can now be evaluated.

D.4 Reactions (Shear) Loads

At r = b (Case 5c and 8c, Table 24, Ref. 7)

$$Q_b = \frac{\alpha_2(1+\nu)\,D_2\,(T_4 - T_3)}{a\,t_{op}} \times \left(\frac{C_7L_2+C_1(1-L_8)}{C_1C_9-C_3C_7}\right) + \frac{M_b}{a}\left(\frac{C_1L_8-C_7L_2}{C_1C_9-C_3C_7}\right) \qquad \text{Eq. 14}$$

Where

α_2, ν, D_2, $\bar{T}_4$, $\bar{T}_3$ a, M_b and t_{op} are as defined previously

C_1, C_3, C_7, L_9, L_2 and L_8 are constants previously defined

Therefore

$$Q_b = 0.032\,E_2\,\alpha_2\,(T_4 - T_3) + 0.304\,M_b$$

And substituting for M_b,

$$Q_b = 0.032\,E_2\,\alpha_2\,(\bar{T}_4 - \bar{T}_3) + 0.304E\,[6.095\,\alpha_1(\bar{T}_2 - \bar{T}_1] + 1.3722\,\alpha_2\,(\bar{T}_4 - \bar{T}_3)$$

Therefore

$$\theta_b = [0.45\,\alpha_2\,(\bar{T}_4 - \bar{T}_3) + 1.853\,\alpha_1\,(\bar{T}_2 - \bar{T}_1)]\,E$$

The reaction at r = a:

$$Q_a = b/a\ Q_b = \frac{31.82}{35.16}[0.45\alpha_2 E_2(\bar{T}_4 - \bar{T}_3) + 1.853\ \alpha_1 E_1(\bar{T}_2 - \bar{T}_1)$$

$$= 0.406\ (E_2\alpha_2(\bar{T}_4 - \bar{T}_3) + 1.677\ \alpha_1(\bar{T}_2 - \bar{T}_1)$$

Substituting the values of moments and shears thus found into the stress equations 6, 7 and 8 completes the analysis for this loading condition. In these equations the moment at the center of the lid, M_c, equals M_b and the moment at the gasket location is conservatively assumed to be equal to the moment M_b at r = b.

E. Thermal Gradient in Lid in the Radial Direction

For this condition the temperature in the lid, which is a function of the radius, is assumed constant across the thickness. The effect of a gradient through the lid thickness is evaluated in Section 4A.5.3.6D above.

The plate is assumed to be simply supported and free to expand. There is no differential thermal expansion between the lid and the top of the cylinder because the lid and the top of the cylinder are at the same average temperature (See Section 4A.5.3.6F below).

Any effects due to the connection with the top of the cask shell (cylinder) are evaluated in Section 4A.5.3.6G below.

The stresses due to the radial gradient are as follows:

Center of plate:

$$\sigma_t = \sigma_r = \frac{E\alpha}{2}\ (T_1 - T_c)$$

Where

T_1 = average temperature of inner plate, °F
= (228 + 215)/2 (See Figure 5.1-9)
= 221.5°F

T_L = average temperature at center of inner plate, °F
= 215°F (Note: the greatest portion of plate is at 221.5°F)

E and α are taken from Table 4A.5-9)

At the outer plate (i.e., lid flange) at junction between inner and outer plates

$$\sigma_r = \sigma_t = E\alpha\,(\bar{T}_2 - Ta)$$

Where

$\bar{T}_2$ = average temperature of outer portion of lid
= (228 + 215)/2 (Fig. 5.1-9)
= 221.5°F

Ta = average temperature of junction between inner and outer plates

$$= \left(228 + \frac{228 + 215}{2}\right)/2 \qquad \text{(Fig. 5.1-9)}$$

= 225°F

E and α are taken from Table 4A.5-9

F. Differential Expansion Between Lid and Cask Cylinder

The thermal analysis of the cask performed in Chapter 5.0 shows that the lid and the cylinder at the lid end are at the same average temperatures. Figure 5.1-14 shows that all but a small portion of the lid is at the same temperature as the top of the cylinder. A more detailed temperature distribution shown in Figure 5.1-9 confirms this. The latter shows that the lid except for a small portion in the center and the top surface are at the same temperature as the top of the cylinder. Therefore, there is no differential thermal expansion between the lid and top of the cylinder.

Discontinuity effects due to other thermal gradient effects are described in Section 4A.5.3.6G below.

G. Effect of Discontinuity of Cylinder on Lid

The displacement and rotation of the cylinder at the junction with the lid introduce shear forces and bending moments at the junction. This induces stresses in the outer plate (i.e. lid flange) and lid bolts. The effect on the lid bolts is described in Section 4A.5.4.2.

The displacements, rotations, edge shear forces and edge bending moments acting on the end of the cylinder are calculated in Section 4A.5.5.6G.d. The loads which induce the discontinuity effects are internal pressure, radial gradient through the cylinder wall, and an axial gradient along the cylinder.

The effect on the lid flange is obtained by assuming the rotation of the cylinder is applied to the lid flange (i.e. outer plate). The moment on the lid flange can be calculated with Eq. 10a of Section 4A.5.3.6B. This expression gives at the junction with the thicker inner plate:

$$\theta = 63.46 \frac{(M_b)}{E}$$

Where

θ = rotation imposed on outer plate (lid flange) by the cylinder
= 0.00041 rad. (Section 4A.5.5.6G.d)

E = Young's modulus, 29×10^6 psi

$(M_b)\theta$ = moment due to rotation of cylinder, in-lbs/in.

Therefore

$$M_b = \frac{0.00041 \times 29 \times 10^6}{63.46}$$

= 20 in-lbs/in.

The shear force at the interface of the cylinder with the lid flange would also induce a moment if there were no relative motion between the lid flange and the cylinder. Making that assumption the shear force also contributes a moment on the lid flange which is calculated as follows:

$$(M_b)_Q = Q \times \frac{t}{2}$$

Where

$(M_b)_Q$ = moment due to shear force, in-lb/in.

Q = shear force
= 135 lbs/in. (Section 4A.5.5.6Gd)

t = thickness of outer plates, 3.5 in.

Therefore

$$(M_b)_Q = 135 \times \frac{3.5}{2}$$

= 240 in-lbs/in.

The bending stress in the lid flange is given by

$$\sigma_b = \frac{M_b}{t^2}$$

Where

σ_b = bending stress, psi
This is both the radial and tangential stress

M_b = total moment, in-lbs/in.
= 240 - 20, Use 240 in-lbs/in.

t = thickness, in.

Therefore, σ_r and σ_t in lid flange is

$$\sigma_r = \sigma_t = \frac{6 \times 240}{3.5^2} = 120 \text{ psi}$$

And σ_r and σ_t at seal are

$$\sigma_r = \sigma_t = \frac{6 \times 240}{3.24^2} = 140 \text{ psi}$$

As indicated above the displacements and rotations of the cylinder have a very small effect on the lid. This is principally due to two reasons. First, the cylinder is a very rigid structure therefore the applied load does not induce significant displacements and rotations. Second, the normal operating loads on the cylinder are small. The internal pressure is only 250 psi which induce pressure stresses of less than 1000 psi. The end of the cylinder and the lid are at almost uniform temperatures, therefore, thermal gradients and resulting thermal stresses are also small.

4A.5.3.7 Analysis Results

The tangential stress σ_t, the longitudinal stress σ_l, the radial stress σ_r, and the shear stress τ, due to the applied loads were calculated at the most critical locations and are listed on Table 4A.5-10 through 4A.5-12. The stresses at the center of the lid, i.e. the inner plate are presented in Table 4A.5-10. The stresses at the junction (the step in thickness) between the inner and outer plates are given in Table 4A.5-11. The stresses at the seal in the outer plate, i.e. the lid flange, are given in Table 4A.5-12.

These stresses are combined, principal stresses and stress intensities determined and compared with the allowable stress intensity values in Section 4.2

4A.5.4 Bolt Stresses

4A.5.4.1 Bolt Preload

The lid is secured to the cylinder by forty eight 1.5 in. diameter UN-8 bolts. The selected bolt preload is such that the corresponding tensile stress in the bolts at temperature is S_m = 25000 psi which is the stress allowable for the bolt material for normal operation. The load per bolt is (See Section 4a.5.3.6B):

$$F_B^* = A_B \times S_m$$

The torque required to preload the bolt is:

$$T = 0.2 \quad D_N \; F_B^*$$

Where

A_B = Bolt stress area = 1.492 $in.^2$
D_N = Bolt nominal dia = 1.5 in.
S_M = 25,000 psi allowable stress

The residual torque in the bolt is:

$$T_R = 0.5625T$$

The shear stress in the bolt is due to the residual torque from preload given by (Ref. 9):

$$= \frac{T_R \times r}{J} = \frac{16T_R}{\pi(D_N)4} = \frac{16(0.5625 \times 0.2 \; D_N \; A_B \; S_M)}{\pi(D_N)4}$$

Therefore

$$\lambda = \frac{16 \times 0.5625 \times 0.2 \times 1.5 \times 1.492 \times 25000}{3.14 \; (1.378)^4}$$

$$= 8900 \text{ psi}$$

4A.5.4.2 Effect of Discontinuity of Cylinder at Lid End

The effect of discontinuities of the cylinder at the lid is described in Section 4A.5.5.6G. This results in an outward deflection of the cylinder relative to the lid of 0.002054 in. It is assumed that the cylinder moves through this distance but the lid does not move. Therefore the end of the bolt in the cylinder moves relative to the end on the lid. This induces a bending in the bolts as shown on Figure 4A.5-11. The moment on the bolt is calculated assuming the bolts are fixed on the ends by the cylinder and lid. If any rotation occurs the moment is reduced. For a bolt simply supported on one end, the bending moment is reduced by on-half. Therefore the assumption of fixed ends is the most conservative and results in the highest stresses. The moment due to the offset from the bolt centerline is also included in the analysis (See Figure 4A.5-11).

THe total moment then is:

$$M_T = M_B + F_B * \delta$$

The bending moment, M_B, is calculated as follows:

$$M_B = \frac{P\ell}{2}$$

And

$$P = \frac{12DI\delta}{\ell^3} \quad \text{for a fixed-fixed beam.}$$

Where

P = lateral load to deflect the bolt and distance δ, lb.
δ = lateral displacement
= 0.002054 in.
E = Young's modulus, 29 x 10^6 @ 200°F

ℓ = bolt length in bending

= 3.5 in.

$I = \pi D^4/64 = 3.14\ (1.378)^4/64$

= 0.177 in.^{4} (D based stress area of 1.492 in.^{2})

F_B^* = bolt preload

= 1.492 x 25000

= 37300 lb.

Therefore

$$M_B = \frac{12DI\delta}{\ell^3} \times \frac{\ell}{2} = \frac{6EI\delta}{\ell^2}$$

$$= \frac{6 \times 29 \times 10^6 \times 0.177 \times 0.002054}{3.5^2}$$

= 5160 in-lbs.

M_T = 5160 + 37300 x 0.002054

= 5240 in-lbs.

The bending stress in the bolt is

$$\sigma_b = \frac{M_T\ C}{I} = \frac{5240 \times 1.5/2}{0.177}$$

= 22200 psi

The shear stress due to the lateral force is

$\tau = P/A = 2950/1.492 = 1980$

It should be noted that the lateral displacement of the cylinder is very small. This is due to the fact that the cylinder is very rigid and the applied loads are small.

The maximum axial stress, σ_a, at the periphery of the bolt is

$\sigma_a = S_m + \sigma_b$

= 25000 + 22200

= 47200 psi

4A.5.4.3 Bolt Load Due to Differential Thermal Expansion

Normal Condition

There is a load on the bolts due to a difference in the thermal expansion coefficients of the bolt and lid material. As shown in Figures 5.1-9 and 5.1-14 of Chapter 5.0 the area of the lid at the bolt location is at a uniform temperature and therefore no differential expansion occurs due to a difference in temperatures.

The temperature of the lid under normal conditions is approximately 225°F (Figure 5.1-9, Chapter 5.0). The effect of a difference in thermal expansion coefficients is calculated as follows:

The resulting effect on bolt length, δ, is:

$$\delta = (\alpha_{\ell} - \alpha_{b})\, \ell \Delta T$$

Where

α_{ℓ} = Thermal expansion coefficient of lid
= 6.0×10^{-6} in/in. °F (Table 4A.5-9)

α_{b} = Thermal expansion coefficient of bolt
= 6.6×10^{-6} in/in. °F (Table 4A.5-9)

ℓ = length of bolt, 3.5 in.

ΔT = difference between ambient and normal temperature
= 225 - 70
= 155°F

δ = $(6.0 - 6.6) \times 10^{-6} \times 3.5 \times 155$
= -0.000 326 in. (bolt expands more than lid)

The resulting axial stress, σ_a, is:

$$\sigma_a = \frac{E\delta}{l}$$

Where

σ_a = direct axial stress, psi
E = Young's modulus at 225°F
= 29×10^6
δ = -0.000 326 in.
l = bolt length, 3.5 in.

Therefore

$$\sigma_a = \frac{29 \times 10^6 \times (-326 \times 10^{-6})}{3.5}$$

$$= -2700 \text{ psi}$$

This would result in a reduction in bolt load. Therefore the preload will be increased at room temperature by 2700 psi to account for this effect.

Fire Condition

As a result of a major fire the lid of the cask body will increase in temperature. The maximum temperature that the lid in the seal and bolt area reaches is 479°F (Table 5.1-3, Chapter 5.0). This is the maximum temperature which will occur for any thermal accident events.

The decrease in bolt stress which would occur is calculated as follows:

$$(\sigma_a)_F = (\sigma_a)_N \times \frac{\Delta T_F}{\Delta T_N}$$

Where

$(\sigma_a)_F$ = stress reduction for fire condition

$(\sigma_a)_N$ = stress reduction for normal condition
= -2700 psi

ΔT_F = temperature difference for fire condition
= 479 - 70
= 409°F

ΔT_N = temperature difference for normal condition
= 155°F

Therefore

$$(\sigma_a)^F = -2700 \times \frac{409}{155}$$
$$= -7130 \text{ psi}$$

The preload bolt stress at normal conditions in 25000 psi, therefore a reduction in the bolt stress of 7130 psi is not critical. The bolt load to seal the gaskets is about one-half of the preload stress of 25000 psi. Therefore, a seal would be maintained on the gaskets under the major fire.

4A.5.4.4 Analysis Results

The lid bolt stresses are presented in Table 4A.5-13. The stress listed in the table for the accident condition (i.e., rotation about the trunnions) comes from Section 4A.5.7.2B.

4A.5.5 Stress Analysis of Cask Cylindrical Shell

4A.5.5.1 Description

The section describes the analysis and reports the results obtained for the cylinder. The geometry and dimensions of the cylinder are shown in Figure 4A.5-1.

4A.5.5.2 Loading Conditions

The loading conditions analyzed are listed below:

1) Internal pressure and bolt preload
2) Effect of inertia loads as a result of handling operations
3) Loads imposed by the trunnions
4) Discontinuity loads at the junction with the bottom plate and lid
5) Thermal radial gradient across the cylinder wall
6) Thermal gradient in the axial direction
7) Differential thermal expansion between cylinder and lid and between cylinder and bottom plate
8) Distributed loads due to weight, wind, water, seismic and handling

4A.5.5.3 Method of Analysis

The most critical areas of the cylinder are at the junction of the cylinder with the lid and bottom plate and at the trunnion attachments. Stresses at the junction of the cylinder with the bottom plate are available from the discontinuity analysis described in Section 4A.5.2. This also includes the stresses in the cylinder away from the bottom plate due to internal pressure, handling, and radial and axial thermal gradients.

The method used to analyze the cylinder at the junction with the lid, which is presented herein, considers the cylinder to

lid junction as a pinned connection with a uniformly distributed moment applied by the bolts, gaskets, etc. to the cylinder. Stress components are calculated for each load and categorized in accordance with the ASME Code, Subsection $N_B(1)$. The formulas are in Section 4A.5.2 and are used as appropriate. The analysis of the cylinder is carried out at the lid, at the center, and at the bottom locations.

4A.5.5.4 Assumptions

The analysis is based on the following assumptions:

1. The thickness of the cylinder is small compared to the radius of curvature.
2. Deflections are small compared to the thickness.
3. The material is isotropic and stresses are in the elastic range (i.e. Hooks Law is valid).

4A.5.5.5 Material Used

The cylinder is made of SA-350 Gr. LF1. For the material properties, see Table 4A.5-9.

4A.5 5.6 Analysis

A1. Internal Pressure

The free body stresses due to internal pressure are given by Eqs. 5, 6, and 7 in Section 4A.5.2.4A.1b.

The discontinuity stresses at the bottom end of the cylinder at the junction with the bottom plate are given in Section 4A.5.2.4A.2 and by Eqs. 15 and 16.

The discontinuity stresses in the cylinder at the lid end are given in this section, i.e., 4A.5.5.6G.

A2. Bolt Preload

The preload on the bolts produces a moment on the top end of the cylinder. The moment is induced by the couple from the bolt preload and seal reaction (See Fig. 4A.5-12). The couple or moment acting on the cylinder is the bolt load, F_B, times the moment arm, d, which is the distance from the bolt circle diameter to the center of the seal. Based on the data in Fig. 4A.5-12 the moment on the cylinder is calculated as follows:

$$M = F_B (d_2 - d_1)$$

Where

M = edge moment on cylinder in-lb/in.
F_B = bolt preload
= 8108 lb/in (See Section 4A.5.3.6B)
d_2 = 1.22 in.
d_1 = 3.325 in.

Note: F_B is selected to exceed the effect of internal pressure and handling loads, i.e. $F_B > F_p$

Therefore

M = 8108 (3.325 - 1.22)
= 17100 in-lbs/in.

The bending stress, which is a longitudinal stress is calculated as follows:

$$\sigma_b = \sigma_l = \frac{6M}{t\ cyl^2}$$

Where

t_{cyl} = cylinder thickness
= 9.75 in.

$$\sigma_b = \sigma_1 = \frac{6 \times 17100}{9.75^2}$$

= 1080 psi

The tangential stress is $\nu\sigma_\ell$ or

σ_t = 0.3 x 1080 = 320 psi

B. Inertia Loads Due to Vertical Lifting and Handling

The loading condition is described and evaluated in Section 4A.5.2.4B. There it is shown that the equivalent pressure acting on the bottom plate which simulates the inertia loads caused by lifting and handling is

P_E = 81 psi

The discontinuity analysis for the inertia loads at the junction of the cylinder with the bottom plate is found in Section 4A.5.2.4B. The equations to calculate stresses in the cylinder are given at the end of Section 4A.5.2.4B.

A handling inertia load on the lid would induce an edge moment on the cylinder. However the preload in the bolts exceeds the load due to internal pressure and handling inertia loads. Therefore the edge moment calculated in Section 4A.5.5.6A2. above is conservative.

C. Loads Imposed by the Trunnions

The local stresses in the cylinder at the trunnions are determined in Section 4A.5.1. The stresses due to the trunnion loads are given in Table 4A.5-4.

D. Thermal Radial Gradient Across the Cylinder Wall

This loading condition is described and evaluated in Section 4A.5.2.4.C.b. The equations to calculate thermal stresses at a free end (i.e. lid) and away from the ends are presented at the beginning of Section 4A.5.2.4C.b.

The equations to calculate discontinuity stresses in the cylinder at the cylinder-to-bottom plate junction are given at the end of Section 4A.5.2.4.Cb.

E. Thermal Gradient in the Axial Direction

This loading condition is described and evaluated for the cylinder in Section 4A.5.2.4.C.d. The evaluation includes the center of the cylinder away from the ends and the discontinuity loads and stresses at the junction of the cylinder with the bottom plate. The equations to calculate discontinuity stresses are given at the end of Section 4A.5.2.4.C.d.

The thermal stresses at a free end (i.e. the lid) due to an axial gradient are zero.

The discontinuity stresses in the cylinder at the lid end due to an axial gradient are given in this Section, i.e., 4A.5.5.6G. below.

F. Differential Thermal Expansion

This loading condition is described and evaluated for the cylinder at the bottom end in Section 4A.5.2.4.C.a. The equations to calculate stresses in the cylinder at the cylinder-to-bottom plate junction are given at the end of Section 4A.5.2.4.C.a. There is no differential thermal expansion at the lid end.

G. Discontinuity Loads at the Junction with the Lid

The discontinuity loads are determined by calculating the displacement and rotation of the cylinder at the lid end, for each applied load. The following conservative assumptions are then made to calculate the discontinuity loads at the end of the cylinder:

1) The rotation of the cylinder is zero. This assumption is very conservative and yields the maximum longitudinal edge moment.

$$M_l = M_B + M_d \qquad \text{(See Figure 4A.5-12)}$$

Where

M_l = total longitudinal moment, in-lb/in.
M_B = moment due to preload and seal reaction, in-lb/in.
M_d = discontinuity moment determined in this section, in-lb/in.

A rotation in the clockwise direction would relax the bolt moment and reduce M_l.

2) The calculated differential growth between cylinder and lid is entirely absorbed by the cylinder. This results in a tangential load, N_t and a tangential stress.

This second conservative assumption yields for N_t:

$$N_t = E_t W_{CYL}/R_m$$

The stresses at the end of the cylinder due to the interaction between lid and cylinder are then calculated as follows:

$$\sigma_l = \pm 6M_x/t^2$$

$$\sigma_t = N_t/t \pm 6M_t/t^2$$

Where

$$M_t = \nu M_l$$

The loading conditions which result in discontinuity between the cylinder and lid are:

a) Internal pressure
b) Temperature gradient in axial direction
c) Temperature gradient in radial direction

G.a. Cylinder Deflection Due to Internal Pressure

The radial displacement of the mid surface of a closed end cylinder under internal pressure is given by[2]:

$$W_{CYL} = \frac{p \quad R_i^2}{E(R_o^2 - R_i^2)R_m} \left(R_m^2 \quad (1-2\nu) + R^2{}_o(1+\nu) \right)$$

$$= 105.4 \; P/E$$

Where

p = 250 psi and $E = 28.3 \times 10^6$ at T = 300°F
$(W_P)_{CYL}$ = 0.000931 in.
$(\theta_P)_{CYL}$ = 0

G.b. Displacement and Rotation of Cylinder Upper End Due to Axial Temperature Gradient

The expressions of the displacement and rotation of the cylinder upper end due to a temperature gradient in the axial direction are found in Section 4A.5.2.4.C.d.

$$W_{CYL} = 0$$

$$\theta_{CYL} = +\frac{Rm}{L_v}\,\alpha(\bar{T}_3 - \bar{T}_1)$$

(Note: θ is plus because rotation at top end is counterclockwise)

Where

$$\frac{\bar{T}_3 - \bar{T}_1}{\alpha} = \text{axial gradient}$$

= 0.5 °F/in. (See Section 4A.5.2.4.C.d.

Therefore

$$\theta_{CYL} = +36.375 \times 6.26 \times 10^{-6} \times 0.5$$

= +0.000114 radians

G.c. Displacement and Rotation of Cylinder Upper End Due to Temperature Gradient in the Radial Direction

The expressions of the deflection and rotation of the cylinder upper end due to a temperature gradient in the radial direction are found in Section 4A.5.2.4.C.b.

$$W_{CYL} = + \frac{(1 + \nu)_x}{2\beta^2} \frac{\alpha\,(T_1^* - T_2^*)}{t_{CYL}}$$

$$\theta_{CYL} = - \frac{(1 + \nu)_x}{\beta} \frac{\alpha\,(T_1^* - T_2^*)}{t_{CYL}}$$

Where

ν = Poisson's Ratio, 0.3

α = thermal expansion coefficient at 250°F

$$\beta = \left(\frac{3\ (1 - \nu^2)}{R_m^{\ 2}\ t_{CYL}^{\ 2}} \right)^{1/4}$$

$$= 0.068\ in^{-1}$$

R_m = ream radius of cylinder, 36.375 in.
t_{CYL} = cylinder thickness, 9.75 in.
T_1^* = temperature at inner surface at lid end of cylinder, °F
T_2^* = temperature at outer surface at lid end of cylinder, °F

T_1^* and T_2^* are obtained from Fig. 5.1-9, Chapter 5.0. The values chosen to give the maximum difference at 241°F and 228°F respectively.

Therefore

W_{CYL} = + 1141 x 10^6 in. at lid end
θ_{CYL} = -155 x 10^6 radian at lid end

G.d Combined Displacement and Rotation of Cylinder at Lid End

Adding all the contributions of displacements and rotations from the various loading conditions at the lid end yields:

$$(W_{CYL})_T = W_p + W_{AX} + W_R$$
$$(\theta_{CYL})_T = \theta_p + \theta_{AX} + \theta_R$$

Where

$(W_{CYL})_T$ = total radial displacement

W_p = pressure displacement
= 0.000931 in.

W_{AX} = axial gradient displacement, in.
= 0

W_R = radial gradient displacement, in.
= 0.001141 in.

$(\theta_{CYL})_T$ = total rotation, radians

θ_p = pressure rotation
= 0

θ_{AX} = axial gradient rotation
= 0.000114 radians

θ_R = radial gradient rotation
= -0.000155 radians

Therefore

$$(W_{CYL})_T = 0.00913 + 0 + 0.001141$$
$$= 0.002054 \text{ in.}$$

$$(\theta_{CYL})_T = 0.000114 - 0.000155$$
$$= 0.000041 \text{ radians}$$

The moment and shear acting at the lid end of the cylinder due to the displacement and rotation above is calculated using the Equations 11a and d 113 of Section 4A.5.2.4.A.2 as follows:

$$W_{CYL} = 23 \frac{Q_L}{E} - 1.43 \frac{M_L}{E} + 0.002054$$

$$\theta_{CYL} = -1.43 \frac{Q_L}{E} + 0.184 \frac{M_L}{E} - 0.000041$$

Note that M_L is minus because a counter clockwise moment at the lid end produces an inward or negative displacement. By the same logic, a positive shear load at the lid (i.e., outward) produces a negative or clockwise rotation.

From the above equations

M_L = 39480 in-lb/in
Q_L = 1640 lb/in.

Using Eqs. 15 and 16 of Section 4A.5.2.4A.2, the stresses can be calculated.

H. Distributed Loads

Distributed loads act on the cask due to wind, water, earthquake and handling. These are considered as uniformly distributed loads that induce axial stresses and/or bending stresses in the cylinder wall. The magnitudes of these loads are listed in Table 3.2-2 and the manner in which they act on the cask are shown in Figs. 3.2-1 and 3.2-6 of Chapter 3.0.

The cask is taken as a beam:

- cantilevered from its base when vertical
- or simply supported at both ends when horizontal

and subjected to distributed forces.

The maximum bending moment under these conditions results when the cask is horizontal and supported at the trunnions (See Fig. 3.2-6 of Chapter 3.0). This is due to the fact that the uniform load is greater than the other loads.

The weight of the cask and contents is distributed uniformly between the trunnion supports.

$$M = \frac{w\ell^2}{8} = \frac{(3670 + 1230)\ (131)^2}{8}$$

$$= 10.51 \times 10^6 \text{ in-lbs}$$

The bending stress is calculated as follows:

$$\sigma_B = \frac{MC}{I}$$

Where

$$I = \frac{\pi}{64} (D_o^4 - D_i^4)$$

$$= (82.5^4 - 63^4)$$

$$= 1.5 \times 10^6 \text{ in}^4$$

$$C = D_o/2 = \frac{82.5}{2} = 41.25 \text{ in.}$$

$$\sigma_B = \frac{10.51 \times 10^6 \times 41.25}{1.5 \times 10^6}$$

$$= 290 \text{ psi}$$

The axial stress is due to a vertical handling load condition is shown in Fig. 3.2-6 of Chapter 3.0. The stress is due to the weight of the cask body below the top trunnions and the contents. As shown in Fig. 3.2-6, the axial stress is 290 psi.

I. Cold Rain on a Hot Cask

Because the cask thermal inertia is large, the cask temperature response to changes in atmospheric conditions will be relatively slow. Therefore, ambient temperature variations due to changes in atmospheric conditions will have negligible effects on the cask. This has been confirmed through INEL tests on the TN-24P which has a very similar cask body. Variation of ambient conditions due to snow, rain and wind will also have negligible effects on the cask. Snow or ice will melt as it contacts the cask because the outer surface temperature will be above 32°F for ambient temperatures above -20°F. The cyclical variation of insolation during a day will also create insignificant thermal gradients. The thermal effects due to ambient variations and conditions are discussed in further detail in Section 5.1.3.6.

The most severe thermal effect from ambient variations is expected to be an extremely cold rain after an extended period of time at maximum temperature conditions. Local thermal stresses can occur on exposed surfaces of the cask body under such conditions. The only surfaces that are exposed to direct infringement of rainwater are those at the ends of the cylinder beyond the outer shell. The maximum normal temperature at the end of the cylinder obtained from the analysis presented in Section 5.1.3.6 is 228 F. If an extremely cold rain occurred, it could conservatively be assumed that the outer surface temperature is rapidly cooled to 32 F (as an upper bound thermal shock condition).

The number of these thermal cycles that the cask body cylinder ends could be subjected to without fatigue damage can be readily determined. The surface skin temperature is assumed to be 228° - 32° or 196°F below the bulk temperature of the cask. The tensile stress developed in this skin of material is $E\alpha\Delta T/1-\nu$. For the cylinder material properties in Table 4A.5-9 ($E = 29.5 \times 10^{6}$, $\alpha = 5.53 \times 10^{-6}$), the stress is 45,678 psi. Since this is the stress range, the alternating stress is 22,839 psi. Appendix I of the Code indicates that the fatigue life at this alternating stress is 70,000 cycles.

Therefore, even under these severe assumptions, cold rain on a hot cask is not a problem.

4A.5.5.7 Analysis Results

The tangential stress, σ_t, the longitudinal stress, σ_l, the radial stress, σ_r, and the shear stress, τ, due to the applied loads are reported at the most critical locations. Tables 4A.5-14 and 4A.5-15, list the stresses in the cylinder at the lid junction and away from the ends. The stresses at the junction with the bottom plate are given in Table 4A.5-6. The stresses due to the distributed loads are listed in Table 4A.5-17.

As shown in Section 4A.5.5.6H above the stress due to the cask weight and contents in a horizontal position are very small. The effects of wind, water and seismic loading in a vertical position are even less. Therefore the maximum stress due to distributed loads occurs in the vertical lift position. As shown above the longitudinal stress, σ_l, is 290 psi. The tangential stress, σ_t, is $\nu\sigma_l$ or 90 psi.

These stresses are combined, principal stresses and stress intensities determined and compared with the allowable stress intensity values in Section 4.2

4A.5.6 Containment Vessel Stresses Due to Cask Drop Accidents

4A.5.6.1 Introduction

The description of the drop accidents and the magnitudes of the deceleration inertia g loading are determined as described in Section 3.1.11. Two vertical drop conditions are considered with the cask falling a distance of 8 feet before impacting the concrete storage pad. In the first drop condition the cask axis is vertical and the peak deceleration is 100 g (Section 3.1.11.3). In the second drop accident considered, the cask center of gravity is located over the corner of the cask. The peak deceleration for this case is 27 g.

Drops from a clear height of 7 feet are considered for the cask in a horizontal orientation. "Slap down" effects are considered for cases where the cask axis is within a few degrees of the horizontal. These cases are found to be only slightly more severe than drops with the cask axis oriented in the horizontal direction. The peak deceleration for this case is found to be 69 g.

4A.5.6.2 Method

Stresses induced in the cask by the accident drop conditions are treated in two stages. First the peak deceleration induced in the cask after it impacts the storage concrete pad is calculated. The method and the results of this calculation are given in Section 3.2.11. The peak decelerations are computed based on the assumption that the cask is rigid relative to the impact target. The target is assumed to be a concrete slab resting on an elastic foundation. The concrete is taken to have a crushing strength of 4000 psi (27.6 MPa). The soil is taken to have a foundation modulus of 380 psi/inch. It should be noted that any cask flexibility would tend to reduce the magnitude of the deceleration.

The peak decelerations are then applied as equivalent static loads to the cask. The method of applying the loads to the cask depends on the drop orientation under evaluation. Where possible the methods previously developed in Sections 4A.5.2, 4A.5.3, 4A.5.4 and 4A.5.5 are used for these evaluations. The particular methods used for the various drop orientations are described in the appropriate sections which follow.

The rise time of the dynamic loads applied to the cask as it is decelerating is small compared to the period of vibration of the cask. The dynamic amplification is not significant for the drops as shown by application of Fig. 8.20 of Reference 11 (See Section 4A.5.6.3D below).

4A.5.6.3 Stresses Resulting from Drop Accidents

A. Drop with Cask Oriented Vertically

The cask, when oriented vertically, is handled by the upper trunnions. If the cask were dropped, it would impact on the bottom end and not the lid end. Therefore for this drop condition only the bottom end is evaluated.

A.1 Bottom Plate-Cylinder Junction

The method used for analysis of the bottom plate and connected cylinder follows that in Section 4A.5.2.4B. An equivalent pressure due to the deceleration loads acting on the bottom is calculated. Then the stresses can be calculated using the equations at the end of Section 4A.5.2.4B.

The loads acting on the bottom of the cask due to a vertical drop are shown in Figure 4A.5-14. The first load is a pressure loading equal to the total weight of the cask multiplied by the deceleration and divided by the area.

$$p_1 = W_1 G_A / A$$

Where W_1 = Total Weight of Cask, 214,000 lb. (Table 3.2-3, Chapter 3.0)
G_A = Deceleration, 100g (See Section 3.2.11, Chapter 3.0)
A = Area of cask end based on outer diameter, $in.^2$

This pressure loading acts on the interface between the cask and concrete pad.

$$p_1 = 214000 \times 100/(\pi \times 82.5^2/4) = 4000 \text{ psi}$$

The second load is a pressure loading resulting from the weight of the internals, i.e., fuel and basket.

$$p_2 = W_2 \times G_A / A$$

Where W_2 = Weight of basket and fuel assemblies

= 17372 + 36000 (See Table 3.2-3, Chapter 3.0)

= 53372 lb. (use 54000 lb)

A = Area of cavity, $in.^2$

$$p_2 = \frac{54000 \times 100}{(\pi/4) \times (63)^2} = 1740 \text{ psi}$$

This pressure loading acts on the inner surface of the bottom plate. The difference between P_1 and P_2 is an equivalent external pressure, p_E, acting on the bottom plate.

$$p_E = 4000 - 1740 = 2260 \text{ psi}$$

The stresses due to this equivalent pressure can be determined with the equations at the end of Section 4A.5.2.4B. Since the accident load results in an external pressure, the signs of the stress components are reversed.

Discontinuity Stresses

Cylinder

Tangential Stresses, σ_t:

σ_t (inside) = $(-1.52\ p_E)$ = (-1.52 x 2260)
= -3435 psi

σ_t (outside) = $(+3.72\ p_E)$ = (3.72 x 2260)
= +8410 psi

Longitudinal Stresses, σ_ℓ:

σ_ℓ (inside) = $(-8.74\ p_E)$ = (-8.74 x 2260)
= -19750 psi

σ_ℓ (outside) = $(8.74\ p_E)$ = (8.74 x 2260)
= +19750 psi

The radial stresses are zero.

Shear Stress, λ, = $(10.19\ p_E)/t$ = (10.19 x 2260)/9.75
= +2360 psi

Plate at Center and Junction with Cyl'nder

σ_t (inside) = $(-2.71)\ p_E$ = (-2.71 x 2260)
= -6125 psi

σ_t (outside) = $(-4.4)\ p_E$ = (-4.4 x 2260)
= +9950 psi

$\sigma_r = \sigma_t$, inside and outside

$\sigma_\ell = 0$

Equivalent Pressure Stresses

Cylinder

There is no pressure acting on the cylinder for this case; therefore there are no stresses acting on the cylinder due to the equivalent pressure from loads p_1 and p_2. However there are stresses due to the load p_3 as calculated below.

Plate

The stresses in the plate are calculated with the equations at the end of Section 4A.5.2.4B. These equations are also given at the end of Section 4A.5.2.4A.1b.

At Junction with Cylinder

σ_t (inside) = (-6.26) p_E = (-6.26 x 2260)
= -14150 psi

σ_t (outside) = (+6.26) p_E = (6.26 x 2260)
= +14150 psi

σ_ℓ (inside) = 6440 psi (interface between cylinder and plate)

σ_ℓ (outside) = -4000 psi (outer surface of plate at interface with target.)

σ_r (inside) = (-2.14) p_E = (-2.14 x 2260)
= -4840 psi

σ_r (outside) = (+2.14) p_E = (2.14 x 2260)
= +4840 psi

Shear stress, $\lambda = \frac{(W_L + W_B)G}{2\pi R_m t_{pl}} = \frac{(143562)\ 100}{2\pi \times 36.375 \times 11.25}$

= 5600 psi

At Center of Plate

$$\sigma_t = \sigma_r \text{ (inside)} = (-11.84\ p_E)$$
$$= (-11.84 \times 2260$$
$$= -26760 \text{ psi}$$

$$\sigma_t = \sigma_r \text{ (outside)} = (+11.84\ p_E)$$
$$= +26760$$

The third load acting at the bottom is load P_3 shown in Figure 4A.5-14. This is a pressure load acting on the cylinder due to the deceleration of the body and lid. It acts on the cross sectional area of the cylinder. This load produces an additional longitudinal stress in the shell calculated as follows:

$$\sigma_\ell = \frac{-(W_L + W_B)\ G_A}{A}$$

Where:

$W_L + W_B = 11624 + 131938$

$G_A = 100$

A = Area of cylinder, $in.^2$

Therefore

$$\sigma_\ell = \frac{(143562)\ 100}{.785\ (82.5^2 - 63^2)}$$

$$= -6440 \text{ psi}$$

And

$$\sigma_t = \mu\sigma_\ell = 0.3 \times -6440 = -1930 \text{ psi}$$

Note the body weight includes the cylinder, outer shell, resin, aluminum fins, trunnions and basket rails (see Table 3.2-3, Chapter 3.0).

A2. Lid

As the cask body is decelerated by the impact of the bottom plate on the concrete pad, the lid is also decelerated. Therefore an upward load would occur at the interface of the lid outer plate (i.e., 3.5 in. thick section) and the top of the cylinder (see Figure 4A.5-15).

The upward load is assumed to act at the bolt circle diameter. This is conservative since as the lid is driven into the cylinder the force would move inward on the lid thus reducing the moment arm on the lid outer plate (i.e. lid flange).

The resulting force, moment and stress are calculated as follows:

$$F_{BC} = W_L \, G_A / \pi D_{BC}$$

Where

W_L = Weight of lid, 11624 lb. (Table 3.2-3, Chapter 3.0)
G_A = Deceleration, 100 g
D_{BC} = Diameter of bolt circle, 70.32 in.

The bending moment, M_L, on the lid flange at the interface between the center lid section and the reduced thickness section (i.e. lid flange) would be

$$M_{LID} = F_{BC} \times a$$

Where a = moment arm,
= (70.31 - 63.63)/2 (Fig. 4A.5-4)
= 3.34 in.

The resulting bending stress, σ_b, which is a radial bending stress is:

$$\sigma_b = \sigma_r = \frac{6\ M_{LID}}{t^2}$$

Where

t = thickness of reduced section of lid, 3.5 in. and 3.28 in. at the seal.

Therefore

$$\sigma_r = \frac{6}{t^2} \times F_{BC} \times a$$

$$= \frac{6}{(3.28)^2} \times \frac{11624 \times 100 \times 3.34}{3.14 \times 70.32}$$

$$= 9820 \text{ psi}$$

Also $\sigma_r = \sigma_t$

The shear stress, λ, due to F_{BC} is as follows:

$$\lambda = \frac{F_{BC}}{t} = \frac{5264}{3.28}$$

$$= 1600 \text{ psi}$$

The longitudinal stress, σ_ℓ, is a compressive stress at the junction with the cylinder.

$$\sigma_\ell = -(W_L \times G_A)/\text{contact area}$$

$$= -(11624 \times 100)/.785\ (68.25^2 - 63^2)$$

$$= -2150 \text{ psi}$$

The bending stress in the inner portion of the lid is calculated using the moment, M_L, as follows:

$$\sigma_r = \sigma_t = \frac{6\ M_{LID}}{t^2}$$

$$= \frac{6 \times 17608}{(11.5)^2}$$

$$= 835 \text{ psi}$$

$$\lambda = \frac{F_{BC}}{t} = \frac{5264}{11.25}$$

$$= 470 \text{ psi}$$

B. Side Drop

Two possible side drop orientations were evaluated to determine the maximum deceleration values. The results of these evaluations, which are presented in Section 3.2.11 and 3.2.12, gave a maximum deceleration for a drop orientation with the cask axis parallel with the impact surface of 65 g. The maximum deceleration for a drop orientation with the cask axis at a slight angle with the horizontal (i.e., slapdown case) is 69g. Therefore the latter value will be used for the stress evaluation of the side drop condition. It is assumed that the 69 g value acts uniformly along the cask length. This produces the highest stresses in the cask body shell, i.e., cylinder.

B1. Ovalization Effect

Under this drop orientation the cylinder will tend to ovalize away from the ends. At the bottom plate and lid ends the ovalization is basically eliminated since these components are very rigid in the radial direction.

The loads acting on the cylinder during the horizontal drop are shown in Fig. 4A.5-16. One load is the weight of the body decelerating against the target. This is assumed to be reacted at a single point or line along the cylinder (Fig. 4A.5-16a). The second load is due to the deceleration of the internals, i.e. basket and fuel assemblies. Again this is reacted as a line load (Fig. 4A.5-16b). Actually the reaction on the cylinder is spread over a finite area as the cask deforms the target, i.e. storage pad. This load is shown as W_3 on Fig. 4A.5-16c and is equal to the line loads R_{c1} and R_{c2}. The effects of these loads are determined using Table 17 of Reference 7. The cylinder is assumed to act as a ring section over its length.

The loads are calculated as follows:

R_{c1} (Fig. 4A.5-16a):

$$R_{c1} = \frac{W_B \times G}{L}$$

Where W_B = Weight of cask without lid bottom and internals
= 105,758 + 2186 + 10484 + 10344 + 1453 + 1413 + 523
(see Table 3.2-3, Chapter 3.0)
= 132161 lb.

G = 69 g (Higher value for slapdown used)

L = Length of outer shell
= 154 in. (Fig. 4A.5-1)

Therefore

$$R_{c1} = \frac{132161 \times 69}{154} = 59215 \text{ lb/in}$$

And

$$W_1 = \frac{R_{c1}}{\pi D}$$

Where

D = diameter of cylinder, in.
= 72.75

Therefore

W_1 = 59215/3.14 x 72.75
= 260 psi

R_{c2} (Fig. 4A.5-16b):

$$R_{c2} = \frac{W_I \, G}{L}$$

Where

W_1 = Weight of fuel and basket
= 17372 + 36000
= 53372 lb.

G and L are defined above

Therefore

$$R_{c2} = \frac{53372 \times 69}{154} = 23915 \text{ lb/in}$$

And

$$W_2 = \frac{R_{c2}}{D} = \frac{23915}{72.75}$$

$$= 328 \text{ psi}$$

Note that the internals are assumed to be uniformly distributed over the projected area based on the mean cylinder radius R_m of 36.375 in. (i.e., 72.75/2).

R_{c3} (Fig. 4A.5-16c):

$$R_{c3} = 2W_3 R \sin \alpha = R_{c1} + R_{c2}$$

Therefore

$$W_3 = \frac{R_{c1} + R_{c2}}{2R \sin \alpha}$$

Where α = Angle based on depth cask moves into target (i.e. storage pad)

= 166.2° (See Section 3.1.11.2.2 of Chapter 3.0)

R_{c1} and R_{c2} are defined above

R_m = cylinder radius, 36.375

And

$$W_3 = \frac{59215 + 23915}{2 \times 36.375 \sin (166.2)}$$

$$= 4790 \text{ psi}$$

The bending moments caused by these loads are calculated using Table 17 of Reference 7.

R_{c1}:

$$M_{c1} = \frac{3}{2} W_1 R_m 2 \qquad \text{(Table 17, Case 13)}$$

$$= 1.5 \times 260 \times 36.375^2$$

$$= 516030 \text{ in-lb/in}$$

R_{c2}:

$$M_{c2} = 0.5 W_2 R_m 2 \qquad \text{(Table 17, Case 12)}$$

$$= 0.5 \times 328 \times 36.375^2$$

$$= 217000 \text{ in-lb/in}$$

R_{c3}:

$$M_{c3} = 0.026 W_3 R_m 2 \qquad \text{(Table 17, Case 12)}$$

$$= 0.026 \times 4790 \times 36.375^2$$

$$= 164800 \text{ in-lb/in}$$

Note that the bending moment due to R_{c3} is opposite to bending moments for R_{c1} and R_{c2}.

The bending stresses due to the sum of the effects of these is:

$$\sigma_b = \frac{6}{t^2} (516030 + 217000 - 164800)$$

$$= \frac{6 \times 568200}{9.75^2}$$

$$= 35900 \text{ psi}$$

This stress is corrected for thick shell effects using Table 16, Case 1 of Reference 7.

Therefore

$$\sigma_b = 1.1 \times 35900 = 39490 \text{ psi}$$

This is a tangential stress in the cylinder, i.e. $\sigma_b = \sigma_t$. The longitudinal stress, σ_ℓ is $\nu\sigma_t$.

$$\sigma_\ell = 0.3 \times 39490$$
$$= 11850 \text{ psi}$$

As stated above these are the highest cylinder stresses that occur during a side drop, including slapdown.

B2. Moment on Lid

This drop condition causes a moment on the lid pulling it off the cask body, i.e. tensile forces acating on lid bolts (See Fig. 4A.3-17).

If the pivot point is conservatively assumed to be at point O, then the moment on the lid is as follows:

$$M_L = W_L G \times a$$

Where

M_L = moment acting on lid, in. lbs.
W_L = weight of lid, 11624 lb.
G = deceleration, 69 g
a = moment arm, 6 in.

Therefore

$$M_L = 11624 \times 69 \times 6$$
$$= 672400 \text{ in. lb.}$$

It is shown in Section 4A.5.7.2B that this is much less severe than the worst condition postulated.

C. Drop with Cask Center of Gravity Over Corner

The cask is handled vertically from the trunnions at the top. Therefore it is postulated that the cask would drop onto the bottom corner of the cask. As described in Section 3.2.11 of Chapter 3.0 the maximum deceleration load is 27 g. This acts on the cask normal to the target surface (See Fig. 4A.5-18). The axial, G_A, (along cask longitudinal axis) and lateral, G_L, (perpendicular to cask longitudinal axis) components are calculated as follows:

$$G_A = G \sin 69°$$
$$= 27 \times 0.934$$
$$= 25.2 \text{ g}$$

$$G_L = G \cos 69°$$
$$= 27 \times 0.358$$
$$= 9.7 \text{ g}$$

This is a less severe condition than the vertical and horizontal drop orientation. The axial, G_A, value of 25.2 g is less than the 100 g value for the vertical drop and the lateral, G_L, value of 9.7 is less than the 69 g value for the side drop. Therefore stresses resulting in the cask body are less severe for the corner over center of gravity drop accident.

D. Dynamic Effects

The dynamic effect of the impact force on the cask from the drop or tipping accidents depends on the duration of the loading and the natural vibration period of the cask. The peak impact force does not occur instantly, it increases with time after the cask strikes the foundation. A finite time is required before the maximum force is developed since the slab and soil must deform to reach this force. In the end impact case approximately .005 sec is required to develop a peak force. In the side drop case concrete crushing results in a more gradual rate of loading; approximately .010 sec is required to develop the maximum force.

The Shock and Vibration Handbook[11] provides curves to determine dynamic amplification factors for gradually applied impact forces. Figure 8.20 is used to determine the TN-24 factors. The fundamental natural period of the cask for axial vibration is .00363 sec (f_n = 275 cps) and for lateral vibration (bending as a beam) is .00557 sec (f_n = 179 cps). The calculated force vs. time curves for the TN-24 end and side drop cases are enveloped as indicated in Figure 4A.5-19 to determine the Figure 8.20 factors. For the end impact case $\tau/2$ = .005 sec, and for the side impact case $\tau/2$ = .010 sec. The ratio τ/T is then 2.75 for the end case and 3.59 for the side case. The dynamic load factors are both less than 0.5. Therefore it is conservative to perform quasistatic stress analyses without applying dynamic load factors.

4A.5.6.4 Analysis Results

The tangential stress, σ_t, the longitudinal stress, σ_l, the radial stress, σ_r, and the shear stress, τ, are presented for the drop accident conditions in Tables 4A.5-18a, 18b, 18c, 18d, 18e and 19. The stresses are reported only for the highest stressed locations, and the applicable ASME code stress category indicated.

These stresses are combined with the stresses due to the other loads acting at the same time as the accident. The combined stresses, principal stresses and stress intensities are determined and compared with the allowable stress intensity values in Section 4.2.

4A.5.7 Containment Vessel Stresses Due to Cask Tipping Accidents

4A.5.7.1 Introduction

The description of the tipping accidents and the magnitude of the deceleration inertia g loadings are determined in Section 3.2.12. One accident involves the cask tipping about the trunnions which are fixed at a point 8 feet off the ground (see Figure 3.2-11). This could occur while tilting the cask up on a cradle support either on the storage pad or transport vehicle and for some reason the handling gear free wheels when the cask would be just vertical on the lower trunnions. The peak rotational deceleration for this accident is 135 rad/sec^2 (0.350 g/inch) for the 4000 psi crushing stress for the concrete pad on an elastic soil. This translates into a peak deceleration at the lid of 55 g.

The second accident involves tipping of the cask about its base. The peak angular deceleration for this case is 155 rad/sec^2. This translates to a peak deceleration at the lid end of 62 g.

4A.5.7.2 Rotation About the Trunnions Support as a Pivot

The cask starts in a vertical position and then rotates about the trunnions (point "O" on Fig. 4A.5-20) until it hits the target. The peak rotational deceleration is 135 rad/sec^2 (0.350 g/inch). This translates to a peak deceleration of 55 g normal to the cask surface at the lid end. These values of deceleration are determined in Section 3.2.12-1a.

There are three loading conditions which are evaluated for the tipping about the trunnion. First, the deceleration on the lid end results in ovalization of the cylinder near the lid. A short length of cylinder will be in direct contact with the target, i.e. forms part of the footprint. This results in ovalization of the end of the cylinder away from the lid.

A second result is a load on the lid tending to throw it off the cask body and cause tensile loads in the lid bolts.

The third effect is a linearly varying load on the cask body caused by the rotational deceleration. This type of loading results in bending of the cask body as a beam. An analysis of the cask as a beam under a uniformly distributed load is presented in Section 4A.5.5.6H. A 3 g load was applied statically to the cask body supported at the trunnion locations. The stress due to a 3 g load is 290 psi. The load distribution due to cask tipping accidents is not the same, however the effects would not be much different. Multiplying the 3 g case by the maximum inertia load of 62 g would yield a bending stress in the cask body of 18000 psi. This is approximately one-half the stress in the cylinder due to ovalization as calculated in Section 4A.5.6.3.B1. Therefore the effects of this loading condition are less severe than the side drop and no further evaluation is presented.

A. Ovalization of Cylinder at Lid End

This accident causes a peak deceleration load of 55 g at the lid end which acts normal to the cask surface. However this is less than the peak load of 69 g at the lid end due to the slapdown case. Therefore the ovalization of the cask shell (cylinder) and the resulting stresses due to ovalization are less for the tipping case compared to the slapdown case. Since this tipping case is less severe no further evaluation is required.

B. Effect on Lid Bolts and Lid

There are two effects acting on the lid tending to push or throw it off the cask body (i.e. tensile forces in the lid bolts). There is a small axial (parallel to cask longitudinal axis) inertia load due to the internals acting on the lid and the lid weight itself. This effect is calculated in Section 4A.5.7.2C. below.

The load of 55 g acting normal to the cask surface will result in a couple acting on the lid due to its inertia effect. The effect is the same as described in Section 4A.5.6.3.B2 and shown in Fig. 4A.5-17. However the magnitude of the tipping case is less than the slapdown case, which results in a deceleration load of 69 g. In order to evaluate this effect on the lid bolts and lid a conservative approach which uses the results of the cask center of gravity over the corner accident case described in Section 4A.5.6.3C. In this section it is postulated that the cask can only drop on the bottom corner of the cask. However, for the evaluation of the lid bolts and lid it is assumed herein that the cask drops on the ocrner at the lid end. There is no other accident condition which is postulated that would cause greater load on the lid bolts and lid for the design of the TN-24.

The results as presented in Section 4A.5.6.3C and shown in Fig. 4A.5-18 are used except the lateral, G_L, load is 69 g rather than 9.7 g. The 69 g value is the maximum lateral deceleration load of any of the accident cases evaluated. Again this is to provide a measure of conservatism. The axial load value used is 25.3 g.

The system of loads acting on the cask are shown in Fig. 4A.5-21. The system of loads projected onto the lid are shown in Fig. 4A.5-22. Also shown is the reaction load at the cask interface and the pivot point, O, for analysis of lid rotation. Fig. 4A.5-23 shows the lid bolt loads resisting rotation of the lid about pivot point O . The bolt load varies uniformly from pivot point O, to the bolt farthest from O.

The moment acting on the lid about pivot point, O, due to the inertia load is calculated as follows:

$$M_I = W_I \times 25.2 \times R_T + W_L \times 25.2 \times R_T + W_L \times 69 \times a + P_A \times R_T$$

Where

M_I = Total moment about pivot point, in-lb

W_I = Weight of internals
= 17372 x 36000
= 53372 lb

W_L = Weight of lid, 11624 lb

P_A = Internal pressure load
= p * A = 250 x .785 x 63^2
= 780000 lb

R_T = Distance from center of lid to pivot point
= 36.875 in.

a = Moment arm of lid inertia load, W_L, in.
= 1 in.

Therefore

M_I = (53372 x 25.2 x 36.875) + (11624 x 25.2 x 36.875)
+ (11624 x 69 x 1) + (780,000 x 36.875)
= 49.8 x 10^6 + 10.8 x 10^6
+ 0.80 x 10^6 + 28.76 x 10^6
= 90.16 x 10^6 in-lb

This moment is reduced by the effect of the preload on the lid bolts. The moment due to preload is calculated as follows:

$$M_p = nF_B^* R_T$$

Where

M_p = moment due to bolt preload, in-lb
n = number of bolts, 48
F_B^* = preload per bolt
= $A_B \times S_m$
= stress area bolt x S_m
= 1.492 x 25000
= 37300 lb.
R_T = distance from center of lid to pivot point
= 36.875 in.

Therefore

$$M_p = 48 \times 37300 \times 36.875$$
$$= 66 \times 10^6 \text{ in-lb.}$$

The increase in bolt load due to the inertia g loads is due to the difference between M_I and M_p which is

$$M_T = M_I - M_p$$
$$M_T = 90.16 \times 10^6 - 66 \times 10^6$$
$$= 24.16 \times 10^6 \text{ in-lbs.}$$

The lid bolts resist the above moment which tends to unseat the lid from the seals. The lid bolt loads are proportional to the distance from the pivot point, O. The resisting moment, M_R, applied by the bolts about point O is obtained from the following expressions. Refer to Fig. 4A.5-24 for terminology.

$$M_R = F_{BO} \ell_{BO} + 2 F_{B1} \ell_{B1} + 2F_{B2} \ell_{B2} + \ldots$$

And $F_{B1} = F_{BO} \frac{\ell_{B1}}{\ell_{BO}}$

Where

ℓ_{BO}, ℓ_{B1}, etc., are the distances between the pivot point O and the bolt centerlines.

Therefore the moment, M_R, can be expressed in general terms as follows:

$$M_R = \frac{F_{BO}\,[2R+b^2]}{2R+b} + 2 \sum_{N=1}^{N=23} [R+R \cos \theta+b]^2$$

Substituting yields

$$M_R = 1230\, F_{BO}$$

Equating M_R and M_T yields F_{BO}

$$F_{BO} = \frac{24.16 \times 10^6}{1230} = 19640 \text{ lb.}$$

The direct axial stress, σ_a, in the bolt is:

$$\sigma_a = \frac{F_{BO}}{A_B}$$

Where

A_B = bolt area, 1.492 in.^{2}

$$\sigma_a = \frac{19640}{1.492} = 13200 \text{ psi}$$

The bending stress in the lid flange, i.e. outer reduced thickness portion (3.5 in. and 3.28 in. at seal) is obtained as follows:

$$\sigma_b = \frac{6M_b}{t^2}$$

And $M_b = 3.34\ F_B$

Where M_b = edge moment, in-lb/in

F_B = bolt load per inch of bolt circle circumference

$$= \frac{48 \times F_{BO}}{6.28 \times 35.16}$$

$$= 4270 \text{ lb/in}$$

Note this assumes the bolt load at each bolt is equal to F_{BO}. However the bolt load varies proportional to the distance from the pivot point. An equivalent average bolt load per inch of circumference would be approximately one-half F_B or

$$F_B = 4270/2 = 2135 \text{ lb/in}$$

Therefore the bending stress in the outer portion of the lid at the seal is

$$\sigma_b = \frac{6 \times 3.34 \times 2135}{(3.28)^2}$$

$$= 3980 \text{ psi}$$

Note: 4200 psi was used for load combinations.

C. Effect of Rotational Deceleration on Lid and Lid Bolts

Analyses to determine the dynamic response of the TN-24 under various drop and tipping accidents are described in Sections 3.2.11 and 3.2.12. The lid loading is directly determined for the translational cases by applying quasistatic inertia forces at the CG's of the various components and performing typical static solutions to determine interface reactions.

In the rotational impact cases, other effects occur. The cases where the lid impacts onto the concrete foundation after a tipping accident about the bottom are more severe than an impact after tipping about the cask bottom. Several inertia effects may occur although probably not at the same time. These effects include:

(1) The centrifugal force required to hold on the lid as the cask reaches the maximum rotational speed,

(2) The centrifugal force required to hold in the cask contents at that speed,

(3) The gravitational force to keep the lid on and contents in the cask as the cask reaches the greatest tipping angle, and finally

(4) The moment required to halt the rotation of the lid as the cask is subjected to the highest rotational deceleration.

The three rotational cases that are to be studied are the trunnion tipping case, the tipover case, and the slapdown case. In the trunnion tipping case the cask CG drops approximately 115 in. while it drops 46 in. in the tipover case and 84 in. in the slapdown case. Therefore, somewhat more potential energy is converted into rotational energy during the trunnion tipping case than in the other rotational cases and a higher rotational speed is developed. Thus the highest centrifugal forces ((1) and (2)) are developed for this case. In addition, the greatest tipping angle is developed in this case so the lid and contents tend to develop the greatest gravity forces ((3)). The greatest moment to react the rotary inertia force ((4)) is developed in the slapdown case which has the greatest rotational deceleration.

If we examine the trunnion tipping case where the CG drops approximately 115 in., we can determine the following numbers:

Rotational Energy at Impact = Change in Potential Energy

$$Wh = \frac{1}{2} I\omega^2$$

$$\omega^2 = \frac{2Wh}{I}$$

Where

h = drop height, 115 in.
W = load cask weight, 215000 lb.
I = cask moment of inertia about trunnion, 4.46×10^6 lb. in. $sec.^2$
ω = cask rotational velocity, rad/sec

The centrifugal force developed on a particle is:

$$F = m\ r\ \omega^2$$

Where:

m = particle mass, $\frac{w}{g}$, lb. $sec.^2/in.$
r = distance from pivot point

The centrifugal force on the lid, which is at a distance of ℓ = 155.75 from the pivot point and has a weight, w, of 11620 lb. is:

$$F_{lid\text{-}centrifugal} = \frac{w}{g}\ell\omega^2 = \frac{w}{g}\ell\left(\frac{2Wh}{I}\right)$$

$$= \frac{11620}{386} \times 155.75 \times \frac{2 \times 215{,}000 \times 115}{4.46 \times 10^6} = 51{,}985 \text{ lb.}$$

The centrifugal force applied to the lid by the cask contents at this time is (w = 52,850 lb., r = 68.37 in.):

$$F_{contents\text{-}centrifugal} = \frac{52850 \times 68.37 \times 2 \times 215{,}000 \times 115}{386 \qquad 4.46 \times 10^6} = 103{,}800 \text{ lb.}$$

The cask reaches an angle of 26.6 degrees below horizontal for this case. Therefore the gravitational forces acting on the lid and contents at this angle, in the direction of the axis of the cask are:

$$F_{lid} = \text{gravitational} = w \sin\alpha$$
$$= 11620 \sin 26.6 = \underline{5200 \text{ lb.}}$$

$$F_{contents\text{-}gravitational} = 52850 \sin 26.6$$
$$= \underline{23660 \text{ lb.}}$$

The greatest rotational acceleration is 175 rad/sec^2 during the slapdown accident. At the time of peak rotational deceleration, the lid rotary deceleration is also the 175 rad/sec^2. The moment required to halt the lid rotation is then:

$$M_{lid} = I\theta''$$

Where:

M_{lid} = Moment to hold lid on cask, in. lb.
I = Lid moment of inertia about point where it pivots on cask, lb. in. sec.^{2}
θ'' = Max. rotary acceleration, rad/sec.^{2}

The moment of inertia of the lid about its edge where it pivots on the cask is:

$$I = \frac{1}{4} m R^2 + \frac{1}{12} m t^2 + m R^2$$

Where, R, the lid radius, is 32 in. and the thickness, t, is 11.5 in.

$$I = \frac{11620}{386}\left(\frac{32^2}{4} + \frac{11.5^2}{12} + 32^2\right)$$

$$= 38,860 \text{ lb. in. sec.}^2$$

M_{edge} = 18"

= 38,860 x 175 = <u>6,801,025 in. lb.</u>

It is clear that the forces and moments acting on the lid and lid bolts are less severe than those calculated in Section 4A.5.7.2B above.

4A.5.7.3 Tipping of Cask About the Bottom

The cask is assumed to be standing vertically and then for some reason tips and pivots about the outer edge of the bottom (See Fig. 3.2-12, Chapter 5.0). The peak rotational deceleration in 155 rads/sec^2 (0.XXX g/inch). This translates to a peak deceleration of 62 g normal to the cask surface at the lid end. These values of deceleration are determined in Section 3.2.12.1.

Again there are three loading conditions which are evaluated for the tipping about the base of the cask. They are evaluated, basically, by comparing the deceleration loads with those of previously evaluated accidents. The first load is the deceleration load on the cask which causes ovalization of the cylinder. In this case the cask body is basically in contact with the target along its entire length. The maximum deceleration is at the lid end and is 62 g. This is less than the peak load of 69 g at the lid end due to the slapdown case. Therefore the ovalization of the cask shell (cylinder) and the resulting stresses due to ovalization are less for tipping about the cask base compared to the slapdown case. Therefore no further evaluation is required.

The second effect is composed of two components: (1) the axial load on the lid due to its own weight and the internals and (2) the couple due to the deceleration load normal to the cask surface at the lid. These two components for this tipping case are less severe than the components evaluated for the tipping about the trunnion case presented in Section 4A.5.7.2B. Therefore no further evaluation of this case is required.

The third effect is a linearly varying load on the cask body caused by the rotational deceleration. The value for this case is 155 rads/sec^2 which is greater than the value of 135 rads/sec^2 for tipping about the trunnions. The higher value is used in evaluating this effect in Section 4A.5.7.2C. Therefore no further evaluation is necessary in this section.

4A.5.7.4 Summary of Stresses

Stresses induced by the tipping accidents are summarized in Tables 4A.5-20a and 20b.

The tangential stress, σ_t, the longitudinal stress, σ_l, the radial stress, σ_r, and the shear stress, τ, are presented.

These stresses are combined with other loading conditions acting simultaneously. The combined stresses, principal stresses and stress intensities are determined and compared with the allowable stress intensity values in Section 4.2.

4A.5.8 Containment Vessel Stresses Due to Tornado Missile Impact

4A.5.8.1 Introduction

The description of the tornado missile impact analysis for the three types of missiles defined in NUREG-0800 (Ref. 6) is provided in Section 3.2.1.2. For review, these missiles are:

Missile A - massive (1800 kg) high kinetic energy missile (automobile) that deforms on impact contacting the cask at a horizontal speed of 35% of the tornado wind speed or 126 mph.

Missile B - rigid missile (125 kg, 8 in. diameter) that impacts on the cask at a horizontal velocity of 126 mph or at a vertical velocity of 70% of the horizontal velocity or 88.2 mph.

Missile C - rigid steel one inch diameter sphere that impacts the cask at the same velocities and orientations as Missile B.

This section describes the analyses performed to determine the global cask body stresses that could occur during impact of each of these missiles. Tables 4A.5-21a through 21c summarize the key stresses for the missiles and cask orientations of interest.

4A.5.8.2 Method

Impact Forces

The impact analysis for each of the three types of tornado missiles is described in Section 3.2.1.2. In that section the magnitudes of the impact forces from each of the missiles are determined and general cask stability is evaluated. It was found that:

Missile A, the high kinetic energy missile, cannot cause a vertical cask to tip or fall over nor can it cause a horizontal cask to roll from its support cradle. This missile can slide a vertical cask a short distance (less than two feet). The peak force due to impact of this missile is 683,314 lb and the force is applied over a very large area (3 ft. by 6 ft.) as the missile crushes. The average contact pressure on this large area is only 266 psi which is well below the yield stress of the cask material and therefore does not cause any local damage.

Missile B, the rigid missile, has a lower initial kinetic energy than Missile A so that it has less effect on cask stability than Missile A. However, it does develop a peak contact force of 1,382,000 lb. which is concentrated on an eight in. diameter "footprint" on the cask. Missile B develops a contact pressure equal to the cask body yield stress of 27,300 psi.

Missile C, the one inch steel sphere, impacts on a very localized area with a peak force of only 11,350 lb. Since there are no small recessed areas on the cask that are vulnerable to such a missile, Missile C is trivial (compared to Missiles A and B) and is not analyzed in any depth.

Models

For a vertical cask, Missile A impact as illustrated in Figure 4A.5-25(a) is conservatively assumed to occur on the side of the cask away from the ends and to be reacted by a three foot high ring of the cask body cylinder. The automobile is assumed to be upright with the front impacting the cask. The impact is represented as a 266 psi pressure on a 3 ft. by 6 ft. projected area on the outside of the cask. (3 ft. on the cask length and 6 ft. on its diameter). The pressure loading is balanced by inertial loading of the full 360° ring and a quasistatic analysis is performed. The remainder of the cask body is conservatively assumed to be ineffective in resisting this crushing or denting load.

For a horizontal cask, Missile A is assumed to be upright and to impact near the center of the cask as illustrated in Figure 4A.5-26. The cask is conservatively assumed to be supported in cradles located near the end of the cask. The section bending and shear stresses are determined with the cask assumed held at the ends (simply supported) in rigid supports.

The stresses due to Missile B impact are determined similarly. In the vertical case (Figure 4A.5-25(b)), the same ring of the cask body is analyzed for the 1,382,000 lb. load concentrated on a local eight in. diameter area. For the horizontal cask, the section bending and shear stresses are determined as for Missile A. The Missile B impact force due to a 126 mph impact is also applied at the center of the cask bottom and the center of the top since the full horizontal velocity impact can occur on these locations on a horizontal cask (Missile A would apply a smaller force on a larger area, and is therefore much less critical on the ends.). Plug shear through (punching shear) due to Missile B is also evaluated on the cask wall thickness.

4A.5.8.3 Stress Analysis

Missile A - Vertical Cask

As described above, it is assumed that the entire crush loading is reacted by a 3 ft. long ring section of the cask body and that the ends do not stiffen the ring. The outer shell and resin are neglected, however θ is determined assuming the resin transmits the load to the cask body. Referring to Figure 4A.5-27(a) and (b):

$$\text{Angle } \theta = \pi - \sin^{-1}\left(\frac{72}{2} \cdot \frac{1}{47.375}\right) = 130.5°$$

$$\text{Pressure on cask} = \frac{47.375}{36.375} \times 266 = 346.4 \text{ psi}$$

Unit load on 36 in. ring of cask = w_1 (load per inch of arc length)

$$w_1 = 36 \times 346.4 = 12,472 \text{ lb/in}$$

The inertial load, w_2, required to react this impact load in Figure 4A.5-27(c) is:

$$w_2 = w_1 \frac{2 R \sin (\pi - \theta)}{2 \pi R} = .2420\ w_1$$

$$w_2 = (.2420)\ (12472) = 3,018 \text{ lb/in}$$
(load per in. along circumference)

For all cases in Roark (Ref. 7), Table 17, the moment in the ring at angle x is:

$$M = M_A - T_A R (1 - \cos x) + V_A R \sin x + LT_M$$

Substituting to find these parameters for Cases 12 and 13:

Case 12 where w_1 = 12,472 lb/in, R = 36.375 in, θ = 130.5°

$$M_{A1} = -504,278 \text{ in lb}$$
$$T_{A1} = -28,893 \text{ lb}$$
$$V_{A1} = 0$$
$$LT_{M1} = 16,502,209\ (1 - \cos (x - \theta))\ \langle x - \theta \rangle$$

Case 13 where w_2 = 3,018 lb/in, R = 36.375

$$M_{A2} = 1,996,619 \text{ in lb}$$
$$T_{A2} = 54,889 \text{ lb}$$
$$V_{A2} = 0$$
$$LT_{M2} = -3,993,238\ (x \sin x + \cos x - 1) \text{ in lb}$$

Substituting in the moment equation above, for Cases 12 and 13 and adding gives a general expression for M as a function of x:

$$M = 4,508,438 - 3,011,062 \cos x - 3,993,238\ x \sin x - 16,502,209\ (1 - \cos (x - \theta))\ \langle x - \theta \rangle$$

Where $\langle x - \theta \rangle = 0$ if $x \leq \theta$

$\langle x - \theta \rangle = 1$ if $x > \theta$

The maximum absolute value of M occurs
at $x = 98.22°$ and $M_{max} = -1,853,302$ in lb

Correcting for thickness and curvature using Table 16.1:

for $R = 36.375$ in and $c = \frac{t}{2} = 4.875$ in

$$\frac{R}{c} = 7.46$$

$k_i = 1.099$ $\qquad$ $k_o = 0.904$

The bending stress in the circumferential direction:

$$\sigma_{\theta i} = k_i \times \frac{6M}{bt^2} = \frac{1.099 \times 6 \times 1,853,302}{36 \times (9.75)^2}$$

$$= 3570 \text{ psi}$$

Similarly $\sigma_{\theta o} = 2936$ psi

If we assume a plane strain condition (i.e., that ends of ring do not warp), the longitudinal stress is ν x circumferential stress:

$\sigma_{\phi i} = .3 \times 3570 = 1071$ psi

$\sigma_{\phi o} = .3 \times 2936 = 881$ psi

The shear stress on the end of the ring is negligible.

The shear stress around the loaded area is:

$$\tau = \frac{F}{t \times \text{circumference}} = \frac{683314 \text{ lb}}{9.75 \times 12 \ (2x3+2x6)}$$

τ = 324 psi Again negligible

Missile A - Horizontal Cask

When the cask is horizontal and simply supported in rigid cradles located near the ends of the cask, Missile A impact is illustrated in Figure 4A.5-26. Longitudinal (beam) bending stresses can be determined assuming all of the load is reacted at the supports:

Total Force = 683,314 lb.

Load per inch of length = w (on ℓ, the center 72 in.)

$$W = \frac{683314}{72} = 9{,}490 \text{ lb/in}$$

The moment of inertia of the section:

$$I = \frac{\pi}{64} (OD^4 - ID^4)$$

$$= \frac{\pi}{64} (82.5^4 - 63^4) = 1{,}500{,}703 \text{ in}^4$$

The maximum bending moment is:

$$M = \frac{W \times \ell}{2} \left(\frac{L}{2} - \frac{\ell}{4} \right)$$

$$= \frac{9490 \times 72}{2} \left(\frac{179.5}{2} - \frac{72}{4} \right) = 24{,}512{,}670 \text{ in lb}$$

The longitudinal bending stress is then:

$$\sigma_b = \frac{MR}{I} = \frac{(24,512,670)(41.25)}{1,500,703} = 673.8 \text{ psi}$$

Missile B - Vertical Cask

The same ring section described above is analyzed under the impact from Missile B. It is assumed that the impact force is concentrated at one point so the complete free body diagram is as illustrated in Figure 4A.5-27(c). The bending moment in the ring is:

$$M = M_A - T_A R (1 - \cos x) + V_A R \sin x + LT_M$$

The impact loading is 1,382,000 lb. which is reacted by the inertia loadiny of the ring.

$$w = \frac{\text{Load}}{2\pi R} = \frac{1,382,000}{2\pi x 36.375} = 6046 \text{ lb/in}$$

$$M_A = \frac{wR^2}{2} = \frac{(6046)\ (36.375)^2}{2} = 3,999,854 \text{ in lb}$$

$$T_A = \frac{wR}{2} = \frac{6046 \text{ x } 36.375}{2} = 109,961 \text{ lb}$$

$$V_A = 0$$

$$LT_M = -wR^2 (x \sin x + \cos x - 1)$$

$$= -7,999,708 (x \sin x + \cos x - 1)$$

Then:

$$M = 7,999,708 - 3,999,854 \cos x - 7,999,708 \text{ x } \sin x$$

The maximum moment occurs at $x = \pi$:

$$M_{max} = 11,999,562 \text{ in lb}$$

k_i and k_o are again 1.099 and 0.904

The circumferential bending stress is:

$$\sigma_{\theta i} = \frac{1.099 \times 6 \times 11,999,562}{36 \times (9.75)^2} = 23,121 \text{ psi}$$

$$\sigma_{\theta o} = 19018 \text{ psi}$$

The longitudinal stresses, assuming plane strain, are:

$$\sigma_{\phi i} = .3 \times 23,121 = 6,936 \text{ psi}$$

$$\sigma_{\phi o} = .3 \times 19,018 = 5,705 \text{ psi}$$

The shear stress in the cask around the plug of material loaded by the missile contact is:

$$\tau = \frac{\text{Load}}{\pi \times 8 \text{ in} \times t} = \frac{1,382,000 \text{ lb}}{\pi \times 88 \times 9.75}$$

$$= 5640 \text{ psi}$$

If the missile penetrated 1.27 in. into the wall, the local thickness would be decreased to 9.75 - 1.27 = 8.48 in. This would increase the shear stress, τ, to:

$$\tau_{\text{damaged wall}} = \frac{1,382,000}{\pi \times 8 \times 8.48} = 6484 \text{ psi}$$

Missile B could impact on the protective cover and deform it onto the lid while the cask is in the vertical orientation. However, the vertical velocity of Missile B is only 70% of the horizontal velocity. Missile B may strike the cask ends at the full horizontal velocity when the cask is in the horizontal orientation. Horizontal impact on the lid as discussed below is therefore a more severe case than vertical impact on the lid.

Missile B - Horizontal Cask - Side Impact

Again, it is assumed that the cask is horizontal and simply supported in rigid cradles located near the ends of the cask. Longitudinal bending stresses are determined assuming the load is reacted at the supports.

Total Force = 1,382,000 lb.

Since the load is assumed to be concentrated at the center, the bending moment is:

$$M = \frac{FL}{4} = \frac{(1,382,000)(179.5)}{4} = 62,017,250 \text{ in lb}$$

The longitudinal bending stress is:

$$\sigma_b = \frac{MR}{I} = \frac{62,017,250 \times 41.25}{1,500,703} = 1704 \text{ psi}$$

The circumferential stress and shear stress are small. The shear stress in the wall around the plug of material loaded by the missile contact is the same as calculated above.

Missile B - Horizontal Cask - Impact on Bottom

As described above, when the cask is horizontal Missile B can impact on the bottom (or top) at the full horizontal velocity, 126 mph. This is more severe than Missile A impact on these locations because the Missile A total force is lower and the Missile A force is also distributed over a greater area.

An analysis is performed for Missile B impact on the center of the bottom plate. The analysis uses the discontinuity analysis equations from Section 4A.5. See Figure 4A.5-28(a) for clarification of force and displacement sign conventions. Conservatively rewriting the equations for the radial deflection and rotation of the edge of the bottom plate and the end of the cask cylinder (equations 10a, 10b, 11a, 11b) with pressure set to zero:

$$(W_L)_{cyl} = 23.0 \frac{Q_L}{E} + 1.43 \frac{M_L}{E} \qquad 10a'$$

$$(\theta_L)_{cyl} = 1.43 \frac{Q_L}{E} + 0.184 \frac{M_L}{E} \qquad 10b'$$

$$(W_L)_{plate} = -8.36 \frac{Q_L}{E} + 1.11 \frac{M_L}{E} \qquad 11a'$$

$$(\theta_L)_{plate} = 1.11 \frac{Q_L}{E} - 0.200 \frac{M_L}{E} \qquad 11b'$$

From Roark (Ref. 7), Case 16, Table 24, we have the plate edge displacements due to application of center force, F_B, as indicated in Figure 4A.5-28(b):

$$\theta = \frac{-F_B R}{4\pi D(1+\upsilon)}$$

$$W = \left(\frac{t}{2}\right)(-\theta) = \frac{F_B R}{8\pi D}\ \frac{(t)}{(1+\upsilon)}$$

Where:

$R = 41.25$ in.

$t = 11.25$ in.

$\upsilon = .3$

$$D = \frac{Et^3}{12(1-\upsilon^2)} = 130.4\ E$$

Then:

$$\theta = -0.01936\ \frac{F_B}{E}$$

$$W = .936\ \frac{F_B}{E}$$

The total displacements of the plate are then equal to those of the cylinder.

$$23 \frac{Q_L}{E} + 1.43 \frac{M_L}{E} = -8.36 \frac{Q_L}{E} + 1.12 \frac{M_L}{E} + .109 \frac{F_B}{E}$$

$$1.43 \frac{Q_L}{E} + 0.184 \frac{M_L}{E} = 1.12 \frac{Q_L}{E} - 0.200 \frac{M_L}{E} - 0.01936 \frac{F_B}{E}$$

Solving these equations:

$$Q_L = .00398 F_B$$

$$M_L = -.0539 F_B$$

The highest bending stresses are at the center of the bottom plate:

$$M_{\text{simply supported plate}} = \frac{F_B}{4\pi} \left[(1+\upsilon) \ln \frac{R_{plate}}{R_{load}} + 1 \right]$$

$$= F_B \left(\frac{1}{4\pi} \right) \left[1.3 \ln \left(\frac{41.25}{4} \right) + 1 \right] = .321 F_B$$

$$Net_M = M_{\text{simply supported plated}} + M_L - Q_L \left(\frac{t}{2} \right)$$

$$Net_M = .321 F_B - .0539 F_B - .00398 F_B \left(\frac{11.25}{2} \right)$$

$$= .2447 F_B$$

$$= (.2447)(1,382,000) = 338,192 \text{ in lb/in}$$

$$\sigma_r = \sigma_t \text{ at center} = \frac{6M}{t^2} = \frac{6 \times 338,192}{11.25^2}$$

$$= 16,032 \text{ psi}$$

The shear stress around the plug of material loaded by F_B is less than the value calculated above for the side of the cask because of the greater thickness of the bottom.

Missile B - Horizontal Cask - Impact on Top

Missile B may impact on the top or lid of the cask at the full 126 mph horizontal velocity when the cask is stored horizontally. If the weather protective cover is in place on the cask, finite element analysis indicates that a significant amount of the missile kinetic energy is absorbed deforming the cover until it (the cover) contacts the lid. However, the cover does "bottom out" against the lid and the missile is assumed to penetrate the lid and apply the full 1,382,000 lb. impact force, calculated above, on the lid (Missile B frontal area multiplied by cask yield stress).

A quasistatic analysis of the lid is performed for the instant of time when the missile develops the maximum force as it impacts near the center of the lid assuming that the force is reacted by the cask at the lid flange. It is assumed that the lid bolts hold the lid flange against the cask body at the diameter of the bolt circle and that the force deforms the lid inward so that the inner edge of the flange is also in contact with the cylinder.

The overall lid free body diagram is illustrated in Figure 4A.5-29(a). The lid has a thick inner region and a thinner peripheral support flange. The lid is loaded in the center by force F_B due to Missile B impact and is assumed to be held flat at two locations on the flange where it is bolted to and bears against the cask body. A discontinuity analysis is performed for the inner plate shown in Figure 4A.5-29(b) and the outer flange in Figure 4A.5-29(c). The unknowns from each analysis are the slope, θ, and moment, M, at the interface between plate and flange. The slopes are equated and the moment is then determined.

The inner plate solution is obtained by superimposing cases 16 and 13a from Table 24 of Roark, (Ref. 7). The resulting equations are:

$$\theta = \frac{F_B b}{4\pi D(1+\upsilon)} - \frac{M\, b}{D(1+\upsilon)}$$

$$M_{center} = \frac{F_B}{4\pi}\left[(1+\upsilon)\ \ln\left(\frac{b}{r}\right) + 1\right] - M\, L_8$$

Where:

θ = slope at junction between plate and flange
M = moment at junction between plate and flange
b = radius at junction between plate and flange
D = plate flexural rigidity
υ = Poisson's ratio
r = radius of loaded region of plate
M_{center} = bending moment at center of plate
L_8 = constant defined by Roark

The outer flange solution is obtained by summing cases 1a and 5a (each with signs reversed) from Table 24:

Deflection y at radius b is determined:

$$y_b = \frac{Wa^3}{D}\left(\frac{C_1\ L_9}{C_7} - L_3\right) + \frac{Ma^2}{D}\left(\frac{C_1\ L_8}{C_7} - L_2\right)$$

Since this is zero, W can be determined as a function of M.

$$\theta = \frac{-(Wa^2)}{DC_7} L_9 + \frac{Ma}{DC_7} L_8$$

Substituting for W:

$$\theta = \frac{Ma}{D}\left\{\frac{\left(\frac{C_1\ L_8}{C_7} - L_2\right) L_9}{\left(\frac{C_1\ L_9}{C_7} - L_3\right) C_7} + \frac{L_8}{C_7}\right\}$$

Where:

θ, M, D are as defined above

C_1, C_7, L_2, L_8, L_9 are constants defined by Ref. 7.

If we equate slopes from the equations for the inner plate and rim:

$$\theta_{\text{flange}} = \theta_{\text{plate}}$$

$$M = .00007466\ F_B$$

Since F_B is 1,382,000 lb, M = .00007466 x 1,382,000 = 103.2 in lb/in.

Then the moment at the center of the inner plate is:

$$M_{center} = .294\ F_B - .655\ M$$

$$M_{center} = 406,240 \text{ in lb/in}$$

The bending stress at the flange and plate center can then be found:

$$\sigma_{b\ flange} = \frac{6M}{t^2} = \frac{6 \times 103.2}{3.5^2} = 50 \text{ psi}$$

$$\sigma_{b\ plate\ center} = \frac{6M_{center}}{t^2_{center}} = \frac{6 \times 406,240}{11.5^2} = 18430 \text{ psi}$$

The shear stress at the flange:

$$\lambda = \frac{F_B}{2\pi tb} = \frac{1,382,000}{2\pi \times 3.5 \times 31.875} = 1971 \text{ psi}$$

If Missile B penetrates the protective cover, it may also partially penetrate the lid. The maximum depth of penetration of the missile, ignoring the energy absorbed in deforming the cover, is shown above to be 1.27 in. This will not penetrate the 11.50 inch thick lid. The flange of the lid is 3.5 in. thick; therefore Missile B will not penetrate the thinnest portion of the containment. The flange is backed up by the cask body so shearing out of a plug of material is impossible. The shear stress around a plug of lid material loaded by F_B is less than the value calculated above for the side of the cask because of the greater thickness of the lid.

TABLE 4A.5-1

COMPUTATION SHEET FOR LOCAL STRESSES
IN CYLINDRICAL SHELLS

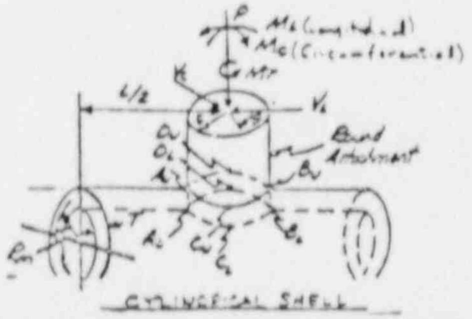

Compute absolute values of stress and enter result →	Stresses - if load is opposite that shown, reverse signs shown							
	A_U	A_L	B_U	B_L	C_U	C_L	D_U	D_L
$K_n\left[\frac{N_\phi}{P/R_m}\right]\cdot\frac{P}{R_mT}$ =	−	−	−	−	−	−	−	−
$K_b\left[\frac{M_\phi}{P}\right]\cdot\frac{6P}{T^2}$ =	−	+	−	+	−	+	−	+
$K_n\left[\frac{N_\phi}{M_c/R_m^2\beta}\right]\cdot\frac{M_c}{R_m^2\beta T}$ =					−	−	+	+
$K_b\left[\frac{M_\phi}{M_c/R_m\beta}\right]\cdot\frac{6M_c}{R_m\beta T^2}$ =					−	+	+	−
$K_n\left[\frac{N_\phi}{M_L/R_m^2\beta}\right]\cdot\frac{M_L}{R_m^2\beta T}$ =	−	−	+	+				
$K_b\left[\frac{M_\phi}{M_L/R_m\beta}\right]\cdot\frac{6M_L}{R_m\beta T^2}$ =	−	+	+	−				
Summation of ϕ* Stresses, σ_ϕ =								
$K_n\left[\frac{N_x}{P/R_m}\right]\cdot\frac{P}{R_mT}$ =	−	−	−	−	−	−	−	−
$K_b\left[\frac{M_x}{P}\right]\cdot\frac{6P}{T^2}$ =	−	+	−	+	−	+	−	+
$K_n\left[\frac{N_x}{M_c/R_m^2\beta}\right]\cdot\frac{M_c}{R_m^2\beta T}$ =					−	−	+	+
$K_b\left[\frac{M_x}{M_c/R_m\beta}\right]\cdot\frac{6M_c}{R_m\beta T^2}$ =					−	+	+	−
$K_n\left[\frac{N_x}{M_L/R_m^2\beta}\right]\cdot\frac{M_L}{R_m^2\beta T}$ =	−	−	+	+				
$K_b\left[\frac{M_x}{M_L/R_m\beta}\right]\cdot\frac{6M_L}{R_m\beta T^2}$ =	−	+	+	−				
Summation of x* Stresses, σ_x =								
$\tau_{\phi x}=\tau_{x\phi}=\frac{M_T}{2\pi r_0^2 T}$	+	+	+	+	+	+	+	+
$\tau_{x\phi}=\frac{V_c}{\pi r_0 T}$	+	+	−	−				
$\tau_{\phi x}=\frac{V_L}{\pi r_0 T}$						−	+	+
Summation of Shear Stresses, τ =								

* ϕ and x represent tangential (circumferential) and longitudinal respectively

TABLE 4A.5-2

LIST OF BIJLAARD PARAMETERS

Parameter Symbol	Parameter Description	Parameter Value
R_m	Mean radius of shell	36.375 in.
T	Wall thickness of shell	9.75 in.
$\gamma = \frac{R_m}{T}$	Shell Parameter	3.731
r_o	Outside radius of attachment (bolt circle of trunnions	6.30 in.
$\beta = \frac{.875\ r_o}{R_m}$	Attachment parameter	0.152

TABLE 4A.5-3

ATTACHMENT LOADS APPLIES TO CASK BODY

Load Symbol	Load Description	Load Magnitude
V_L	Maximum possible longitudinal shear	337,500 lb.
V_C	Maximum possible circumferential shear	337,500 lb.
M_L	Maximum possible longitudinal moment	2.6×10^6 in.-lb.
M_C	Maximum possible circumferential moment	1.3×10^6 in.-lb.
P	Radial Load	225,000 lb.
M_T	Torsional Moment	0 in.-lb.

TABLE 4A.5-4

STRESS COMPONENTS IN CYLINDER AT TRUNNIONS DUE TO ATTACHMENT LOADS

LOAD	SURFACE	STRESS (PSI)				CLASSFICATION
		CIRCUMF. σ_t	LONGIT. σ_l	RADIAL σ_r	SHEAR τ	
Radial Load, P	Inner	-600	-550	0	0	P_L
	Outer	-600	-550	0	0	
Radial Load, P	Inner	2500	2300	0	0	Q
	Outer	-2500	-2300	0	0	
Circumferential Moment, M_c	Inner	±150	±100	0	0	P_L
	Outer	±150	±100	0	0	
Circumferential Moment, M_c	Inner	±1650	±1050	0	0	Q
	Outer	±1650	±1050	0	0	
Longitudinal Moment, M_L	Inner	±250	±100	0	0	P_L
	Outer	±250	±100	0	0	
Longitudinal Moment, M_L	Inner	±2000	±3100	0	0	Q
	Outer	±2000	±3100	0	0	
Circumferential Shear, V_C	Inner	0	0	0	1800	P_L
	Outer	0	0	0	1800	
Longitudinal Shear, V_L	Inner	0	0	0	1800	P_L
	Outer	0	0	0	1800	

TABLE 4A.5-5

APPLIED LOADS AT THE OUTER SHELL CLOSURE PLATE CONNECTION COMPARED TO APPLIED LOADS AT TRUNNION

TOTAL APPLIED LOAD	OUTER SHELL CLOSURE PLATE	TRUNNION
RADIAL LOAD P (lb)	11,530	225,000
LONGITUDINAL SHEAR V_L (lb)	31,030	337,500
LONGITUDINAL MOMENT M_L (in-lb)	178,750 (1)	2.5×10^6

(1) This moment is distributed around the entire cask body while the moment at the trunnion is concentrated locally.

TABLE 4A.5-6

STRESS COMPONENTS IN CYLINDER AT JUNCTION WITH BOTTOM PLATE

LOAD	SURFACE	STRESS (PSI)				CLASSFICATION
		σ_t	σ_l	σ_r	τ	
Internal Pressure	Inner	950	350	-250	0	P_m
	Outer	700	350	0	0	
Discontinuity Effects of Internal Pressure	Inner	-610	+2230	0	350	$P_L + P_b$
	Outer	-730	-2230	0	350	
Handling Acting as Equivlanet Pressure	Inner	0	0	0	0	----
	Outer	0	0	0	0	
Discontinuity Effects of Handling	Inner	125	+710	-81	150	$P_L + P_b$
	Outer	-300	-710	0	150	
Discontinuity Effects Due to Differential Thermal Expansion	Inner	-3430	-290	0	560	Q
	Outer	-3260	+290	0	560	
Discontinuity Effects Due to Thermal Gradient Across Cylinder Wall	Inner	-2550	-1430	0	200	Q
	Outer	-1690	+1430	0	200	

TABLE 4A.5-6

(CONTINUED)

LOAD	SURFACE	STRESS (PSI) σ_t	σ_l	σ_r	τ	CLASSFICATION
Discontinuity Effects Due to Thermal Gradient Across Bottom Plate	Inner	-470	-2700	0	320	Q
	Outer	1150	2700	0	320	
Discontinuity Effects Due to Thermal Axial Gradient in Cylinder	Inner	-130	575	0	0	Q
	Outer	-470	-575	0	0	
Local Effects From Trunnion Loads	Inner	-850	-650	0	1800	$P_L + P_b$
	Outer	-850	-550	0	1800	
Local Effects From Trunnion Loads	Inner	4500	5400	0	1800	Q
	Outer	-4500	-5400	0	1800	

TABLE 4A.5-7

STRESS COMPONENTS IN BOTTOM PLATE AT JUNCTION WITH CYLINDER

LOAD	SURFACE	STRESS (PSI)				CLASSFICATION
		σ_t	σ_l	σ_r	τ	
Internal Pressure	Inner	-1565	-250	-535	400	P_L
	Outer	1565	0	535	400	
Discontinuity Effects of Internal Pressure	Inner	435	0	435	400	P_L
	Outer	-990	0	-990	400	
Handling Acting as Equivlanet Pressure	Inner	-510	-61	-170	150	P_L
	Outer	+510	0	170	150	
Discontinuity Effects of Handling	Inner	220	0	220	150	P_L
	Outer	-360	0	-360	150	
Discontinuity Effects Due to Differential Thermal Expansion	Inner	1600	0	1600	0	Q
	Outer	-700	0	-700	0	
Discontinuity Effects Due to Thermal Gradient Across Cylinder Wall	Inner	-370	0	-370	0	Q
	Outer	+380	0	+380	0	

TABLE 4A.5-7

(CONTINUED)

LOAD	SURFACE	STRESS (PSI)				CLASSFICATION
		σ_t	σ_l	σ_r	τ	
Discontinuity Effects Due to Thermal Gradient Across Bottom Plate	Inner	-835	0	-835	0	Q
	Outer	1350	0	1350	0	
Discontinuity Effects Due to Thermal Axial Gradient in Cylinder	Inner	-1620	0	-1620	0	Q
	Outer	1300	0	1300	0	
Thermal Radial Gradient in Bottom Plate	Inner	-2090	0	0	0	Q
	Outer	-2090	0	0	0	

TABLE 4A.5-8

STRESS COMPONENTS IN BOTTOM PLATE AT CENTER

LOAD	SURFACE	STRESS (PSI)				CLASSFICATION
		σ_t	σ_l	σ_r	τ	
Internal Pressure	Inner	-2960	-250	-2960	0	P_L
	Outer	2960	0	2960	0	
Discontinuity Effects of Internal Pressure	Inner	435	0	435	0	P_L
	Outer	-990	0	-990	0	
Handling Acting as Equivlanet Pressure	Inner	-960	0	-960	0	P_L
	Outer	960	0	960	0	
Discontinuity Effects of Handling	Inner	220	0	220	0	P_L
	Outer	-360	0	-360	0	
Discontinuity Effects Due to Differential Thermal Expansion	Inner	1600	0	1600	0	Q
	Outer	-700	0	-700	0	
Discontinuity Effects Due to Thermal Gradient Across Cylinder Wall	Inner	-370	0	-370	0	Q
	Outer	380	0	380	0	

TABLE 4A.5-8

(CONTINUED)

LOAD	SURFACE	STRESS (PSI)				CLASSFICATION
		σ_t	σ_l	σ_r	τ	
Discontinuity Effects Due to Thermal Gradient Across Bottom Plate	Inner	-835	0	-835	0	Q
	Outer	1350	0	1350	0	
Discontinuity Effects Due to Thermal Axial Gradient in Cylinder	Inner	-1620	0	-1620	0	Q
	Outer	1300	0	1300	0	
Thermal Radial Gradient in Bottom Plate	Inner	1040	0	1040	0	Q
	Outer	1040	0	1040	0	

TABLE 4A.5-9

MATERIAL PROPERTIES USED FOR THE CASK LID AND CYLINDRICAL SHELL

SA-350 Gr. LF1

T°F	RT	100	200	250	300	350	400
Su (ksi)	60	60	60	60	60	60	60
Sy (ksi)	30	30	27.3		26.6	26.8	25.7
Sm (ksi)		20	18.3		17.7		17.2
$\alpha x 10^{-6}$ in/in/F		5.53	5.89	6.09	6.26	6.43	6.61
$Ex10^{6}$ lb/in^2	29.5		28.8		28.3		27.7

MATERIAL PROPERTIES USED FOR THE BOLTS

SA-320 Gr. L43

Su (ksi)	125	125	118		114	111.5	109
Sy (ksi)	105	105	99		95.7	93.7	91.8
Sm (ksi)		35	33		31.9		30.6
$\alpha x 10^{-6}$ in/in/F		6.27	6.54	6.65	6.78	6.88	6.98
$Ex10^{6}$ lb/in^2	29.7		29.0		28.5		27.9

TABLE 4A.5-10

STRESS COMPONENTS IN LID AT CENTER

LOAD	SURFACE	STRESS (PSI)				CLASSFICATION
		σ_t	σ_l	σ_r	τ	
Bolt Preload	Inner	-1030	0	-1030	0	P_b
	Outer	1030	0	1030	0	
Internal Pressure	Inner	-3000	-250	-3000	0	P_b
	Outer	3000	0	3000	0	
Handling	Inner	-970	81	-970	0	P_b
	Outer	970	0	970	0	
Thermal Gradient Across Lid Thickness	Inner	-905	0	-905	530	Q
	Outer	905	0	905	530	
Thermal Gradient in Radial Direction	Inner	600	0	600	0	Q
	Outer	600	0	600	0	
Effect of Displacement and Rotation of Cylinder at Lid End	Inner	0	0	0	0	---
	Outer	0	0	0	0	

TABLE 4A.5-11

STRESS COMPONENTS IN LID AT STEP IN LID FLANGE

LOAD	SURFACE	STRESS (PSI)				CLASSFICATION
		σ_t	σ_l	σ_r	τ	
Bolt Preload	Inner	-11100	0	-11100	1230	P_b
	Outer	11100	0	11100	1230	
Internal Pressure	Inner	-6850	-250	-6850	3980	P_b
	Outer	6850	0	6850	3980	
Handling	Inner	-2220	-81	-2220	360	P_b
	Outer	2220	0	2220	360	
Thermal Gradient Across Lid Thickness	Inner	-9770	0	-9770	1750	Q
	Outer	9770	0	9770	1750	
Thermal Gradient in Radial Direction	Inner	-610	0	-610	0	Q
	Outer	-610	0	-610	0	
Effect of Displacement and Rotation of Cylinder at Lid End	Inner	120	0	120	0	Q
	Outer	-120	0	-120	0	

TABLE 4A.5-12

STRESS COMPONENTS IN LID AT SEAL LOCATION

LOAD	SURFACE	STRESS (PSI)				CLASSFICATION
		σ_t	σ_l	σ_r	τ	
Bolt Preload	Inner	-12950	0	-12950	2660	P_b
	Outer	12950	0	12950	2660	
Internal Pressure	Inner	-8000	-250	-8000	1275	P_b
	Outer	8000	0	8000	1275	
Handling	Inner	-2590	-81	-2590	350	P_b
	Outer	2590	0	2590	350	
Thermal Gradient Across Lid Thickness	Inner	-11400	0	-11400	1890	Q
	Outer	11400	0	11400	1890	
Thermal Gradient in Radial Direction	Inner	-610	0	-610	0	Q
	Outer	-610	0	-610	0	
Effect of Displacement and Rotation of Cylinder at Lid End	Inner	140	0	140	0	Q
	Outer	-140	0	-140	0	

TABLE 4A.5-13

LID BOLT STRESSES, PSI

LOAD	DIRECT STRESS	BENDING STRESS	SHEAR STRESS
Preload	25000	---	8900
Effect of Displacement and Rotation of Cylinder at Lid End	---	22200	1980
Inertia Loads Due to Drop and Tipping Accidents	13200	---	---

TABLE 4A.5-14

STRESS COMPONENTS IN CYLINDER AT JUNCTION WITH LID

LOAD	SURFACE	STRESS (PSI)				CLASSFICATION
		σ_t	σ_l	σ_r	τ	
Bolt Preload	Inner	320	1080	0	0	P_L
	Outer	-320	-1080	0	0	
Internal Pressure	Inner	950	350	-250	0	P_m
	Outer	700	350	0	0	
Handling	Inner	0	0	0	0	---
	Outer	0	0	0	0	
Thermal Gradient Across Cylinder Wall	Inner	-4750	0	0	0	Q
	Outer	4750	0	0	0	
Thermal Axial Gradient in Cylinder	Inner	0	0	0	0	---
	Outer	0	0	0	0	
Effects of Displacement and Rotation of Cylinder at Lid End	Inner	1140	-1670	0	170	Q
	Outer	2140	1670	0	170	

TABLE 4A.5-15

STRESS COMPONENTS IN CYLINDER AWAY FROM THE ENDS

LOAD	SURFACE	STRESS (PSI)				CLASSFICATION
		σ_t	σ_l	σ_r	τ	
Bolt Preload	Inner	0	0	0	0	---
	Outer	0	0	0	0	
Internal Pressure	Inner	950	350	-250	0	P_m
	Outer	700	350	0	0	
Handling	Inner	0	0	0	0	---
	Outer	0	0	0	0	
Thermal Gradient Across Cylinder Wall	Inner	-3660	-3660	0	0	Q
	Outer	3660	3660	0	0	
Thermal Axial Gradient in Cylinder	Inner	-190	-630	0	0	Q
	Outer	190	630	0	0	
Effects of Displacement and Rotation of Cylinder at Lid End	Inner	0	0	0	0	---
	Outer	0	0	0	0	

TABLE 4A.5-16

DELETED

TABLE 4A.5-17

STRESS COMPONENTS IN CYLINDER DUE TO DISTRIBUTED LOADS

LOAD	SURFACE	STRESS[3] (PSI) σ_t	σ_l	σ_r	τ	CLASSFICATION
Distributed Load Maximum Effect of Wind, Water, Weight and Handling (1)	Inner	90	290	0	0	P_m
	Outer	90	290	0	0	P_m
Distributed Load Maximum Effect of Wind, Water, Weight and Handling (2)	Inner	0	290	0	0	P_b
	Outer	0	290	0	0	

(1) Axial Load inducing P/A Stresses

(2) Bending Load inducing $\frac{Mc}{I}$ Stresses

(3) These stresses are added to those of Tables 4A.5-14 through 4A.5-16

TABLE 4A.5-18a

STRESS COMPONENTS DUE TO 8 FT. VERTICAL DROP

CYLINDER AT JUNCTION WITH BOTTOM PLATE

LOAD	SURFACE	STRESS (PSI)				CLASSFICATION
		σ_t	σ_l	σ_r	τ	
Inertia Loads Acting as Equivalent Pressure	Inner	-1930	-6440	0	0	P_m
	Outer	-1930	-6440	0	0	
Discontinuity Effects of Equivalent Pressure from Inertia Loads	Inner	-3435	-19750	0	2360	$P_L + P_b$
	Outer	8410	19750	0	2360	

TABLE 4A.5-18b

STRESS COMPONENTS DUE TO 8 FT. VERTICAL DROP

BOTTOM PLATE AT JUNCTION WITH CYLINDER

LOAD	SURFACE	STRESS (PSI)				CLASSFICATION
		σ_t	σ_l	σ_r	τ	
Inertia Loads Acting as Equivalent Pressure	Inner	-14150	-6440	-4840	5600	$P_L + P_b$
	Outer	14150	-4000	4840	5600	
Discontinuity Effects of Equivalent Pressure from Inertia Loads	Inner	-6125	0	-6125	0	$P_L + P_b$
	Outer	9950	0	9950	0	

TABLE 4A.5-18c

STRESS COMPONENTS DUE TO 8 FT. VERTICAL DROP

BOTTOM PLATE AT CENTER

LOAD	SURFACE	STRESS (PSI)				CLASSFICATION
		σ_t	σ_l	σ_r	τ	
Inertia Loads Acting as Equivalent Pressure	Inner	-26760	-1740	-26760	0	$P_L + P_b$
	Outer	26760	-4000	26760	0	
Discontinuity Effects of Equivalent Pressure from Inertia Loads	Inner	-6125	0	-6125	0	$P_L + P_b$
	Outer	9950	0	9950	0	

TABLE 4A.5-18d

STRESS COMPONENTS DUE TO 8 FT. VERTICAL DROP

AT SEAL IN LID FLANGE

LOAD	SURFACE	STRESS (PSI)				CLASSFICATION
		σ_t	σ_l	σ_r	τ	
Inertia Loads Acting at Lid Flange - Cylinder Interface	Inner	9820	-2150	9820	1600	$P_L + P_b$
	Outer	-9820	0	-9820	1600	

TABLE 4A.5-18e

STRESS COMPONENTS DUE TO 8 FT. VERTICAL DROP

CENTRAL PORTION AT STEP IN LID

LOAD	SURFACE	STRESS (PSI)				CLASSFICATION
		σ_t	σ_l	σ_r	τ	
Inertia Loads Acting at Lid Flange - Cylinder Interface	Inner	835	0	835	470	$P_L + P_b$
	Outer	-835	0	-835	470	

TABLE 4A.5-19

STRESS COMPONENTS DUE TO HORIZONTAL 7 FT. DROP

CYLINDER AWAY FROM ENDS

LOAD	SURFACE	STRESS (PSI)				CLASSFICATION
		σ_t	σ_l	σ_z	τ	
Bending Due to Ovalization of Cylinder	Inner	39490	11850	0	0	$P_L + P_b$
	Outer	-39490	-11850	0	0	

TABLE 4A.5-20a

STRESS COMPONENTS DUE TO TIPPING ACCIDENTS

AT SEAL IN LID FLANGE

LOAD	SURFACE	STRESS (PSI)				CLASSFICATION
		σ_t	σ_l	σ_r	τ	
Inertia Loads from Lid and Internals Acting on Lid	Inner	-15530	0	-15530	5230	$P_L + P_b$
	Outer	15530	0	15530	5230	

TABLE 4A.5-20b

STRESS COMPONENTS DUE TO TIPPING ACCIDENTS

CENTRAL PORTION AT STEP IN LID

LOAD	SURFACE	STRESS (PSI)				CLASSFICATION
		σ_t	σ_l	σ_r	τ	
Inertia Loads from Lid and Internals Acting on Lid	Inner	-1270	0	-1270	1480	$P_L + P_b$
	Outer	1270	0	1270	1480	

TABLE 4A.5-21a

STRESS COMPONENTS DUE TO TORNADO MISSILES

CASK IN VERTICAL ORIENTATION - CYLINDER AWAY FROM ENDS

LOAD	SURFACE	STRESS (PSI)				CLASSFICATION
		σ_t	σ_l	σ_r	τ	
Missile A:						
Bending Due to Ovalization of Cylinder	Inner	3570	1070	0	325	$P_L + P_b$
	Outer	2940	880	-260	325	
Missile B:						
Bending Due to Ovalization of Cylinder	Inner	23120	6940	0	6485	$P_L + P_b$
	Outer	19020	5710	-27300	6485	

TABLE 4A.5-21b

STRESS COMPONENTS DUE TO TORNADO MISSILES

CASK IN HORIZONTAL ORIENTATION - IMPACT ON CENTER OF CASK

LOAD	SURFACE	STRESS (PSI)				CLASSFICATION
		σ_t	σ_l	σ_r	τ	
Missile A:						
Cask Bending as Beam	Inner	±150	±520	0	325	$P_L + P_b$
	Outer	±200	±675	-260	325	
Missile B:						
Cask Bending as Beam	Inner	±390	±1300	0	6485	$P_L + P_b$
	Outer	±510	±1700	-27300	6485	

TABLE 4A.5-21c

STRESS COMPONENTS DUE TO TORNADO MISSILES

CASK IN HORIZONTAL ORIENTATION - IMPACT ON CENTER OF CASK BODY, LID OR BOTTOM

LOAD	SURFACE	STRESS (PSI) σ_t	σ_l	σ_r	τ	CLASSFICATION
Bottom-Missile B*						
Missile Force Acting on Center of Bottom Plate	Inner	16030	0	16030	<6485	$P_L + P_b$
	Outer	-16030	-27300	-16030	<6485	
Lid-Missile B*						
Missile Force Acting on Center of Lid	Inner	18430	0	18430	<6485	$P_L + P_b$
	Outer	-18430	-27300	-18430	<6485	
Lid Flange-Missile B						
Missile Force Acting on Center of Lid	Inner	50	0	50	1970	$P_L + P_b$
	Outer	-50	0	50	1970	

* These stresses are at the center of the bottom plate and lid.

FIGURE 4A.5-1
TN-24 STORAGE CASK - LONGITUDINAL SECTION

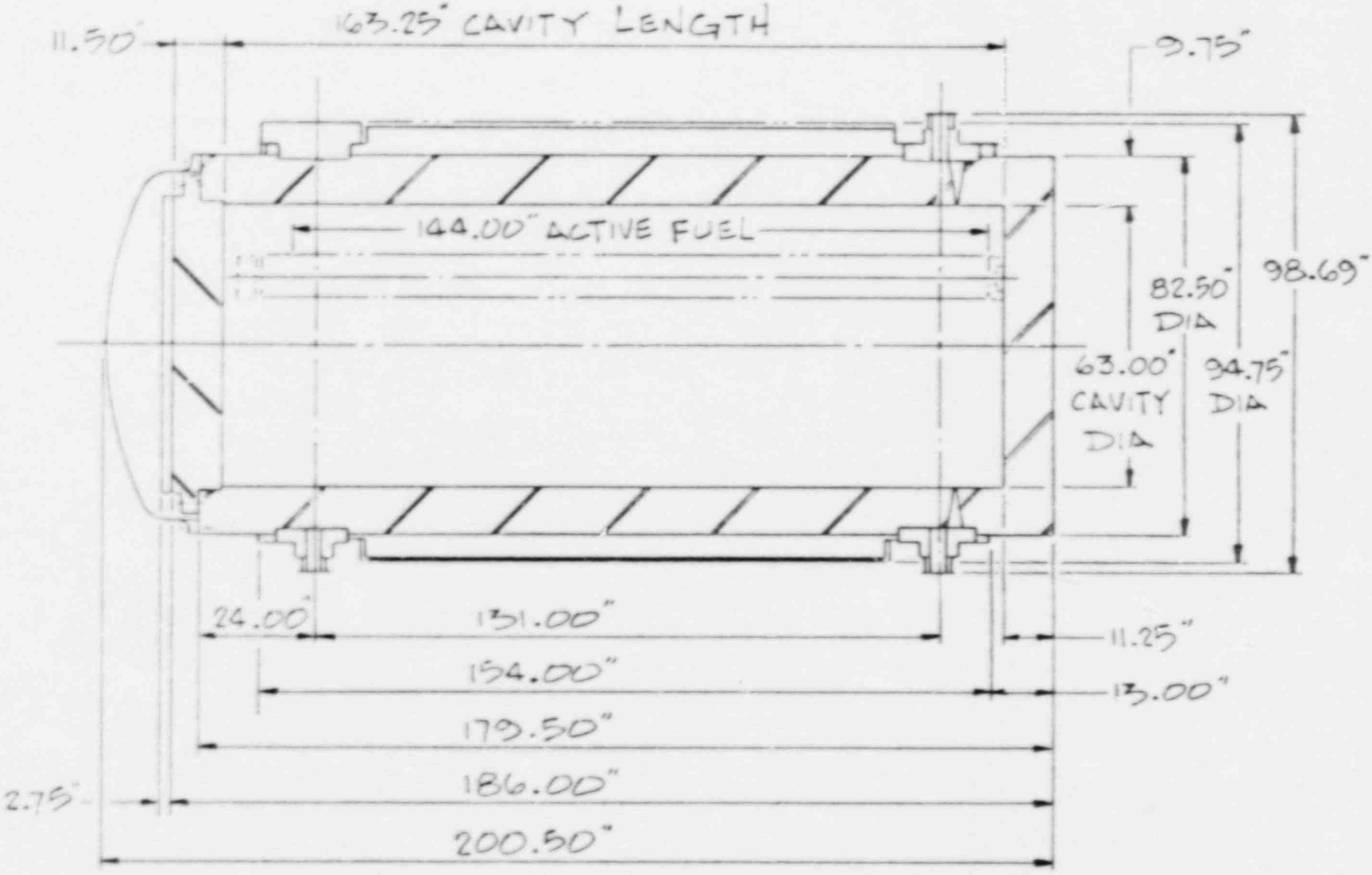

FIGURE 4A.5-2

SIGN CONVENTION FOR DISCONTINUITY
MOMENTS AND SHEARS AT JUNCTION
OF CYLINDER TO PLATE

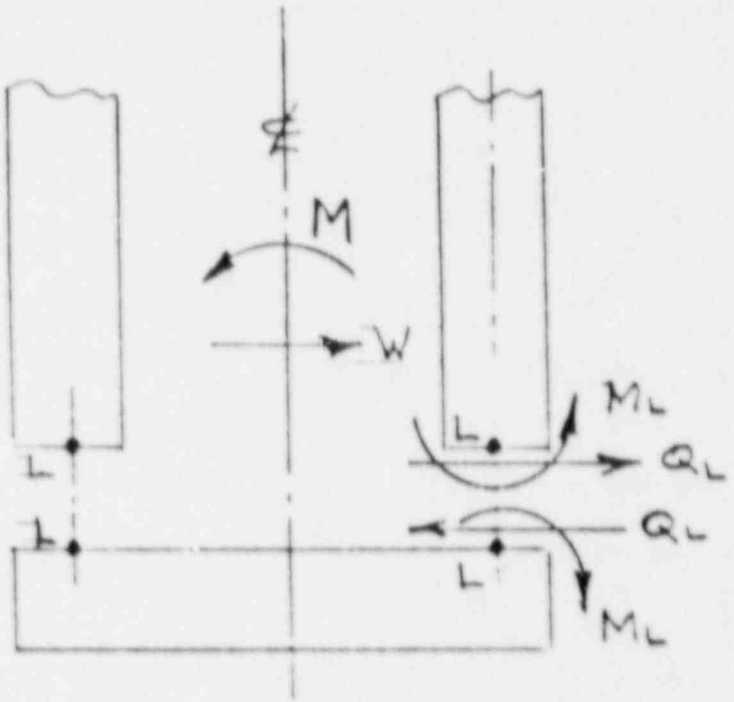

FIGURE 4A.5-3
MODEL OF THE CYLINDER
AND PLATE AT THE JUNCTION

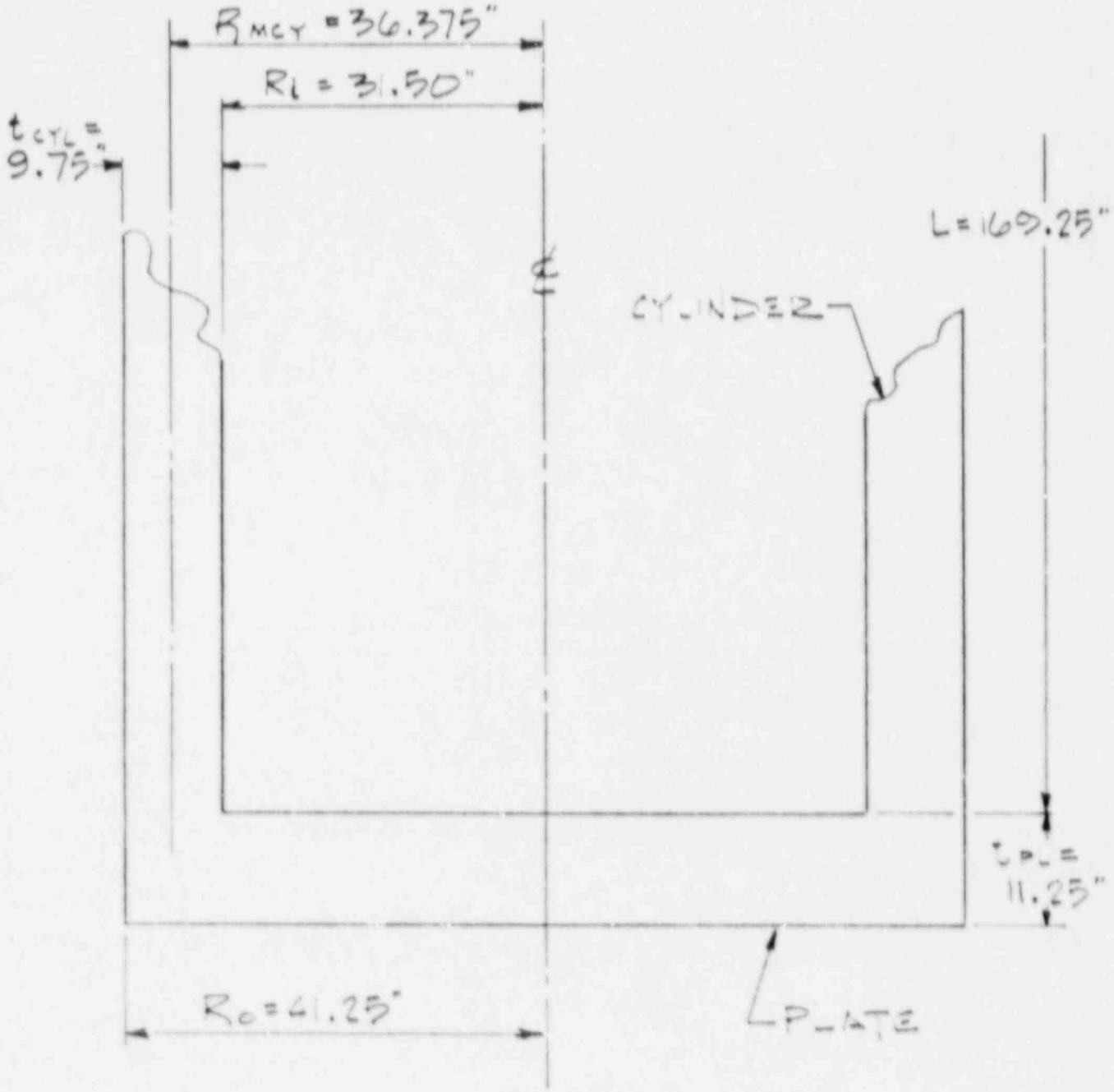

FIGURE 4A.5-4
LID AND JUNCTION OF LID AND CASK BODY CYLINDER

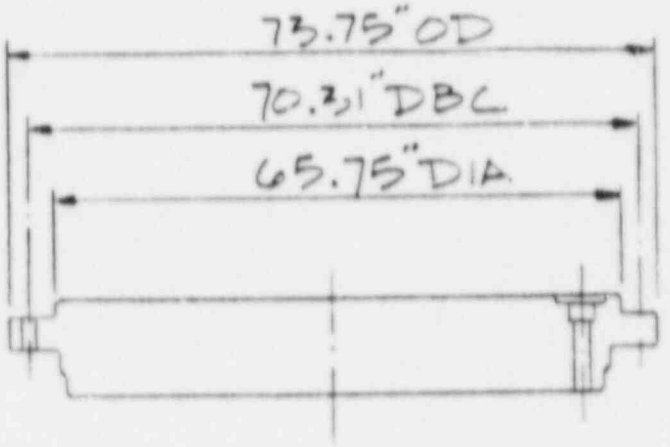

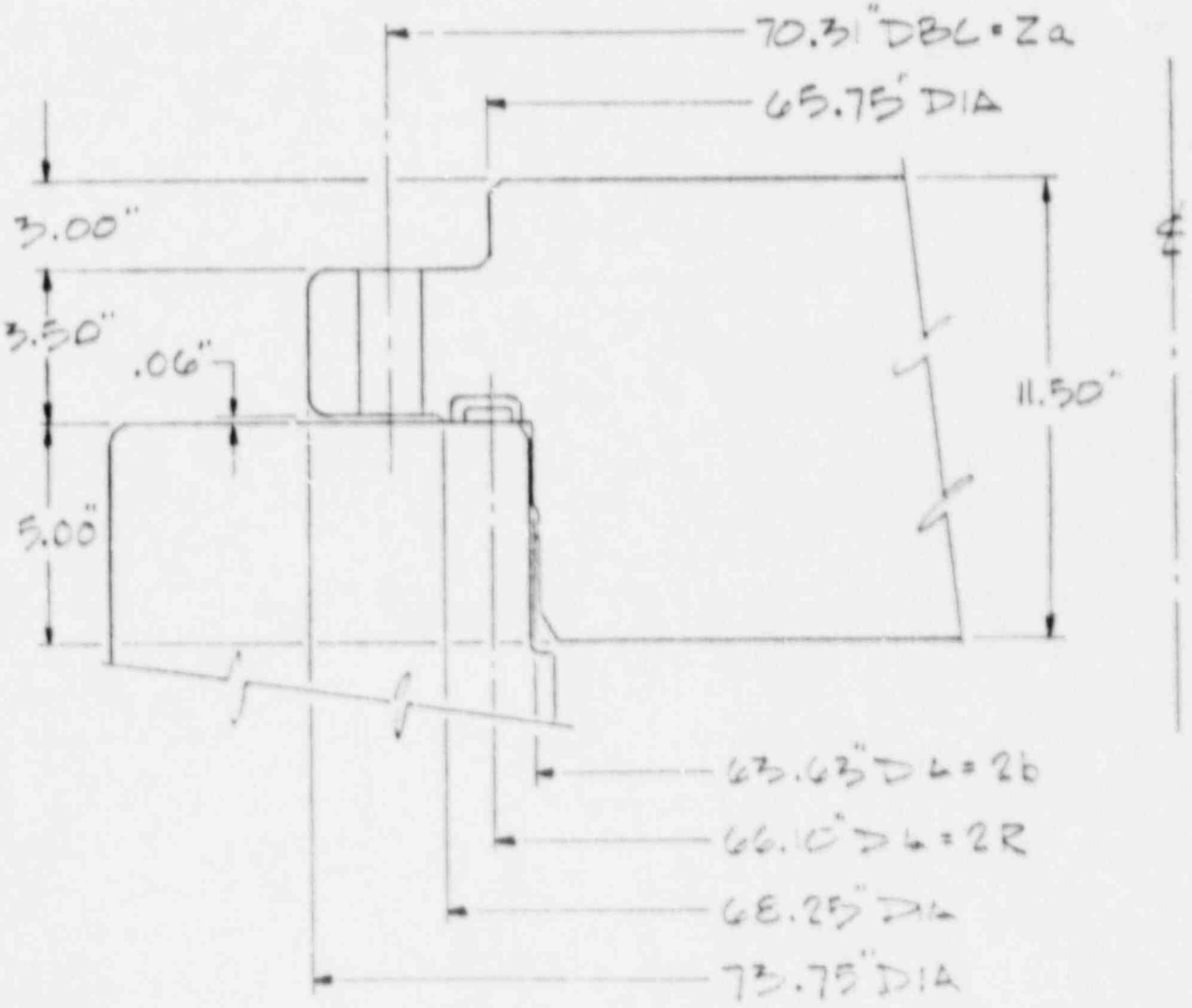

FIGURE 4A.5-5
MODIFIED LID FLANGE AT JUNCTION
WITH CASK BODY CYLINDER

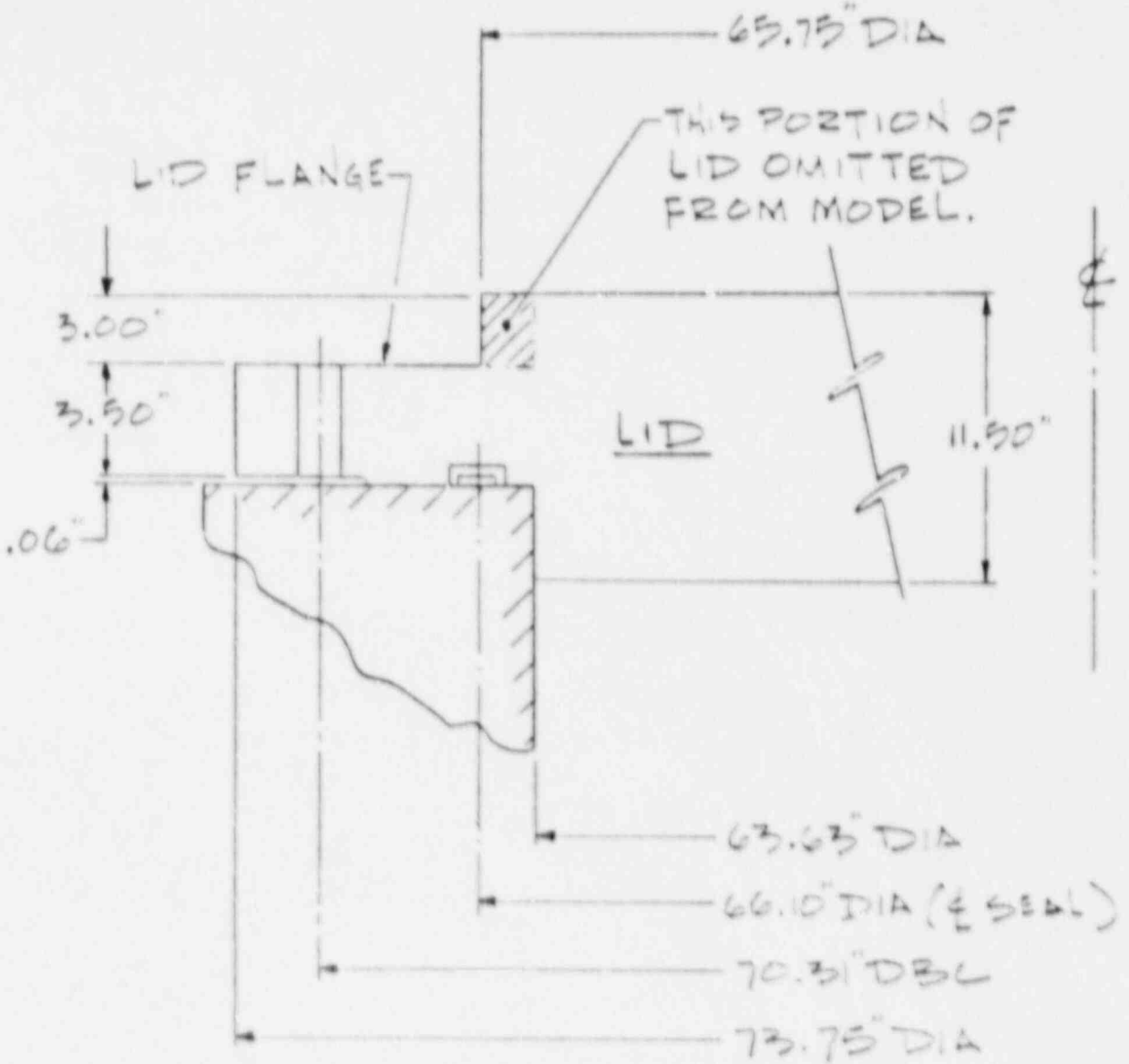

FIGURE 4A.5-6

LID ELEMENTS AND SIGN CONVENTION

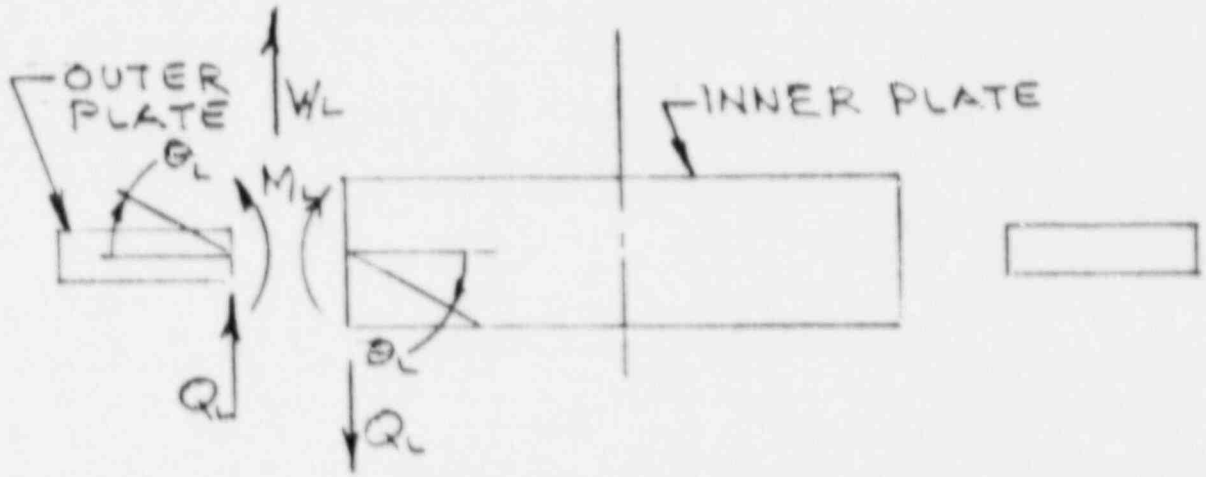

FIGURE 4A.5-7
MODEL OF LID USED FOR ANALYSIS PURPOSES

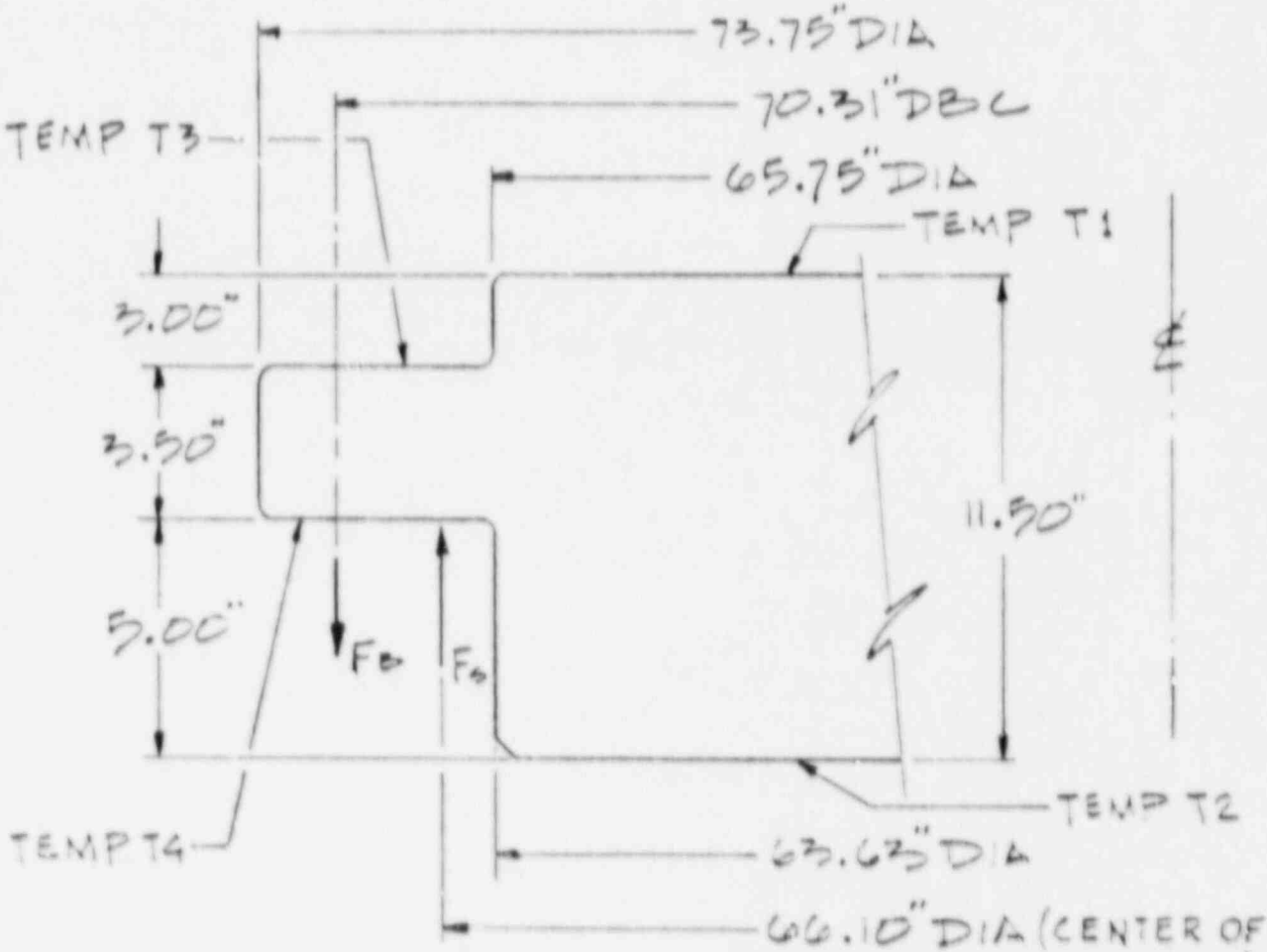

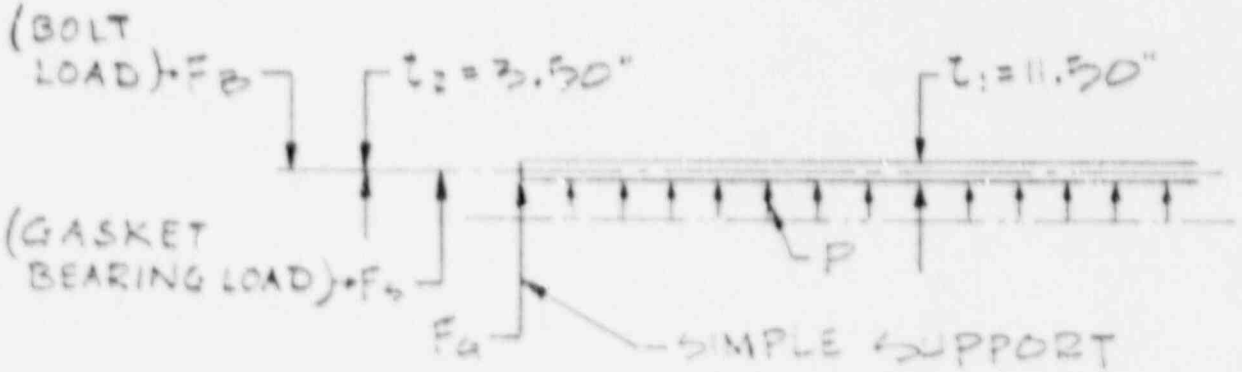

FIGURE 4A.5-8

MODEL OF LID FOR PRESSURE LOAD

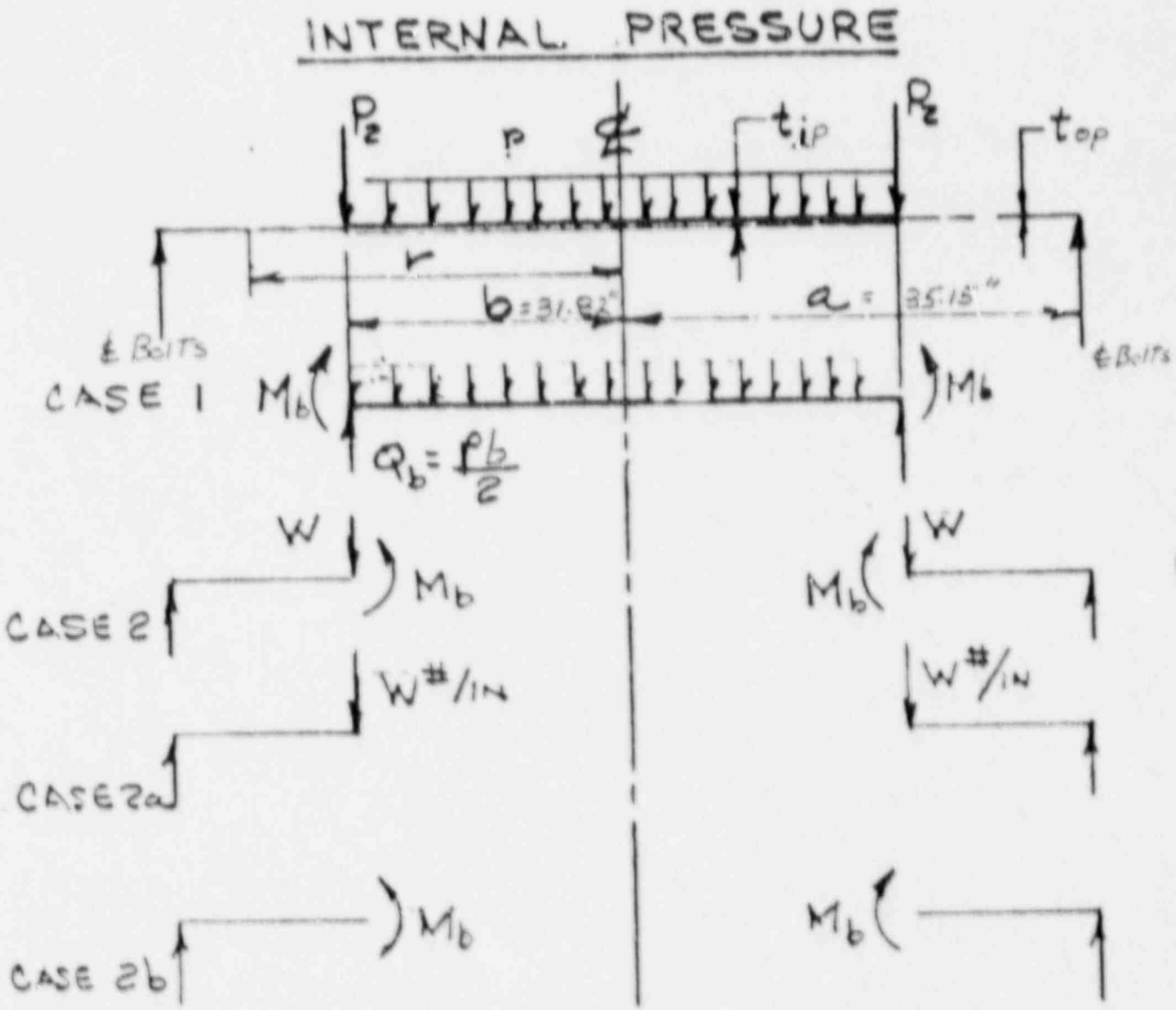

$$P_2 = \frac{\pi (r^2 - b^2)}{2\pi b} p = 1.254\, p$$

$$Q_b = \frac{pb}{2} = 15.91\, p$$

$$W = (P_2 + Q_b) = 17.164\, p$$

FIGURE 4A.5-9
MODEL OF LID FOR BOLT PRELOAD

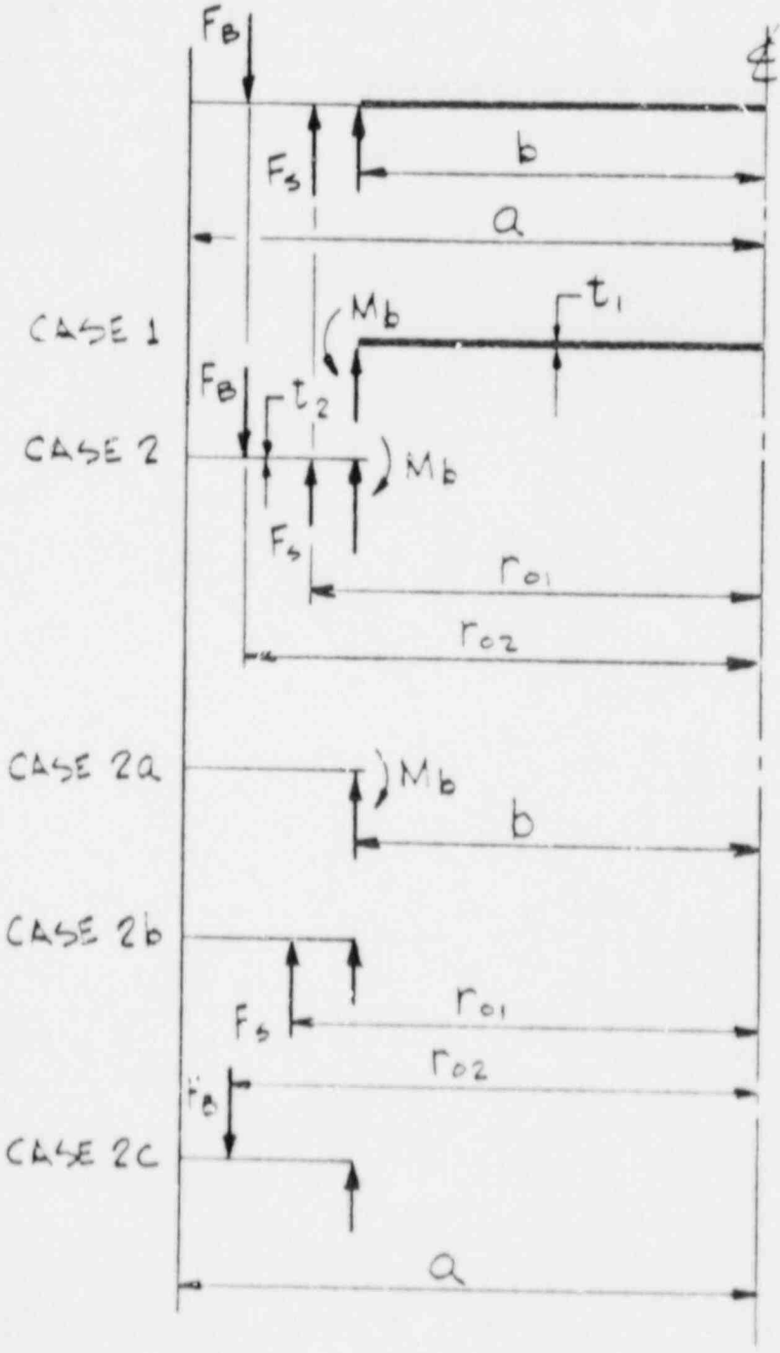

b = 31.82"
a = 36.88"
t_1 = 11.50"
t_2 = 3.50
r_{o1} = 33.05"
r_{o2} = 35.[illegible]"

FIGURE 4A.5-10

MODEL OF LID FOR ANALYSIS OF THERMAL GRADIENT ACROSS LID THICKNESS

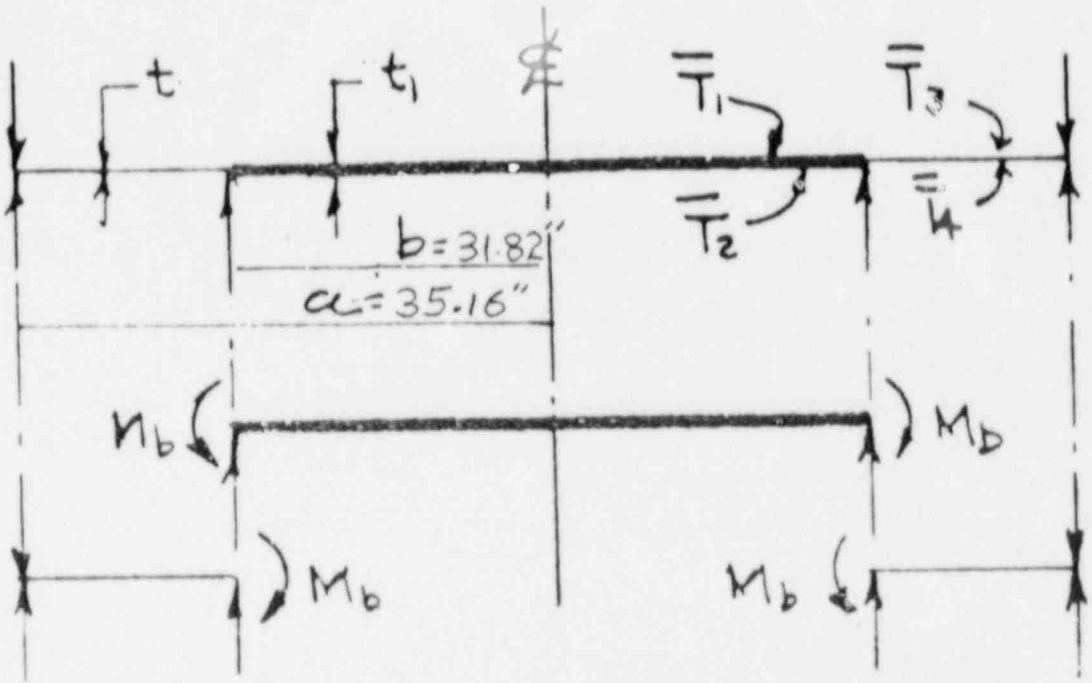

$\bar{T}_2 > \bar{T}_1$; $\bar{T}_4 > \bar{T}_2$

FIGURE 4A.5-11
MODEL OF LID & BOLTS FOR ANALYSIS OF DIFFERENTIAL THERMAL EXPANSION BETWEEN LID & CYLINDER

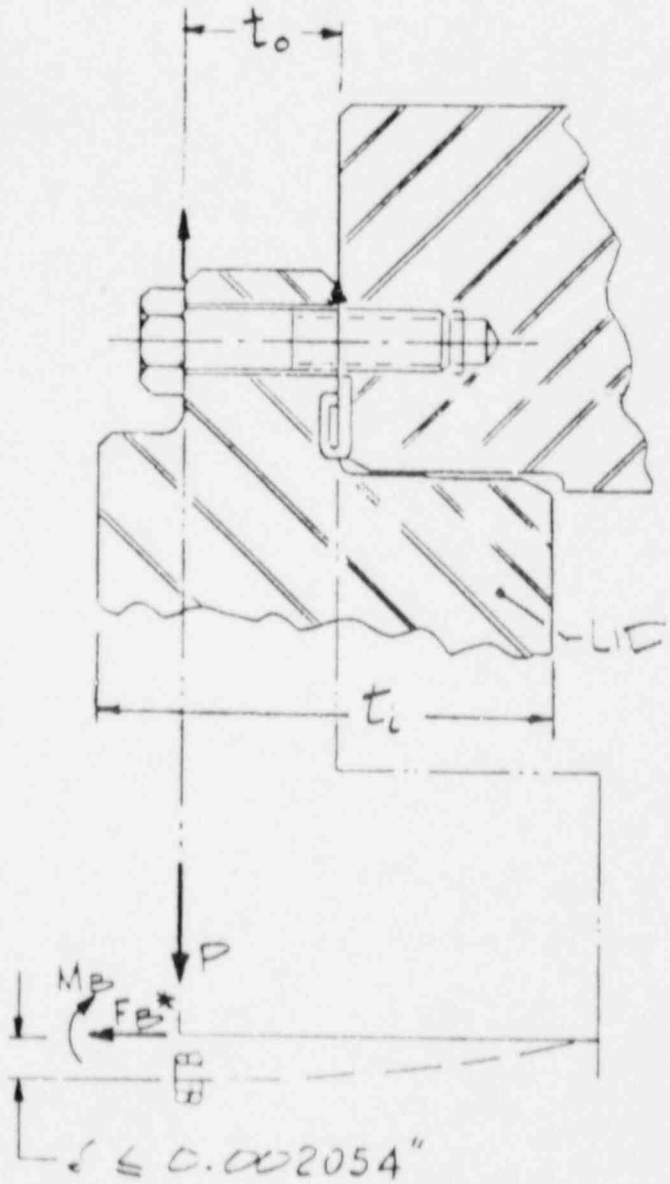

$P < f F_B^*$

$M = M_B + F_B^* \delta$

FIGURE 4A.5-12
LOADS ACTING AT JUNCTION OF LID AND CYLINDER

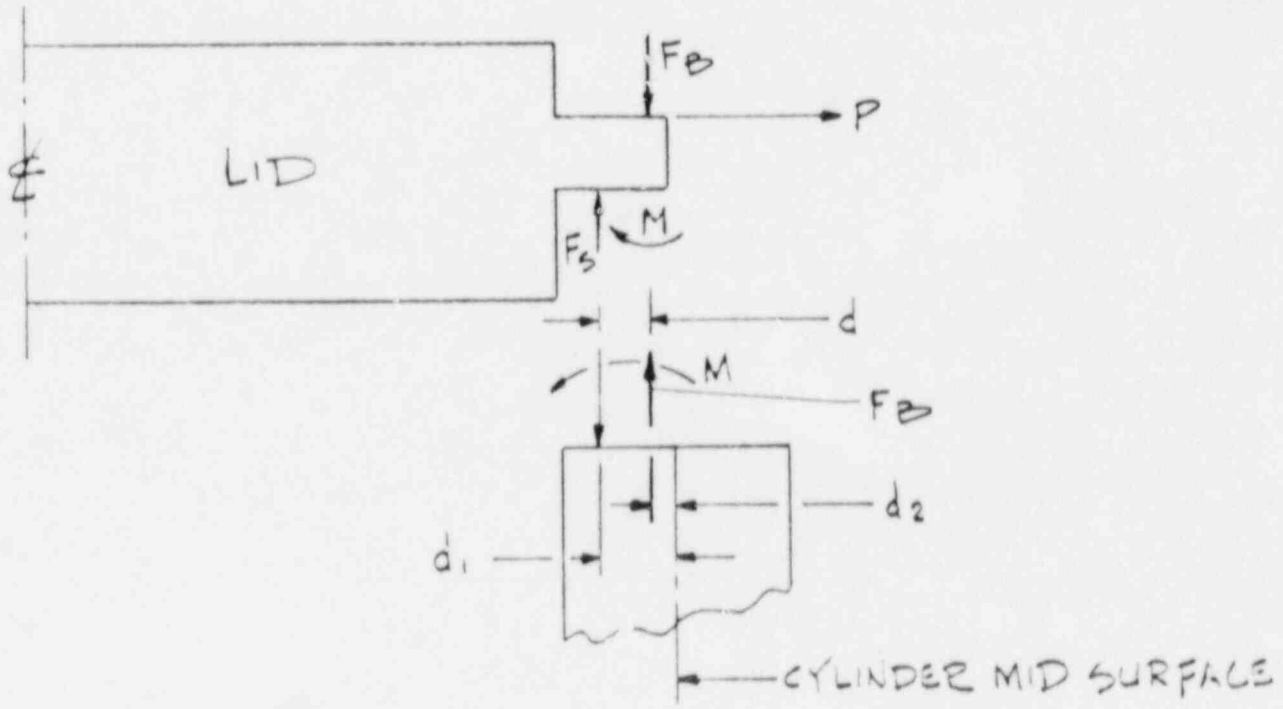

- $d_1 = 3.325"$, $d_2 = 1.22"$
- $M_B = F_S \times d_1 - F_B \times d_2$
- $M = \frac{Pl}{2}$ BENDING MOMENT FROM BOLTS (SEE FIG 4A.1-11).
- $F_S = 4474$ LB/IN FORCE REQ'D TO SEAT THE SEAL.
- $F_B = \frac{n A_B S_M}{2\pi R\, B.C.} = 8104$ LB/IN BOLT PRELOAD
- P = LATERAL FORCE ON BOLT (SEE FIG 4A.1-11).

FIGURE 4A.5-13
LOADINGS IMPOSED ON SHELL BY TRUNNIONS

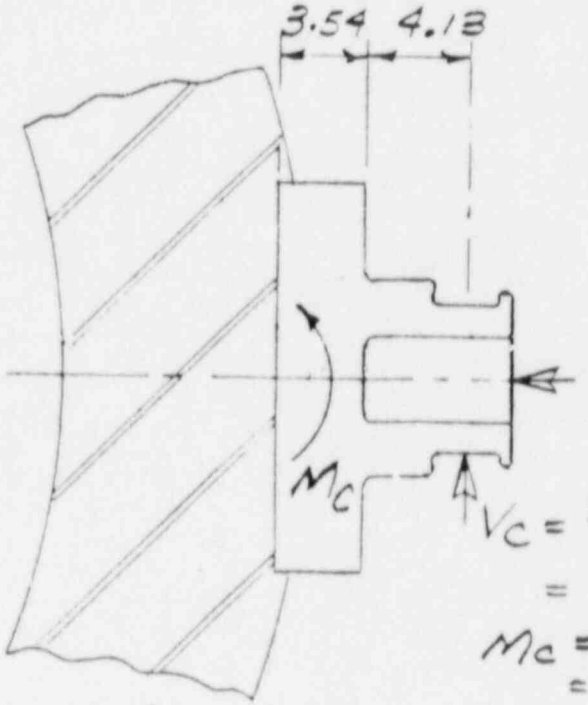

$$P = \frac{2 \times 225000}{2} = 225000 \text{ LB}$$

$$V_C = \frac{3 \times 225000}{4} = 168{,}750 \text{ LB}$$

$$M_C = 7.67 \times 168750 = 1.3 \times 10^6 \text{ IN.-LB.}$$

PARTIAL CROSS SECTION THRU TRUNNION

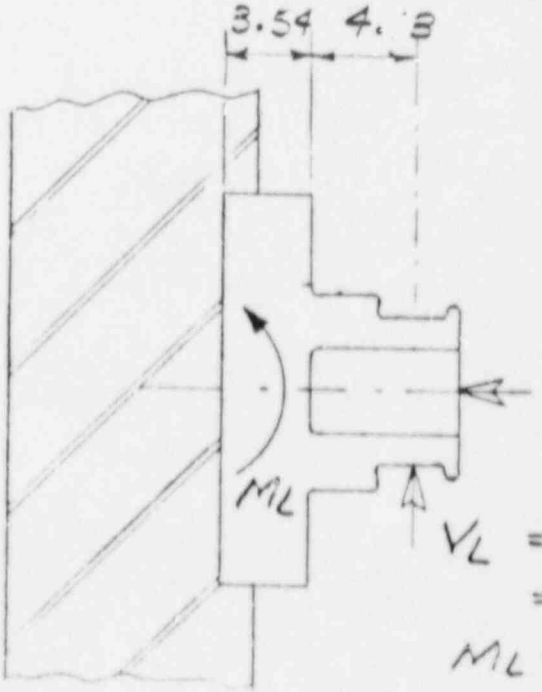

$$P = \frac{2 \times 225000}{2} = 225000$$

$$V_L = \frac{3 \times 225000}{2} = 337{,}500 \text{ LB}$$

$$M_L = 7.67 \times 337{,}500 = 2.6 \times 10^6 \text{ IN-LB}$$

PARTIAL LONGITUDINAL SECTION THRU TRUNNION

FIGURE 4A.5-14
LOAD DISTRIBUTION ON LID OR BOTTOM PLATE DUE TO VERTICAL CASK DROP ACCIDENT ONTO CONCRETE STORAGE PAD

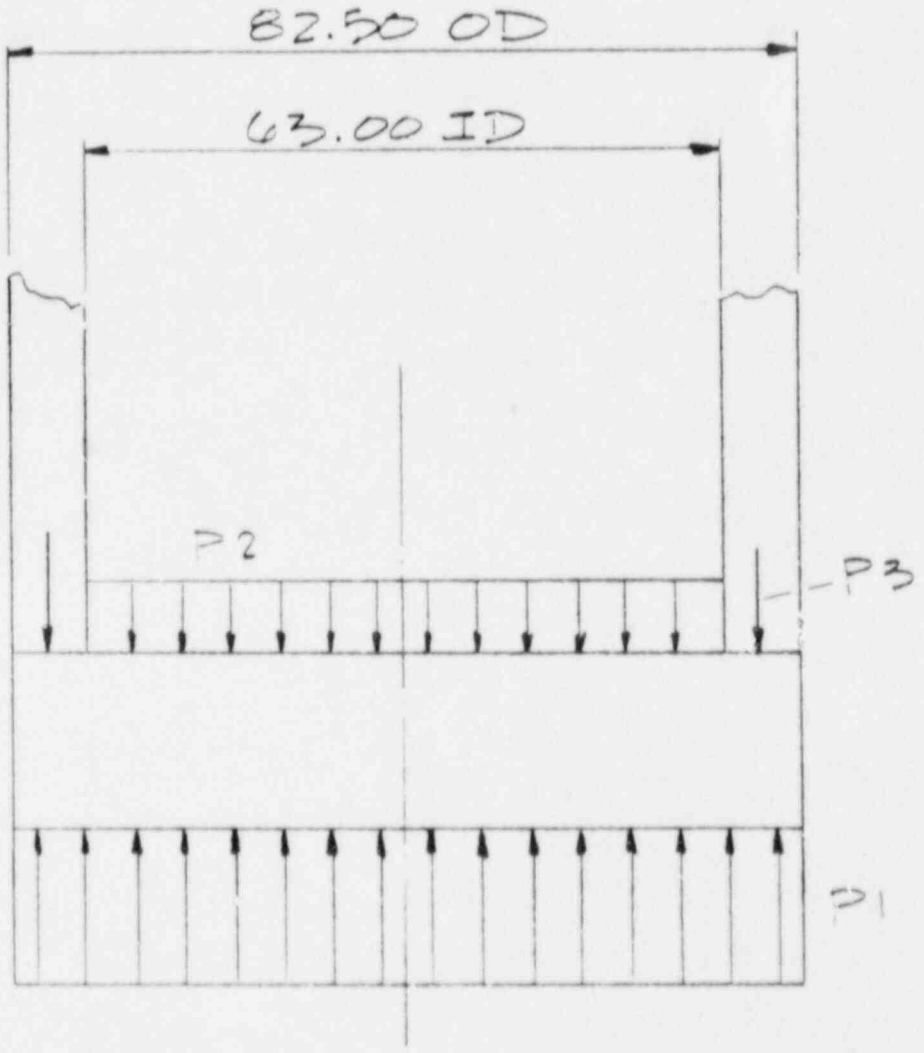

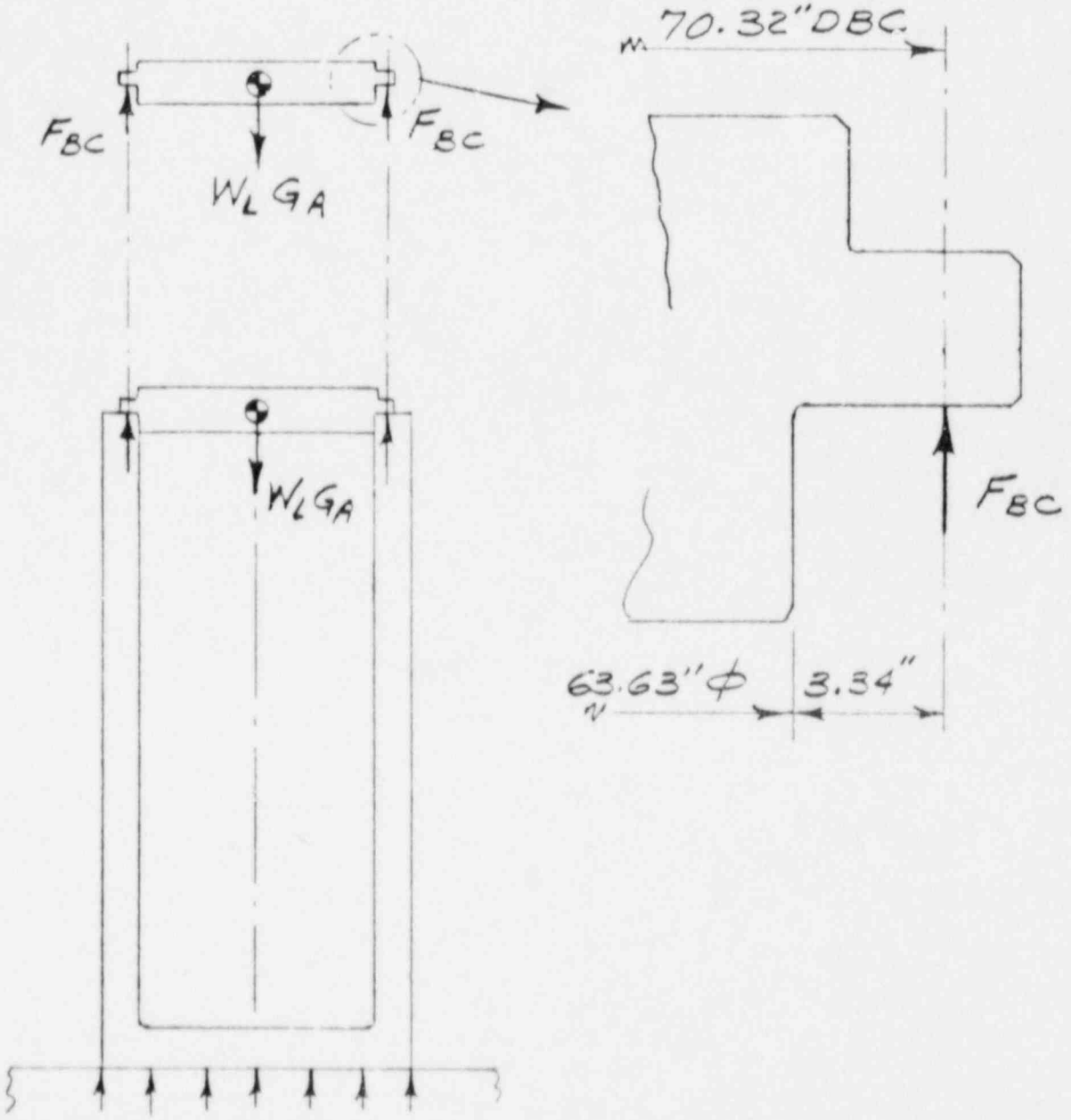

FIGURE 4A.5-15

LOAD ACTING ON LID FLANGE
DUE TO VERTICAL DROP ON BOTTOM PLATE

FIGURE 4A.5-16
LOAD DISTRIBUTION & REACTIONS ON A RING SECTION OF THE CYLINDER DUE TO HORIZONTAL CASK DROP INTO A CONCRETE STORAGE PAD.

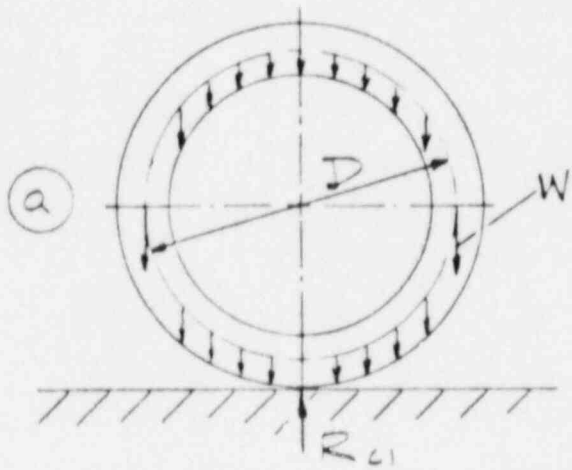

$$W1 = \frac{(\text{WEIGHT OF BODY} \times \text{ACCEL})}{(\text{LENGTH OF CASK} \times \text{CIRCUMFERENCE})}$$

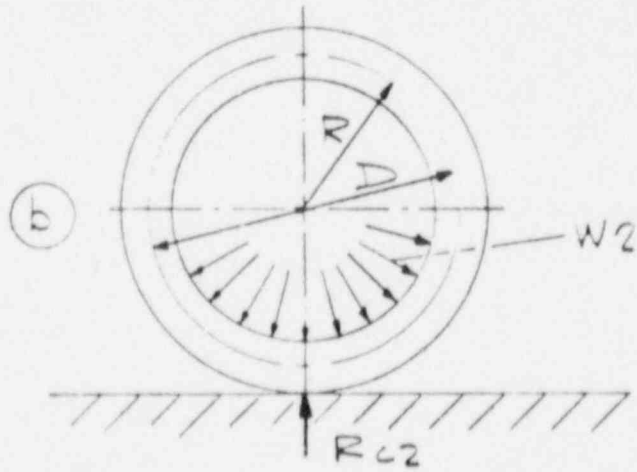

$$W2 = \frac{(\text{WEIGHT OF INTERNALS} \times \text{ACCEL.})}{(\text{LENGTH})}$$

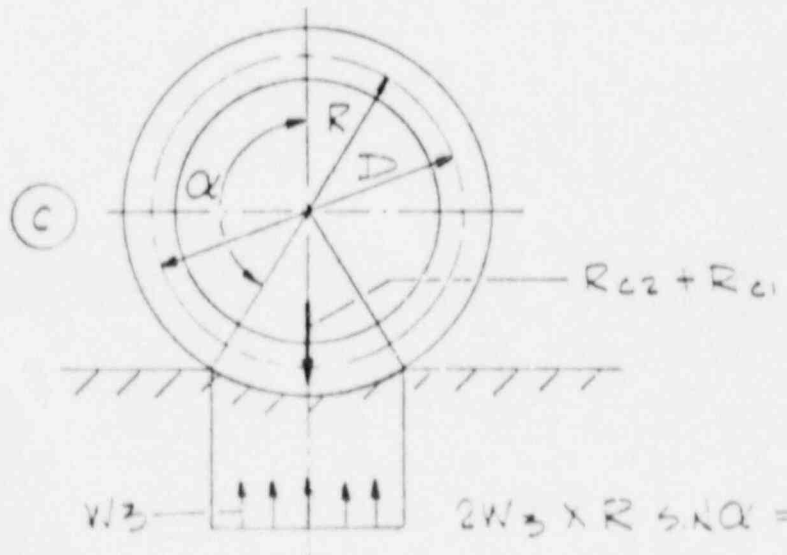

$$2W_3 \times R \sin\alpha = R_{C2} + R_{C1}$$

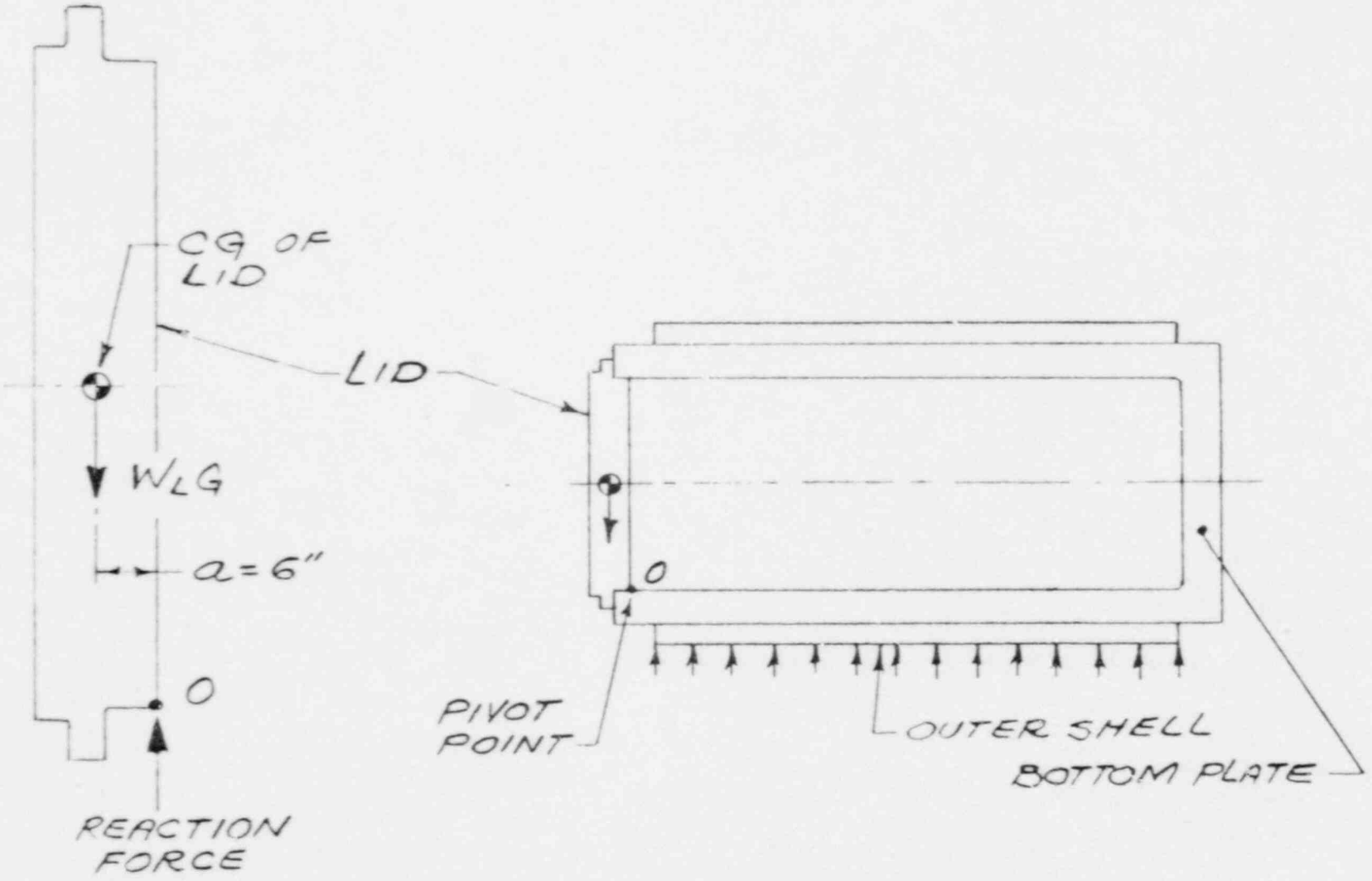

FIGURE 4A.5-17
LOAD ON LID AND LID BOLTS
FOR HORIZONTAL DROP ACCIDENT

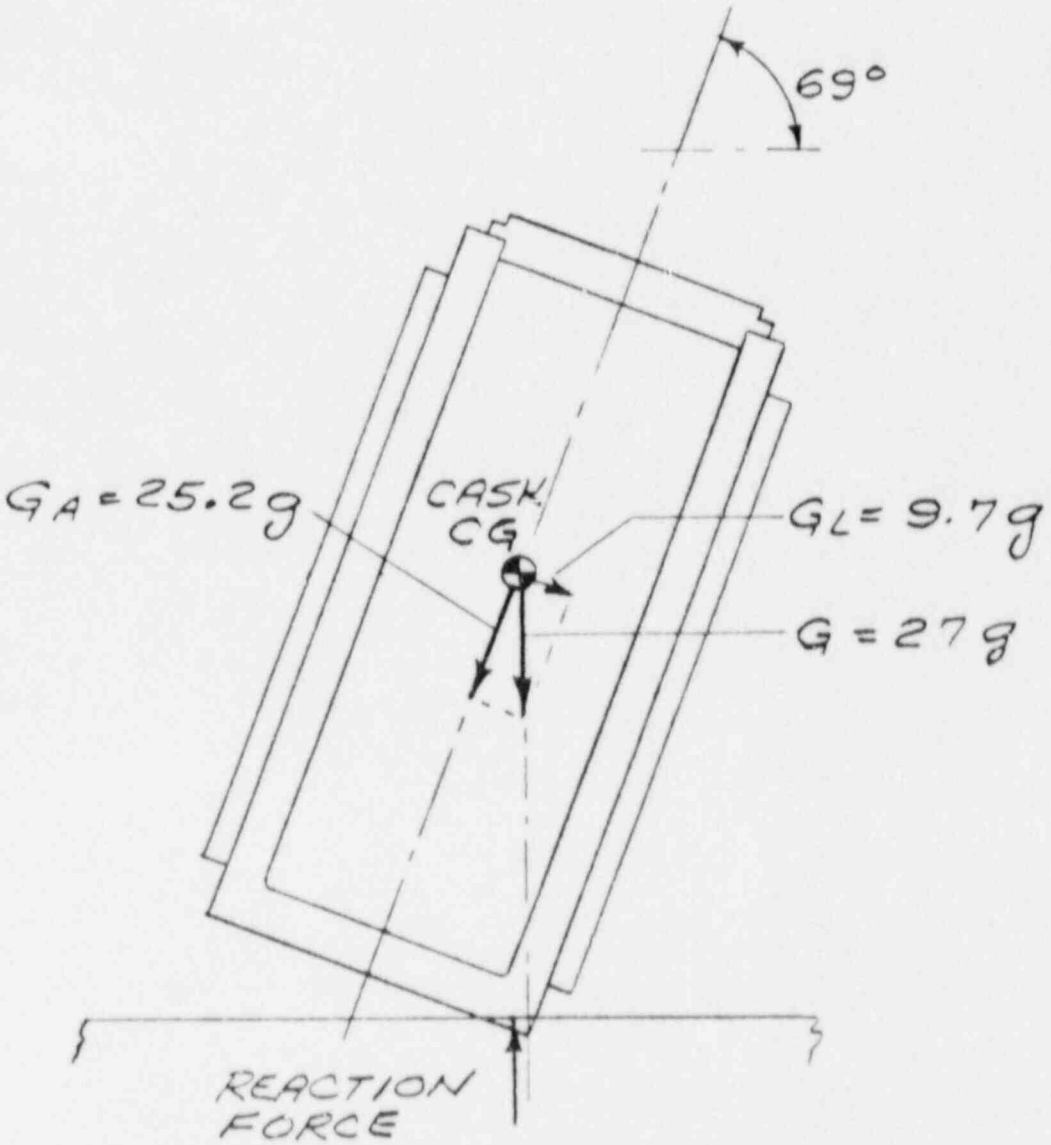

FIGURE 4A.5-18

LOADING ON CASK
DUE TO CASK CENTER OF GRAVITY
OVER BOTTOM CORNER

FIGURE 4A.5-19

ENVELOPING THE CALCULATED FORCE VS TIME CURVE TO DETERMINE DYNAMIC LOAD FACTORS

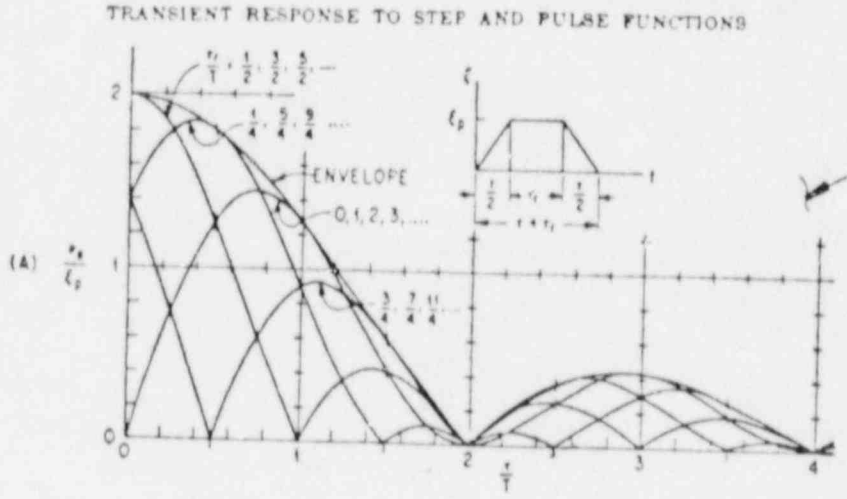

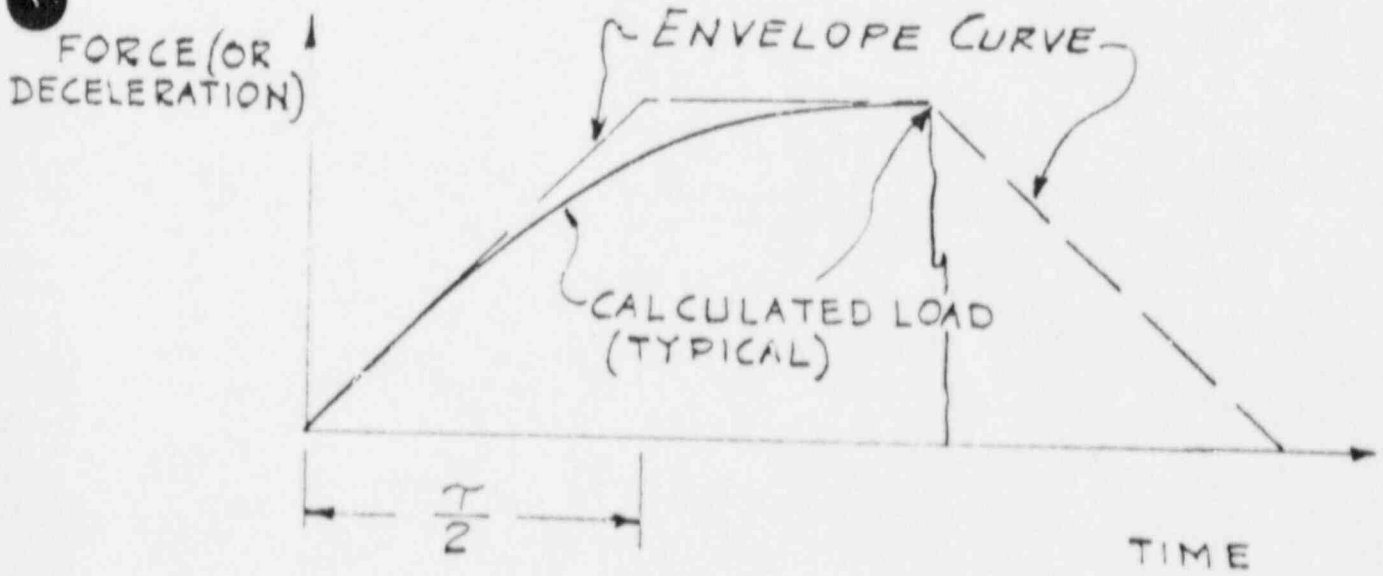

4A.5-20

LOAD DISTRIBUTION ON CYLINDER & REACTION AT CONCRETE STORAGE PAD DUE TO CASK TIPPING ACCIDENT (I.E. ROTATION ABOUT TRUNNION).

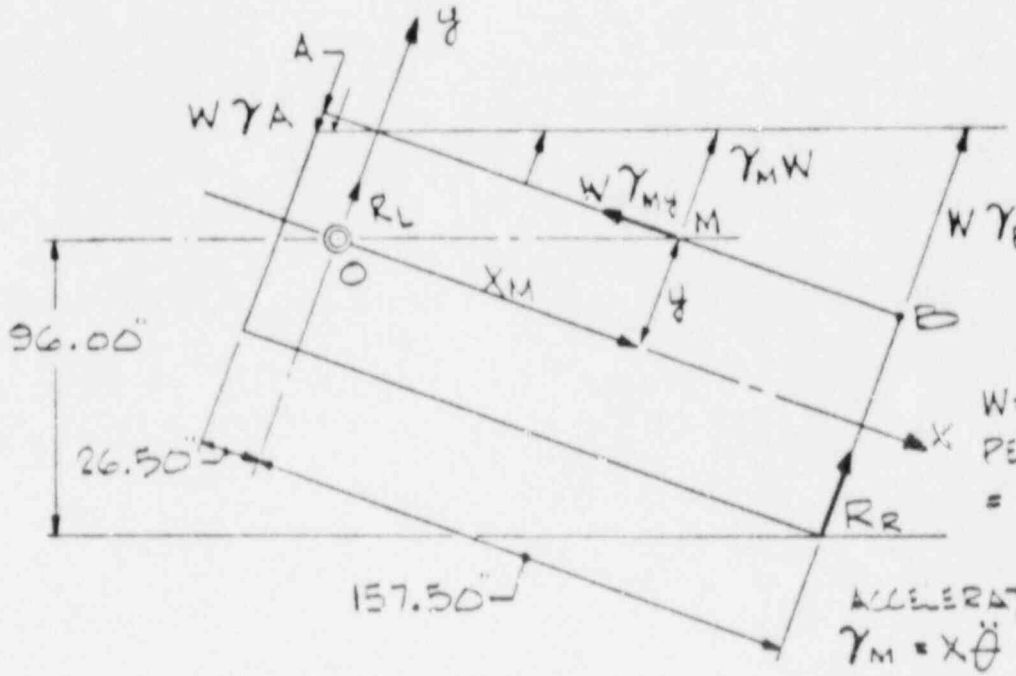

W = WEIGHT OF CASK PER UNIT LENGTH = 1189 LB/IN

ACCELERATION AT M =
$\gamma_M = X\ddot{\theta}$ AND $\gamma_{My} = y\ddot{\theta}$

$\ddot{\theta}$ = ANGULAR ACCELERATION

4A.5-19a

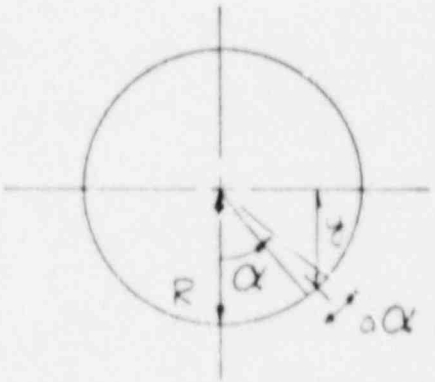

$$W_y = \frac{W}{2\pi R}$$

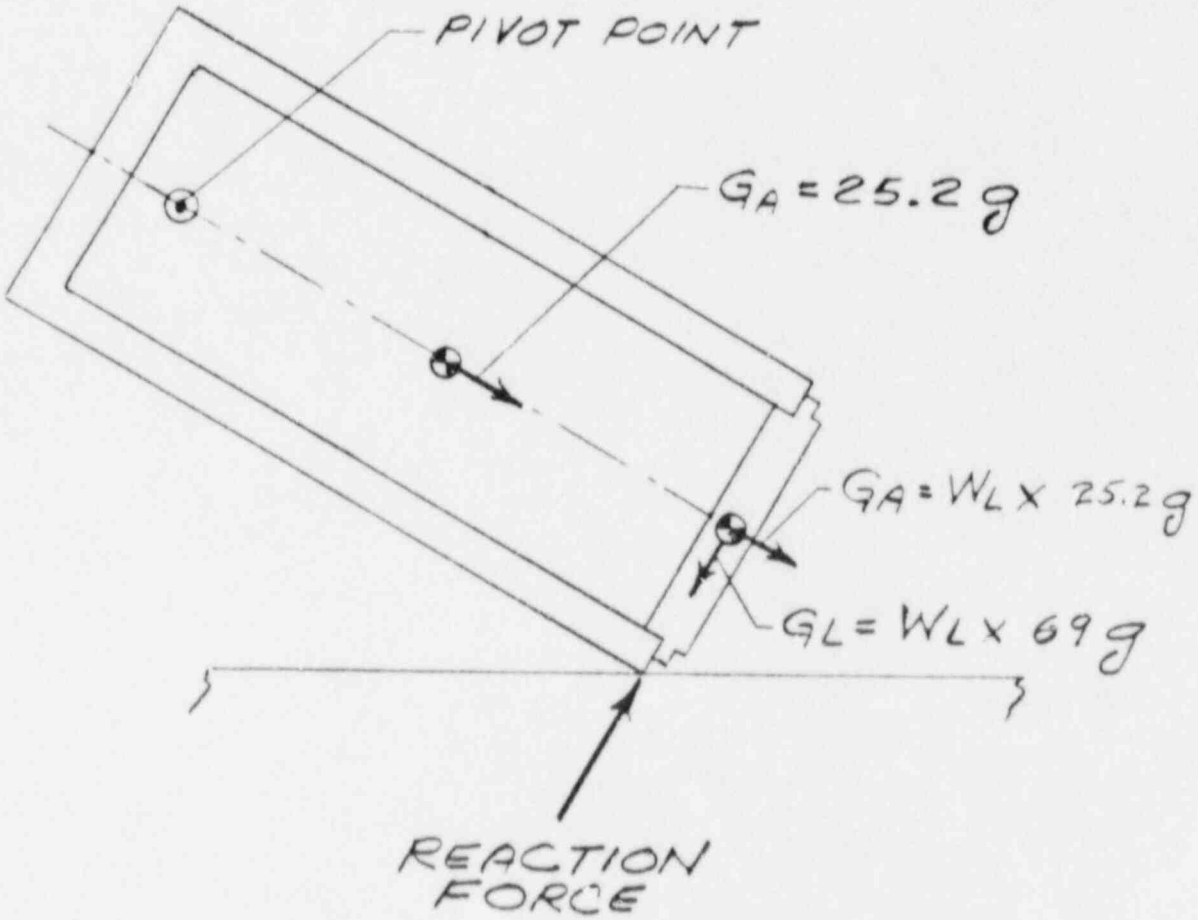

FIGURE 4A.5-21
SYSTEM OF INERTIA LOADS
APPLIED ON CASK
FOR TIPPING ABOUT TRUNNION

FIGURE 4A.5-22
INERTIA LOADS APPLIED ON LID FOR TIPPING ABOUT TRUNNION

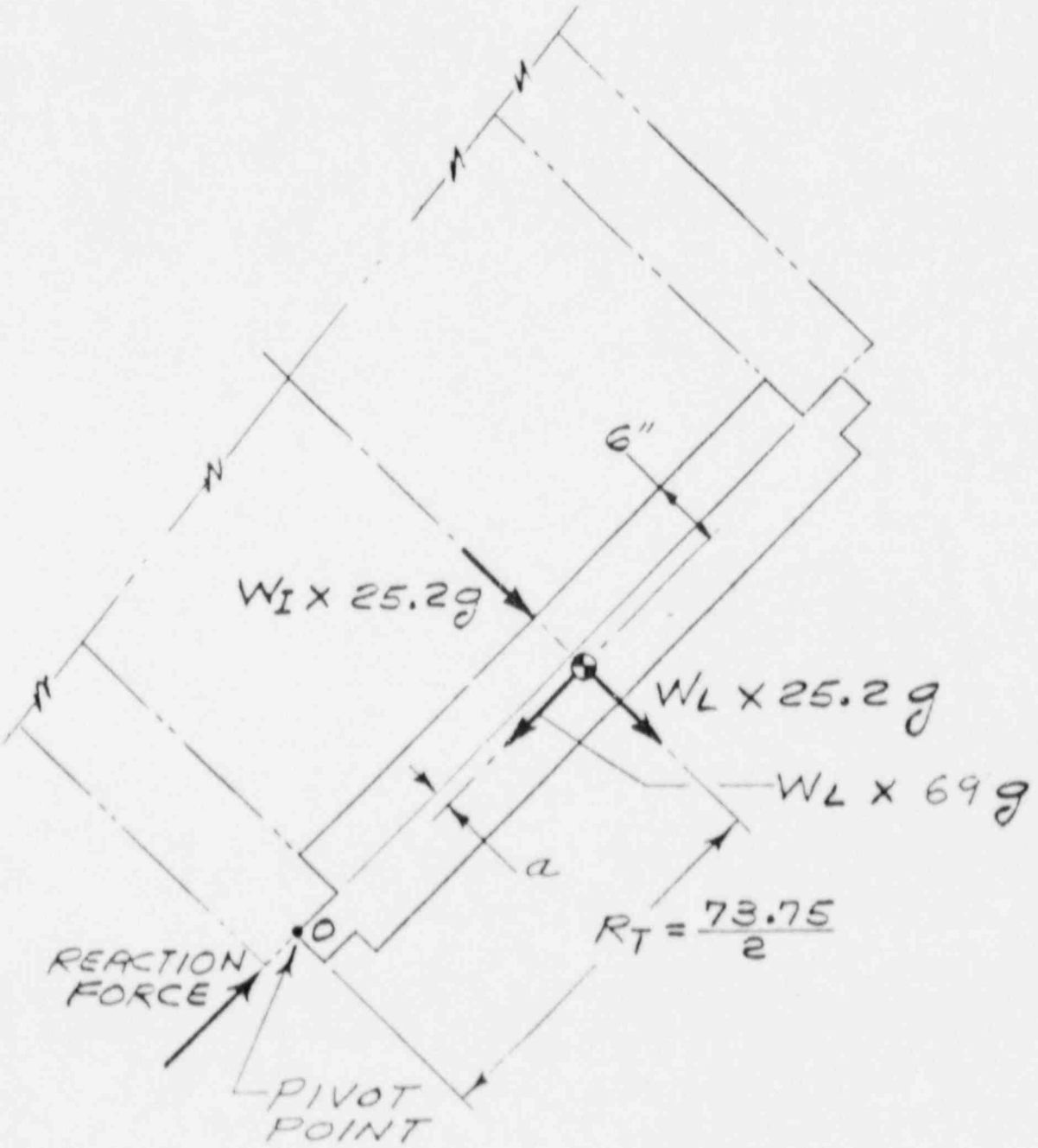

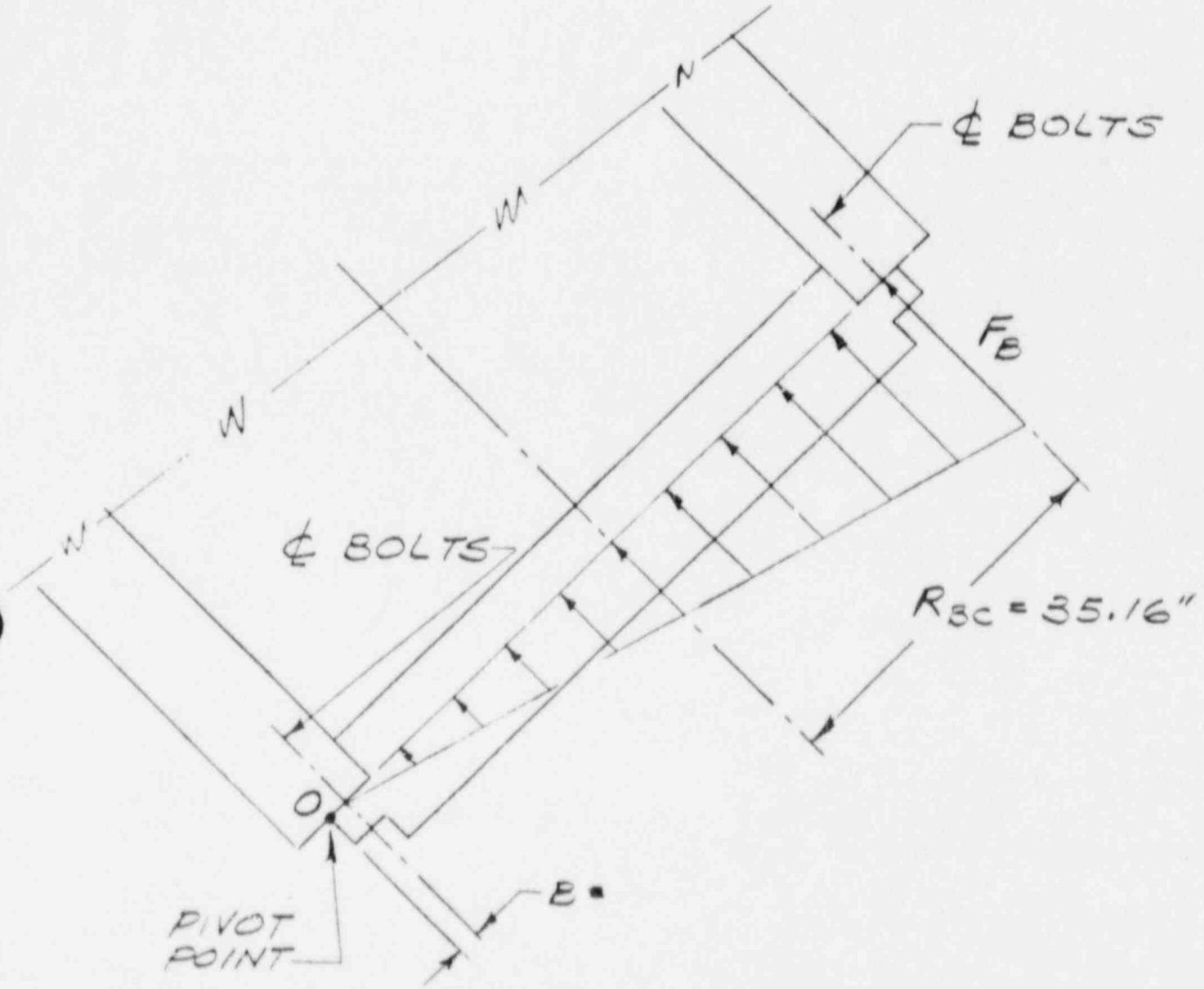

FIGURE 4A.5-23

LID BOLTS REACTING INERTIA LOADS

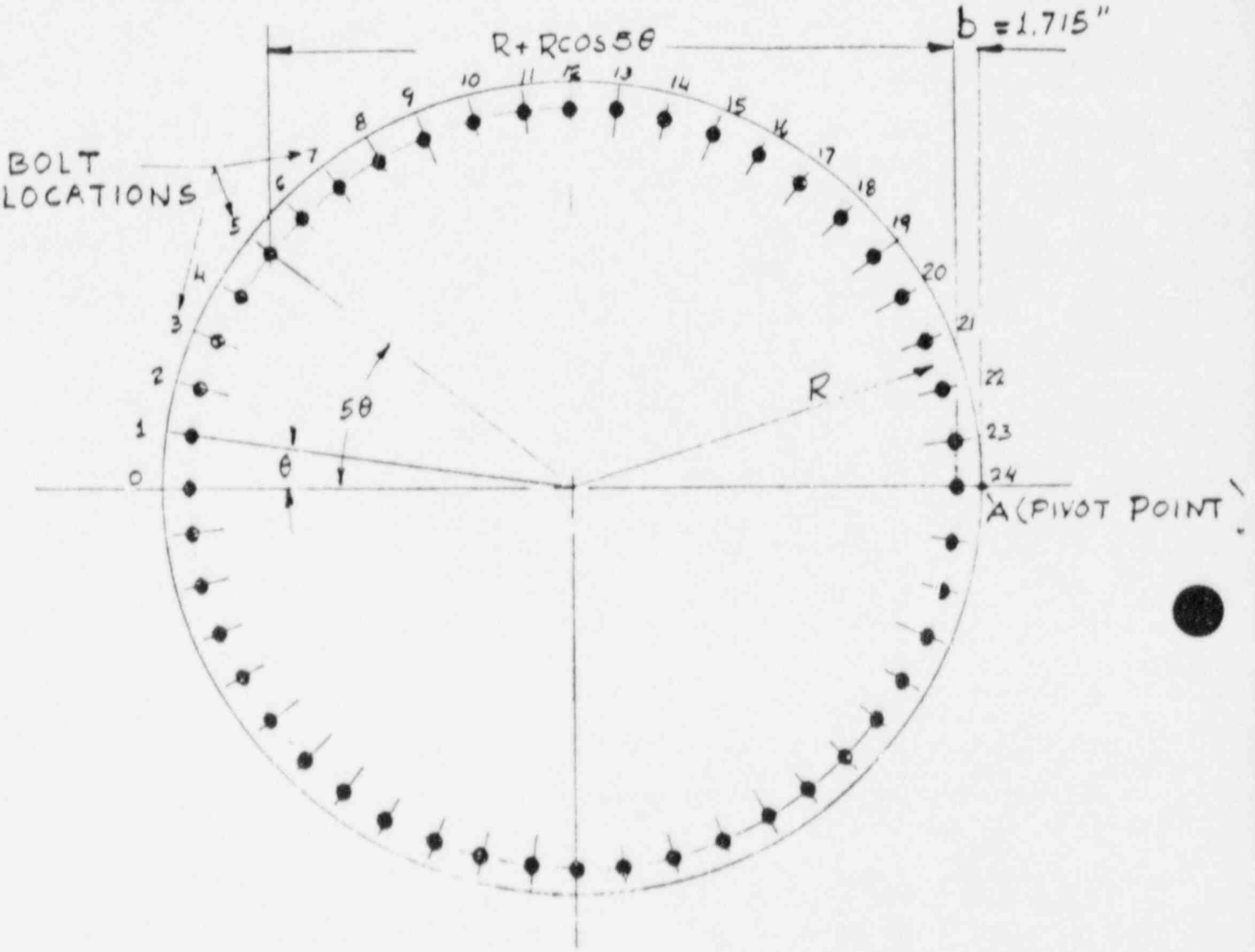

FIGURE 4A.5-24
GEOMETRY TERMS FOR LID BENDING MOMENT

FIGURE 4A.5-25
ANALYSIS MODEL
TORNADO MISSILE IMPACT ON VERTICAL CASK

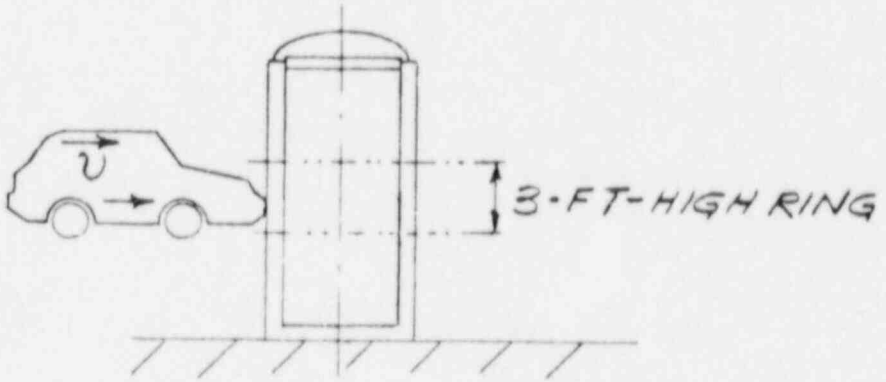

A) MISSILE A

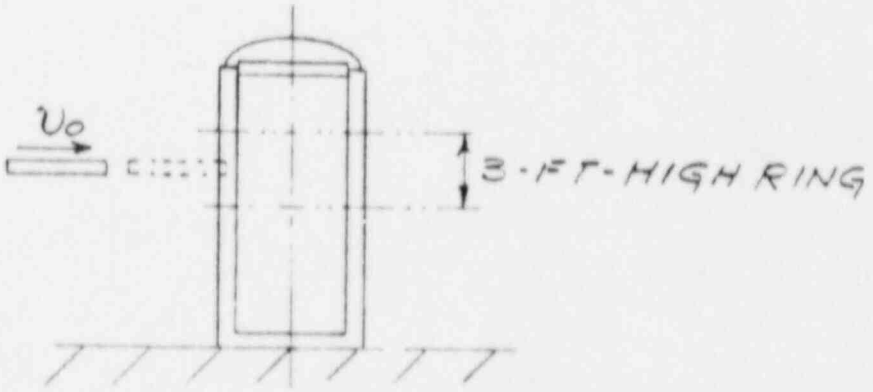

B) MISSILE B

FIGURE 4A.5-26
ANALYSIS MODEL
TORNADO MISSILE IMPACT ON HORIZONTAL CASK

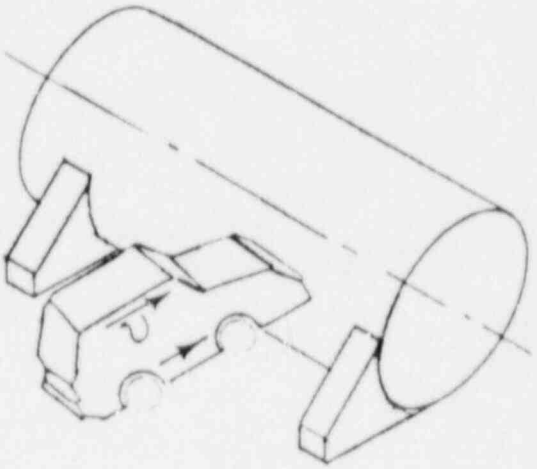

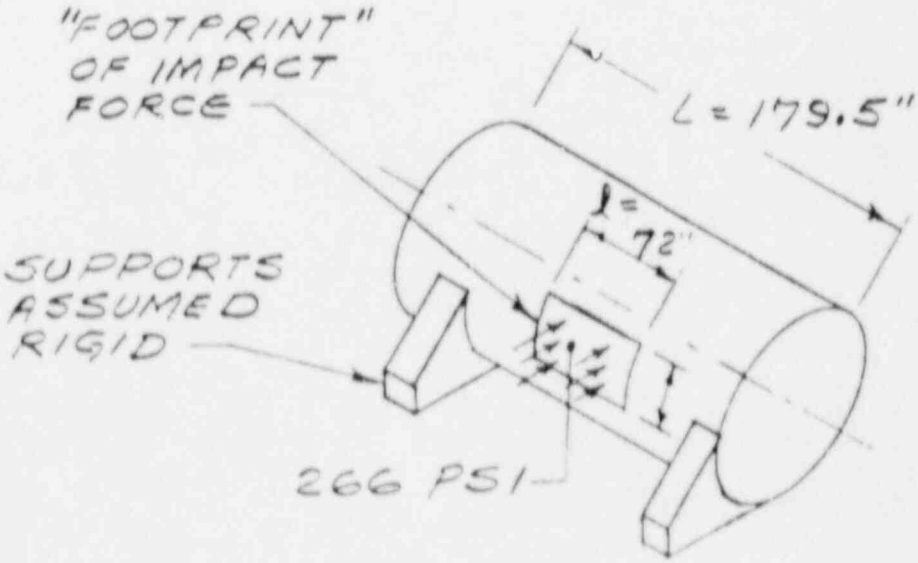

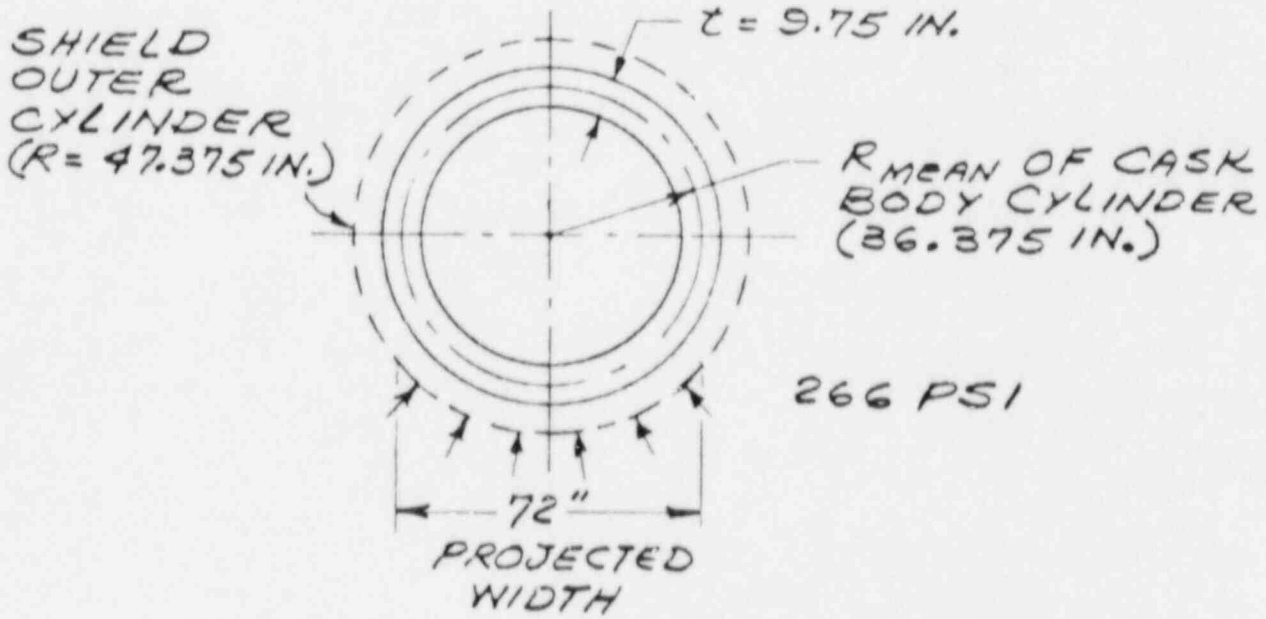

A) CASK BODY LOADING

THE ABOVE IMPACT LOADING IS APPLIED TO A 36-IN.-RING OF CASK BODY CYLINDER AND REACTED BY INERTIA LOADING AS INDICATED BELOW:

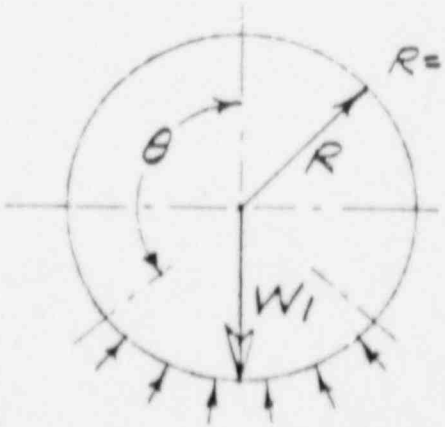

w_1, LB/IN.

B) ROARK, REF 7
TABLE 17, CASE 12

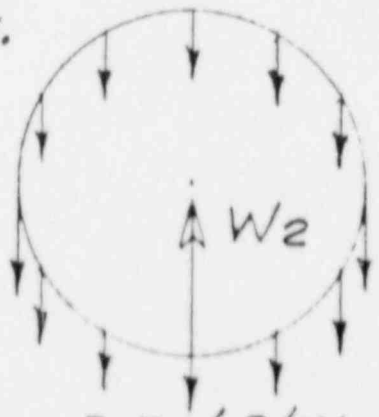

w_2 LB/IN.

C) ROARK, REF 7
TABLE 17, CASE 13

FIGURE 4A.5-27
MISSILE A IMPACT
ON RING SECTION OF VERTICAL CASK

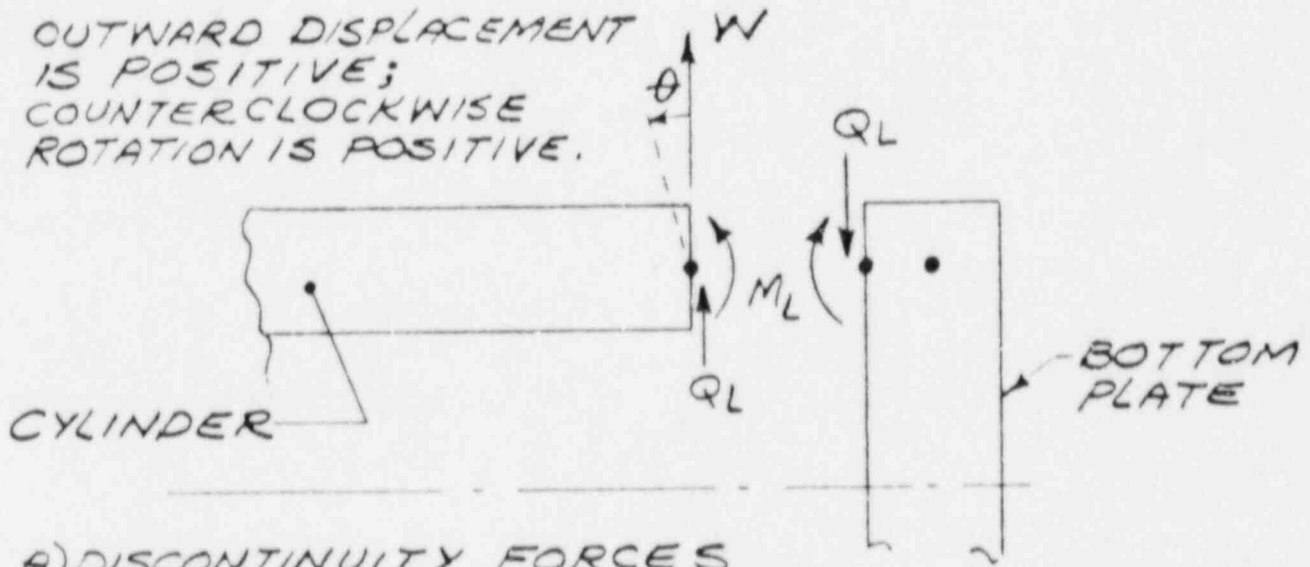

A) DISCONTINUITY FORCES BETWEEN CASK CYLINDER AND BOTTOM PLATE

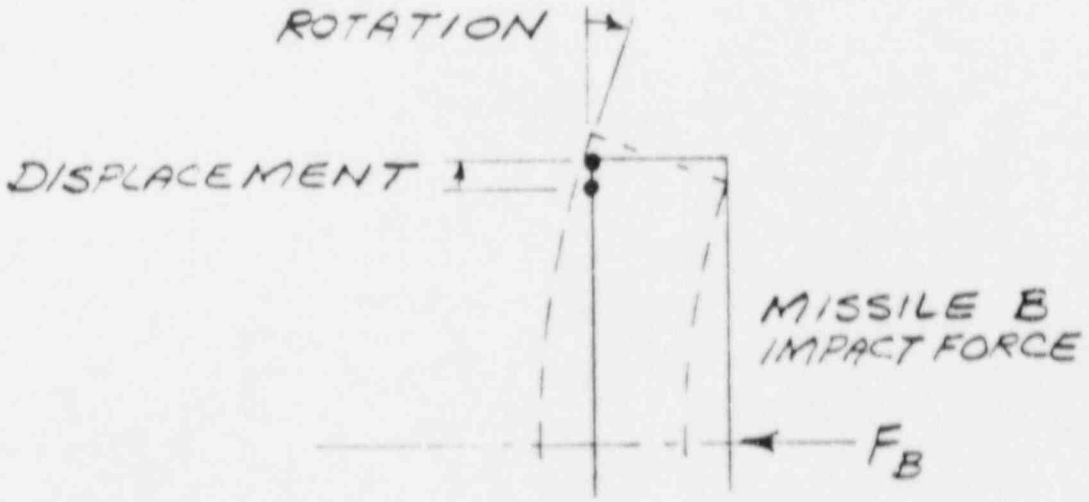

B) SIMPLY SUPPORTED BOTTOM PLATE DISPLACEMENTS DUE TO IMPACT FORCE.

FIGURE 4A 5-28
MISSILE B IMPACT
ON CASK BOTTOM

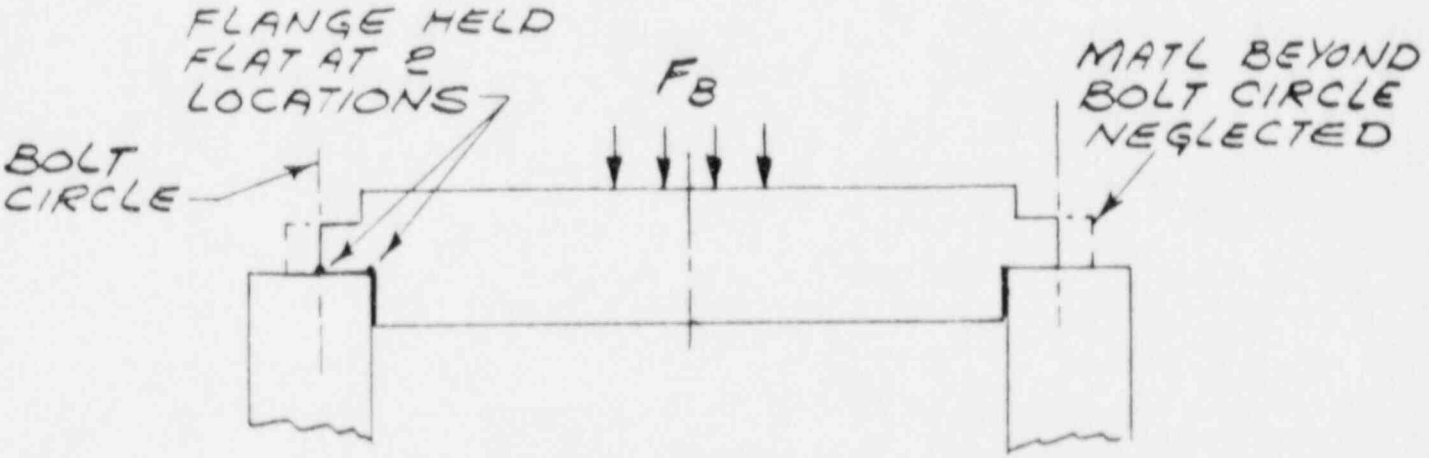

A) OVERALL CONFIGURATION

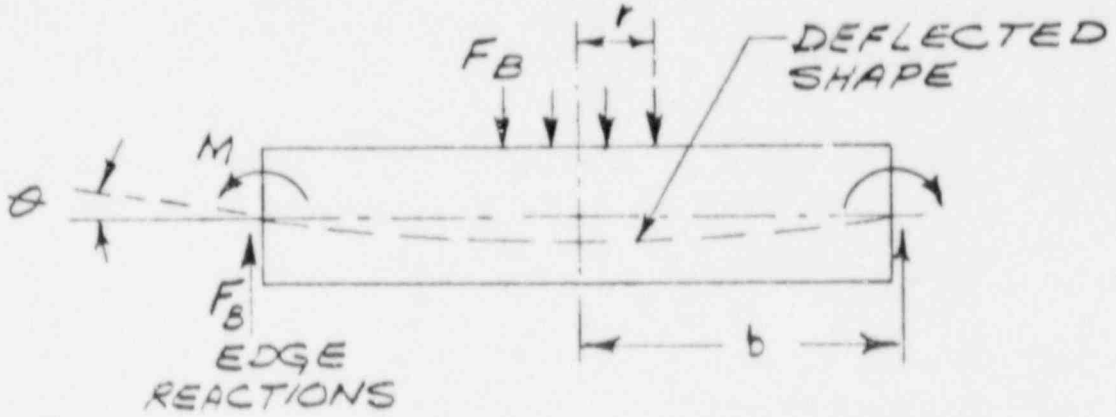

B) INNER PLATE

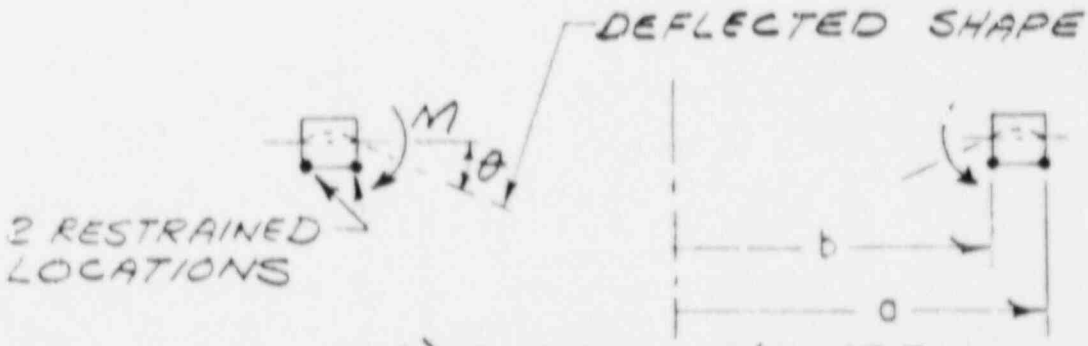

C) OUTER FLANGE

FIGURE 4A5-29

MISSILE B IMPACT ON CASK LID

4A.6 STRUCTURAL ANALYSIS OF THE BASKET

4A.6.1 Introduction

This appendix presents the structural analysis of the TN-24 basket. The basket consists of borated stainless steel plates which are slotted along the top and bottom edges. When assembled, they interlock to form an egg crate structure which has a total height of 161.8 in.

This egg crate structure is designed to provide sufficient structural rigidity to maintain separation of the fuel assemblies and a subcritical configuration under the applied loadings. The deformations and stresses induced in the basket structure due to the applied loads are determined using the ANSYS computer program[15]. The loads are established based on normal handing and storage accident conditions. The inertia g loads due to the fuel assemblies are applied to the basket structure as distributed loads on the plates. A quasistatic stress analysis is then performed with applied loads in equilibrium with the reactions at the periphery of the basket.

The calculated stresses in the basket structure are compared with the stress limits to demonstrate that the established design criteria are met.

4A.6.2 Description

Geometry

The details of the TN-24 basket are shown on drawings 971-005 and 971-006 in Appendix 1A. The basket is constructed of 1.0% borated stainless steel plates which are 0.276 in. thick and 16.18 in. wide. The length of the plates varies from 18.75 in. to 62 in. depending on their location in the cavity. The plates are slotted on the top and bottom edges at intervals of approximately 9 in. as

shown in drawing 971-006. The plates interlock by sliding into the slots in mating plates and, when assembled, form the egg crate structure which provides 24 compartments each having a cross section of 8.7 in. by 8.7 in. to house 24 fuel assemblies.

Rails are used at the periphery of the basket to provide restraint against bending and buckling at the ends of those plates which have the greatest length beyond the adjacent intersecting plates. The basket plates are copper-coated on both surfaces to improve heat transfer. The copper is not considered to have load carrying capability for structural analysis.

Weight

A conservative value of 1550 lb is assumed for the fuel assembly weight. Each assembly is supported by ten plates. In addition to the fuel assembly weight, the weight of the basket structure is included in the analysis.

Temperature

A thermal analysis was conducted to obtain a steady-state temperature distribution for the basket structure. The results of this analysis are presented in Section 5.1.3.6.

4A.6.3 Material Properties and Design Criteria

Material Properties

The material properties of the 1.0% borated stainless steel plates are taken from Reference 10. The elevated temperature properties not available in this reference are obtained by extrapolating stainless steel properties found in the ASME Code Section III Appendices[2]. The material properties used in the analysis are listed in Table 4A.6-1. A stress-strain curve was established based on this table and is shown on Figure 4A.6-1.

Design Criteria

The basket structure is designed to provide a minimum nominal gap of 1/8 in. between the fuel assembly and the inside surfaces of the compartment walls. The compartment wall (the plate) thickness is determined to meet heat transfer, nuclear criticality, and structural requirements. The basket structure must provide sufficient rigidity to maintain a subcritical condition under the applied loads while providing sufficient area to transfer heat without exceeding fuel cladding temperature limits.

The minimum mechanical properties for the borated stainless steel at 650°F are used to establish quantitative acceptance criteria for comparison with analysis results. Under normal handling conditions, the primary membrane stress and the primary membrane plus bending stress are limited to 67% of the minimum yield strength and 100% of the minimum yield strength, respectively, at any location in the basket. During accident conditions, the primary membrane stress is limited to 70% of the minimum ultimate strength. The membrane plus bending stress is limited to 90% of the ultimate strength. The maximum local strain at any slot location is limited to 50% of the ductility of the material (local strain limit = 0.5 x minimum ductility = 0.5 x 20% = 10%).

4A.6.4 Loading Conditions

The loading conditions considered in the evaluation of the fuel basket consist of inertial loads resulting from normal handling and hypothetical accident drops and thermal loads. The inertial loads of significance for the basket analysis are those transverse to the cask and basket structure longitudinal axes, so that the loading from the fuel assemblies is applied normal to the basket plates and transferred to the cask wall by the basket. The inertial loading analysis is described in detail in Sections 4A.6.5 and 4A.6.6, below.

The effect of thermal loads on the fuel basket is evaluated by calculating the thermal expansion of the basket plates in comparison to the space available in the cask cavity to accommodate the thermal expansion. Drawing 971-006 shows the five different plate types (L1 - L5) which make up the basket structure. The dimensions shown are room temperature values. The maximum basket plate temperatures under hot conditions from Section 5.1.3.6 are used to calculate thermal expansion. The primary parameters used in this analysis and the resulting calculated minimum gaps are summarized in Table 4A.6-2. In all cases it is shown that sufficient gap exists between the plate ends and the cask cavity wall to permit free, unrestrained thermal expansion of the basket plates. Therefore, no thermally induced stresses need be included in the fuel basket analysis.

4A.6.5 Fuel Basket Plate Panel Analysis

An elastic-plastic structural analysis of the fuel basket is performed using the ANSYS computer program. The basket plate assembly is a redundant structure assembled from many similar interlocking plates. It is impractical to model even a single transverse slice or layer of basket plates using a three-dimensional finite element model with plate or shell elements. Therefore, the analysis of the TN-24 fuel basket is conducted by developing a frame model of a slice of one layer of basket plates. The elements used in the model to represent the plates are beams which vary in width since there are slots in the plates which reduce the width of the plates where they intersect. The plate panel spanning one compartment between the centers of intersecting plates is divided into a number of beam elements so that this variable width can be modeled properly. The two outer end beams are given the actual width of the plate at the slots, 8.08 in.

The central portion of the plate between slots is not fully effective in resisting normal loads because the overhanging tabs of material beyond the slots are cantilevered from the center region of the plate rather than supported at the ends. The equivalent width in this region is determined using two ANSYS finite element models: (1) a detailed 3D shell model of a plate panel, shown in Figure 4A.6-2, and (2) a simple beam model of the same plate panel, shown in Figure 4A.6-3. The two models are run for the same loads and boundary conditions. When the input value for the plate width, b, in the beam model is the actual value of 16.18 in., the stress, strain and displacement results are significantly less than those from the detailed shell model. The beam model plate width is varied until the results agree with those from the shell model. The effective width of plate, b, in Figure 4A.6-3, that satisfactorily reproduces the panel behavior determined from the shell model is found to be 75% of the actual plate width. Therefore, the width of the beam elements representing the unslotted portions of the plates in the frame model of the overall basket structure described below is 0.75 x 16.18 in. or 12.135 in.

4A.6.6 Fuel Basket Frame Analysis

4A.6.6.1 ANSYS Model

This section describes the nonlinear frame analysis performed for a load orientation perpendicular to the plates of the basket. Results are presented for a 3 g inertial loading due to the normal handling condition and for a 75 g loading due to the most severe accident condition. This 90 degree load orientation has been found (in analyses of previous designs) to be the critical orientation as stresses due to loadings at other angles are lower.

The frame model of the basket is comprised of STIF 23 two-dimensional beam elements. These elements properly model both the tensile and flexural stiffnesses of the basket plates. Two

different element widths are used; the actual plate width of 8.08 in. is used in the slotted regions and an equivalent width of 12.135 in. in the unslotted center regions. A typical frame compartment model with details of the beam span and real constants (section properties) is presented in Figure 4A.6-4.

Since the basket structure and the loading are symmetric, only one-half of the basket is modeled. Five nodes and four elements are used to define each of the horizontal and vertical plates that form the fuel compartments. In order to model the slotted connection at the intersections of the horizontal and vertical plates, two nodes (one in each plate) are used at each intersection. These two nodes have the same coordinates and are coupled in the X and Y directions, but their rotations are not coupled. The finite element model of the basket is shown in Figure 4A.6-5.

4A.6.6.2 Boundary Conditions, Loading and Assumptions

The boundary condition at each point of contact between the basket plates and the containment vessel cavity depends on the direction of the applied inertia load. As the basket is forced in a particular lateral direction, it separates from the cask wall on one side and reacts against the wall on the other side. At the locations where the basket loses contact with the wall, no restraint or support is provided in the model. For vertical inertial loading on a horizontal cask and basket, contact is lost between the basket and cask wall at the top half of the structure except at the rails which provide local vertical support to the horizontal plates and horizontal support to the vertical plates. In the bottom half of the model, the rails also provide support to the vertical plates in the vertical direction. The boundary conditions are shown on Figure 4A.6-6.

The maximum transverse containment vessel and basket decelerations for the normal handling and accident conditions are 3 g and 75 g, respectively. The inertial loads applied to the plate panels as the plates deflect away from the fuel assemblies shift to the outer slotted portions of the panels. Therefore, the loading is assumed to vary linearly from the edges of each panel to the center as represented by the triangular transverse loading shown on Figure 4A.6-7. A nonlinear iterative analysis of the basket frame model is performed since the basket structure is redundant and the support is indeterminant without considering deflections. The total load is applied in small steps, and an actual increasing load history is followed. During each of the steps sufficient iterations are allowed for proper convergence.

4A.6.6.3 Results

The maximum stresses, strains, and deflections at the slotted and central basket plate regions are summarized for the two loading cases in Table 4A.6-3. The maximum stresses for the normal handling and accident conditions are presented in Figures 4A.6-8 to 11.

Based on the results of this analysis, it is concluded that:

1. The maximum stresses, both in the slotted (4,380 psi) and central (2,970 psi) regions of the plates, are below the material yield strength (25,840 psi) during the 3 g normal handling condition.

2. During the accident (drop) condition, the maximum stress in the slotted region for 75 g is 47,700 psi and in the central region of the plate is 39,500 psi. Both of these stresses are below the allowable stress ($0.9 \times S_u$ = 67,312 psi). The maximum strain of 0.0927 in/in. occurs at the slot and is less than the criteria which is 0.100 (i.e. 0.5 x 20% strain). It should be noted that these high strains and stresses are at the surface of the plates and are much lower through the thickness (See Figs. 4A.6-10 and 4A.6-11). Also, the allowable values of stress are taken at 650°F and the plates with the highest stresses are at the periphery where temperatures are lower.

3. The maximum deflections occur in plates at the periphery of the basket. Deflection in plates in the remainder of the basket are considerably less. The plates deflect in the same direction therefore the relative spacing between fuel assemblies remains approximately the same.

4. The basket plate is structurally adequate under these loads. The plates will remain in place and maintain separation of adjacent fuel assemblies.

TABLE 4A.6-1

MATERIAL PROPERTIES FOR TN-24 BASKET

Temperature (°F)	Ultimate Strength (psi)		Yield Strength (psi)		Modulus of Elasticity (psi x 10^6)		Thermal Expansion in./in./° F	Poisson's Ration
	1.0% Borated SS	304 SS	1.0% Borated SS	304 SS	1.0% Borated SS	304 SS	1.0% Borated SS	
75	92,500	70,000	42,500	25,000	31.94	28.3	8.71×10^{-6}	0.2
212	-	-	-	21,000	31.1*	27.5	8.71×10^{-6}	0.306
650	74,792	56,600	25,840	15,200	28.3*	25.05	9.28×10^{-6}	0.306

* Extrapolated Value

NOTE: The extrapolated values in the above table, are based on the assumption that the variation of the 1.0% borated S.S. properties with temperature is the same as that for 304 S.S.

TABLE 4A.6-2

BASKET PLATE THERMAL EXPANSION CALCULATION SUMMARY

PLATE NO.	BASKET PLATE LENGTH AT ROOM TEMP (in)	BASKET PLATE AVG. TEMP (°F)	BASKET PLATE LENGTH AT TEMP (in.)	CAVITY DIMENSION AVAILABLE AT TEMP (in)	CLEARANCE AT EACH END AT TEMP (in)
L-1	62.00	498	62.246	62.25	0.002
L-2	58.71	566	58.98	60.316	0.668
L-3	45.00	490	45.175	45.35	0.088
L-4	18.75	424	18.81	24.9	3.04
L-5	43.30	556	43.395	59.22	7.91

TABLE 4A.6-3

SUMMARY OF STRESSES, STRAINS AND DEFLECTIONS

LOADING	STRESS/STRAIN/DEFLECTION TYPE	MAGNITUDE	ALLOWABLES	MARGIN OF SAFETY
NORMAL HANDLING CONDITION (3G)	MEMBRANE (Slot)	830 (psi)	17312 (psi)	19.85
	MEMBRANE PLUS BENDING (Slot)	4380 (psi)	25840 (psi)	4.89
	MAX. STRAIN (Slot)	0.000156 (in/in)	0.100 (in/in)	large
	MEMBRANE (Center)	0	17312	large
	MEMBRANE PLUS BENDING (Center)	2970 (psi)	25840 (psi)	7.7
	MAX. STRAIN (Center)	0.000105 (in/in)	0.100 (in/in)	large
	MAX. DEFLECTION (Center)	0.0052 (in)		
ACCIDENT CONDITION (75G)	MEMBRANE (Slot)	35100 (psi)	52354 (psi)	0.49
	MEMBRANE PLUS BENDING (Slot)	47700 (psi)	67312 (psi)	0.41
	MAX. STRAIN (Slot)	0.0927 (in/in)	0.100 (in/in)	0.08
	MEMBRANE (Center)	11250 (psi)	52354 (psi)	3.65
	MEMBRANE PLUS BENDING (Center)	39500 (psi)	67312 (psi)	0.7
	MAX. STRAIN (Center)	0.046 (in/in)	0.100 (in/in)	1.17
	MAX. DEFLECTION (Center)	1.219 (in)		

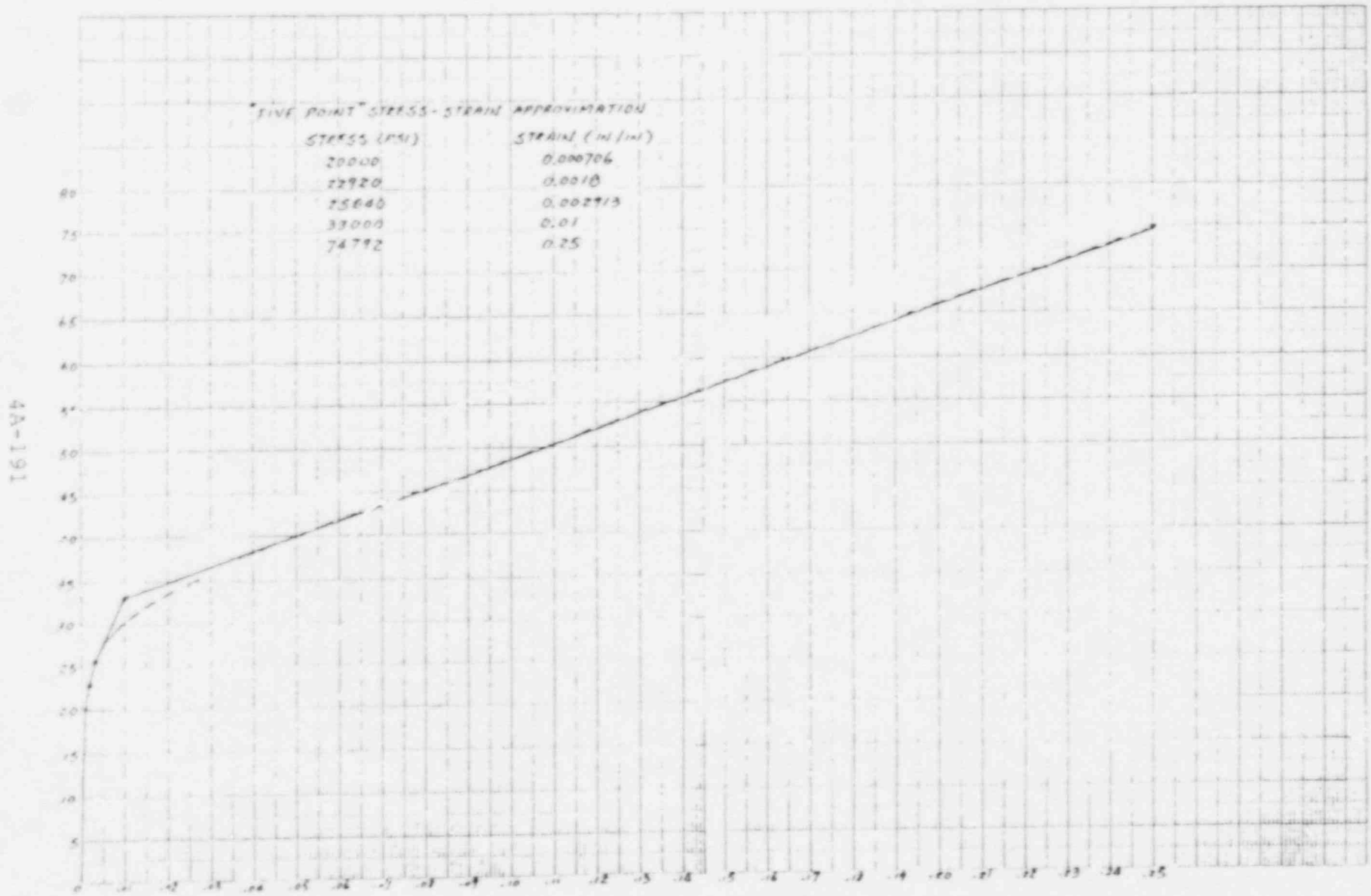

FIGURE 4A.6-1

STRESS-STRAIN CURVE FOR 1.0% BORATED STAINLESS STEEL AT 650°F

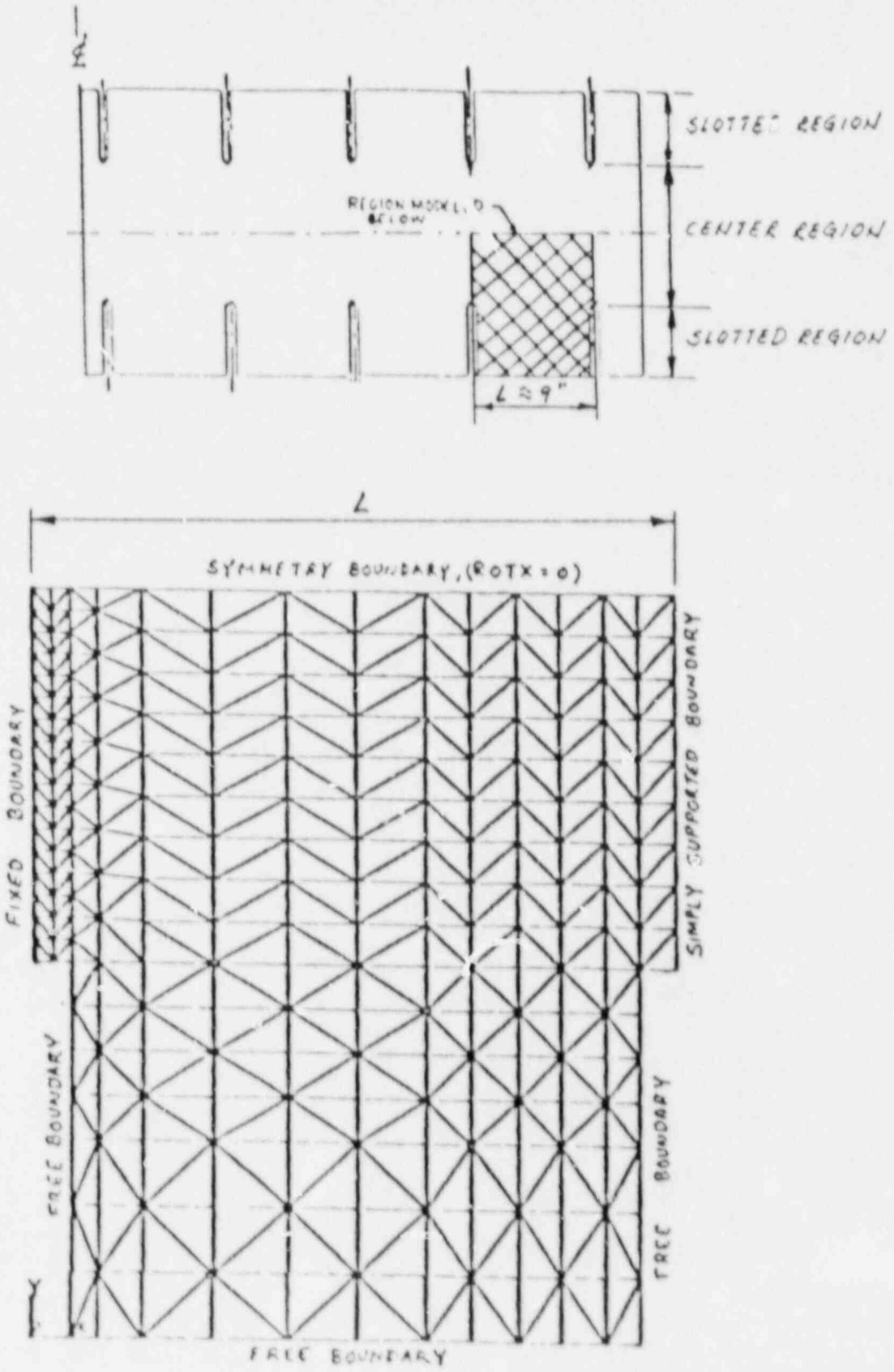

FIGURE 4A.6-2

TN - 24 FUEL BASKET PLATE SHELL MODEL

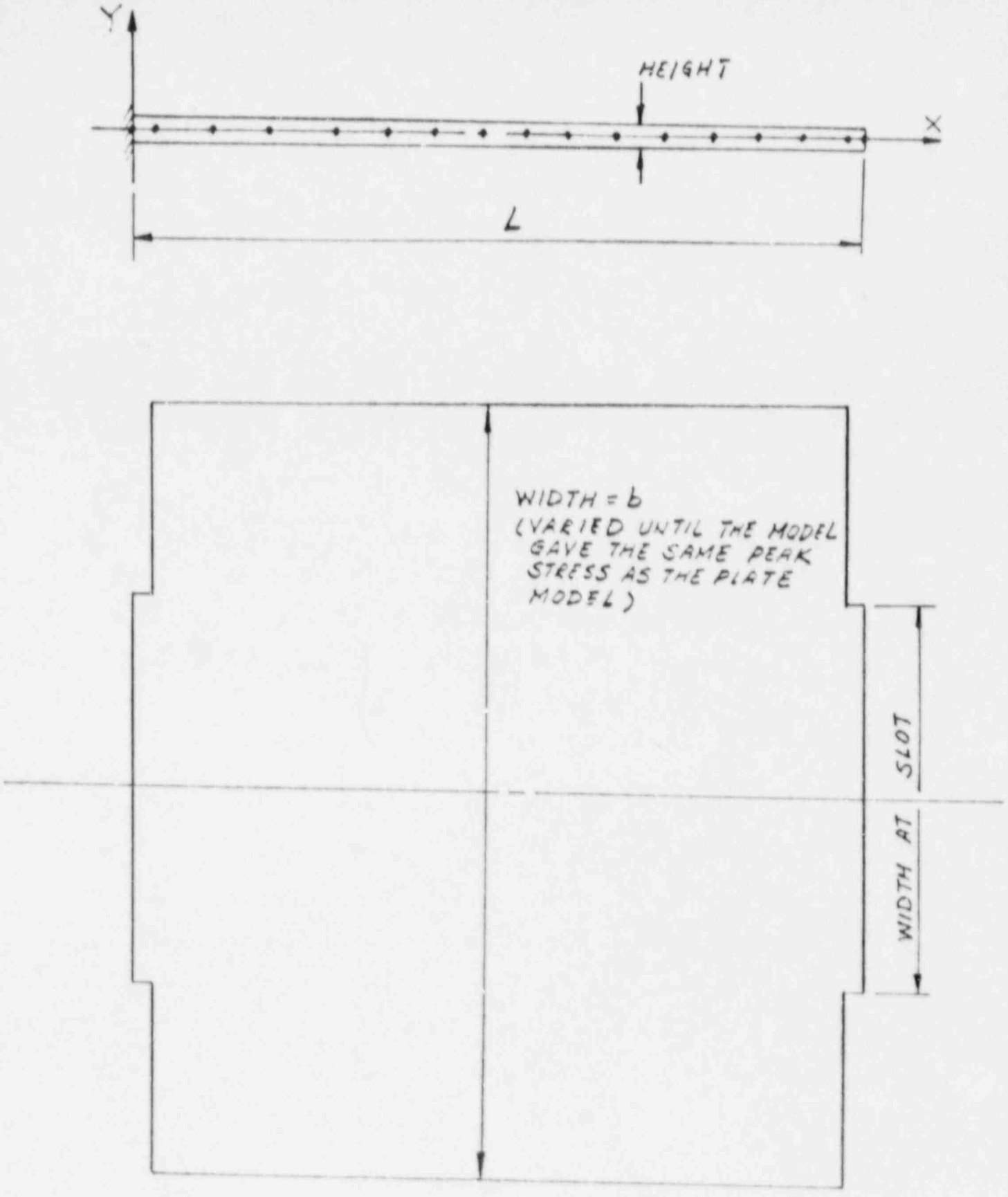

FIGURE 4A.6-3

TN-24 FUEL BASKET PLATE
EQUIVALENT BEAM MODEL

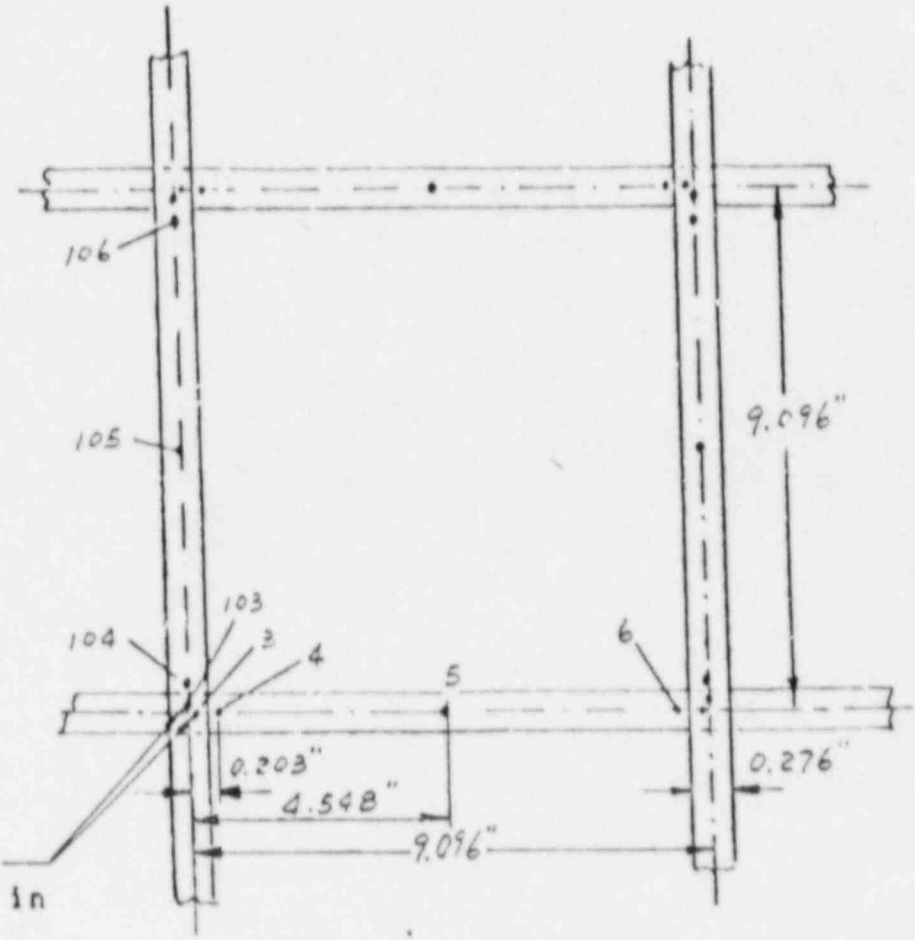

These are coincident nodes and are coupled in x and y directions. Coupling provides pin joint between interlocking plates.

Slot Elements (between nodes 3 and 4 or 103 and 104)

Area = $8.08 \times 0.276 = 2.23\ IN^2$

Moment of Inertia = $\frac{8.08 \times (0.276)^3}{12} = 0.01415\ IN^4$

Middle Section Elements (between nodes 4 and 5 or 5 and 6)

Area = $12.135 \times 0.276 = 3.35\ IN^2$

Moment of Inertia = $\frac{12.135 \times (0.276)^3}{12} = 0.02126\ IN^4$

FIGURE 4A.6-4

FRAME MODEL COMPARTMENT DETAIL

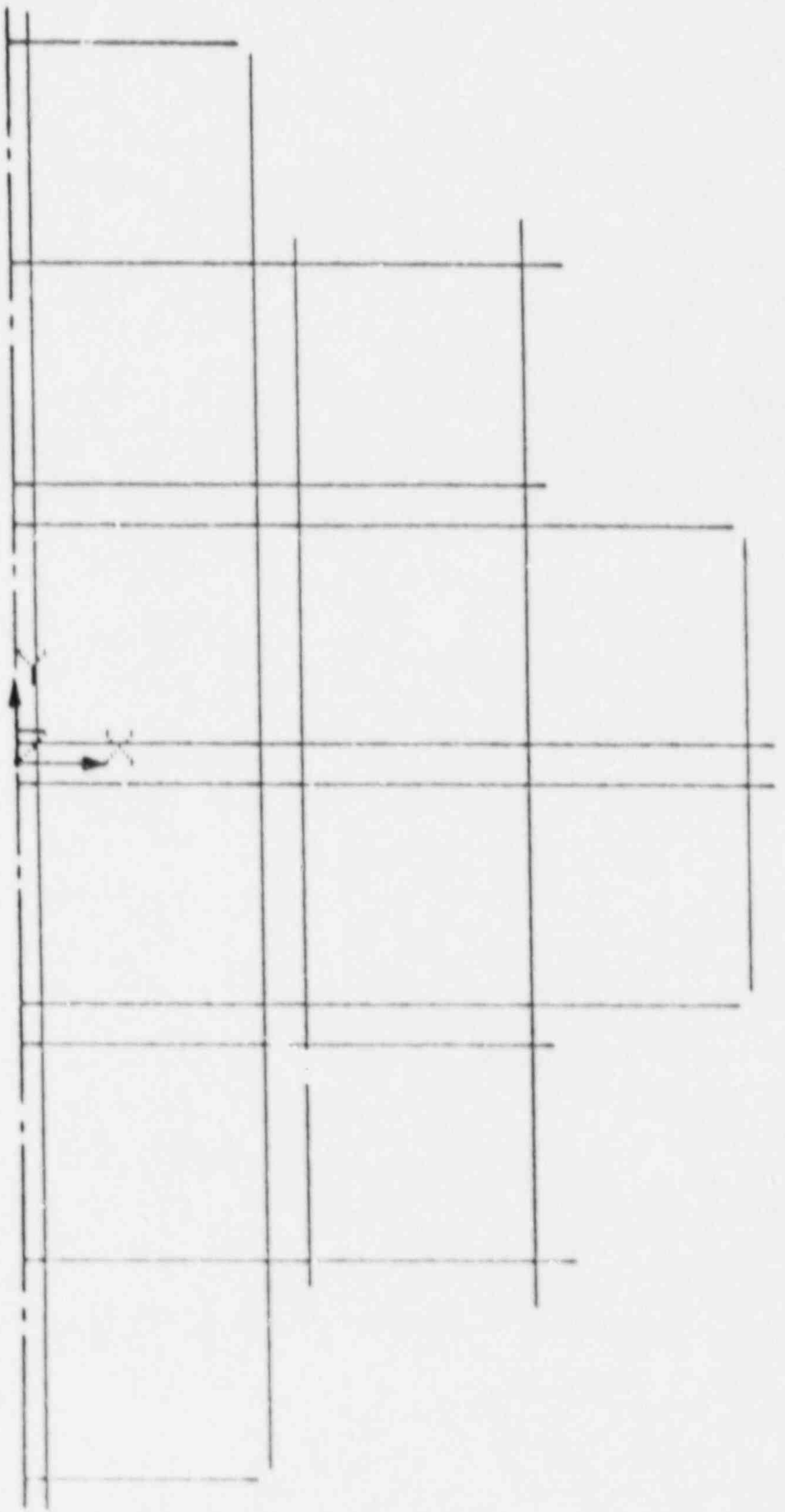

FIGURE 4A.6-5

TN-24 FUEL BASKET FRAME MODEL

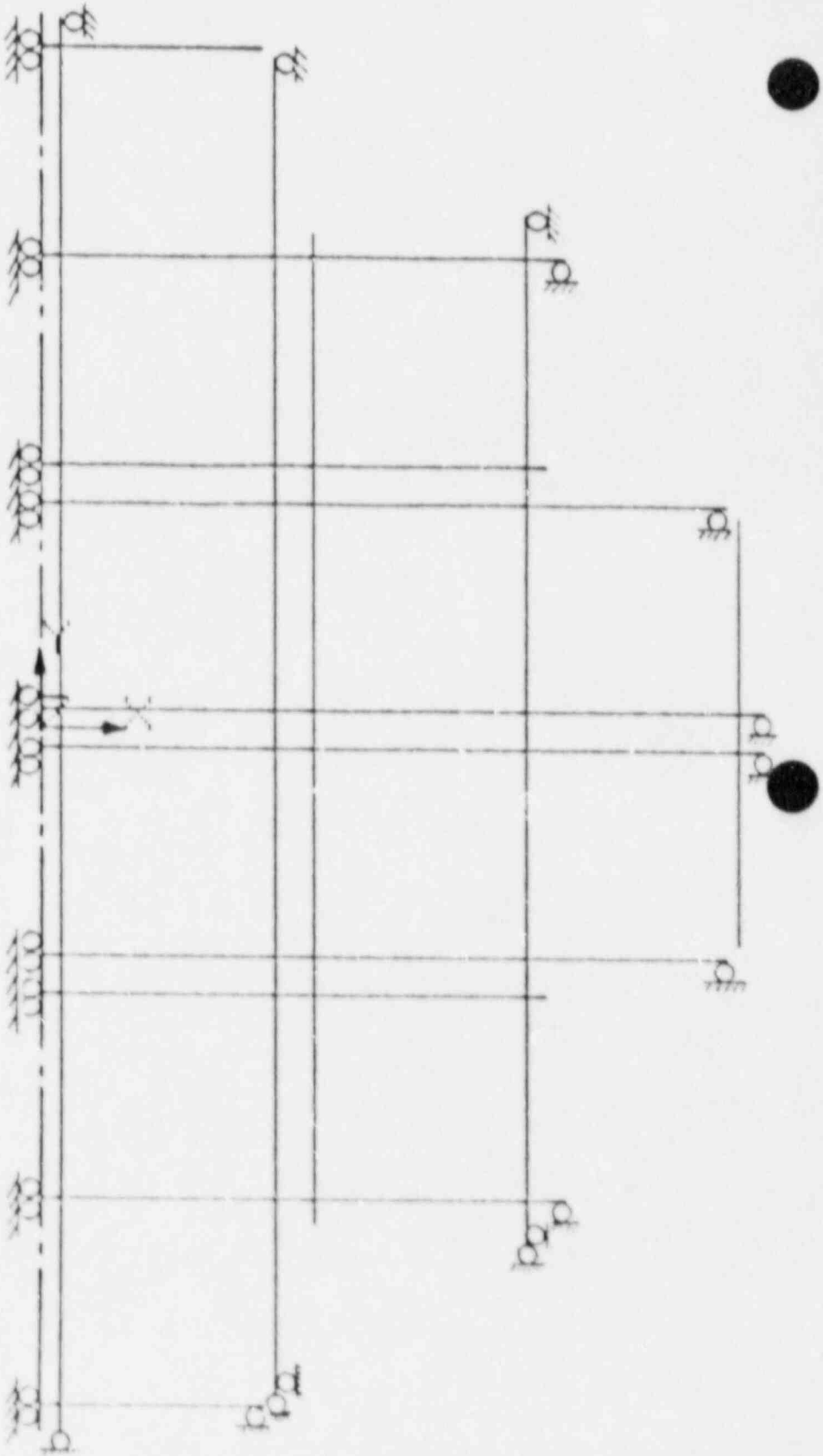

FIGURE 4A.6-6

BOUNDARY CONDITIONS

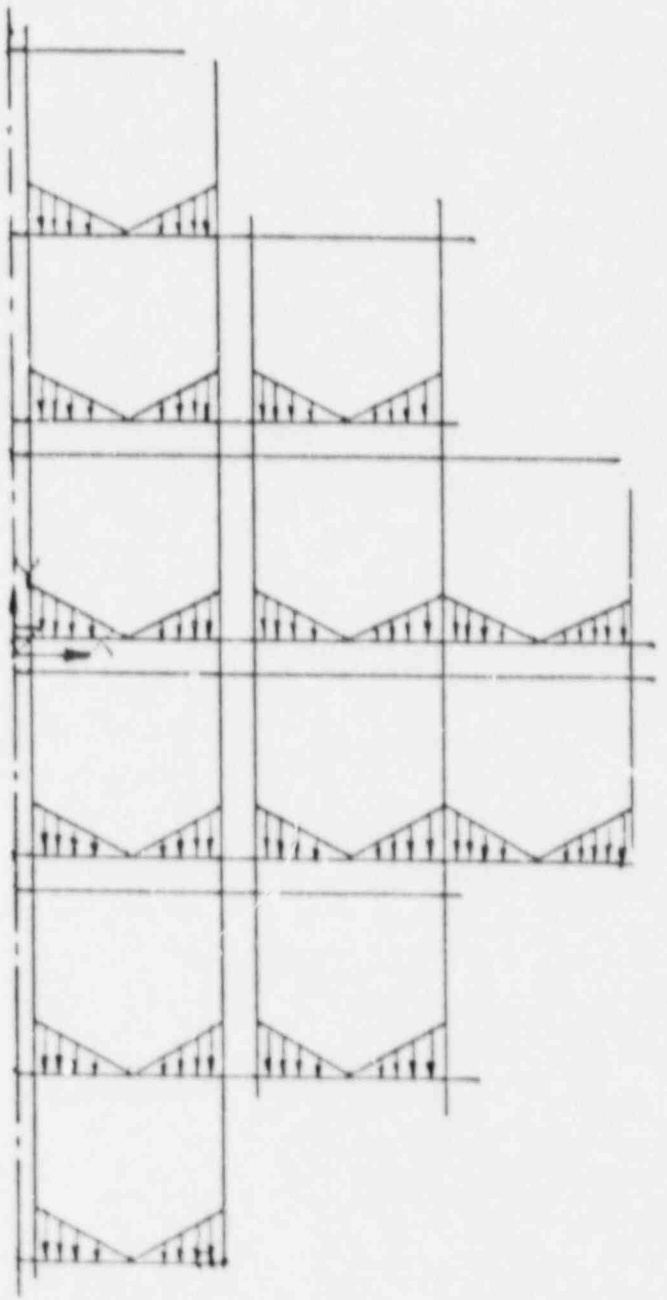

FIGURE 4A.6-7

LOAD DISTRIBUTION

NOTE:

1. Numbers in circle are stresses in Ksi. Upper number is maximum surface stresses, $P_m + P_b$. Lower number is membrane stresses, P_m.

2. The maximum stress is shown by *.

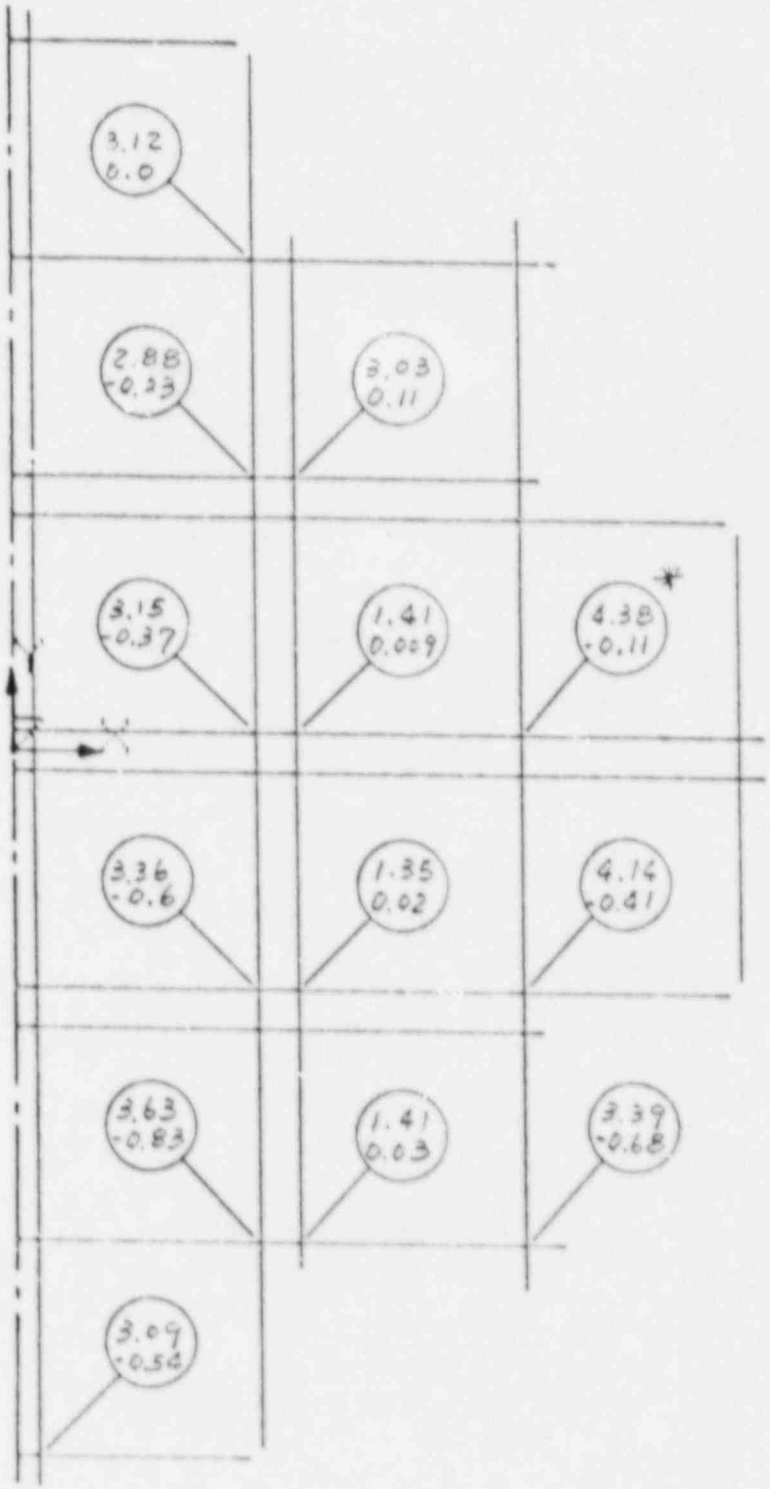

FIGURE 4A.6-8

PLATE SLOT REGION STRESSES (3C)

NOTE:

1. Numbers in circle are stresses in Ksi. Upper number is maximum surface stresses, $P_m + P_b$. Lower number is membrane stresses, P_m.

2. The maximum stress is shown by *.

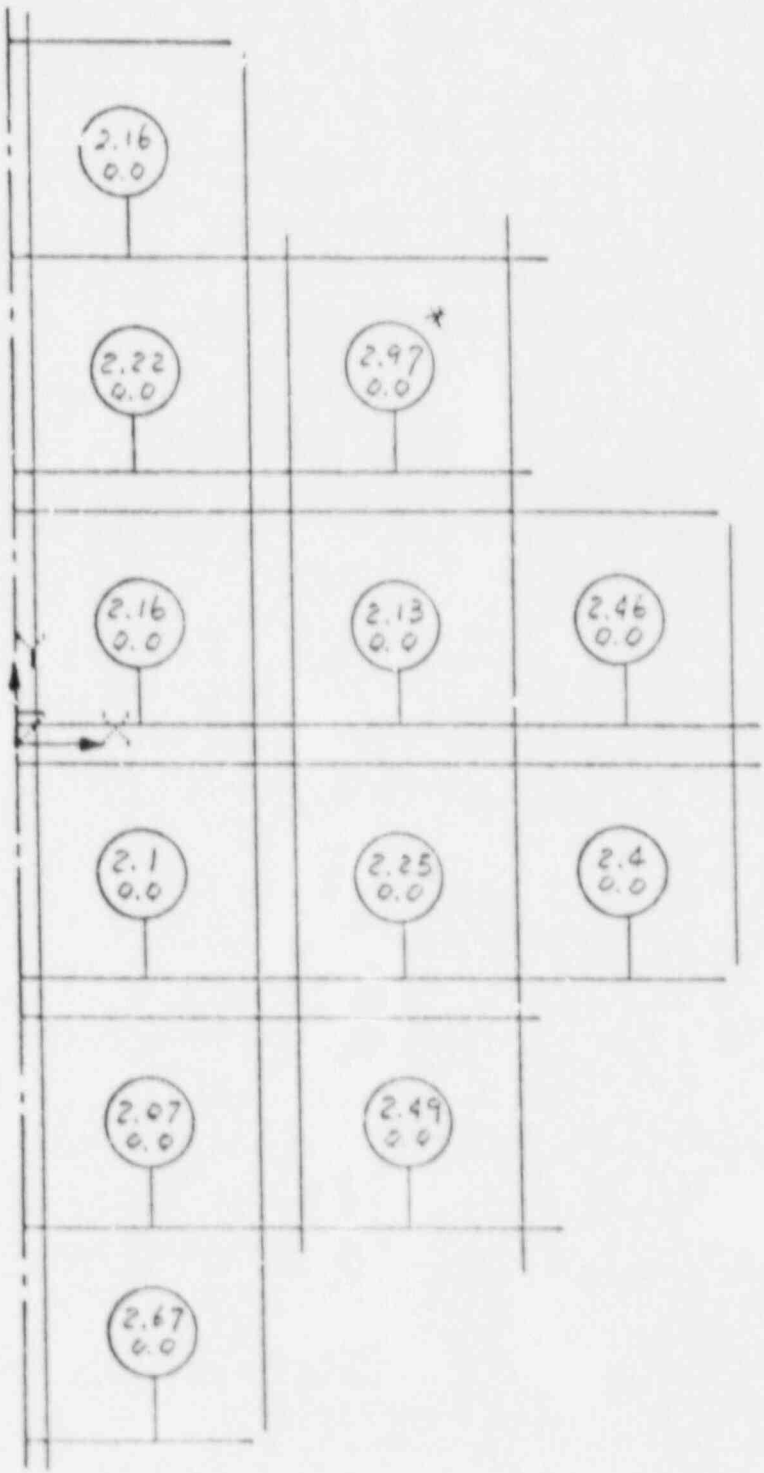

FIGURE 4A.6-9

PLATE CENTER REGION STRESSES (3G)

NOTE:

1. Numbers in circle are stresses in Ksi. Upper number is maximum surface stresses, $P_m + P_b$. Lower number is membrane stresses, P_m.

2. The maximum stress is shown by *.

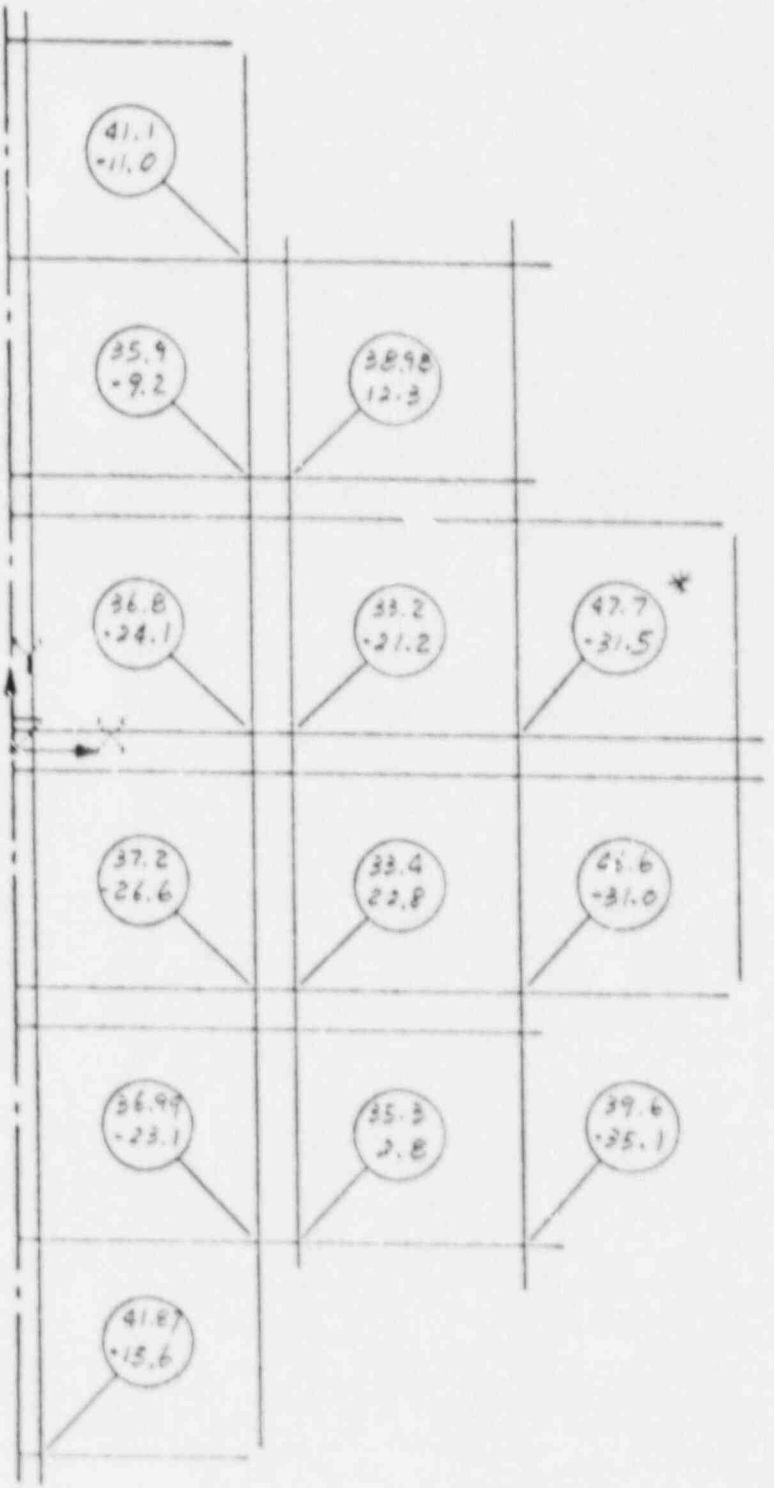

FIGURE 4A.6-10

PLATE SLOT REGION STRESSES (75°)

NOTE:

1. Numbers in circle are stresses in Ksi. Upper number is maximum surface stresses, $P_m + P_b$. Lower number is membrane stresses, P_m.

2. The maximum stress is shown by *.

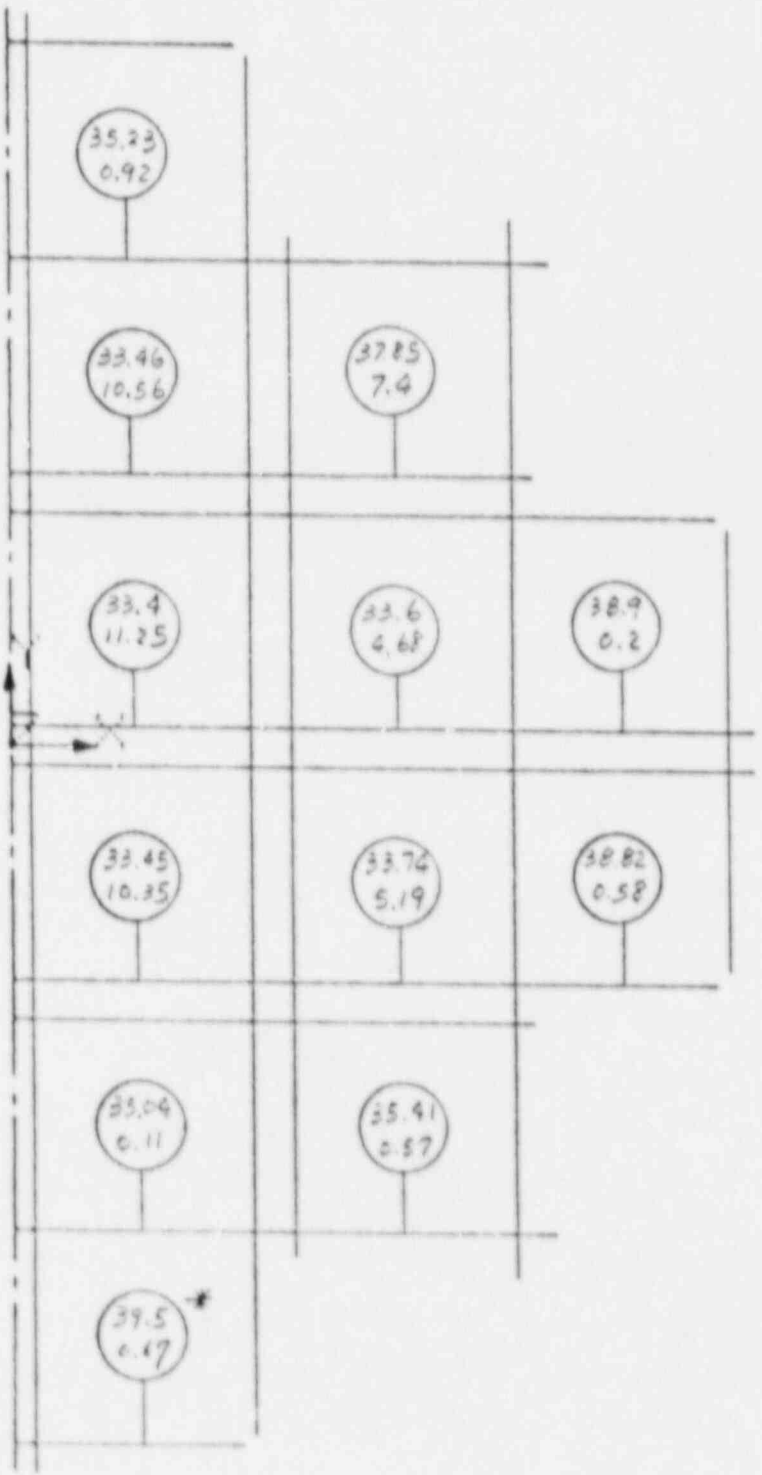

FIGURE 4A.E-11
PLATE CENTER REGION STRESSES (75G)

4A.7 STRUCTURAL ANALYSIS OF THE TRUNNIONS

This section presents the structural analysis of the trunnions of the TN-24 storage cask. The trunnions consist of an outer and inner shoulder, a flange and bolts for attachment to the containment vessel. The loads acting on the trunnions occur during normal handling operations. The trunnion structural analyses include the calculation of attachment bolt stresses, trunnion shoulder and flange stresses, and contact bearing pressure and friction forces at the flange-vessel interface. These stresses are compared to the allowable stress limits of Section 4.2 to assure that the design criteria are met.

4A.7.1 Description

The trunnions (Fig. 4A.7-1) are stainless steel forgings bolted to the outer surface of the containment vessel with twelve 1 1/2 inch diameter bolts on a 12.6 inch diameter bolt circle. The forging and bolt materials were selected for their high strength. A 50,000 psi bolt preload is used.

The trunnions are recessed slightly into the cask body. However, it is assumed that the transverse shear load is transferred from the trunnions to the cask body at the interface by friction.

The trunnion shoulders are designed as hollow cylinders to minimize the inertia g loads that occur during impact since the trunnions punch holes in the concrete foundation. The impact load is based on the crushing strength of the concrete and the trunnion section area.

4A.7.2 Materials Input Data

The trunnions are fabricated from SA-564 Type 630, Condition H 1150 material. The material property data is taken from the Section III, Appendices[2] of the ASME Boiler and Pressure Vessel Code. The yield strength of the material is taken at room temperature and 300°F.

4A.7.3 Applied Loads

The handling loads acting on the trunnions occur during lifting, tilting and transfer operations. The trunnions are designed for a factor of three against yielding and a factor of five against the material ultimate strength as specified by ANSI N14.6[13].

The most severe loads on the trunnions occur for the vertical lift which results in the following loads based on three and five times the fully loaded weight. These loads are applied at the midlength of the outer shoulder as shown in Fig. 4A.7-1. The fully loaded weight of the packaging used for the analysis, (including water), is 225,481 lb. The vertical lift is performed with one set of trunnions. Therefore:

$$F_L = \frac{3 \times 225,481}{2} = 338,222 \text{ lb/Trunnion}$$

or

$$F_L = \frac{5 \times 225,481}{2} = 563,703 \text{ lb/Trunnion}$$

The bending moments and stresses acting at the base of the trunnion shoulders are given in Table 4A.7-1. The key results at the trunnion flange-cask body interface are listed in Table 4A.7-2. Yield and ultimate criteria are met everywhere at both room temperature and 300°F.

A handling load case of 1.5 times the weight is also considered. The bolt preload is selected so that under this loading the flange does not lose contact bearing pressure with the cask body. This requires a bolt prestress of 50,000 psi.

4A.7.4 Method of Analysis

4A.7.4.1 Trunnion Shoulders

The trunnion support shoulders are analyzed as cantilevered beams. The trunnion shoulders are concentric hollow cylinders which are considered fixed at their base, i.e., the outer shoulder is fixed to the inner shoulder and the inner shoulder is fixed to the flange. Under some loading conditions, a loss of local contact between the trunnion flange and the cask body occurs and the contact bearing pressure locally is zero. However, the bending moments and shear loads on the hollow shoulder cylinders do not increase or decrease as a result of this effect.

The maximum bending stress, shear stress and combined stress intensities are calculated at the base of each hollow cylinder for the applied loads. The shear stress, τ, is calculated using the following equation:

$$\tau = \frac{V}{A} = \frac{F_L}{\frac{\pi}{4}(D_o^{\,2} - D_i^{\,2})}$$

Where V = The shear force = F_L

D_i, D_o = Inside and outside shoulder diameters at Section A-A or B-B

The bending stress, σ_B, is calculated using the following equation:

$$\sigma_B = \frac{MC}{I} = \frac{M \times D_O/2}{\frac{\pi}{64}(D_O^4 - D_i^4)}$$

Where M = bending moment at section A-A or B-B

The stress intensity, S, is calculated using the following equation:

$$S = \sigma_B^2 + 4\tau^2$$

4A.7.4.2 Trunnion Flange

The maximum bending and shear stresses in the trunnion flange occur in the region outside of the shoulder diameter, i.e., at a distance $r \geq 3.94$ in. from the centerline of the trunnions. For $r < 3.94$ in. the reinforcing effect of the shoulder reduces the bending and shear stresses in the flange (Fig. 4A.7-1).

The free body diagram of Fig. 4A.7-2 shows the forces acting on the flange:

1) The applied moment M_A
2) The bolt preload σ_b
3) The max. and min. bearing pressure $(\sigma_{br})_{Max}$ and $(\sigma_{br})_{Min}$

The bolt preload causes an average bearing pressure of:

$$\sigma_{br} = \frac{4NA_b}{\pi D^2} \sigma_B$$

Where:

σ_B = bolt stress due to the preload
N = number of bolts
A_b = bolt stress area
D = outer diameter of flange

When the moment, M_A, is applied, if there is no loss of contact, the bolt stress, σ_B, does not change, but the bearing pressure varies from a maximum to a minimum:

$$(\sigma_{br})_{Max} = \frac{4NA_b\sigma_B}{\pi D^2} + \frac{32\ M_A}{\pi D^3}$$

$$(\sigma_{br})_{Min} = \frac{4NA_b\sigma_B}{\pi D^2} - \frac{32\ M_A}{\pi D^3}$$

Loss of contact will not occur if $(\sigma_{br})_{Min} > 0$ or if:

$$\sigma_B > \frac{8\ M_A}{NA_bD}$$

For σ_B = 50000 psi, the maximum moment that can be applied without loss of contact is:

$$M_A < \frac{50000 \times 12 \times 1.492 \times 15.75}{8} = 1,762,425 \text{ in-lb}$$

Hence, in both the 3 g and 5 g cases some loss of contact will occur. The bending moment, M, and the shear force, V, acting on the flange cross section at a distance $x \geq 3.94$ in. from the flange centerline consist of the sum of three pairs of components: the first, M_1 and V_1, are due to the bearing pressure; the second, M_2 and V_2, are due to the bolt loads; and the third, M_3 and V_3 are due to the applied moment. The net moment and shear force can be calculated by conservatively summing the force and moment sets shown on the free body diagram, Fig. 4A.7-2 and/or 4A.7-3. At Section x the bending and shear stresses in the flange are then calculated:

$$\sigma = \frac{MC}{I} = \frac{6(M_1 + M_2 + M_3)}{2\left[\left(\frac{D}{2}\right)^2 - x^2\right]^{1/2} t_f^2} \qquad x \geq 3.94 \text{ in.}$$

$$\tau = \frac{V}{A} = \frac{(V_1 + V_2 + V_3)}{2\left[\left(\frac{D}{2}\right)^2 - x^2\right]^{1/2} t_f}$$

The maximum stress in the flange occurs at Section C-C in Fig. 4A.7-4. An upper limit of this stress can be obtained by conservatively assuming that the resultant trunnion/vessel bearing force, V, is concentrated at point C and determining the moment about Section C-C due to V.

The combined stress intensity in the flange is then:

$$\sigma = \sigma_b^2 + 4\tau^2$$

4A.7.4.3 Trunnion Bolts

Twelve 1.5 inch diameter bolts attach the trunnions to the cask. Trunnion bolt stresses result from preload, residual torque, bending and shear.

The bolts are preloaded to 50,000 psi.

The residual preload torsional shear stress is:

$\tau_R = T_R r/J = 23,787$ psi

Where T_R = the residual torque

$= .5625 (.2D\sigma_B A_B) = 12,589$ in lb

A_B = bolt area = 1.492 sq. in.

σ_B = preload stress = 50000 psi

D = nominal bolt diameter, 1.5 in.

J = .3964 $in.^4$

r = .75 in.

The loads due to lifting result in a bending moment and shear load at the flange-cask interface. The maximum bending moment is $7.67F_L$ where F_L is the applied load. The bending moments for the various load cases are given in Table 4A.7-2.

The applied bending moment is reacted by the bolts and the bearing pressure at the interface between the flange and cask body as shown in Fig. 4A.7-3. The upper limit of the bearing pressure at the cask body-flange interface is the yield value of the cask body material (σ_y = 37,500 psi). Using this upper limit for the bearing pressure with a linear variation as shown in Fig. 4A.7-3, the resultant bearing force is located near point D indicated on Figure 4A.7-4. Taking point D as the pivot point and equating the moment of the bolt forces about D to the applied moment, M_A, yields: (Fig. 4A.7-4)

Bolt Force	Distance from D	Moment About D
$F_o = F_B$	$2r$	$2rF_o$
$F_1 = F_B \frac{r + r\cos\theta}{2r}$	$(r + r\cos\theta)$	$(r + r\cos\theta) F_1$
$F_2 = F_B \frac{r + r\cos 2\theta}{2r}$	$(r + r\cos 2\theta)$	$(r + r\cos 2\theta) F_2$
$F_5 = F_B \frac{r + r\cos 5\theta}{2r}$	$(r + r\cos 5\theta)$	$(r + r\cos 5\theta) F_5$

Or in terms of the load in the highest loaded bolt:

$$M_A = \frac{F_B}{2r}\left[(2r)^2 + 2\sum_{n=1}^{5}(r + r\cos n\theta)^2\right] = 56.70\ F_B$$

The maximum force in the bolt is:

$$F_B = \frac{M_A}{56.70}$$

And the stress is:

$$\sigma_B = \frac{F_B}{A_b}$$

For the 1.5 W and 3.0 W load cases the maximum tensile stress does not exceed the preload stress. Therefore the maximum bolt tensile stress is the preload.

The bolt tensile stresses thus calculated are reported in Table 4A.7-2.

The shear load at the flange-cask interface is equal to the lifting load. Part of this shear load is transferred to the cask by friction and the remainder is taken by the bolts. The frictional force that can be developed between the flange and vessel wall is:

$$V_f = \mu N A_B \sigma_B$$

Where μ = coefficient of friction between flange and vessel wall, .45
N = number of bolts
A_B = bolt area, sq. in.
σ_B = average bolt stress, psi

For the 1.5 W and 3.0 W cases, V_f exceeds the applied shear load, and the bolts are not loaded in shear. For the 5.0 W case, the frictional force, V_f is 403.6 kips, but the applied load is 563.7 kips. The remaining shear load is taken by the bolts. The shear stress in the bolts to react the applied load is:

$$\tau_B = \frac{563,700 - 403,600}{12 A_{SH}} = 7550 \text{ psi}$$

Where A_{SH} is the shoulder area, 1.767 in.^{2}

The maximum stress intensity in the bolts is:

$$S = \sqrt{\sigma_B^2 + 4 (\tau_B + \tau_R)^2}$$

The maximum bearing pressure on the cask body is:

$$(\sigma_{br})_{max} = \frac{4 N A_b \sigma_B}{\pi D^2} + \frac{32 M_B}{\pi D^3}$$

For the 5 W load case, the maximum bearing pressure is the yield strength of the cask material, 37,500 psi.

4A.7.5 Analysis Results

4A.7.5.1 Trunnion Shoulders

The maximum shear, bending stress and stress intensities at the base of the outer (Section A-A) and inner (Section B-B) shoulders of the trunnions are shown in Table 4A.7-1. For all loads the stress intensities are less than the allowable stresses.

4A.7.5.2 Trunnion Flange and Bolts

The loads acting on the trunnion flange and bolts are translated into a force and a moment acting on the flange. The analysis methods described above are used to evaluate the maximum friction force that will be transmitted across the flange/cask interface, the bearing stress at the flange/cask body interface, and the bolt stress, the bending stress in the flange, the shear stress in the flange, and the resulting stress intensity. The results are tabulated in Table 4A.7-2.

TABLE 4A.7-1

SUMMARY OF STRESSES IN TRUNNION SHOULDERS

Condition	Lifting (3xW)		Lifting (5xW)	
	Section		Section	
Quantity	A-A	B-B	A-A	B-B
Lifting Load F_L, kips (1)	338.2	338.2	563.7	563.7
Bending Moment, kip-in (1)	467	1397	778	2328
Bending Stress, ksi	26.26	30.26	43.77	50.43
Shear Stress, ksi	19.0	8.6	31.7	14.4
Combined Stress Intensity, ksi	46.2	34.9	77.0	58.0
Allowable Stress, ksi — At 300°F	Yield = 93		Ult. = 135	
Allowable Stress, ksi — At R. T.	Yield = 105		Ult. = 135	

(1) The values used in the analysis are slightly larger than those listed in Chapter 3.0, Table 3.2-5.

TABLE 4A.7-2

SUMMARY OF STRESSES IN FLANGE AND BOLTS

ITEM	Inertia Loads Due to Lifting 1.5 x W	3 x W	5 x W
Load, kips	169.1	338.2	563.7
Bending Moment, kip-in	1297	2594	4324
Friction Force, kips	402.8	402.8	403.6
Bearing Pressure On Cask Body, ksi	7.98	11.36	37.50
Bolt Preload, ksi	50	50	50
Bolt Tensile Stress, ksi	50	50	51.1
Bolt Twisting Stress, ksi	23.79	23.79	23.79
Bolt Shear Stress, ksi	--	--	7.55
Bolt Stress Intensity, ksi	69.02	69.02	80.87
Allowable Bolt Stress, ksi	95.7	95.7	114.0
Flange Max. Bending Stress, ksi	15.9	31.7	52.8
Shear Max. Shear Stress, ksi	3.5	7.0	11.7
Flange Stress Intensity, ksi	17.33	34.67	57.77
Allowable Flange Stress, ksi	93	93	135

FIGURE 4A.7-1

BOLTED TRUNNION

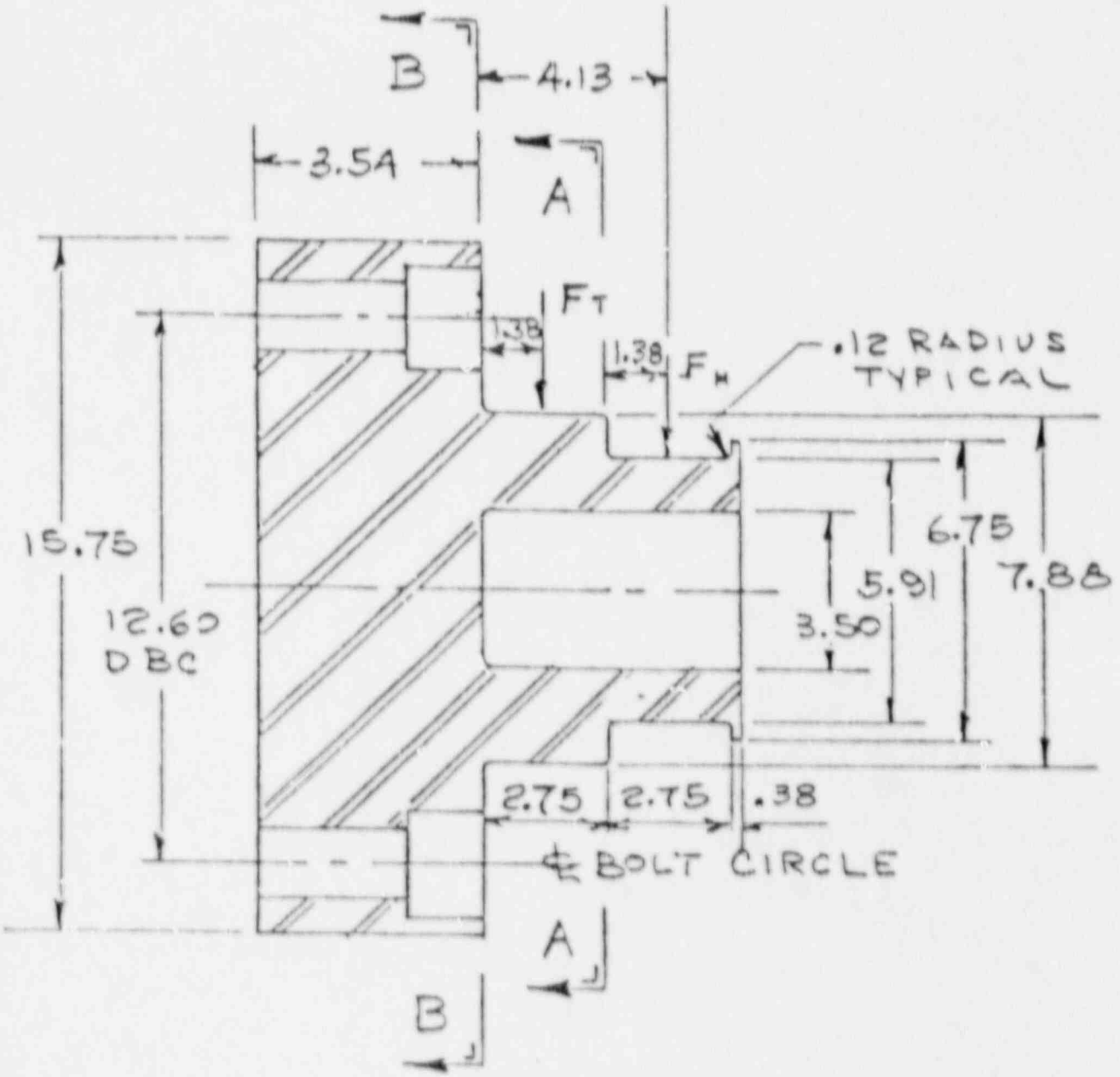

FIGURE 4A.7-2

FREE BODY DIAGRAM
NO LOSS OF CONTACT BEARING PRESSURE

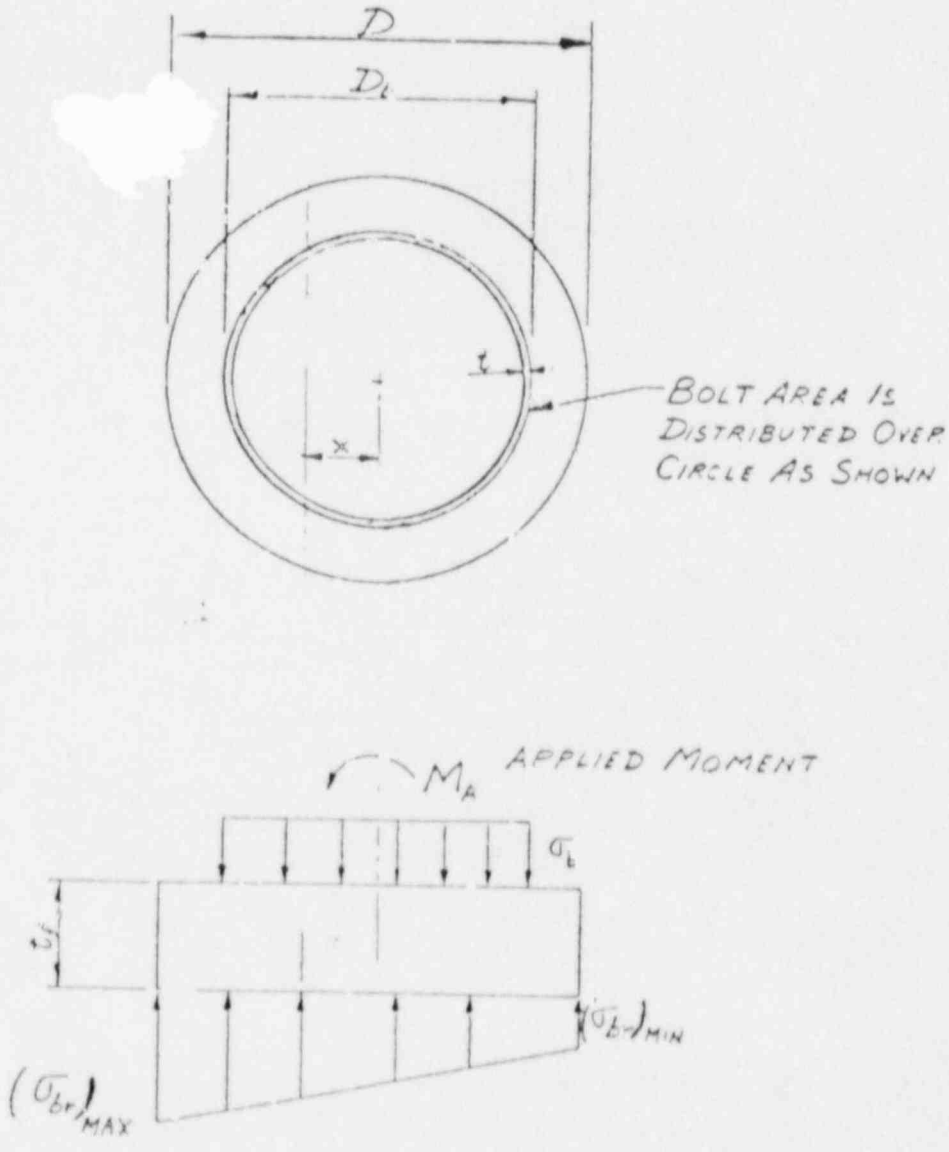

FIGURE 4A.7-3

LOCAL LOSS OF CONTACT BEARING PRESSURE

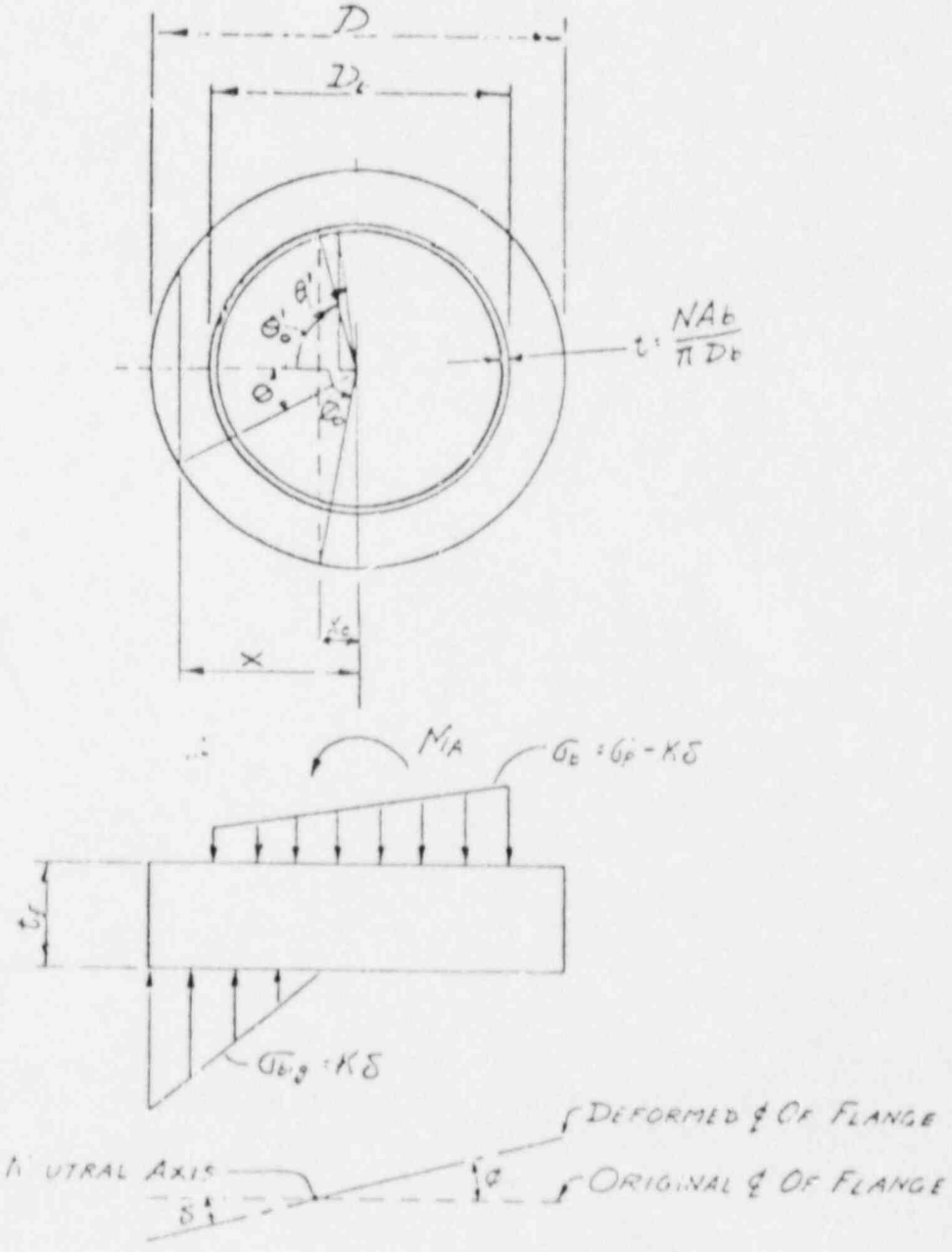

FIGURE 4A.7-4

TRUNNION BOLTS - MOMENTS

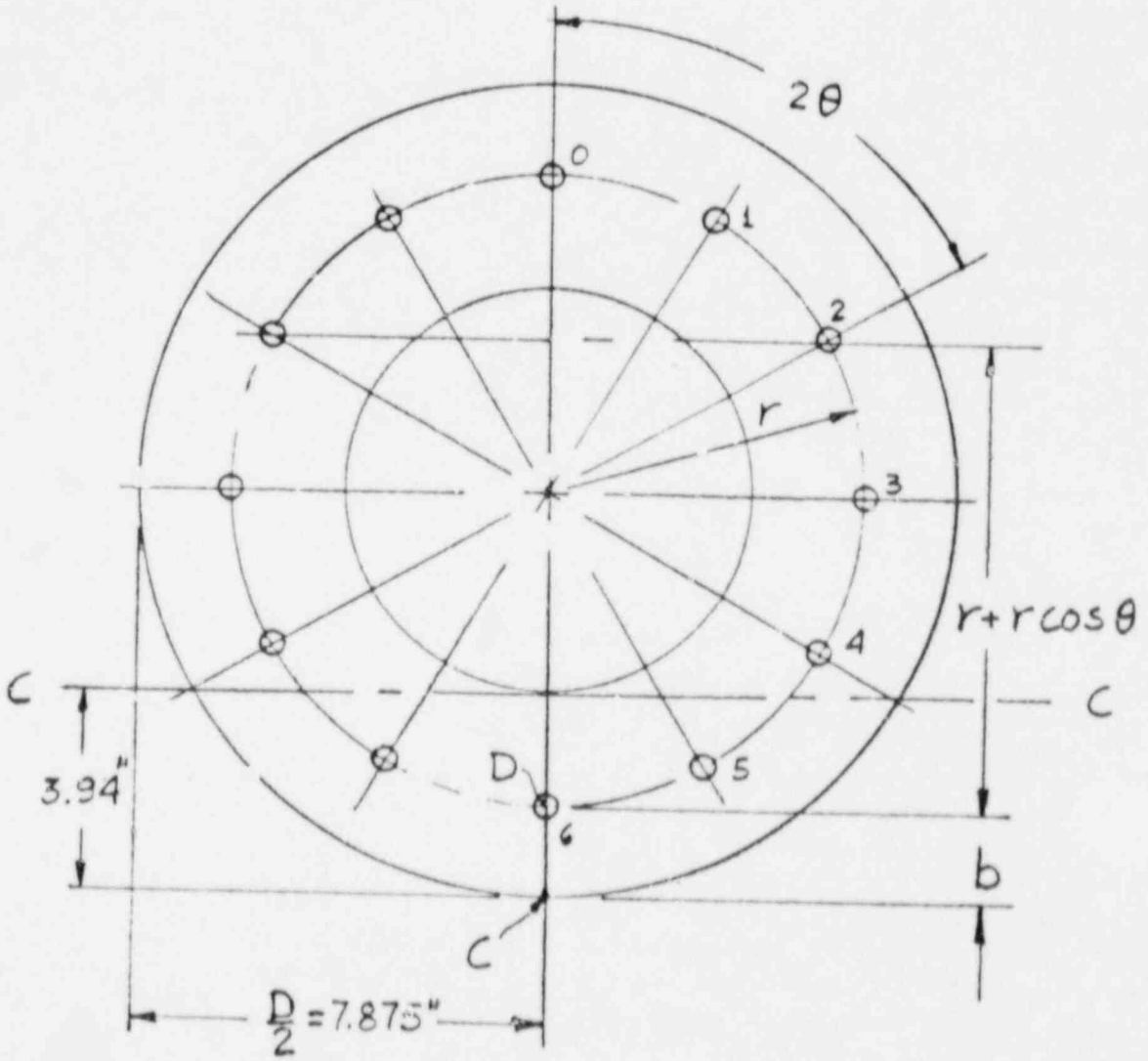

4A.8 OUTER SHELL

This section of the appendix presents the structural analysis of the outer shell of the TN-24 storage cask. The outer shell consists of a cylindrical shell section and closure plates at each end which connect the cylinder to the cask body. The normal loads acting on the outer shell are due to internal and external pressure and the normal handling operations. Membrane stresses due to the pressure difference and bending and shear stresses due to the handling loads are determined. These stresses are compared to the allowable stress limits in Section 4.2 to assure that the design criteria are met.

4A.8.1 Description

The outer shell is constructed from low-alloy carbon steel and is welded to the outer surface of the containment vessel. The cylindrical shell section is 0.75 in. thick and the closure plates are 1.0 in. thick. Pertinent dimensions are shown in Fig. 4A.8-1 and drawing 971-001 in Appendix 1A.

4A.8.2 Materials Input Data

The outer shell cylindrical section and closure plates are constructed from SA 516-GR 55. The material properties are taken from the ASME Boiler and Pressure Vessel Code, Section III, Appendices[2]. The yield strength of the material is also obtained from the Appendices at a temperature of 350°F.

4A.8.3 Applied Loads

It is assumed that a pressure of 25 psi may be applied to either the inside or outside of the outer shell. This bounding assumption envelopes the actual expected pressures described in Sections 3.2.8 and 3.2.13.4.

The handling loads acting on the outer shell are a result of lifting, tilting and transfer operations. The loads applied to the shell as a result of these operations consist of the values given in Table 3.2-4. The weight or inertia g load can include all of the weights of the outer shell, neutron resin shield, and aluminum containers. The most severe normal loading condition is the 3 g or 5 g inertia load in the vertical or horizontal orientations.

4A.8.4 Method of Analysis

4A.8.4.1 Stresses Due to Pressure

An external pressure of 25 psi will not induce any load or stress in the outer shell since it is in contact with and supported by the resin filled aluminum containers.

The membrane stresses due to the internal pressure on the cylinder are determined using the following equations.

Longitudinal:

$$\sigma_l \quad \frac{Pr}{2t} = \frac{25 \times 46.62}{2 \times .75} = 777 \text{ psi}$$

Tangential:

$$\sigma_t = \frac{Pr}{t} = \frac{25 \times 46.62}{.75} = 1554 \text{ psi}$$

The stress in the closure plates due to pressure is determined using the same method as used to determine stresses caused by the weight of the resin filled aluminum containers.

The bending stress due to pressure is calculated as follows: (Ref. 4, Table 3, Case 5)

$$\sigma_B = K \frac{Pa^2}{t^2} = 4890 \text{ psi}$$

Where

K = 0.09
P = 25 psi
a = 46.62 in.
t = 1 in.

4A.8.4.2 Stresses Due to Handling Loads

The outer shell is analyzed using conservative methods and assumptions. The cylindrical shell section is analyzed as a simple beam with the appropriate end restraints.

The maximum stress in the cylinder occurs with the cask in the horizontal orientation. The weight load, which consists of the weight of the cylinder, the resin and the aluminum containers, is assumed to be uniformly distributed over the length of the cylinder. The cylinder is assumed to be simply supported at the ends with no rotational restraint from the closure plates. The maximum bending stresses occur at the center (See Figure 4A.8-2) and are given by:

$$(\sigma_B)_{cyl} = \frac{MC}{I} .$$

Where: $M = \frac{W_o \ell}{8}$

$\ell = 154$ in.

$W_o = 3 \times W = 3 \times 23014$ lb

$M = 1.329 \times 10^6$ in. lb

$C = \frac{D_o}{2} = \frac{94.75}{2} = 47.37$ in.

$$I = \frac{\pi}{64}(D_o^4 - D_i^4) = \frac{\pi}{64}(94.75^4 - 93.25^4)$$

$$= 0.2445 \times 10^6 \text{ in}^4;$$

$$\sigma_B = \frac{1.329 \times 10^6 \times 47.37}{0.2445 \times 10^6} = 257 \text{ psi}$$

For the closure plates the maximum bending moment and stress occurs for a fixed end restraint. The bending stress in the closure plate is given by:

$$(\sigma_B)_R = \frac{6M}{t^2}$$

Where: M is the uniform bending moment per unit length of plate;

$$M = \frac{W\ell^2}{12} \times \frac{1}{\pi D} = \frac{150 \times 154^2}{12} \times \frac{1}{\times 94.75} = 996 \text{ in-lb/in.}$$

$$(\sigma_B)_R = \frac{6 \times 996}{1^2} = 5975 \text{ psi}$$

This is conservative because the closure plate will not be perfectly fixed so the moment and bending stress will be less than the value calculated above.

When the cask is in the vertical orientation, the weight of the cylinder acts on the edge of the closure plate and the weight of the resin plus aluminum containers acts as a distributed load. The bending stresses on the plate are then determined.

The end load due to the weight of the outer cylinder is:

$$F_c = W_c \times g = 10344 \times 3 = 31{,}032 \text{ lbs:}$$

The uniform load due to the weight of the resin and aluminum containers is:

$$w = \frac{3(10484 + 2186)}{0.785\ (D_o^2 - D_i^2)} = \frac{3 \times 12670}{1483} = 26 \text{ psi}$$

Based on the formulas of Ref. 4, Case 5 and 6, Page 62, Table 3:

$$(\sigma_B)_R = \frac{6M}{t^2} = K\frac{F_c}{t^2}^2 + K\frac{Pa}{t^2}\ \frac{.115 \times 31032}{1^2} + \frac{.09 \times 26 \times 46.62^2}{1^2} =$$

$$= 3569 + 5086 = 8655 \text{ psi}$$

4A.8.4.3 Results

The stresses acting on the outer shell and closure plates are listed in Table 4A.8-1. They are compared with the allowable values reported in Section 4.2 of Chapter 4.

TABLE 4A.8-1

STRESS COMPONENTS IN OUTER SHELL AND CLOSURE PLATES

LOAD	SURFACE	STRESS (PSI) σ_t	σ_l	σ_r	τ	CLASSFICATION
Outer Shell Internal Pressure (p = 25 psi)	Inner	+1554	+777	+25	0	P_m
	Outer	+1554	+777	0	0	
Stress in Outer Shell Due to Inertia Loads	Inner	77	257	0	116	P_m
	Outer	-77	-257	0	116	
Stress in Closure Plate Due to Internal Pressure	At Junction with Vessel	1515	+25	4890	278	P_b
		-1515	0	-4890	278	
Stress in Closure Plate Due to Inertia Loads	At Junction with Outer Cylinder	2597	0	8655	533	P_b
		-2597	0	-8655	533	

FIGURE 4A.8-1

OUTER SHELL AND CONNECTION WITH CASK BODY

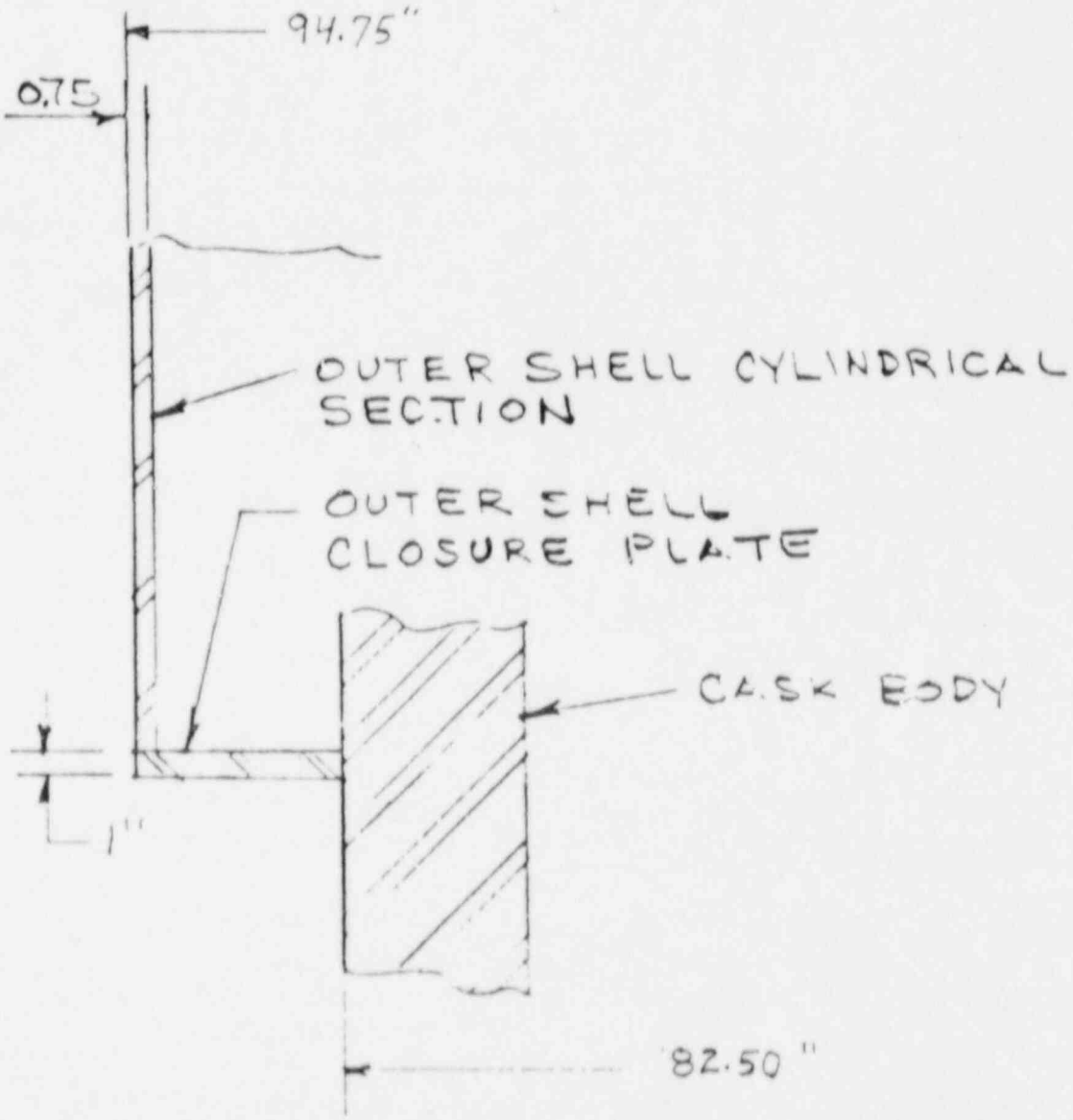

FIGURE 4A.8-2

LOAD DISTRIBUTIONS AND MODELS
USED FOR ANALYSIS OF OUTER SHELL

CASK HORIZONTAL

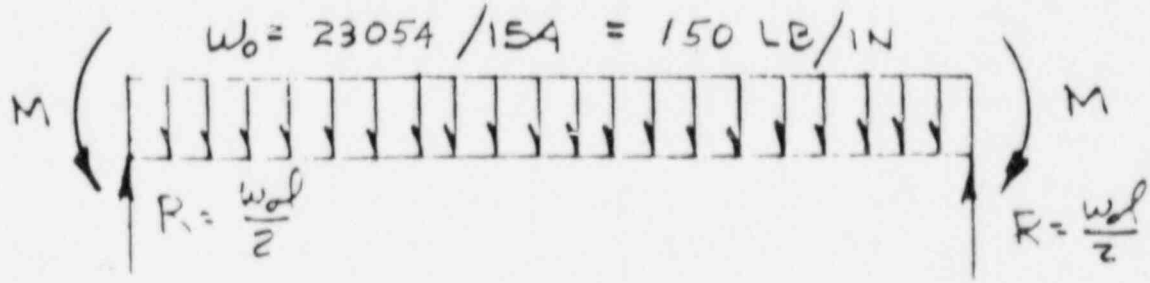

FOR SIMPLY SUPPORTED ENDS

$$M = \frac{W_o l^2}{8}$$

FOR FIXED ENDS

$$M = \frac{W_o l^2}{12} \quad \text{WHERE } W_o = 3W$$

CASK VERTICAL

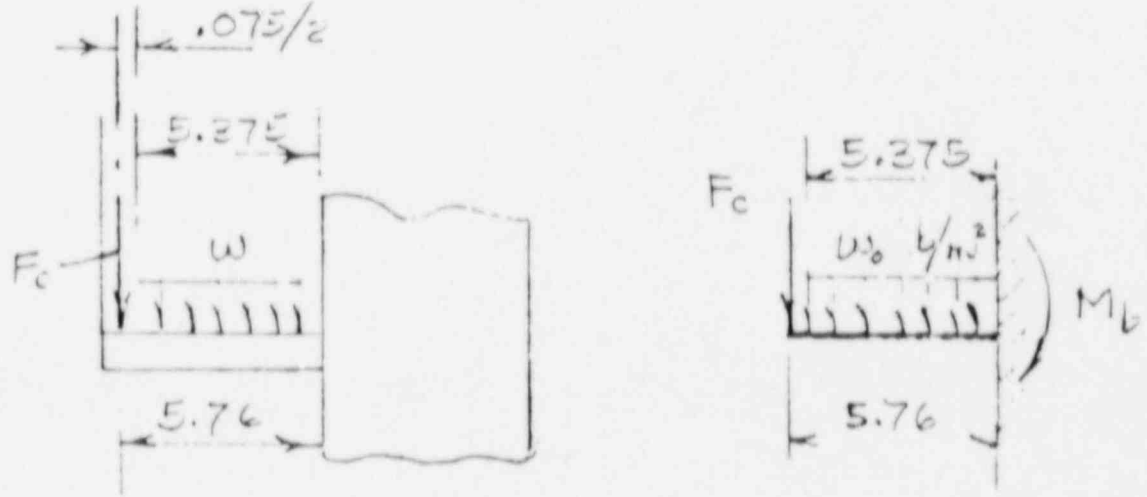

References for Appendix 4A

1. "Rules for the Construction of Nuclear Power Plant Components," ASME Boiler and Pressure Vessel Code, Section III, Division 1 - Subsection NB, The American Society of Mechanical Engineers, New York.

2. "Rules for the Construction of Nuclear Power Plant Components," ASME Boiler and Pressure Vessel Code, Section III, Division 1 - Appendices, The American Society of Mechanical Engineers, New York.

3. Wichman, K.R., Hopper, A.G., and Mershon, J.L., "Local Stresses in Spherical and Cylindrical Shells Due to External Loadings", Pressure Vessels and Piping Design and Analysis, Volume Two, The American Society of Mechanical Engineers, New York, 1972.

4. Timoshenko, S. and Woinowsky-Krieger, S., Theory of Plates and Shells, McGraw Hill Book Co., New York, 1959.

5. Resilient Metal Seals and Gaskets, Catalog H.001.002, Helicoflex Co., 1982.

6. Standard Review Plan, US Nuclear Regulatory Commission, NUREG-0800, Rev. 2, July 1981.

7. Roark, R.J. and Young, N.C., Formulas for Stress and Strain, McGraw Hill Book Co., 1975.

8. Burgreen, D., Elements of Thermal Stress Analysis, Fifth Edition, C.P. Press, Jamaica, New York, 1971.

9. Hopper, A.G. and Thompson, G.V., "Stress in Preloaded Bolts", Product Engineering, McGraw Hill Book Co., New York, Sept. 1974.

10. Carpenter NeutroSorb and NeutroSorb Plus, Alloy Data, Carpenter Technology Corporation, Carpenter Steel Division, May 1987.

11. Harris, C.M. and Crede, C.E., Shock and Vibration Handbook, Second Edition, McGraw Hill Book Co., New York, 1976.

12. Deleted

13. "American National Standard for Special Lifting Devices for Shipping Containers Weighing 10,000 Pounds (4500 kg) or More for Nuclear Materials," ANSI N14.6, American National Standards Institute, New York, Feb. 1978.

14. Deleted

15. DeSalvo, G.J. and Swanson, J.A., ANSYS Engineering Analysis System, User's Manual for ANSYS Revision 4.0, Swanson Analysis Systems, Inc., Houston, Pa., Feb. 1982.

5. OPERATION SYSTEMS

5.1 OPERATION DESCRIPTION

5.1.1 General Description

After arrival, the empty casks are inspected for any damage and stored in a dry, protected area. When required for fuel loading, the cask is transferred to the pool where spent fuel assemblies are loaded into the 24 storage compartments provided by the basket assembly. Nuclear criticality safety is assured as described in Section 3.3.4.1. The lid, with the Helicoflex seals attached, is then placed on the cask body over the two alignment pins and the cask is lifted to the pool surface. The lid bolts are installed and tightened, and the pool water can then be forced from the cavity by pressurizing with inert gas. The cask is then decontaminated to the levels specified by the facility. The cavity is evacuated and dried by means of a vacuum system, and then it is back-filled with helium to an equilibrium pressure of 2.2 atm. The leak detection system pressure tranducers are installed, the seal interspaces pressurized to 5.8 atm, (at equilibrium) and the seals checked for leakage. The external surface temperatures and radiation level are checked to assure that they are within acceptable limits.

The protective cover is then installed and the cask is transferred to its permanent storage location at the ISFSI. (The protective cover could be installed at the ISFSI.) Area radiation and airborne radioactivity monitors are provided by the operator of the ISFSI to assure compliance with the licensing requirements under 10CFR Part 72[1]. Seal interspace pressure can be continuously monitored to assure that design criteria requirements are met. Routine temperature monitoring is not necessary. Periodic maintenance is performed as described in Section 4.5.

5.1.2 Flow Sheets

The sequence of operations to be performed in loading fuel into the TN-24 storage cask and then placing the cask into storage at the ISFSI is outlined in Table 5.1-1 and is shown in simplified flowsheet form in Figure 5.1-1.

Details of the number of personnel and the time required for the various operations are given in Table 5.1-2 for use in the radiation exposure determinations developed in Chapter 7. The data are based on Transnuclear's experience with transport cask operations.

5.1.3. Identification of Subjects for Safety Analysis

5.1.3.1. Criticality Prevention

As discussed in Section 3.3.4, criticality is controlled by utilizing poison materials in the fuel basket plates. These features are only necessary during the loading operations that occur in the cask loading pool (underwater). During storage, with the cavity dry and sealed from the environment, no further criticality control measures within the installation are necessary because of the low reactivity of the dry cask; however, the poison materials are obviously in place during storage.

5.1.3.2 Chemical Safety

There are no chemical safety hazards associated with operations of the TN-24 dry storage cask.

5.1.3.3 Operation Shutdown Modes

The TN-24 dry storage cask is a totally passive system so that consideration of operation shutdown modes is unnecessary.

5.1.3.4 Instrumentation

The only instrumentation pertinent to cask storage are the pressure transducers described in Section 3.3.3 which monitor the cask seals for leakage. The transducers monitor the pressure in an interspace to provide an indication of seal failure before any release occurs.

An initial function check is performed at the manufacturer's plant and another function check of the transducers is performed in preparation for cask storage. Three identical transducers are used to assure a functional system through redundancy.

5.1.3.5 Maintenance Techniques

Maintenance during normal storage is expected to be minimal. Other than visual inspection and possible instrument calibration and paint touch-up, no maintenance is anticipated.

5.1.3.6 Heat Transfer Design

The TN-24 packaging is designed to passively reject decay heat under normal conditions of storage and hypothetical accident conditions while maintaining appropriate packaging temperatures and pressures within specified limits. An evaluation of the TN-24 thermal performance is presented in this section. Objectives of the thermal analyses performed for this evaluation include:

- Determination of maximum and minimum temperatures with respect to material limits.

- Determination of temperature distributions for analysis of thermal stresses.

- Determination of temperatures for containment pressurization.

Section 1.2.2 and Table 1.2-1 present the principal design bases for the TN-24 packaging.

A significant thermal design feature of the TN-24 is the basket described in Section 1.2.5. The basket consists of a multitiered "egg crate" assembly of 0.396 in. thick by 16.18 in. wide electroplated copper on borated stainless steel plates, interlocked together to form 24 fuel compartments. The design of the basket allows the heat from the fuel assemblies to be conducted along the plates to the periphery of the basket and dissipated to the cavity wall.

Another design feature is the conduction path created by the aluminium boxes in the neutron shielding layer described in Section 1.2.5. The neutron shielding is provided by a resin compound cast into long slender aluminum containers placed around the cask shell and enclosed within a smooth outer shell. By butting against the adjacent shell surfaces, the aluminum containers allow decay heat to be conducted across the neutron shield.

The TN-24 dry storage cask falls under the jurisdiction of 10CFR Part 72[1] when used as a component of an ISFSI. The guidelines for the heat transfer design in 10CFR Part 72 are not as specific as those in 10CFR Part 71[2] or the Cask Designers Guide.[3] Use of transport cask thermal criteria for storage cask design provides a conservative design approach.

Several thermal design criteria are established for the TN-24. These are:

- Containment of radioactive material and gases is a major design requirement. Seal temperatures must be maintained within specified limits to satisfy the leak tight containment function under normal and accident conditions. A maximum temperature limit of 700°F (371°C) is set for the Helicoflex seals (double metallic O-rings) in the containment vessel closure lid.

- To maintain the stability of the neutron shield resin during normal storage conditions, a maximum temperature limit of 300°F (149°C) is set for the neutron shield. For accident conditions, the neutron shield temperature limit is 1100°F (593°C). This is to ensure that the conduction path, provided by the aluminum containers, does not deteriorate.

- Maximum temperatures of the containment structural components must not adversely affect the containment function.

- Maintaining fuel cladding integrity during storage is another design consideration. To minimize creep deformation that can occur over the storage duration, the maximum initial storage fuel cladding temperature is determined as a function of the initial fuel age using the guidelines provided by the Commercial Spent Fuel Management Program (CSFM).[4] These temperature limits are reported in Section 3.3.7.

In general, all the thermal criteria are associated with maximum temperature limits and not minimum temperatures. All material can be subjected to the minimum environment temperature of - 20°F (-29°C) without adverse effects. The accident design criteria assume that continued fuel storage in the same packaging would be subject to further inspection, test and analysis.

The TN-24 is analysed based on a maximum heat load of 24 KW from 24 fuel assemblies. The thermal evaluation concludes that with this heat load all design criteria are satisfied for normal and accident conditions. A summary of the results from the analyses performed for normal and accident conditions is provided in Table 5.1-3.

Thermal Properties Of Materials

Table 5.1-4 lists the thermal properties of materials used in the thermal analyses. The values are listed as given in the corresponding references. The analyses use interpolated values when appropriate for intermediate temperatures where the temperature dependency of a specific parameter is deemed significant. The interpolation assumes a linear relationship between the reported values.

Thermal radiation effects at the external surface of the packaging are considered. The external surfaces of the TN-24 are painted white (emissivity = 0.95, solar absorptivity = 0.18[7]). To account for dust and dirt an emissivity of 0.9 and a solar absorptivity of 0.3 are used for exterior surfaces in the thermal models.

The cavity wall and the basket plates are treated to ensure a minimum surface emissivity of 0.9 and 0.7 respectively. An emissivity of 0.7 and 0.9 is used for all steel surfaces under the protective cover for the normal and accident analyses respectively. An emissivity of 0.8[10] is used for the fuel cladding.

Thermal Evaluation For Normal Storage Conditions

Normal conditions of storage are site specific and listed in Table 2.7-1. The evaluation for normal storage conditions assumes steady-state ambient temperatures of -20°F to 115°F (-29°C to 46°C), a 12 hour cumulative insolation of 1475 Btu/ft^2 (400 cal/cm^2), horizontal or vertical orientations, and any location within a prescribed array of casks.

The thermal analyses of the TN-24 packaging are performed using the ANSYS computer program.[8] ANSYS is a large scale, general purpose finite element computer code which can be used for steady state or transient thermal analyses. Three computer models are developed, the first for the temperature distribution through the packaging cross section and the next two for the temperature distribution along the cask body and lid.

Packaging Cross Section Model

The packaging cross section model represents a three dimensional slice through the packaging. The model includes the geometry and material properties of the basket, the cask shell, the neutron shield (resin in aluminum boxes) and the outer shell. Taking advantage of symmetry, one-eighth of the cross section is modeled with a thickness corresponding to one-half the basket plate width (8.09 in). Figure 5.1-2 shows a sketch of the model developed.

The basket is comprised of a multitiered "egg crate" assembly of 0.276 in. thick by 16.18 in. wide borated stainless steel plates interlocked to form 24 fuel compartments. Copper (0.06 in.) is electroplated on each side of the basket plates. The plates butt against each other at the intersections which may not establish good thermal contact between the plates. Heat flow along the plates is disrupted by the slots in the plate causing heat to be conducted axially around the slot. The maximum gap of 0.016 in. (obtained from slot tolerances on the basket plates) is assumed to exist between the slot and the interlocking plate on all sides of the slot. This conservatively causes heat to be transferred across a gaseous medium (helium) from one plate to another.

The fuel basket model is three dimensional allowing heat transfer along the X, Y, and Z axes. The three dimensional isoparametric thermal shell element, STIF57,[8] is used to simulate heat transfer along the plates. At the intersection of the plates, STIF57 elements are used to connect nodes of interlocking plates with the slots and allow gaseous conduction across the gaps in the slot.

Heat transfer from the periphery of the basket to the cavity wall is by radiation and gaseous conduction. Conduction is simulated by filling the void spaces between the basket plates and the cavity wall with the three dimensional isoparametric solid element, STIF70[8]. The thermal properties for helium are assigned to these elements. Radiation heat transfer across the void spaces is simulated using the radiation super element, STIF50[8]. The geometry and emissivities of the element surfaces forming the void spaces are inputed into the ANSYS utility called /AUX12[8]. This utility calculates the view factors and the corresponding gray body exchange cocfficients between element surfaces, and stores this information in a file to be read by the radiation superelement.

STIF70 elements are also used to model the cask shells. The inner shell is 9.75 in. and the outer shell is 0.75 in. thick.

The neutron shield consists of 60 long slender resin-filled aluminum containers placed between the inner and outer steel shells. The aluminum containers butt against the shells. The model does not take any credit for thermal contact; a maximum air gap of 0.01 in. is assumed.

The maximum heat flux corresponding to a 12 hour cumulative solar heat load of 1475 Btu/ft^2(400 cal/cm^2) is applied to the outer surface for a steady state analysis. This is conservative since no credit is taken for the 12 hour night period when the packaging does not receive insolation. A solar absorptivity of 0.3 is used for the heat flux calculation.

Heat dissipation from the outer surface is by radiation and natural convection to an ambient 115°F (46°C). An emissivity of 0.9 is used for radiation heat transfer. For this analysis it is assumed the packaging is standing alone (vertical or horizontal) and not in an array. The total heat transfer coefficient, H_t, for heat dissipation by radiation and natural convection is:

$$H_t = H_c + H_r$$

where,

H_c = natural convection coefficient, Btu/hr-ft^2-°F
= 0.18 $(T_s - T_a)^{1/3}$ for horizontal cylindrical surfaces, and
0.19 $(T_s - T_a)^{1/3}$ for vertical surfaces.[3] For conservatism, the former expression is used.

H_r = radiation heat transfer coefficient, Btu/hr-ft^2-°F
= $(0.1714E-8)(G_{12})\ [(T_s + 460)^4 - (T_a + 460)^4]/(T_s - T_a)$

G_{12} = gray body exchange coefficient
= Outer surface emissivity for large surroundings in comparison with surface area[3]
= 0.9

T_a = ambient temperature, °F
= 115°F

T_s = surface temperature, °F

The total heat transfer coefficient is applied as a boundary condition on the outer surfaces of the finite element model.

The fuel assemblies are not included in the model. Instead, a uniform heat flux corresponding to a decay heat load of 1 kw per assembly is applied to the basket plate surfaces forming the fuel compartments. A fuel assembly active length of 144 in. is used for the heat flux calculation.

A plot of the three dimensional ANSYS finite element model is shown in Figure 5.1-3. Elements representing the same material have the same color. Elements for radiation heat transfer and gaseous conduction have not been included in the plot.

The maximum temperature distribution in the packaging is obtained by performing a steady state analysis. This distribution corresponds to the maximum total payload decay heat of 24 kw, a 115°F ambient temperature and insolation. The resulting calculated packaging temperatures are shown in Table 5.1-5. Figure 5.1-4 shows the temperature distribution in the model. The maximum seal temperature will be less than the maximum cavity wall temperature of 317°F (158°C).

The maximum fuel cladding temperature is calculated for the hottest fuel compartment which is located closest to the center of the basket. The Wooton - Epstein equation[9] is used to calculate the maximum fuel cladding temperature. This is a semi-empirical, semi-theoretical correlation which accounts for natural convection (in air) and radiation cooling of a spent fuel assembly in a horizontal cask. The TN-24 may be stored vertically or horizontally and is back filled with helium. Based on experimental studies performed on the TN-24P[10] lower fuel cladding temperatures were obtained for a helium instead of a nitrogen back-fill gas medium. Hence it is conservative to used the Wooton - Eptstein correlation for the fuel cladding temperature calculation. The correlation is:

$$q=4WL_a[sC_1/(1/E_r+1/E_w-1)(T_r^4-T_w^4)+C_2(T_r-T_w)^{4/3}]$$

where,

q = heat dissipation from the fuel assembly, Btu/hr
W = width of the fuel assembly, ft
L_a = active length of fuel assembly, ft
s = Stefan-Boltzmann constant (0.171E-8 Btu/hr-ft^2-°R^4)
C_1 = $4N/(N+1)^2$ (geometric constant)
E_r = emissivity of fuel cladding
E_w = emissivity of compartment walls
N = number of fuel rods on a side

C_2 = 0.1218 (an experimentally determined constant)
T_f = maximum fuel cladding temperature, °R
T_w = average compartment wall temperature, °R

A W 17 x 17 fuel assembly is selected as the basis assembly. An axial power peak factor of 1.2 is included in the calculation. For a W 17x17 assembly,

W = 0.7 ft
L_a = 12 ft
C_1 = 0.2099
E_f = 0.8 (from Ref. 10)
E_w = 0.7 (basket plate emissivity)
g = (1 kw) x 1.2 x (3412 Btu/hr-kw) = 4094 Btu/hr

The average temperature of the hottest fuel compartment is 563°F (see Table 5.1-5). Substituting the appropriate values in the Wooton - Epstein equation, the maximum fuel cladding temperature is 642°F (339°C).

The cavity gas temperature is maximum at the hottest fuel cladding and minimum at the cooler surfaces in the lid region. For simplicity and conservatism, it is assumed that the average cavity gas temperature is the average value of the maximum fuel cladding and the cavity wall temperatures. From Table 5.1-5, the maximum cavity wall temperature = 317°F.

Average cavity gas temperature = (317 + 642)/2
= 480°F (249°C)

The above analysis using the packaging cross section model does not consider the thermal effects of storage in a 2x10 array and axial heat transfer. It is demonstrated below using the cask body models that by taking credit for axial heat transfer and accounting for the reduction of radiation heat dissipation due to storage in an array, the above calculated temperatures will not be exceeded.

Cask Body Model - Vertical Storage in a 2x10 Array

The finite element cask body model for vertical storage represents the TN-24 cask body stored vertically in a 2x10 array on a concrete pad. The model includes the geometry and material properties of the inner and outer shells, bottom, lid, neutron shielding and protective cover. The model takes advantage of the axisymmetric geometry and is two-dimensional with a radial and an axial axis. Figure 5.1-5 is a sketch of the model. The concrete slab is also included in the model and assumed to be 3 ft thick and extend radially 3 ft from the edge of the packaging as shown in Figure 5.1-5.

The finite element ANSYS model is developed using the two dimensional isoparametric thermal solid element, STIF55[8] to simulate conduction heat transfer. Heat dissipation from the resin disk on the lid to the protective cover is by radiation only. Conduction heat transfer is conservatively neglected. The radiation super element, STIF50, is used to simulate radiation across the void space under the protective cover. The ANSYS utility program, /AUX12, is used to calculate the view factors and the corresponding gray body exchange coefficients between element surfaces forming the void space.

The neutron shield around the inner shell is modeled as a homogenized mixture of the aluminum containers and the resin. The effective thermal conductivity in the radial direction is calculated using the temperature results of the packaging cross section model. The average axial thermal conductivity is a weighted average of the resin and aluminum thermal conductivities.

A uniform heat flux corresponding to the total decay heat load of 24 kw is applied to the cavity wall surface adjacent to the 144 in. active length of fuel assembly. No credit is taken for axial conduction along the basket which would cause the decay heat to be dissipated over a larger surface area resulting in a lower heat flux.

Insolation corresponding to 1475 Btu/ft^2(400 cal/cm^2) for 12 hours a day is included on all external surfaces of the cask body model. A solar absorptivity of 0.3 is used for all surfaces. The maximum heat flux corresponding to the above insolation is applied to the external surfaces rather than the average value over a 24 hour period.

The TN-24 packaging dissipates heat to the environment by radiation and natural convection. If the packaging is stored in an array, partial radiation "blockage" occurs which reduces the overall view factor from the packaging to the environment. The analysis assumes that the packagings will be stored in a 2x10 array and will be placed at least 16 ft (center to center) apart (Figure 5.1-6). Convection heat transfer is assumed to be unaffected. Heat transfer between packagings is neglected.

To simplify the outer shell-environment view factor calculation, the TN-24 is assumed to be a cylinder of radius 3.95 ft and length 12.83 ft. This represents the outer surface dimensions for the outer shell. Based on its location in a 2x10 array, it is possible for 46.5% of the outer shell surface area to be surrounded by other packagings. Radiation heat transfer for this "blocked" region could be approximated as that between two concentric cylinders of radii 3.95 ft and (16-3.95) = 12.05 ft respectively. The equation for the view factor F_{2-1} is obtained from Ref. 11 for two concentric cylinders of finite length and is:

$$F_{2-1} = (1/R) - [1/(\pi R)] \cos^{-1}(B/A) + [1/(2\pi RL)] ([(A+2)^2-2R^2]^{1/2} \cos^{-1}(B/RA)) - [B/(2\pi RL)][\sin^{-1}(1/R)] + [A/(4RL)]$$

where,

$A = L^2 + R^2 - 1$

$B = L^2 - R^2 + 1$

$L = h/r_1$

$R = r_2/r_1$

r_1 = radius of inner cylinder = 3.95 ft.

r_2 = radius of outer cylinder = 12.05 ft

h = height of cylinders = 12.83 ft

Substituting values,

$R = 3.0506$

$L = 3.248$

$A = 18.856$

$B = 2.2433$

$F_{2-1} = 0.2034$

From the reciprocity theorem,

$$A_1F_{1-2} = A_2F_{2-1}$$

$$F_{1-2} = F_{2-1}\ (r_2/r_1)$$

$$= (0.2034)\ (12.05/3.95)$$

$$= 0.6205$$

The view factor from the outer surface to the environment

$= 1-0.6205 = 0.3795$

Hence, 46.5% of the "blocked" surface of the packaging will have a view factor of 0.3795 and the remaining, a value of 1. The overall view factor

$$= [\ 0.3795 \times 0.465 + 1.0 \times (1-0.465)]$$

$$= 0.7115$$

The total heat transfer coefficient, H_t, for heat dissipation by radiation and natural convection is:

$$H_t = H_c + H_r$$

where,

H_c is the natural convection coefficient, Btu/hr-ft^2-$^\circ$F.

$H_c = 0.18\ (T_s - T_a)^{1/3}$ for vertical surfaces [3] and is used for the exposed vertical cylindrical surfaces of the cask inner and outer shells.

H_t is the radiation heat transfer coefficient, Btu/hr-ft^2-°F

$$=(0.1714E-8)(G_{12})[(T_s+460)^4 - (T_a+460)^4]/(T_s-T_a)$$

G_{12} is the gray body exchange coefficient
= (surface emissivity) (view factor)
For the protective cover surfaces, $G_{12} = 0.9$

For the vertical cylindrical surfaces,
$G_{12} = (0.9)\ (0.7115) = 0.6403$
T_a = ambient temperature, = 115°F
T_s = surface temperature, °F

The total heat transfer coefficient is applied as a boundary condition on the exposed surfaces of the finite element model.

A plot of the axisymmetric two dimensional ANSYS model is shown in Figure 5.1-7. Elements representing the same material have the same color.

A steady state analysis is performed to obtain the maximum temperature distribution in the cask body for vertical storage. This distribution shown in Figure 5.1-8, corresponds to the maximum total heat load of 24 kw, a 115°F ambient temperature and insolation. Figures 5.1-9 and 5.1-10 show the temperatur distribution in the lid and the bottom regions. The maximum outer surface temperature is 244°F (118°C) which is approximately the same as that obtained with the packaging cross section model (see Table 5.1-5). All other cask body temperatures are lower than those reported in Table 5.1-5. The maximum lid temperature is 222°F. The results of the [illegible] N-24 cask body stored vertically in a 2x10 array [illegible] packaging component temperatures reported in Table [illegible] be exceeded during normal conditions of storage.

Cask Body Model - Horizontal Storage in a 2 x 10 Array

The TN-24 may also be stored in the horizontal position in a 2x10 array. A 4.0 in. thick resin cap will be placed over the external bottom surface to provide additional neutron shielding. The cask body model developed is the same as that used for the vertical orientation except that model does not include the concrete pad but instead the bottom resin cap. Figure 5.1-11 is a sketch of the model.

The finite element ANSYS model of the cask body is identical to that for the cask body in the vertical orientation and has the same geometry and material properties for the packaging components. The heat transfer modes simulated are identical. The uniform decay heat flux applied to the cavity wall is the same. The maximum heat flux corresponding to the insolation of 1475 Btu/ft^2 for 12 hours a day is included on all external surfaces of the model.

The effect of horizontal storage in a 2x10 array on heat dissipation to the environment is recalculated. The packagings will be placed at least 16 ft apart (center to center) and consequently, convection heat transfer is assumed to be unaffected. Figure 5.1-12 is a sketch showing horizontal storage of the TN-24 in a 2x10 array. The view factor, F_{1-2}, between two packagings in an array is calculated using the view factor equation for infinitely long parallel cylinders of the same diameter. The equation is:

$$F_{1-2} = (1/\pi)\{(X^2 - 1)^{1/2} + \sin^{-1}(1/X) - X\}$$

Where,

$X = 1 + (S/2r)$

r = outer surface radius = 3.95 ft

S = distance between packaging surfaces

= 16-2(3.95) = 8.1 ft

Substituting values,

$$X = 2.0253$$

$$F_{1-2} = 0.08031$$

The effective view factor (outer surface-environment) for a packaging located between two other packagings,

$$= 1-2(0.08031)=0.8394$$

The total heat transfer coeffient, H_t for heat dissipation by radiation and natural convection is:

$$H_t = H_c + H_r$$

Where,

H_c is the natural convection coefficient, Btu/hr-ft^2°F
$= 0.18\ (T_s - T_a)^{1/2}$ for horizontal cylindrical surfaces and
$0.19\ (T_s-T_a)^{1/2}$ for vertical surfaces.(3)
$H_c = 0.18\ (T_s-T_a)^{1/2}$ is used for all surfaces conservatively.

H_r is the radiation heat transfer coeffient, Btu/hr-ft^2°F
$= (0.1714E-8)(G_{12})\ [(T_s+460)^4 - (T_a+460)^4]/(T_s - T_a)$

G_{12} is the gray body exchange coefficient
= (surface emissivity) (view factor)
For the protective cover surface, $G_{12} = 0.9$
For the horizontal cylindrical surfaces, G_{12} =
$(0.9)(0.8394) = 0.7555$

For the bottom surface, $G_{12} = 0$

Figure 5.1-13 is a plot of the axisymmetric two dimensional ANSYS model. Elements representing the same material have the same color.

A steady state analysis is performed to calculate the maximum temperature distribution. Corresponding to a total heat load of 24 kW, a 115°F ambient temperature and insolation. Figure 5.1-14 shows the temperature distribution in the model. The maximum outer surface temperature obtained is 237°F (114°C). All cask body temperatures are lower than those reported in Table 5.1-5. The results of the thermal analysis (TN-24 cask body stored horizontally in a 2x10 array) demonstrate that packaging component temperatures reported in Table 5.1-5 will not be exceeded during normal conditions of storage.

Evaluation of Packaging Performance

The thermal analysis for normal storage concludes that the TN-24 design meets all applicable requirements. The maximum temperatures calculated using conservative assumptions are low. The maximum temperature of any containment structural component is less than 320°F (160°C) which has an insignificant effect on the mechanical properties of the containment materials used. This temperature (320°F) also corresponds to the maximum seal temperature during normal storage and is well below the 700°F long term limit specified for continued seal function. The neutron shield temperature is below 300°F (149°C) and no degradation of the neutron shielding is expected during the 20 year storage life. The maximum fuel cladding temperature is 642°F (339°C) and within allowable fuel temperature limits (Section 3.3.7). The minimum temperature of -20°F (-29°C) is also inconsequential to the packaging function.

Thermal Evaluation for Hypothetical Accident Conditions

A transient analysis is performed to demonstrate the thermal performance of the TN-24 in a thermal accident such as an exposure to a fire. The thermal environment conditions, as specified in 10CFR Part 71, are used to evaluate the response of the TN-24.

The packaging is assumed to be initially at steady state in an ambient temperature of 115°F with a 24 KW heat load. The effects of solar radiation are neglected prior to, during, and following the accident. During the accident the packaging is exposed to a radiation environment of 1475°F (800°C) for 30 minutes. The radiation environment is characterized by an emissivity of 0.9 and the outer surface of the packaging is assumed to have an absorptivity of 0.8. Heat absorption by natural convection on the basis of still air at 1475°F is included. Cooldown of the packaging after 30 minutes of exposure to the accident environment is based on 115°F ambient air temperature and a surface emissivity of 0.8.

The computer model for the packaging cross section is used for the accident analysis. To determine seal temperatures in the lid region, a model for the seal-lid region is developed.

Packaging Cross Section Model

The packaging cross section model, developed for the normal storage analysis, is reused for the transient analysis.

Heat dissipation from the outer surface is by radiation and natural convection to an ambient temperature of 115°F before and after the thermal accident. The total heat transfer coefficient, H_t, is calculated in the same manner for normal storage conditions.

Initial conditions before the thermal accident are established by performing a steady state analysis with a packaging heat load of 24 kw and an ambient temperature of 115°F. Effects of solar radiation are neglected.

During the thermal accident, heat absorption at the outer surface by radiation and convection on the basis of still ambient air at 1475°F is given by the following equation:(3)

$$q_s = H_c(T_f - T_s) + 0.1714E\text{-}8(F_o)x\{E_f(T_f+460)^4 - (T_s+460)^4\}$$

Where,

q_s = Heat flux into packaging from thermal environment

H_c = Convection heat transfer coefficient
= $0.19(T_f - T_s)^{1/3}$ Btu/hr-ft^2 -°F

T_f = Radiation environment temperature
= 1475°F

T_s = Surface temperatures of the packaging, °F

F_o = Outer packaging surface absorptivity
= 0.8

E_f = Radiation environment emissivity
= 0.9

The total heat transfer coefficient for heat absorption is:

$$H_t = H_c + 0.1714E\text{-}8(F_o)[E_f(T_f+460)^4 - (T_s+460)^4]/(T_f - T_s)$$

H_t is used as a boundary input during the 30 minute duration of the radiation environment.

Two computer analyses were performed, the first with the 0.01 in. air gaps and the second with no air gaps in the neutron shielding region. The maximum temperatures obtained for each case are listed in Table 5.1-6. Figure 5.1-15 shows the temperature distribution at the end of the thermal accident. The maximum temperature-time history for the outer surface, neutron shielding, cavity wall and basket plate is shown in Figure 5.1-16. The maximum fuel cladding temperature is calculated for the hottest fuel compartment as in the case for normal storage conditions. The peak temperature for the hottest fuel compartment was calculated to be 613°F at 12.8 hr from the start of the thermal accident. Using the Wooter-Epstein equation, the peak value of the maximum fuel cladding temperature is 675°F(357°C)

The same assumption for the average cavity gas temperature during normal storage condition is used for the accident analysis. The peak value for the average cavity gas temperature is 518°F occuring at 12.8 hr from the start of the accident.

Seal-Lid Region Model

To demonstrate the integrity of the seals during thermal accident conditions, a computer model of the top portion of the TN-24 is developed. The model is an axisymmetric two dimensional model and includes the geometry and material properties of the lid, the resin disk, the protective cover, and the upper portions of the cask inner shell, neutron shield and outer shell.

The finite element ANSYS model is similar to the cask body model developed for normal storage and uses the same ANSYS elements. Heat transfer in the enclosure below the protective cover is by radiation. For conservatism, all surfaces are assigned an emissivity of 0.9.

Figure 5.1-17 is a plot of the axisymmetric two dimensional ANSYS model. Elements representing the same material have the same color.

The initial temperature of the model before the thermal accident is 222°F which corresponds to the lid temperature obtained for normal storage conditions. The boundary input (total heat transfer coeffient, H_t), calculated for the packaging cross section model is applied to the external surfaces of the model.

The results of the computer analysis show that the maximum seal temperature in the lid will not exceed 479°F (248°C).

Evaluation of Packaging Performance

Based on the analysis for accident conditions, the package will withstand the hypothetical thermal accident event without comprising the containment integrity of the package. The design meets all applicable requirements.

Buried Cask Thermal Evaluation

The TN-24 dissipates heat to the environment by radiation and natural convection. If the packaging is accidently buried in medium that will not provide the equivalent cooling of natural convection and unrestricted radiation to the environment, component temperatures will increase to a higher steady state condition after long-term burial. Of interest is the containment integrity which is assured as long as the metallic seals remain below 700°F and the cavity pressure is less than 250 psig.

The temperature response of the TN-24 is evaluated using the finite element packaging cross section model developed for the normal storage analysis. For this analysis, the packaging is assumed to be completely buried in dry soil with such poor heat transfer characteristics that it effectively insulates the packaging. This conservative assumption eliminates any communication between the cask and a final heat sink. The resulting analysis therefore determines the time required to reach limiting temperatures for the containment integrity.

Initial conditions before burial are established by performing a steady state analysis with a packaging heat load of 24 kw and an ambient temperature of 115°F. Effects of solar radiation are neglected.

The results of the analysis show that if the packaging is not uncovered within 4 hours, the resin will start outgassing as its temperature exceeds 300°F (149°C). Thereafter, packaging component temperatures will increase by about 6°F (3.3°C) per hour. The cask body temperatures will reach 700°F about 60 hours after burial. At this time all temperatures in the packaging will be about 380°F (211°C) higher than those for normal storage. The cavity pressure, if all fuel fails, will not exceed 60 psig. Thermal gradients in the packaging are small and less than those during normal storage. Figure 5.1-18 shows the maximum temperature/time history for the outer surface, neutron shielding, cavity wall and basket plate.

The operating and emergency procedures for an ISFSI should consider these time frames in planning for recovery from an accidental cask burial.

TABLE 5.1-1

SEQUENCE OF OPERATIONS

A. Receiving

1. Unload empty cask and separately packaged seals at plant site.
2. Inspect for shipping damage: exterior surfaces, sealing surfaces, trunnions, seals, accessible interior surfaces and basket assembly, bolts, bolt holes and threads, neutron shield vents.
3. Move cask to cask loading pool area.

B. Cask Loading Pool

1. Install plug in neutron shield vent hole. (threaded hole in the top of the steel shell surrounding the resin which contains a pressure relief valve during storage).
2. Remove lid bolts and lid.
3. Install two alignment pins in cask body flange bolt holes, 180° apart.
4. Install protective plate over cask body sealing area.
5. Lower cask into cask loading pool.
6. Load preselected spent fuel assemblies into the 24 basket compartments.
7. Reconfirm identity of the fuel assemblies loaded into the cask.
8. Obtain lid and lid seal from storage.
9. Attach lid seal to lid by means of six retaining screws.
10. Remove protective plate from cask body flange.
11. Lower lid and place on cask body flange over the two alignment pins.
12. Lift cask out of pool. (Cask could remain in pool to drain water)
13. Remove two alignment pins and install 48 lid bolts.
14. Torque the bolts using prescribed procedure.
15. Remove drain port cover and bolts from lid.
16. Connect line from plant readwaste system to "Hansen" quick-disconnect coupling in the drain port.
17. Remove vent port cover and bolts from lid.

18. Bolt special adapter, with quick-disconnect coupling, to vent port bolt holes.
19. Connect plant compressed air line to special adapter quick-disconnect coupling.
20. Pressurize cavity to force water from cavity through drain port to the plant radwaste system.
21. Sample the drain water to determine presence of failed fuel in the cask.
22. Disconnect plant compressed air line and plant radwaste system line from their quick-disconnect couplings.
23. Move cask to the decontamination area.

C. Decontamination Area

1. Decontaminate cask until acceptable surface dose levels are obtained
2. Remove plug from neutron shield vent and install pressure relief valve.
3. Remove special adapter at vent port.
4. Connect Vacuum Drying System (VDS) to vent port bolt holes.
5. Evacuate cavity to remove remaining moisture using prescribed procedure.
6. Break vacuum by closing vacuum valve and opening air valve to admit dry air into the cavity.
7. Disconnect VDS at vent port and install vent port cover with seal and bolts.
8. Torque the bolts using prescribed procedure.
9. Connect Vacuum-Backfill System (VBS) to "Hansen" quick-disconnect coupling in the drain port.
10. Evacuate cavity to 10 millibar and backfill with dry helium gas using prescribed procedure.
11. Pressurize cavity to about 2 atm with helium.
12. Disconnect VBS at the drain port quick-disconnect coupling and install drain port cover with seal and bolts.
13. Torque the bolts using prescribed procedure.
14. Remove leak detection port cover.
15. Install leak detection pressure transducers with seal and bolts.

16. Torque the bolts using prescribed procedure.
17. Connect pressure transducers to pressure recorder (switch)
18. Pressurize overpressure system, (seal interspaces), with Helium to a pressure of about 5.5 atm.
19. Check pressure recorder for any decrease in pressure. Observe pressure for a period of 24 hours.
20. Check external surface temperatures using an optical pyrometer.
21. Check surface radiation levels.
22. Install top neutron shield drum and protective cover with seal and bolts. (could be performed in storage area)
23. Torque bolts using prescribed procedures.
24. Load cask on transfer vehicle.
25. Move cask to Storage Area.

D. Storage Area

1. Unload cask from transfer vehicle.
2. Position cask in preselected location on storage pad.
3. Check for surface defects.
4. Connect pressure instrumentation to pressure recorder in ISFSI control room.
5. Check that pressure instrumentation is functioning.
6. Check surface radiation levels.
7. Check that area radiation monitors and airborne radioactivity monitors are functioning.
8. Remove trunnions and trunnion bolts and store (Optional).
9. Install neutron shield plugs with seals and bolts at the trunnion locations (Optional).

TABLE 5.1-2

ANTICIPATED TIME AND PERSONNEL REQUIREMENTS FOR CASK HANDLING OPERATIONS

Operation	No. of Personnel	Time (min)	Avg. Distance (ft) from Cask
Receiving			
1. Unloading	*	*	*
2. Inspection	*	*	*
3. Transfer to cask loading pool	*	*	*
Cask Loading Pool			
4. Install vent plugs	*	*	*
5. Remove lid	*	*	*
6. Install alignment pins	*	*	*
7. Lower cask into pool	*	*	*
8. Load fuel	*	*	*
9. Place lid on cask	*	*	*
10. Lift cask to pool surface	2	30	5
11. Remove alignment pins	2	15	3
12. Install lid bolts	3	120	3
13. Drain cavity	2	90	6
14. Transfers to decon. area	3	60	10
Decontamination Area			
15. Decontaminate cask	3	120	3
16. Remove vent plugs	2	30	5
17. Drying, evacuating, backfilling	2	480	5

*No personnel radiation exposure during these operations.

TABLE 5.1-2 (continued)

	No. of Personnel	Time (min)	Avg. Distance from Cask (ft)
Operation			
18. Install pressure transducers	2	30	5
19. Pressurize interspace	*	*	*
20. Check leakage	2	30	5
21. Check surface temperature	2	30	5
22. Check surface dose rate	2	30	3
23. Install protective cover	2	30	5
24. Load on transfer vehicle	3	60	5
25. Transfer to storage area	3	60	10
Storage Area			
26. Unload from vehicle position in location	3	60	5
27. Check surface dose rate	2	30	3
28. Connect pressure instr.	2	30	5
29. Remove trunnions and install shield plugs (optional)	3	60	2
Periodic Maintenance (Annual)			
1. Wash down of exterior	2	60	5
2. Surface defects	2	60	3
3. Instrument calibration	2	60	5
Major Maintenance (once in 20 years)			
1. Remove protective cover and install containment cover	3	180	8

*No personnel radiation exposure during these operations.

TABLE 5.1-3

SUMMARY OF RESULTS

Normal Storage Conditions*	
Maximum Temperatures	
Outer Surface	243°F (117°C)
Neutron Shield (resin/aluminum)	291°F (144°C)
Seal	317°F (158°C)
Cavity Wall	317°F (158°C)
Basket Plate	575°F (302°C)
Fuel Cladding	642°F (339°C)
Average Cavity Gas Temperature	480°F (249°C)
Accident Conditions**	
Maximum Transient Temperatures	
Outer Surface	1102°F (594°C)
Neutron Shield (resin/aluminum)	980°F (527°C)
Seal	479°F (248°C)
Cavity Wall	379°F (193°C)
Basket Plate	613°F (323°C)
Fuel Cladding	675°F (357°C)
Average Cavity Gas Temperature (Peak)	518°F (270°C)

*115°F (46°C) ambient temperature, 12-hour cumulative solar heat load of 1475 Btu/ft^2 (400 cal/cm^2).

**1475°F (802°C) radiation environment with convective heat input for a period of 30 minutes, no solar heat load.

TABLE 5.1-4

PROPERTIES OF MATERIALS USED IN THERMAL ANALYSES

Material	Copper[5]*	Borated[5] Stainless Steel	Carbon[6] Steel	Aluminum[6]	Resin	Helium[7]	Air[7]	Concrete[7]
Used For	basket	basket	lid protective cover, inner and outer shells	neutron shield	neutron shield	fill gas	air gaps	concrete pad
Density (lb/ft^3)	559	488	489	169	87.4			
Specific Heat (Btu/lb-°F)	0.0915	0.11	0.110@100°F 0.123@300°F 0.133@500°F 0.143@700°F 0.156@900°F 0.172@1100°F	0.219@150°F 0.221@200°F 0.224@250°F 0.226@300°F 0.229@350°F 0.230@400°F	0.3107			
Thermal Conductivity (Btu/hr-ft-°F)	223@32°F 219@212°F 216@392°F 213@572°F 210@752°F	8.4@32°F 10.0@212°F 10.0@392°F 11.0@572°F 11.0@752°F	25.9@100°F 24.4@300°F 23.7@500°F 22.4@700°F 20.9@900°F 19.2@1100°F	98.0@150°F 99.0@200°F 99.8@250°F 100.6@300°F 101.3@350°F 101.9@400°F	0.104	0.078@0°F 0.097@200°F 0.115@400°F 0.129@600°F	0.0154@100°F 0.0174@200°F 0.0193@300°F 0.0212@400°F 0.0231@500°F	0.81

* Numbers in parenthesis are the reference numbers

TABLE 5.1-5

COMPONENT TEMPERATURES* DURING NORMAL STORAGE

Maximum temperatures	
Outer shell surface	243°F (117°C)
Neutron shield	291°F (144°C)
Cavity wall	317°F (158°C)
Basket plate	575°F (302°C)
Fuel compartment	563°F (295°C)
Fuel cladding	642°F (339°C)
Average Cavity Gas Temperature	480°F (249°C)

*From TN-24 packaging cross section model.

TABLE 5.1-6

MAXIMUM TRANSIENT TEMPERATURES-THERMAL ACCIDENT

	With Air Gaps In Neutron Shield		No Air Gaps In, Neutron Shield	
	Initial	Max. Temp./Time	Initial	Max Temp./Time
Outer Surface	231° F	1102°F @ 0.5 hr.	230°F	993° F @ 0.5 hr.
Aluminum Resin	242° F	873°F @ 0.52 hr.	230°F	980° F @ 0.5 hr.
Cavity Wall	306° F	379°F @ 3.3 hr.	273°F	375° F @ 2.6 hr.
Basket Plate	566° F	613°F @ 12.8 hr.	543°F	602° F @ 9.8 hr.

FIGURE 5.1-1

SEQUENCE OF OPERATIONS

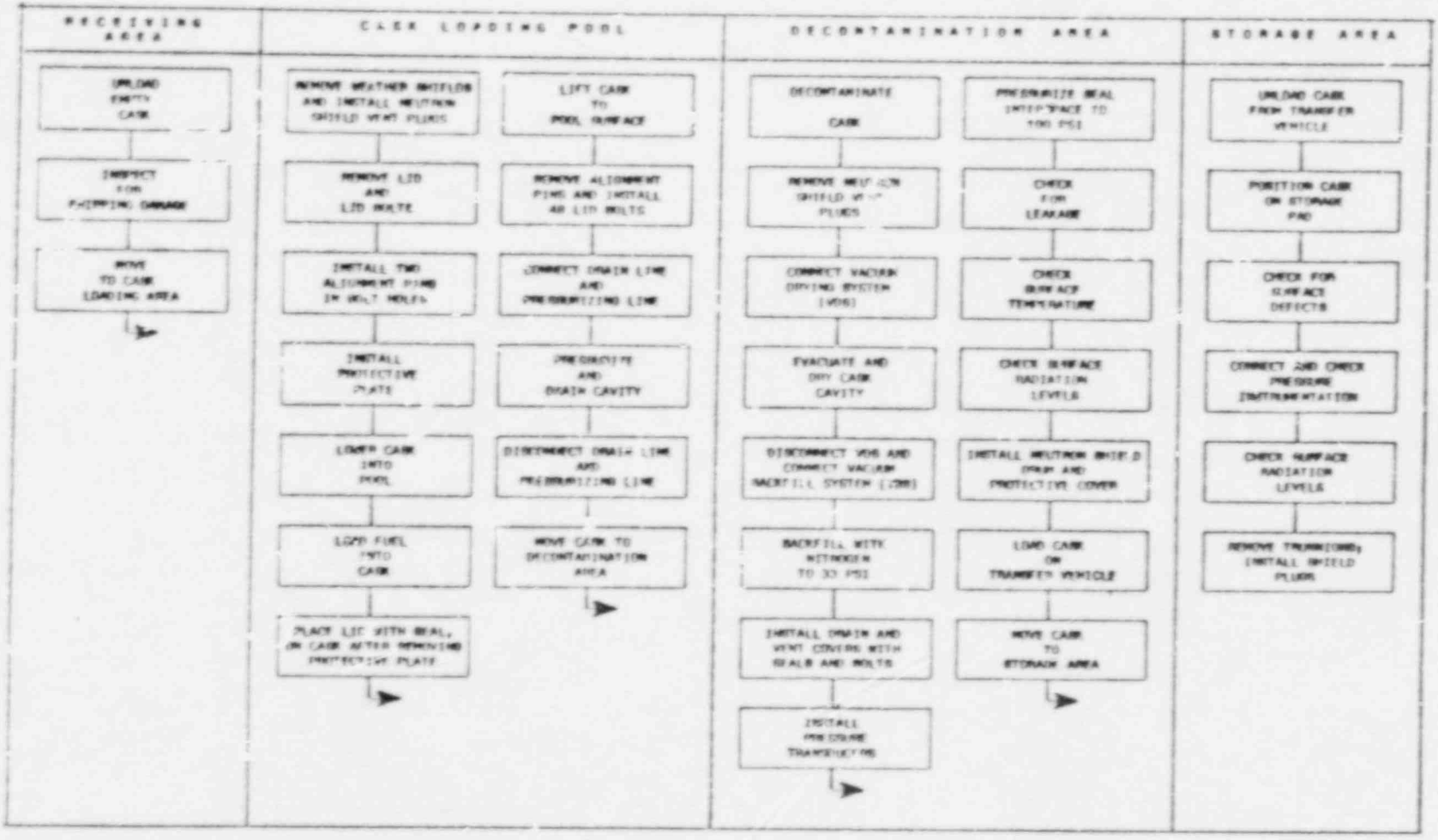

FIGURE 5.1-2

SKETCH OF THERMAL MODEL FOR TN-24 PACKAGING CROSS SECTION

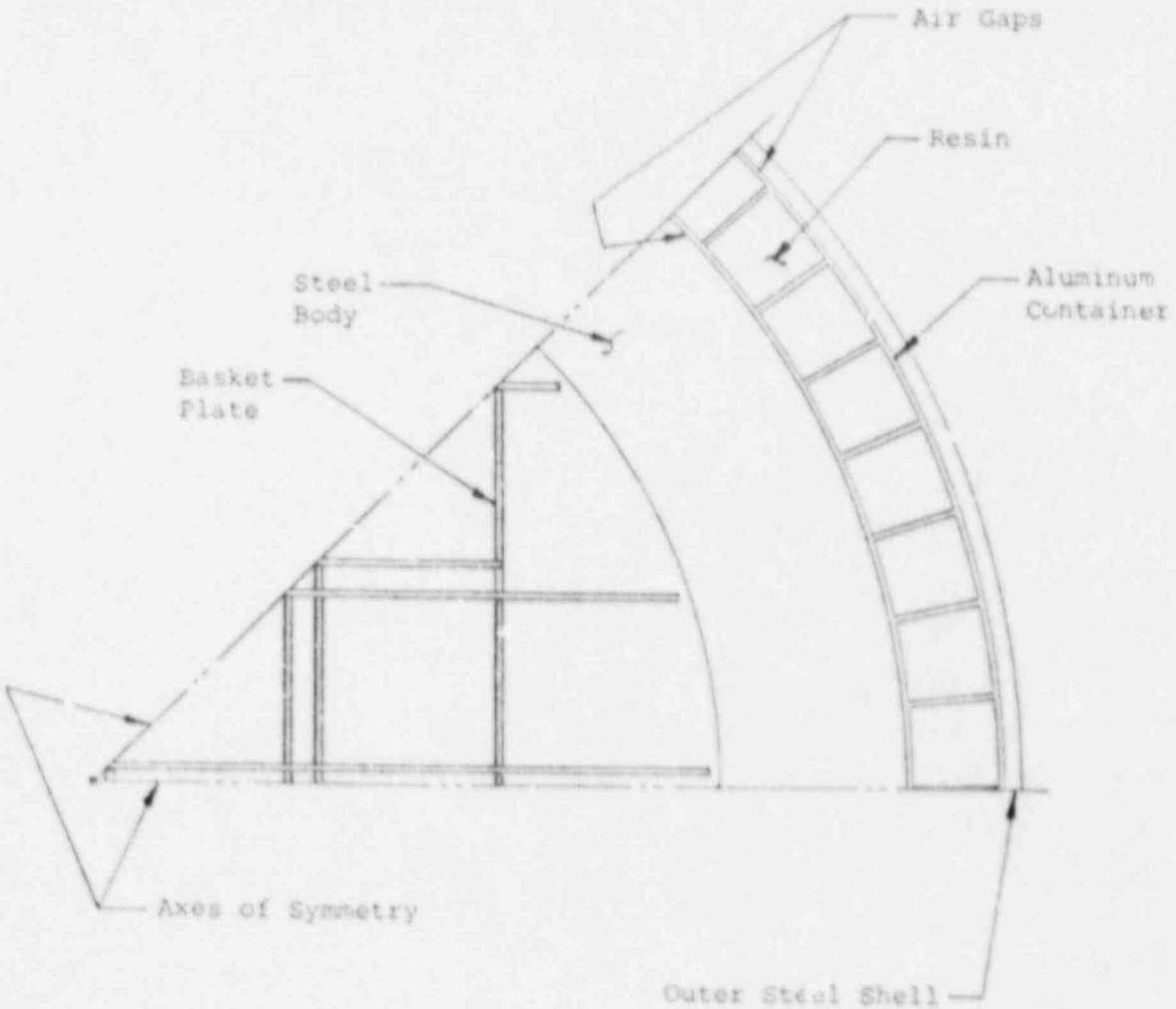

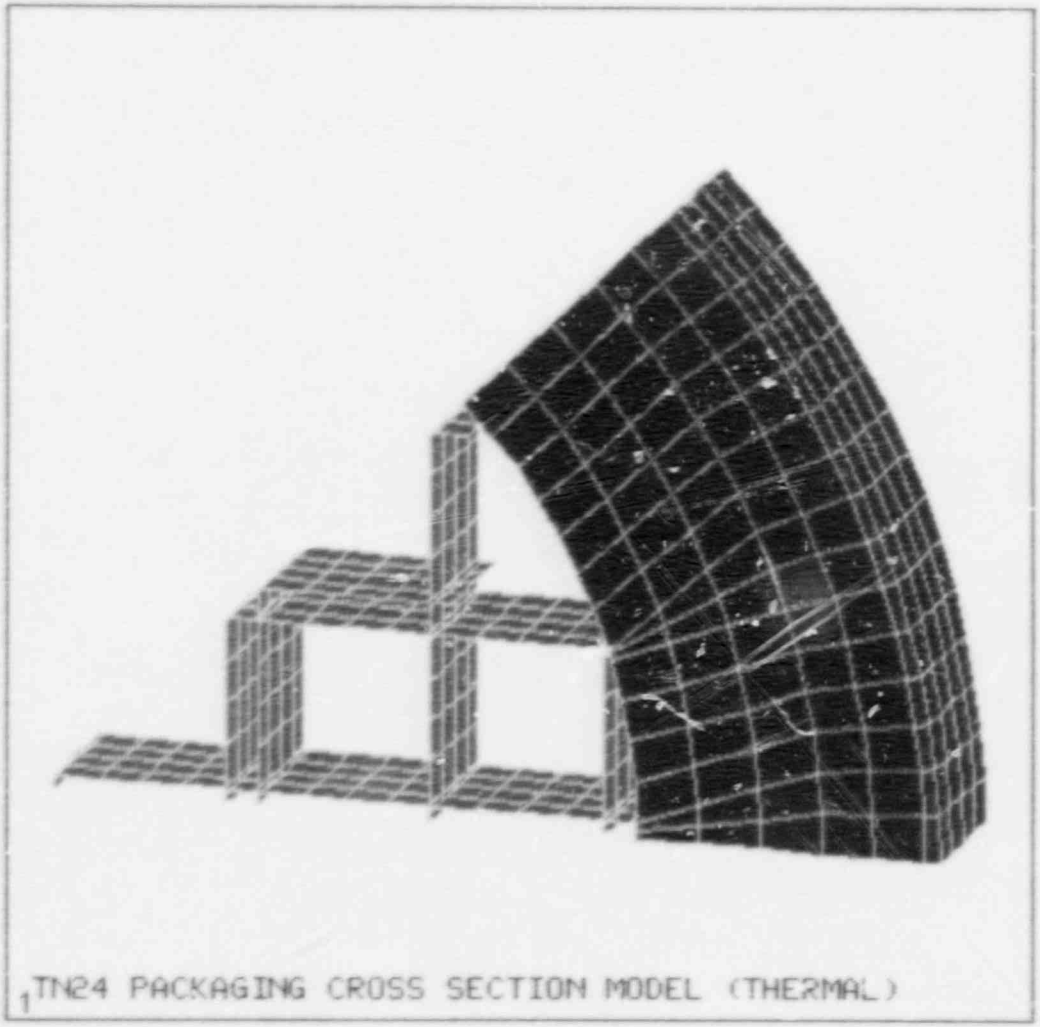

FIGURE 5.1-3

FINITE ELEMENT MODEL FOR TN-24 PACKAGING CROSS SECTION

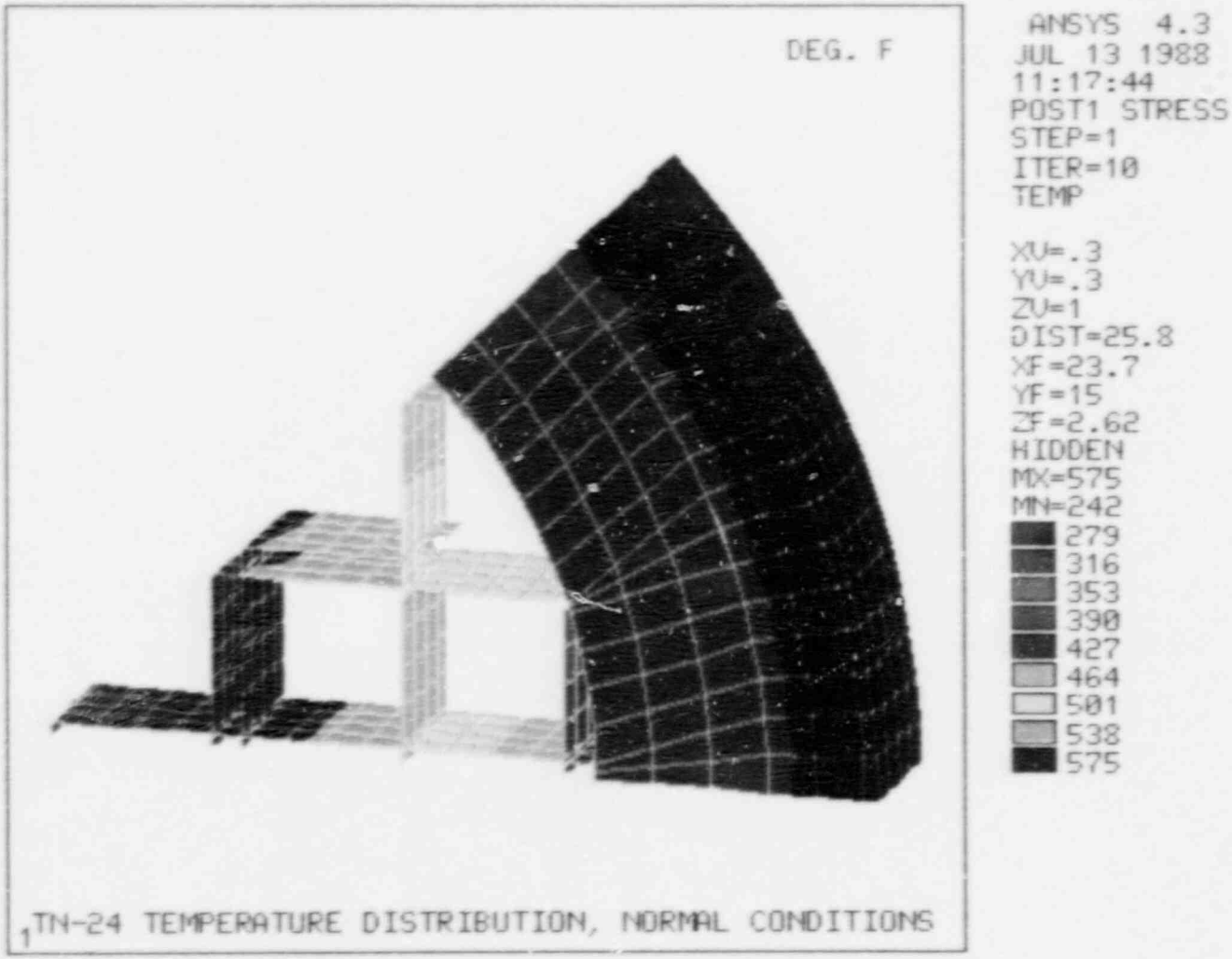

FIGURE 5.1-4

TEMPERATURE DISTRIBUTION IN THE TN-24 PACKAGING

CROSS SECTION MODEL - NORMAL CONDITIONS

FIGURE 5.1-5

SKETCH OF THERMAL MODEL FOR TN-24 CASK BODY - VERTICAL STORAGE

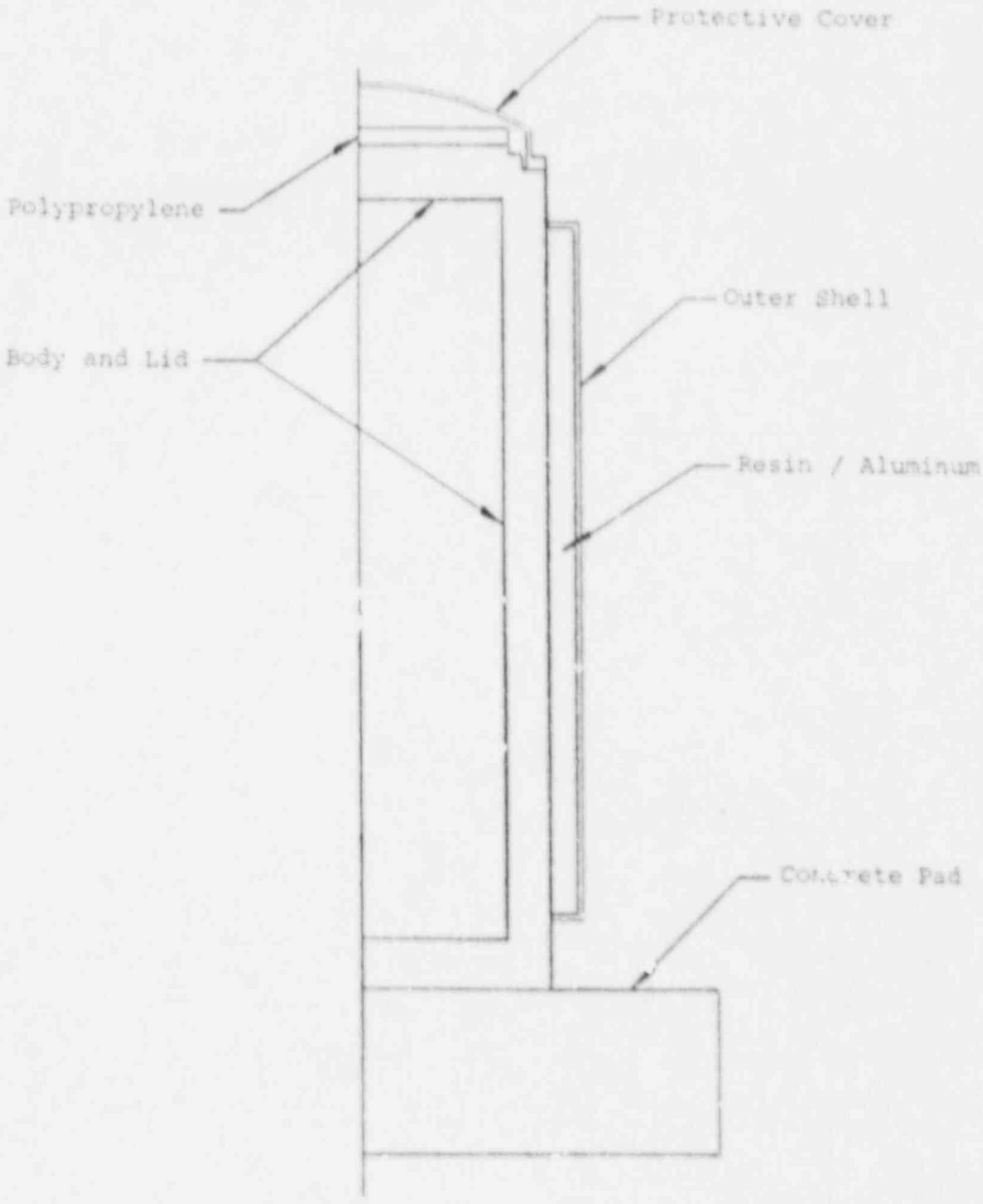

FIGURE 5.1-6
VERTICAL STORAGE OF THE TN-24 IN A 2x10 ARRAY

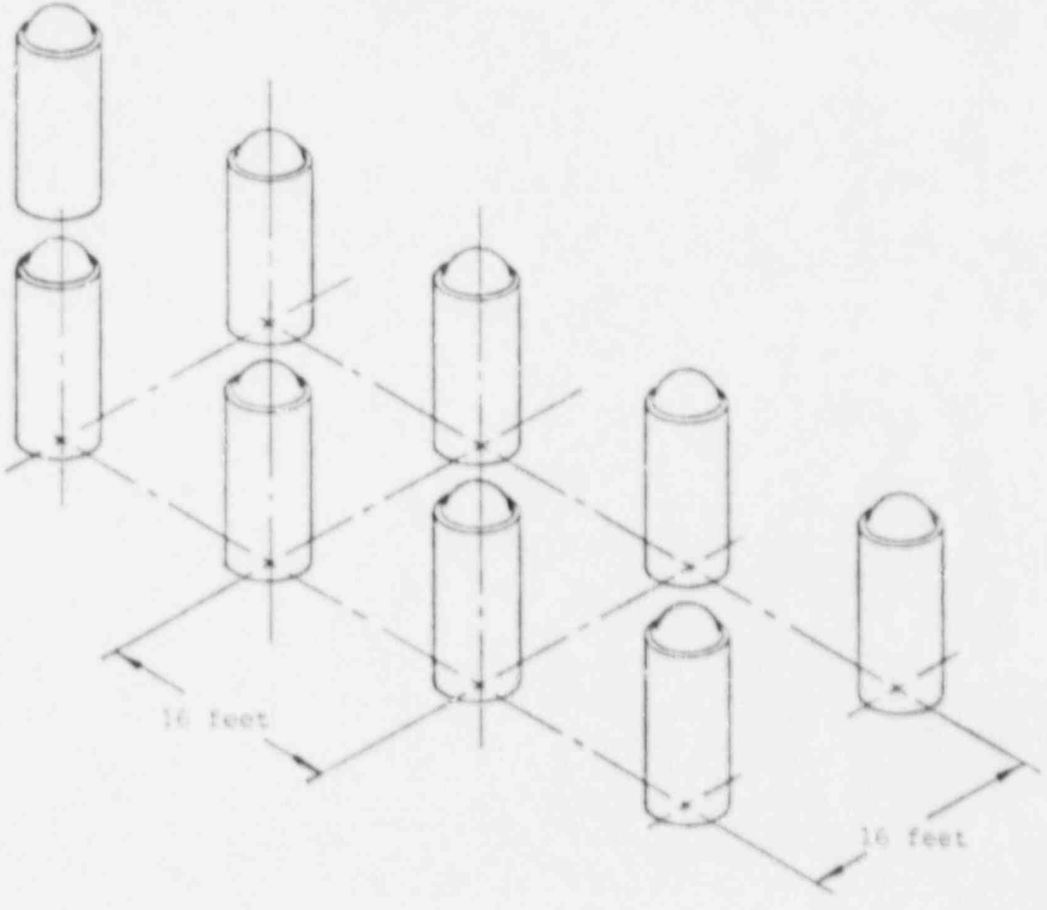

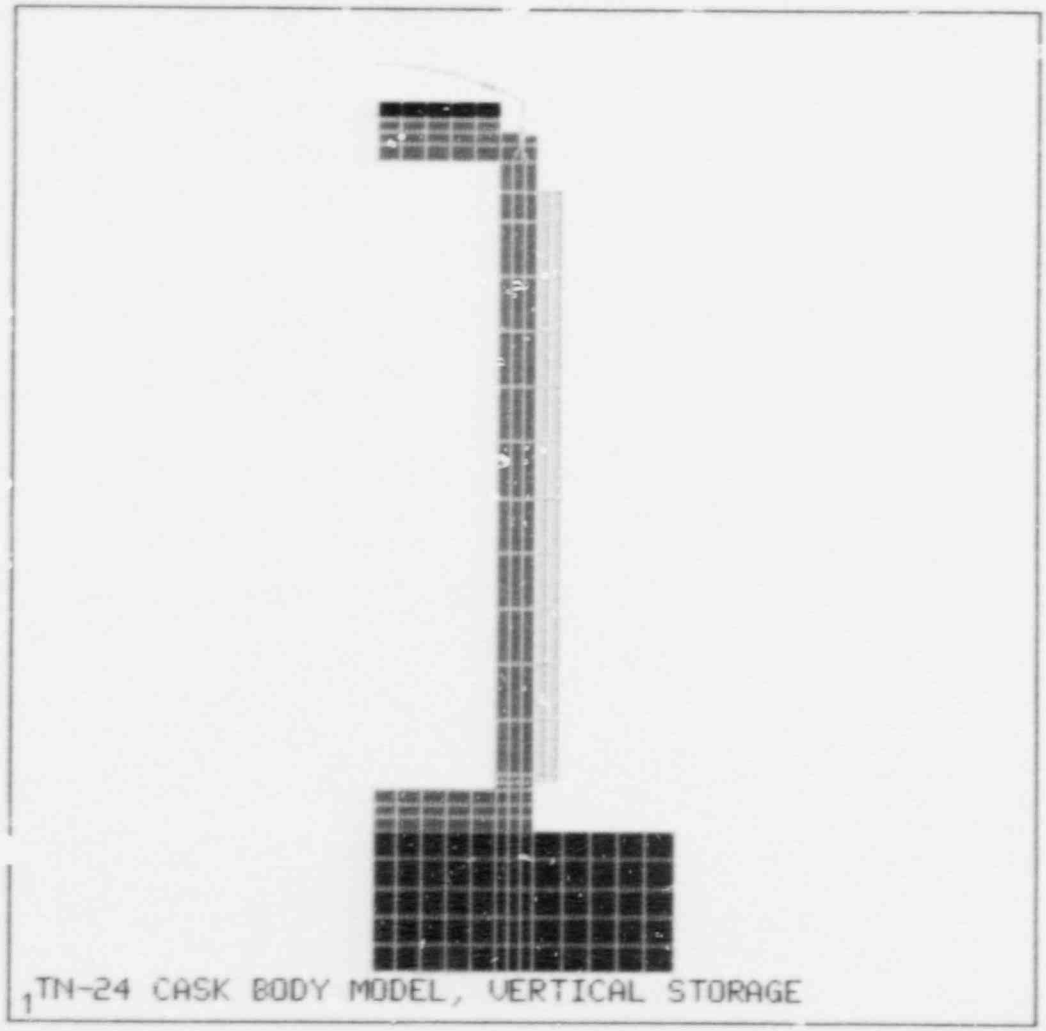

FIGURE 5.1-7

FINITE ELEMENT MODEL FOR THE TN-24 CASK BODY

VERTICAL STORAGE

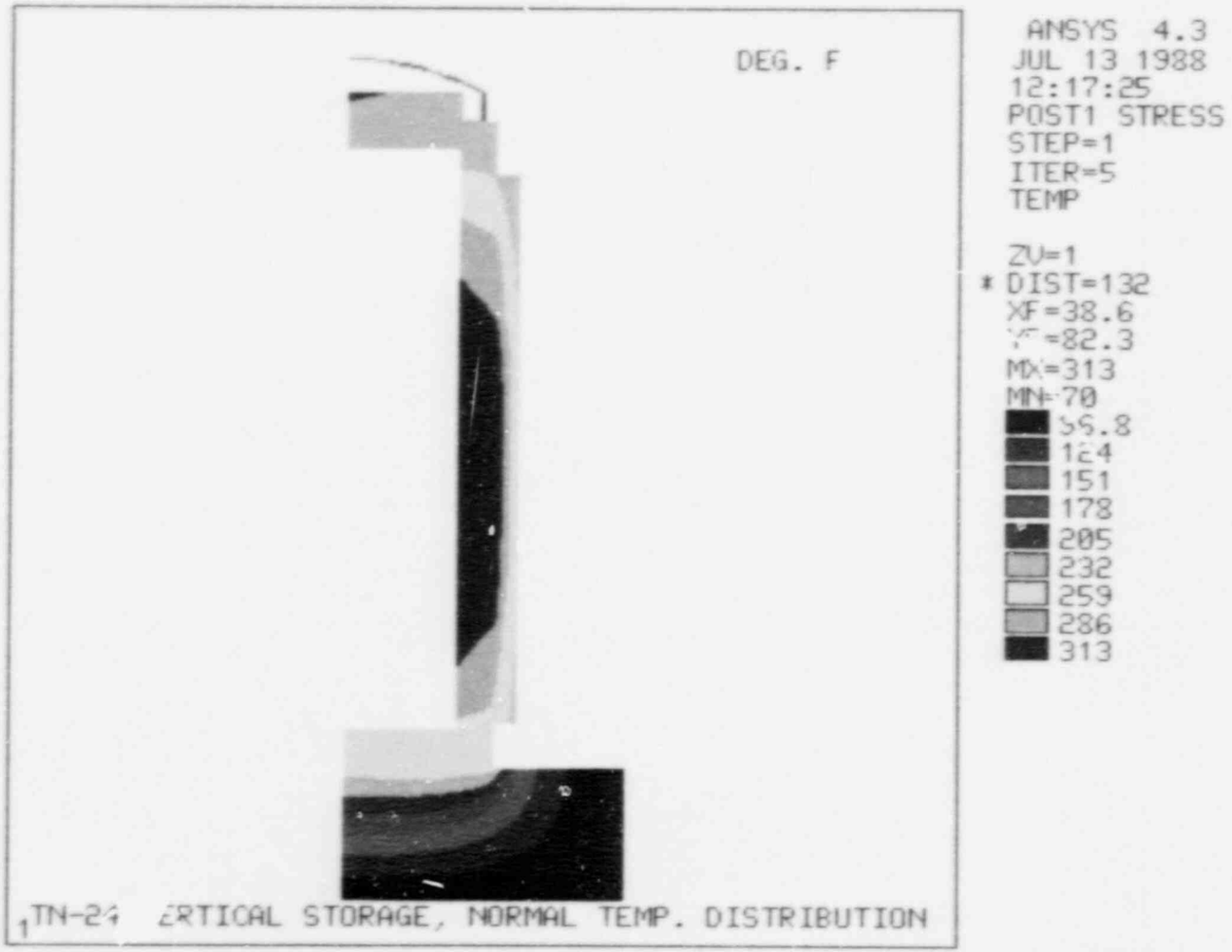

FIGURE 5.1-8

TEMPERATURE DISTRIBUTION IN THE TN-24 CASK BODY

VERTICAL STORAGE - NORMAL CONDITIONS

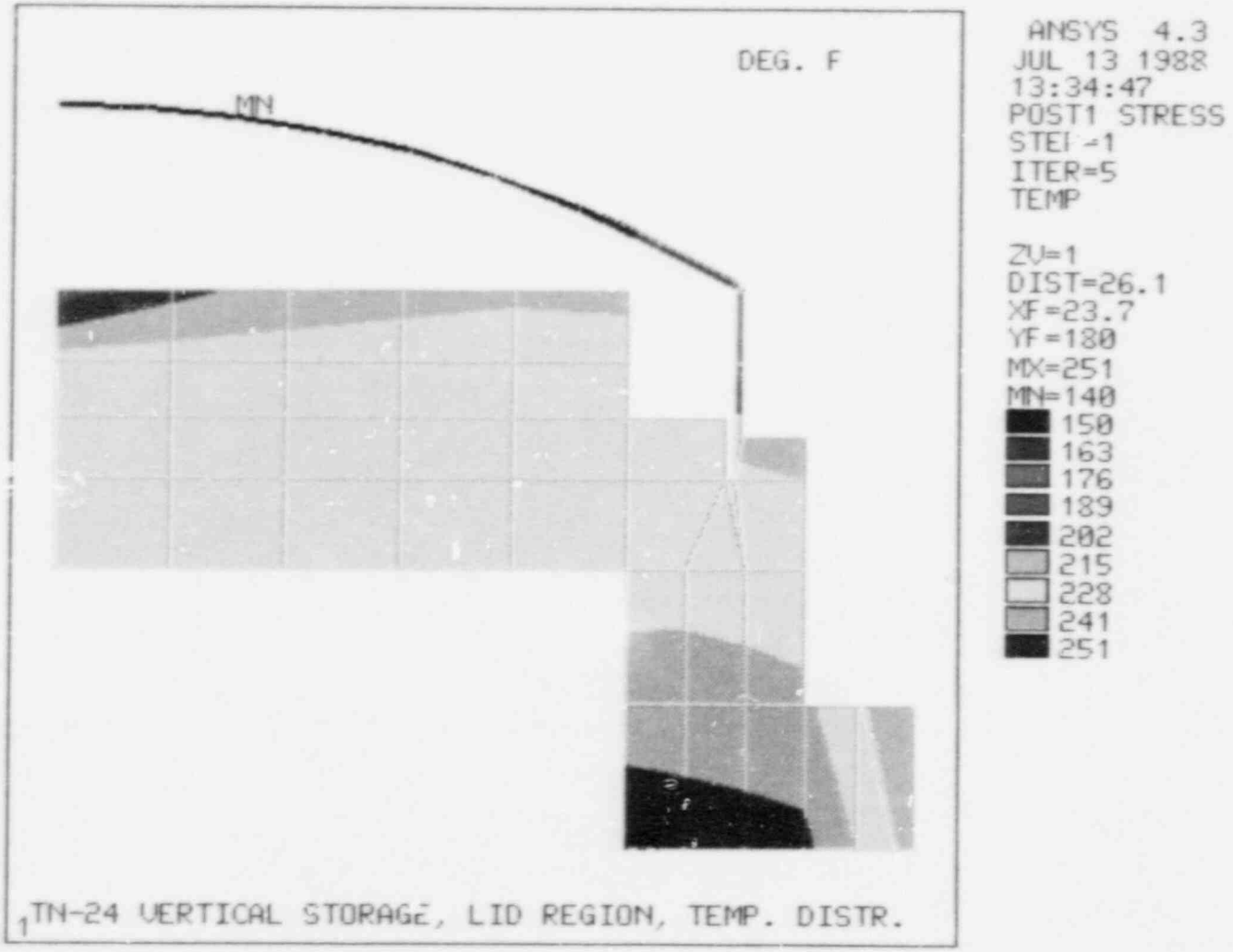

FIGURE 5.1-9

TEMPERATURE DISTRIBUTION IN THE TN-24 LID REGION

VERTICAL STORAGE - NORMAL CONDITIONS

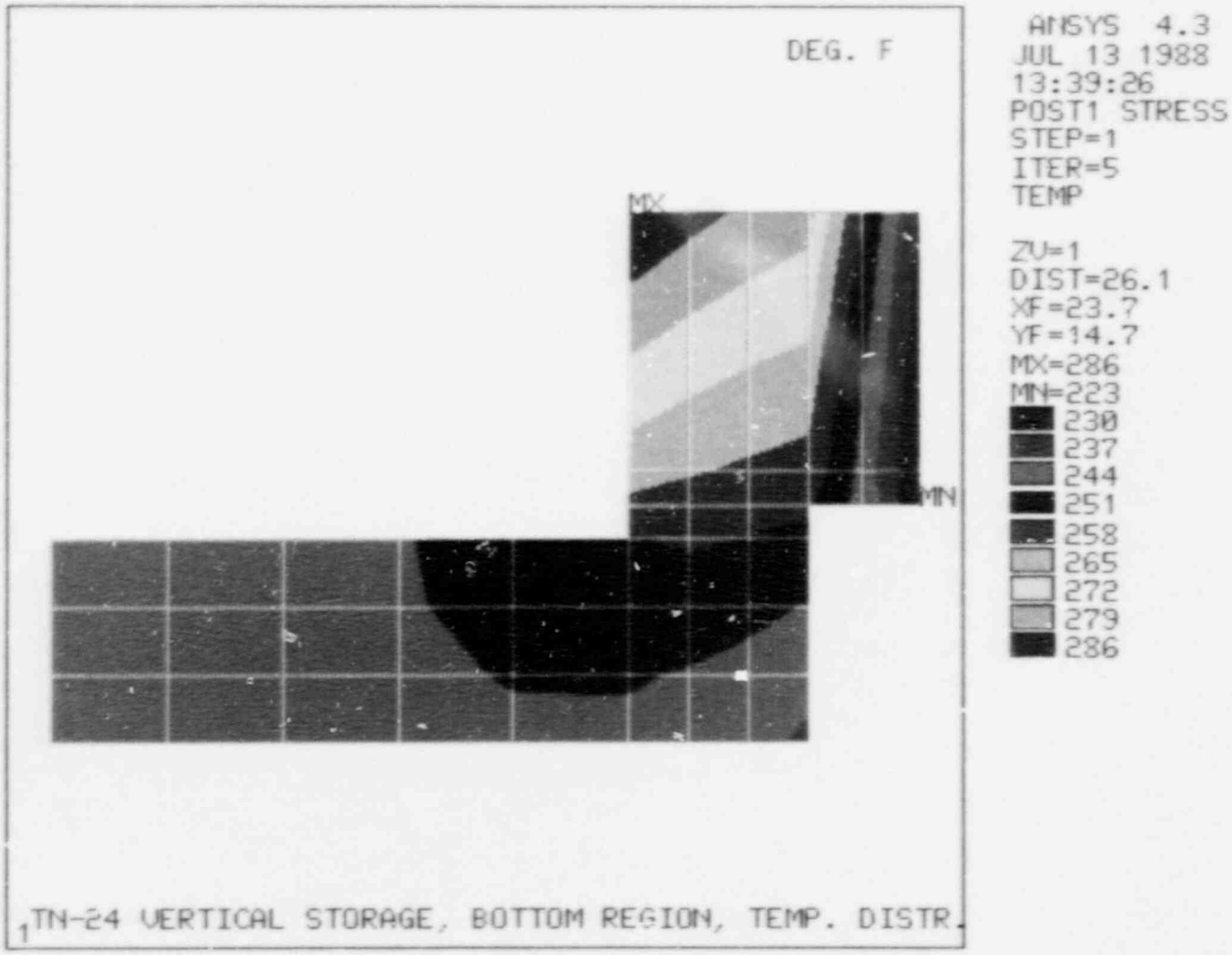

FIGURE 5.1-10

TEMPERATURE DISTRIBUTION IN THE TN-24 BOTTOM REGION

VERTICAL STORAGE - NORMAL CONDITIONS

FIGURE 5.1-11

SKETCH OF THERMAL MODEL FOR TN-24 CASK BODY - HORIZONTAL STORAGE

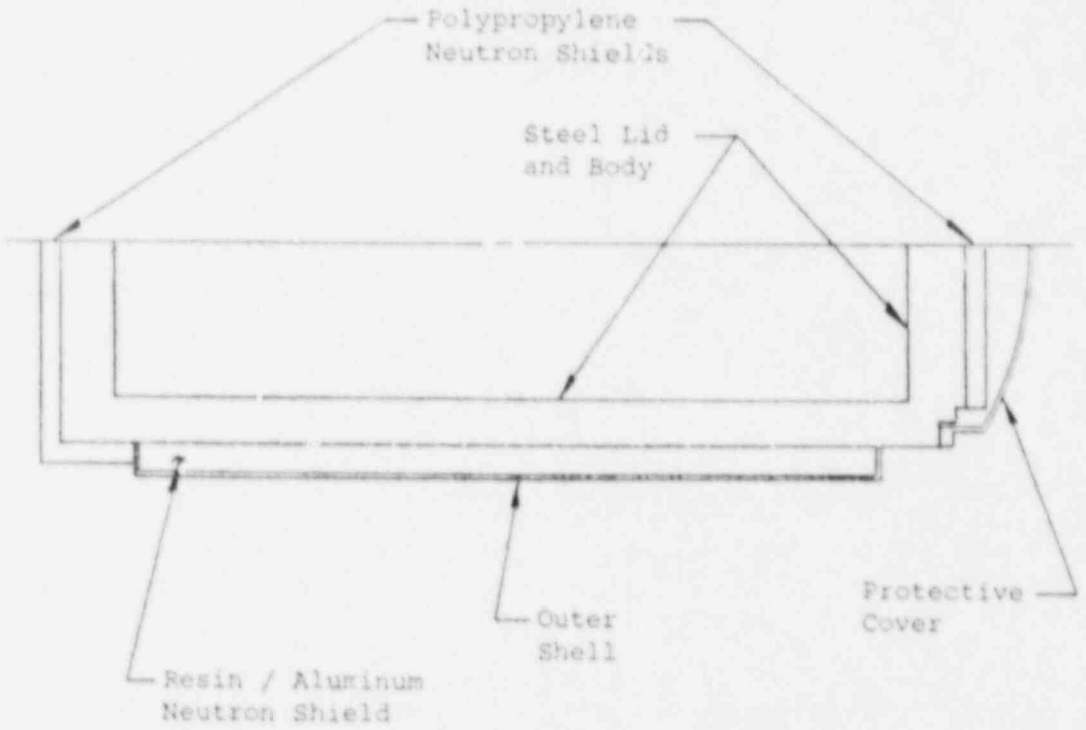

FIGURE 5.1-12

HORIZONTAL STORAGE OF THE TN-24 IN A 2x10 ARRAY

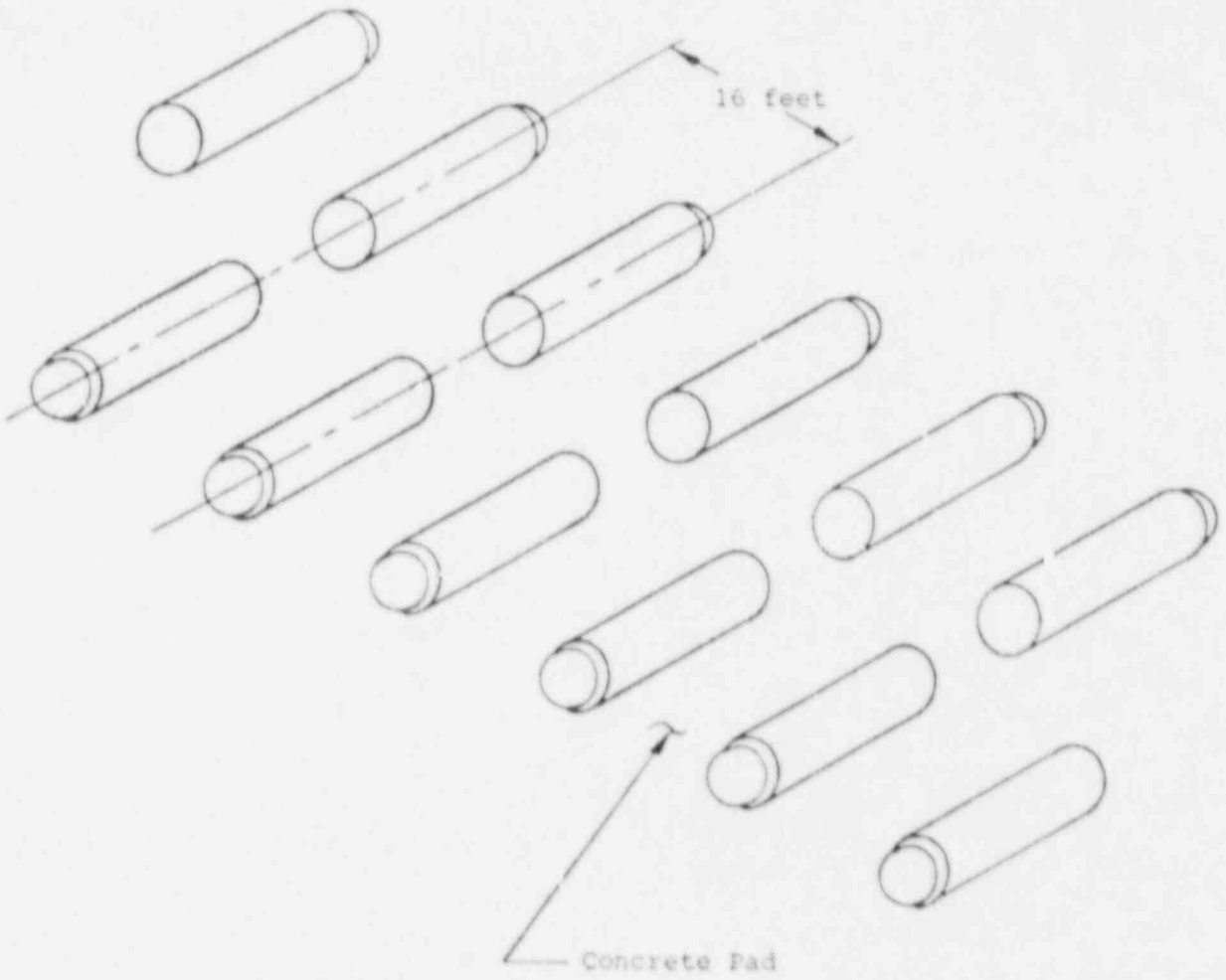

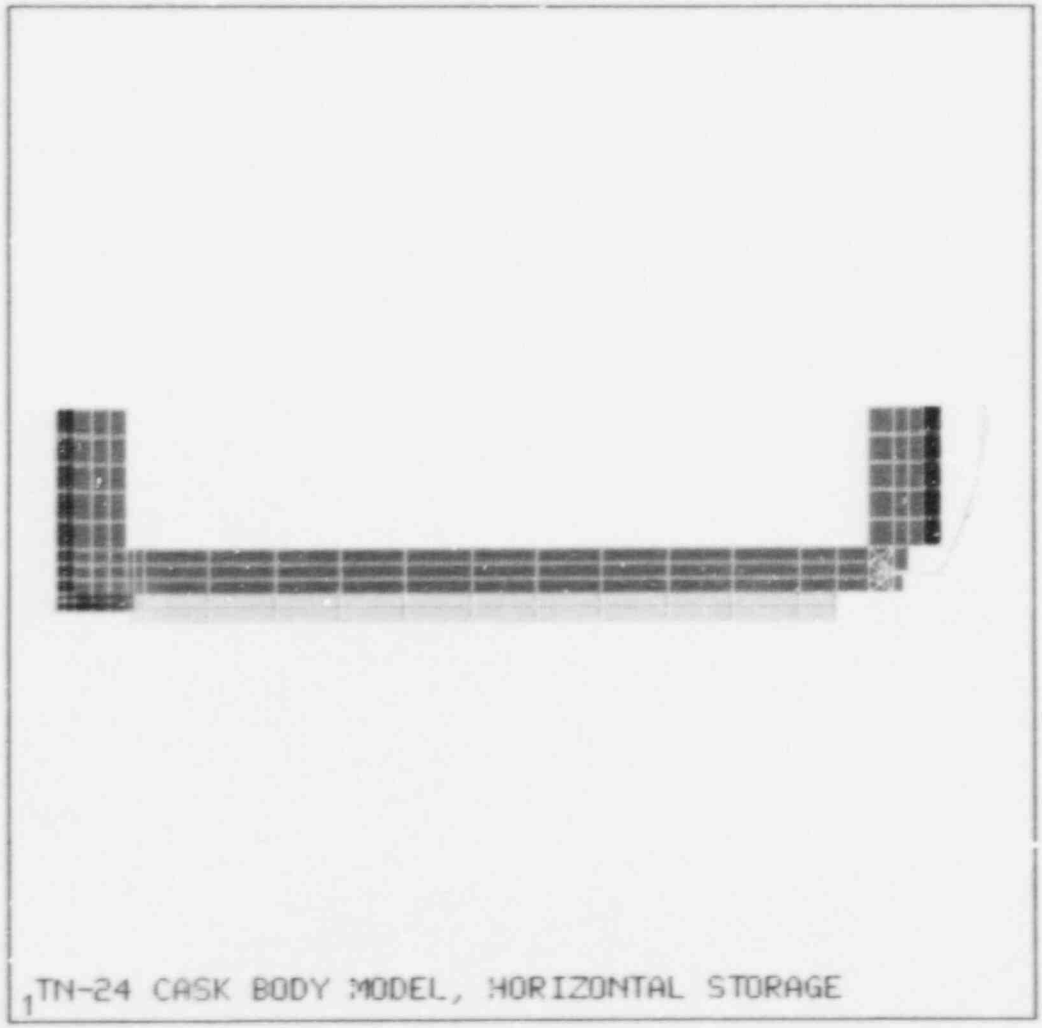

FIGURE 5.1-13

FINITE ELEMENT MODEL FOR THE TN-24 CASK BODY

HORIZONTAL STORAGE

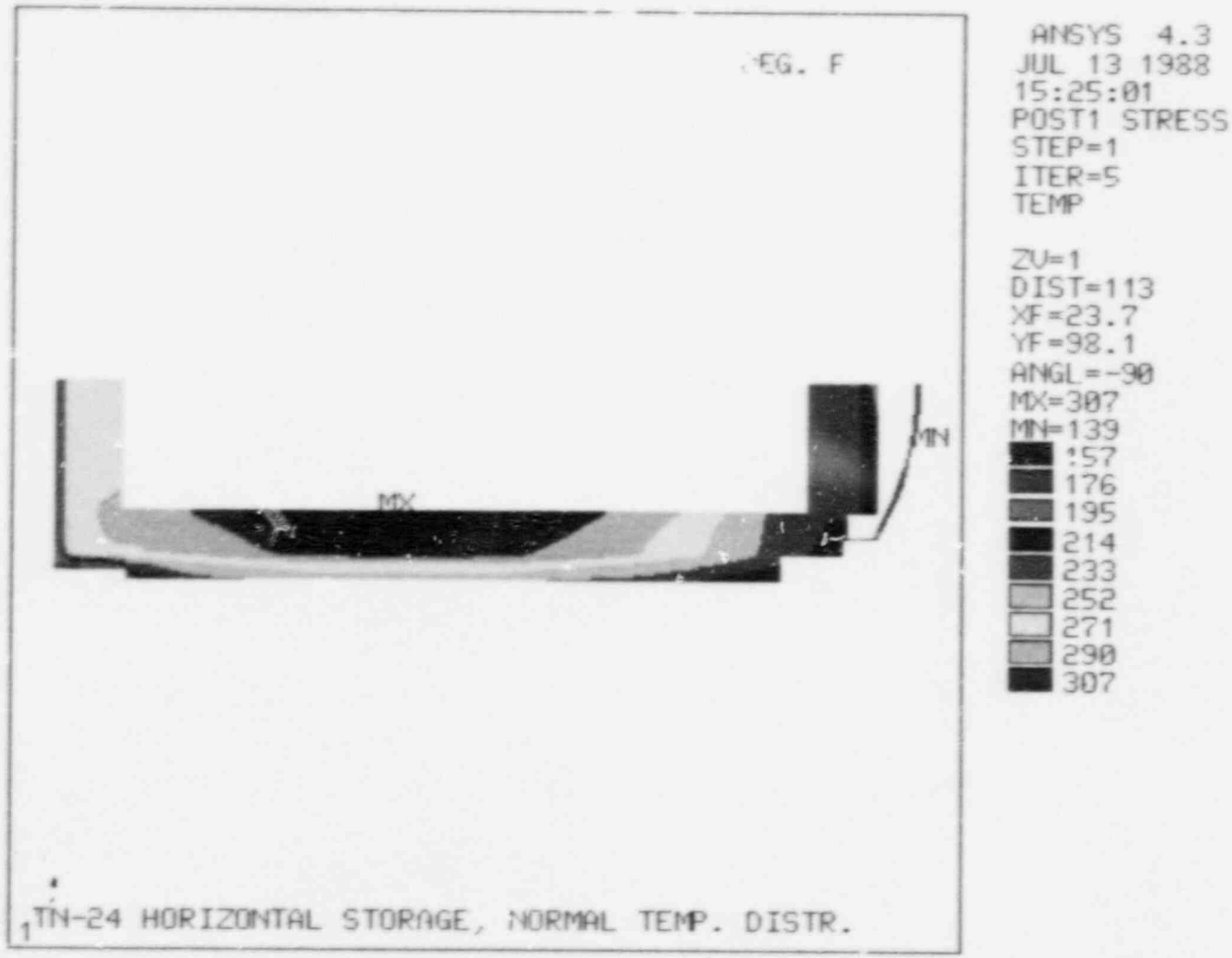

FIGURE 5.1-14

TEMPERATURE DISTRIBUTION IN THE TN-24 CASK BODY

HORIZONTAL STORAGE - NORMAL CONDITIONS

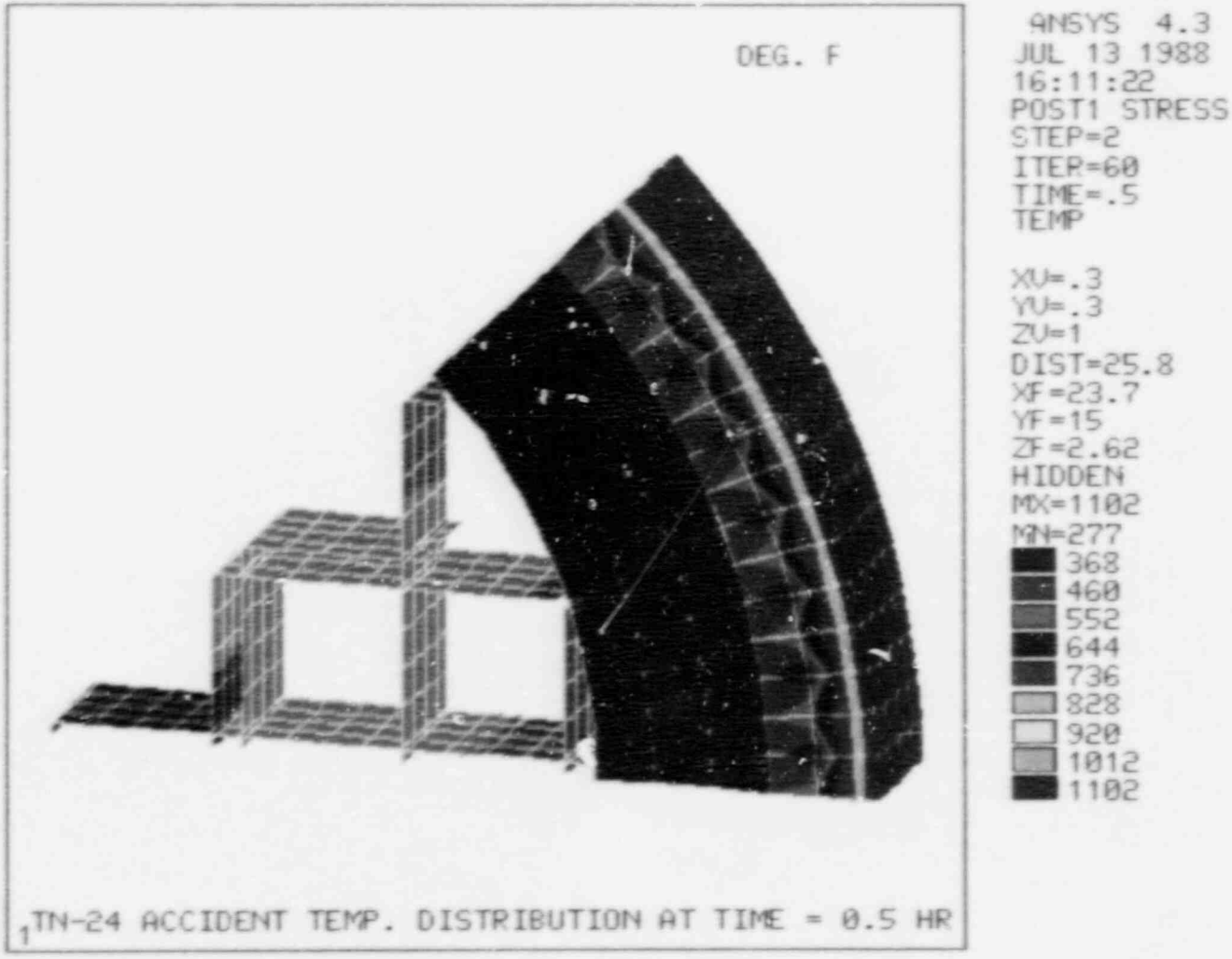

FIGURE 5.1-15

TEMPERATURE DISTRIBUTION IN THE TN-24 PACKAGING CROSS SECTION MODEL AT THE END OF THE THERMAL ACCIDENT

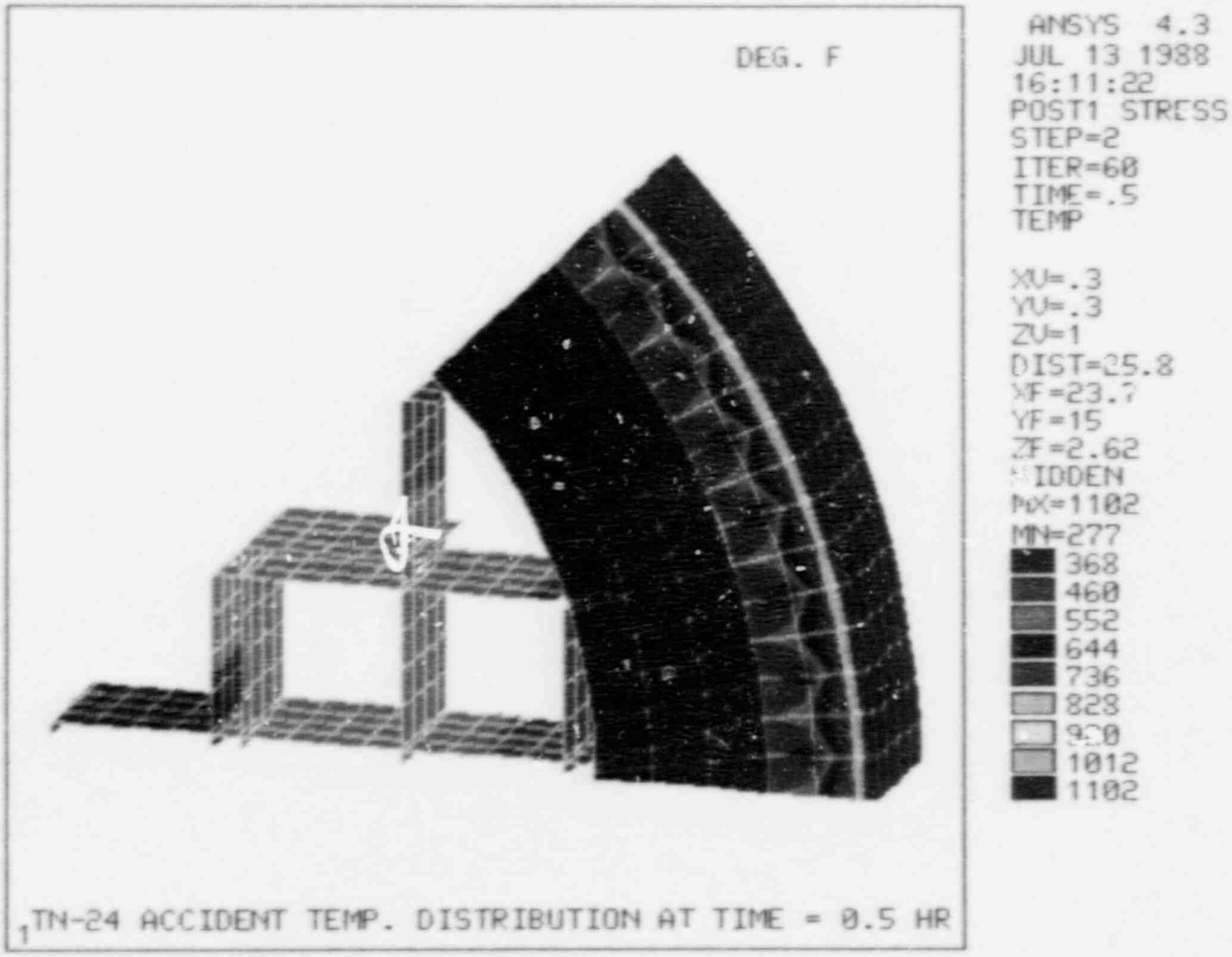

FIGURE 5.1-15

TEMPERATURE DISTRIBUTION IN THE TN-24 PACKAGING CROSS SECTION

MODEL AT THE END OF THE THERMAL ACCIDENT

FIGURE 5.1-16

MAXIMUM TEMPERATURE - TIME HISTORY FOR THE TN-24 PACKAGING DURING ACCIDENT CONDITIONS

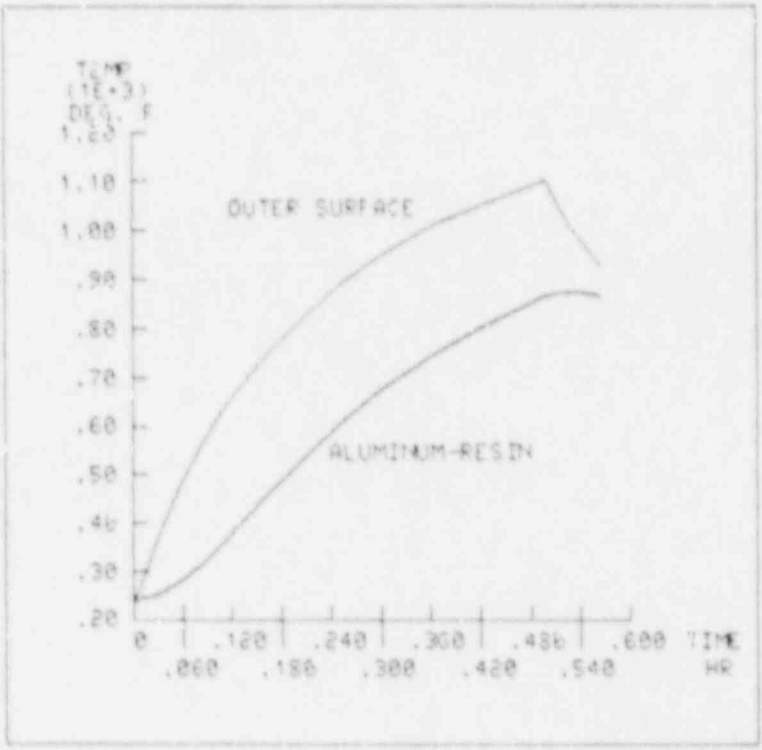

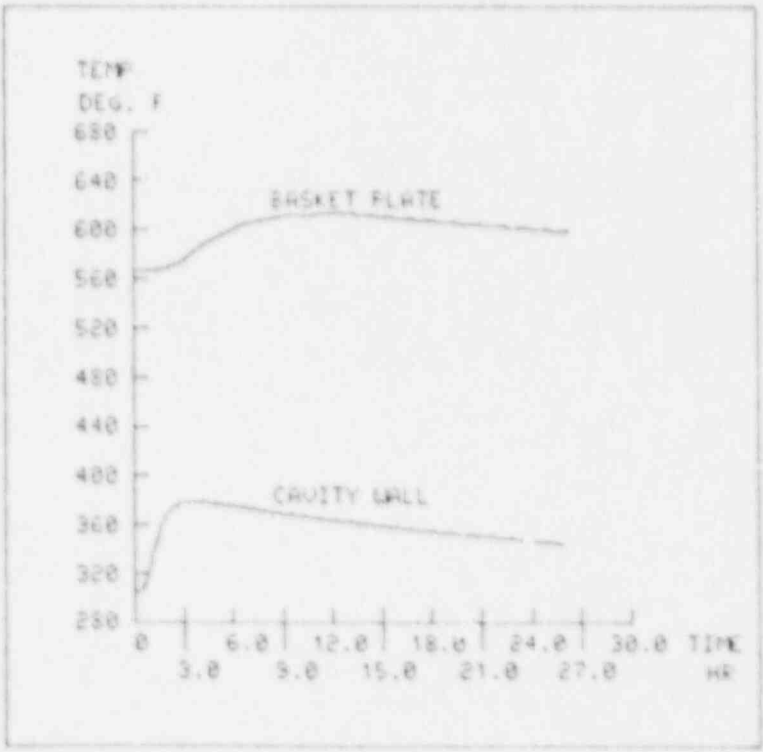

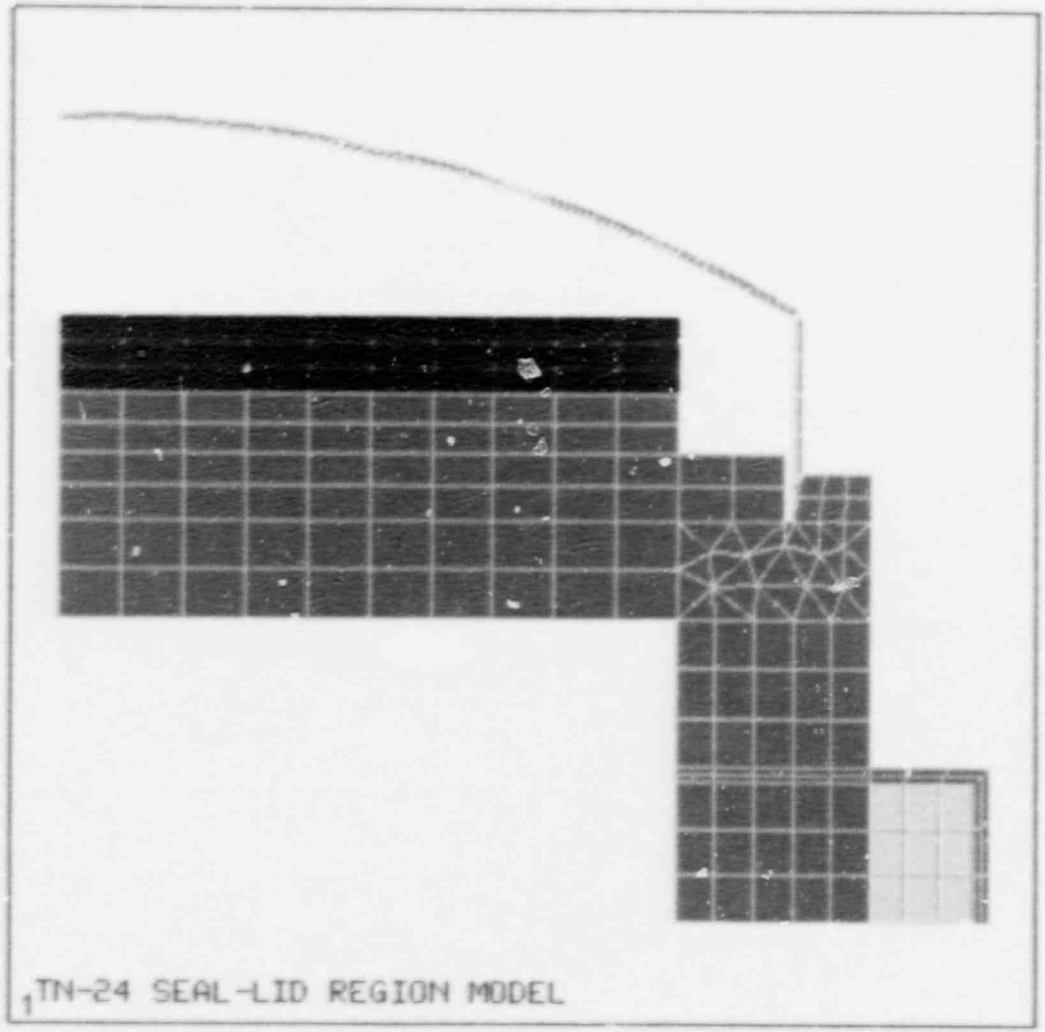

FIGURE 5.1-17

FINITE ELEMENT MODEL FOR THE TN-24 CASK BODY

SEAL-LID REGION MODEL

FIGURE 5.1-18

MAXIMUM TEMPERATURE - TIME HISTORY FOR A BURIED TN-24 PACKAGING

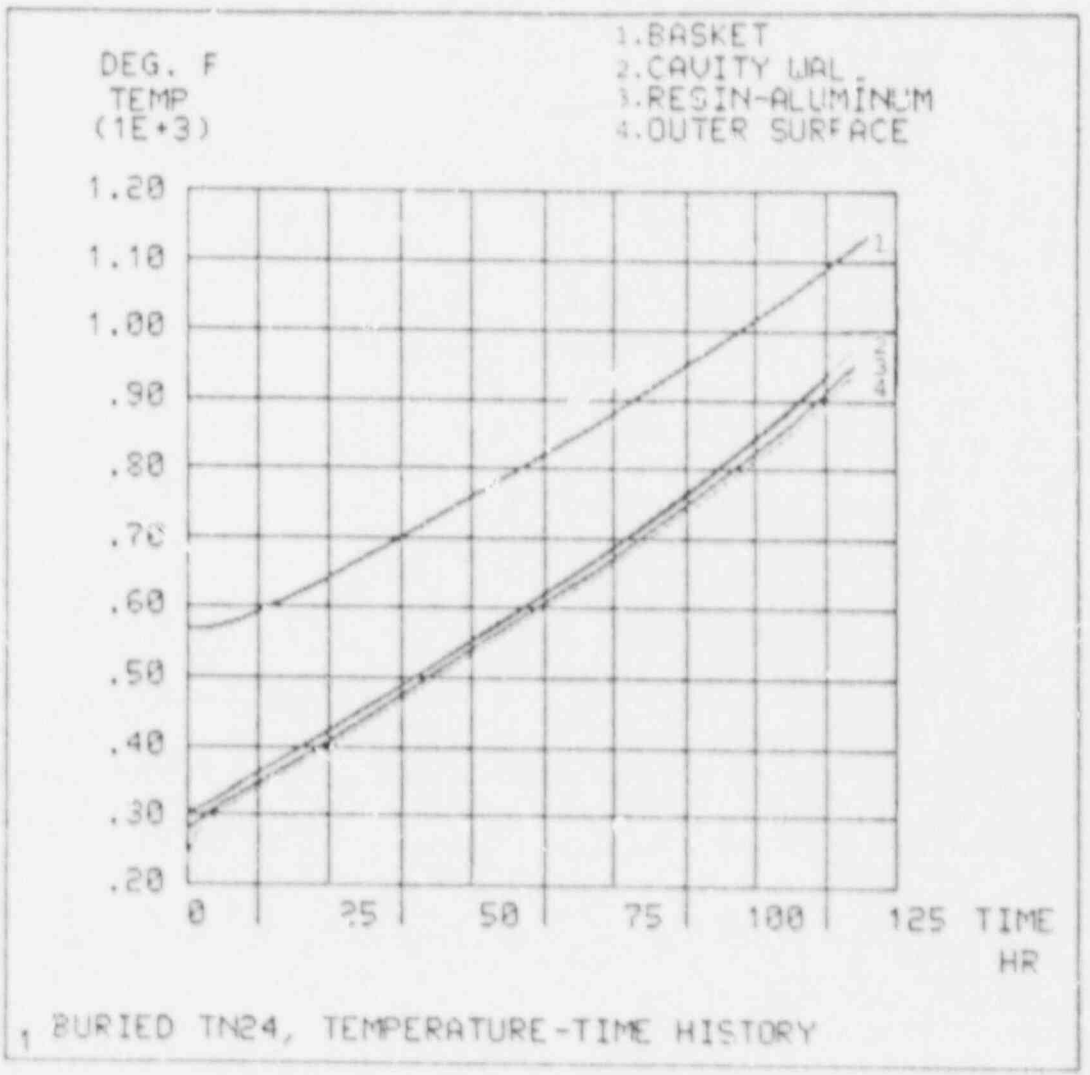

References for Section 5.1

1. "Licensing Requirements for the Storage of Spent Fuel in an Independent Spent Fuel Storage Installation (ISFSI)," 10CFR Part 72, Rules and Regulations, Title 10, Chapter 1, Code of Federal Regulations- Energy, U.S. Nuclear Regulatory Commission, Washington D.C., Jan. 1987.

2. "Packaging and Transportation of Radioactive Material," 10CFR Part 71, Title 10, Chapter 1, Code of Federal Regulations - Energy, U.S. Nuclear Regulatory Commission, Rules and Regulations, Washington, D.C., Jan. 1987.

3. Shappert, L.B., Cask Designers Guide, A Guide for the Design Fabrication and Operation of shipping Casks for Nuclear Applications, Oak Ridge National Laboratory, Oak Ridge, Tenn., Feb. 1970.

4. Levy et. al., Recommended Temperature Limits for Dry Storage of Spent Light Water Reactor Zircaloy-Clad Fuel Rods in Inert Gas, PNL-6189 Pacific Northwest Laboratory, Richland, Wash., May 1987.

5. Rohsenow, W.M., and Hartnett, J.P., Handbook of Heat Transfer, McGraw-Hill Book Co., New York, 1973.

6. "Rules for the Construction of Nuclear Power Plant Components," 1986 ASME Boiler and Pressure Vessel Code, Section III, Division I- Appendices, The American Society of Mechanical Engineers, New York.

7. Kreith, F., Principles of Heat Transfer, Third Edition, Harper & Row, Publishers, New York, 1973.

8. DeSalvo, G.J., and Swanson J.A., ANSYS Engineering Analysis System, User's Manual for ANSYS Revision 4.3, Swanson Analysis Systems, Inc., Houston, PA, June 1987.

9. Bucholz, J.A., Scoping Design Analyses for Optimized Shipping Casks Containing 1-, 2-, 3-, 5-, 7, or 10-year-old PWR Spent Fuel, ORNL/CSD/TM-149, Oak Ridge National Laboratory, Oak Ridge, Tenn., Jan. 1983.

10. Creer et. al, The TN-24P PWR Spent Fuel Storage Cask: Testing and Analyses, EPRI NP-5128, PNL-6054, UC-85, Electric Power Research Institute, Palo Alto, Calif., April 1987.

11. Siegal et. al, Thermal Radiation Heat Transfer, Second Edition, McGraw - Hill Book Co., New York, 1981.

5.2 FUEL HANDLING SYSTEMS

Specific information on fuel handling systems is site-specific and will be provided by the license applicant.

Sections 5-1.1 and 5-1.2 provide a general description of fuel storage operations.

Features of the fuel storage system important to safety are described in Sections 1-2.8 and 3.4.

5.3 OTHER OPERATING SYSTEMS

Component/equipment spares for the TN-24 dry storage cask include the metallic and elastomer seals and the pressure transducer.

The cask is designed with double metallic seals on all containment penetrations. A seal failure can be detected by the pressure monitoring system. Both inner and outer metallic seals would have to fail before seal replacement could become necessary. However, in the unlikely event that this should happen, the protective cover can be replaced by a containment cover (described in Section 4.5).

The containment cover can either be bolted or welded onto the cask. This minimizes radiation exposure by not requiring the lid to be removed and the seals replaced.

Although a pressure transducer can be considered an equipment spare, the design of the pressure monitoring system utilizes three transducers to greatly reduce the possibility of needing to replace one.

Information on any other operating system is site-specific and will be provided by the license applicant.

5.4 OPERATION SUPPORT SYSTEMS

As discussed in Section 3.3, an overpressure system is utilized to provide monitoring of the containment seals. A positive pressure is maintained in the interspace between the double metallic seals. This allows only inleakage to the cavity in case of a seal failure. The pressure in the over pressure system is monitored by pressure transducers. For reliability and redundancy, three transducers are mounted on the over pressure tank. The pressure tranducers employ a four arm strain guage bridge bonded to the reference side of a stainless steel diaphragm. The housing is also stainless steel. It is temperature compensated and has an operating temperature range of -65°F to 250°F. The tranducers produce an output which can be connected to a monitor and/or alarm to provide continuous monitoring. A reduction in pressure in the over pressure system is indicative of a leak which can be investigated. A malfunction of the overpressure system has no safety consequences since the containment is not affected.

5.5 CONTROL ROOM AND/OR CONTROL AREA

Information on control room and/or control areas is site-specific.

5.6 ANALYTICAL SAMPLING

Provisions for analytical sampling are site-specific.

6. WASTE CONFINEMENT AND MANAGEMENT

Since the TN-24 dry storage casks are permanently sealed and completely passive in operation, all radioactive materials are contained and no radioactive waste treatment is required.

Any radioactive wastes generated during loading and decontamination operations within a nuclear plant facility prior to transfer to the ISFSI are handled by the plant's radwaste systems.

The only waste products resulting from cask operation would be a few gloves and swipes that might be slightly contaminated during periodic cask inspection and maintenance.

As shown in Section 3.3.2.2, for normal operations during the twenty year storage life there will be no out leakage of gas from the cavity because the over pressure system will be maintained at a higher pressure than the cavity.

7. RADIATION PROTECTION

7.1 ENSURING THAT OCCUPATIONAL RADIATION EXPOSURES ARE AS LOW AS IS REASONABLY ACHIEVABLE (ALARA)

7.1.1 Policy Considerations

Management policies and organizational structure to maintain exposures As Low As is Reasonably Achievable (ALARA) at an ISFSI are the responsibility of the license applicant.

7.1.2 Design Considerations

The TN-24 dry storage cask incorporates several design features to keep radiation exposures ALARA. The applicable design considerations set out in regulatory position 2 of Regulatory Guide 8.8[1] are followed as described below:

a. Access control of Radiation Areas will be met by a fenced controlled zone surrounding the cask storage area. The cask over pressure system will provide remote signals to an area in the control zone with a low radiation field.

b. Radiation shielding is provided by the cask components. The thick steel lid, bottom and cask wall provide gamma shielding. The radial layer of resin and the disc of polypropylene on the lid provide neutron shielding.

c. Process instrumentation is not utilized. The over pressure system instrumentation is selected for long service and low maintenance requirements. It is designed for a remote signal indication.

d. Control of airborne contamination is provided because no gaseous releases are expected and no significant contamination of the cask surface is expected.

e. Crud control is not applicable to an ISFSI.

f. Decontamination is provided because the casks are decontaminated prior to acceptance for storage.

g. Radiation monitoring is met because the casks are sealed and a pressure monitoring system is utilized to monitor the seals.

h. Resin treatment is not applicable.

i. Other features are not applicable.

7.1.3 Operational Consideration

The TN-24 dry storage cask is designed to be essentially maintenance free. It is a passive system without any moving parts. The double metallic O-ring concept with continuous surveillance of the over pressure system guarantees that in the unlikely event of a failure of one of the seals, adequate time is available to restore the cask leak tightness.

The only cask repair procedures that could conceivably be envisioned are those associated with 1) seal replacement, 2) installation of containment cover, or 3) transducer replacement. For the replacement of a lid seal, the cask would be returned to a spent fuel pool to minimize radiation exposure to personnel. Other seal replacements or transducer replacement can be performed efficiently at the storage site. The replacement of the protective cover with a containment cover would also be performed at the storage site.

The only anticipated maintenance procedures are visual inspection (and possibly paint touch-up) and calibration of the over pressure system.

References for Section 7.1

1. "Information Relavent to Ensuring That Occupational Radiation Exposures at Nuclear Power Stations Will Be As Low As Is Reasonably Achievable", Regulatory Guide 8.8, U.S. Nuclear Regulatory Commission, Washington D.C., June 1978.

7.2 RADIATION SOURCES

7.2.1 Characterization of Sources

There are five principal sources of radiation of concern for radiation protection:

(1) Primary gamma radiation from spent fuel.
(2) Primary neutron radiation from spent fuel.
(3) Gamma radiation from activated fuel structural materials.
(4) Capture gamma radiation produced by attenuation of neutrons by shielding material of the cask.
(5) Neutrons produced by sub-critical fission in fuel.

Primary gamma and neutron radiation sources are generated by using the ORIGEN2[1] computer code. A 3.3% enrichment Westinghouse 17x17 fuel assembly, as described in Section 3.1.1, is modeled in three zones for the ORIGEN2 calculation[2]. The structural material masses are taken from Ref. 2 and are listed in Table 7.2-1. The structural material compositions and fuel impurities are also taken from Ref. 2. In particular, the cobalt impurities in Inconel, Nicrobraze and stainless steel are 0.47%, 0.038% and 0.08% respectively.

The fuel zone is irradiated at a constant specific power of 37.5 MW/MTU to a total burnup of 35,000 MWD/MTU. A conservative three-cycle operating history is utilized with 20% down time each cycle except for no down time in the last cycle. After the fuel zone irradiation, the flux generated by ORIGEN2 for the fuel zone is used to irradiate the plenum and end zones. However, the methodology of Ref. 2 is used to correct the plenum and end zone

irradiations. The cobalt, zircaloy and manganese masses in the structural materials are multiplied by 0.67, 0.40 and 0.80 respectively and the irradiation flux for the plenum and end zones is multiplied by 0.011 and 0.042 respectively. Those factors are used to correct for the spatial and spectral changes of the neutron flux outside of the fuel zone.

Gamma and neutron sources are generated for cooling time from 5 years to 40 years.

Table 7.2-2 shows the total primary gamma source and neutron source. Fission product activities are listed on Table 7.2-3.

The primary gamma source spectrum, group structure and ANSI/ANS-6.1.1 flux-to-dose factors are listed in Table 7.2-4. The energy groups are those output by ORIGEN2.

The neutron source consists of spontaneous fission and alpha-n reactions mainly from Cm244. Spectra for both mechanisms are obtained from Ref. 3. However the spectra of Ref. 3 must be converted into the proper neutron energy groups of the SCALE 27n-18γ library[4]. This is accomplished by apportioning the Cm244 spectra into the SCALE energy groups. For example, SCALE Group 6 contains neutrons with energies between 0.4 and 0.9 MeV. This encompasses two groups and part of a third of the Ref. 3 spontaneous fission spectrum (i.e., 0.4-0.6, 0.6-0.8 and 0.8-1.0). Therefore the fraction in SCALE Group 6 is:

$$0.07973 + 0.08156 + 0.07056 * \frac{0.9-0.8}{1.0-0.8} = 0.1966$$

The spectra from Ref. 3 for both spontaneous fission and alpha-n reactions are converted into "equivalent" neutron spectra in the SCALE energy groups in this manner. A single combined neutron spectrum is then calculated using 93.5% spontaneous fission and 6.5% alpha-n. Those percentages are obtained from the ORIGEN2 output. Table 7.2-5 lists the neutron spectra.

The primary gamma spectrum is also converted into the SCALE 27n-18g energy groups. In addition to simple apportioning of overlapping groups as is done above for the neutrons, the gammas are weighted by the ratio of the ORIGEN2 and SCALE library average group energies because ORIGEN2 weights the photon yields in this fashion. Table 7.2-6 lists this spectrum and ANSI flux-to-dose factors for the SCALE energy groups.

Gamma radiation produced by capture of neutrons in shielding materials is computed in the shielding analysis with the coupled SCALE 27n-18g neutron-gamma library. Similarly, neutrons produced from sub-critical multiplication are accounted for in the shielding calculation.

7.2.2 Airborne Radioactive Material Sources

Since the radioactive sources are safely confined both within the fuel cladding and within the cask containment during storage, provisions for personnel protective measures against airborne sources are not required.

The quantity of fission gas produced in a typical PWR assembly for the design irradiation condition is approximately 550 liters at STP[4]. Of this quantity, only a small fraction is radioactive with Kr85 being the dominant nuclide. Most of the fission products generated are retained within the fuel pellet. A small fraction, nominally 10% for noble gases, is released into the fuel rod plenums. Table 7.2-7 shows the inventory of fission gases and volatile nuclides contained in 24 of the design basis fuel assemblies.

TABLE 7.2-1

MATERIAL DISTRIBUTION IN PWR FUEL ASSEMBLY

	Material	Mass kg/MTU	Mass kg/assembly
Fuel Zone			
Cladding	Zircaloy-4	223.0	102.9
Grid spacers and grid-spacer springs	Inconel 718	12.8	5.9
Grid-brazing material	Nicrobraze 50	2.6	1.2
Miscellaneous	SS 304[a]	9.9	4.6
Fuel-gas Plenum Zone			
Cladding	Zircaloy-4	12.0	
Plenum spring	SS 302	4.2	1.9
End Fitting Zone			
Top end fitting	SS 304	14.8	6.8
Bottom end fitting	SS 304	12.4	5.7
Total		291.7	134.5

[a] Distributed throughout the PWR core in sleeves and so forth.

TABLE 7.2-2

GAMMA AND NEUTRON RADIATION SOURCES (5 YEAR COOLING TIME)

Fission Product Activit/ (Curie/Assembly)	2.24E5
Neutron Source (n/sec/Assembly)	1.43E8
Fuel Zone Gamma Source (γ/sec/Assembly)	8.16E15
Plenum Zone Gamma Source (γ/sec/Assembly)	3.60E11
End Zone Gamma Source (γ/sec/Assembly)	5.12E11*

*Upper Fitting (54.4%), Lower Fitting (45.6%)

TABLE 7.2-3

Fission Product Activities (Curies/MTU)

Nuclide	Discharge	Five -Yr	Ten -Yr
H 3	5.82E+02	4.40E+02	3.32E+02
KR 85	9.83E+03	7.11E+03	5.15E+03
SR 89	8.65E+05	1.12E-05	1.46E-16
SR 90	7.67E+04	6.81E+04	6.05E+04
Y 90	8.10E+04	6.81E+04	6.05E+04
Y 91	1.14E+06	4.59E-04	1.84E-13
ZR 95	1.64E+06	4.18E-03	1.07E-11
NB 95	1.64E+06	9.29E-03	2.37E-11
RU103	1.67E+06	1.68E-08	1.75E-22
RH103M	1.50E+06	1.52E-08	1.58E-22
RU106	5.87E+05	1.88E+04	6.05E+02
RH106	6.65E+05	1.88E+04	6.05E+02
AG110	1.81E+05	4.00E-01	2.52E-03
SB125	1.50E+04	4.34E+03	1.24E+03
TE125M	3.14E+03	1.06E+03	3.03E+02
TE129	3.38E+05	1.43E-12	0.00E+00
CS134	1.68E+05	3.13E+04	5.82E+03
CS137	1.10E+05	9.80E+04	8.73E+04
BA137M	1.04E+05	9.27E+04	8.26E+04
CE141	1.66E+06	2.05E-11	2.53E-28
CE144	1.20E+06	1.39E+04	1.62E+02
PR144	1.21E+06	1.39E+04	1.62E+02
PM147	1.29E+05	3.66E+04	9.77E+03
PM148	2.84E+05	7.73E-11	3.80E-24
SM151	3.71E+02	3.64E+02	3.50E+02
EU154	1.16E+04	7.78E+03	5.20E+03
EU155	7.13E+03	3.55E+03	1.76E+03
Total	1.76E+08	4.85E+05	3.22E+05

TABLE 7.2-4

PRIMARY GAMMA SOURCE SPECTRUM

ORIGEN2 GROUP STRUCTURE

Avg Energy (MeV)	Flux-to-Dose Factor (mrem/hr/ϕ)	γ/s/24 Assemblies			
		Fuel Zone	Plenum Zone	Top Fitting	Bottom Fitting
0.125	3.26E-4	6.465E15	6.218E9	2.813E9	2.357E9
0.225	5.66E-4	6.125E15	3.850E10	9.252E8	7.752E8
0.375	9.33E-4	3.350E15	2.226E11	2.594E8	2.174E8
0.575	1.31E-3	6.038E16	2.858E11	1.495E7	1.253E7
0.850	1.76E-3	1.334E16	1.249E11	1.127E11	9.445E10
1.25	2.32E-3	6.300E15	7.066E12	6.314E12	5.292E12
1.75	2.93E-3	1.017E14	---	---	---
2.25	3.47E-3	5.472E13	---	---	---
2.75	3.96E-3	1.698E12	---	---	---
3.50	4.63E-3	2.171E11	---	---	---

TABLE 7.2-5

NEUTRON SOURCE DISTRIBUTION

SCALE Group	Alpha-n Spectrum	SF Spectrum	Combined Spectrum	n/sec*
1	0.0	0.01883	0.01761	6.041E7
2	0.25271	0.20958	0.21238	7.284E8
3	0.52336	0.22657	0.24586	8.434E8
4	0.13084	0.13081	0.13081	4.488E8
5	0.06978	0.17915	0.17194	5.899E8
6	0.01981	0.19657	0.18508	6.348E8
7	0.00349	0.03849	0.03622	1.242E8
	1.0	1.0	0.99990	3.43E9

* For 24 assemblies

TABLE 7.2-6

Parameters For The SCALE 27n-18g Library

Group No.	Max Energy (eV)	Flux-Dose Factor (rem/hr/ϕ)	Primary Gamma* (γ/sec)
1	2.000E+07	1.492E-04	0.000E+00
2	6.434E+06	1.446E-04	0.000E+00
3	3.000E+06	1.270E-04	0.000E+00
4	1.850E+06	1.281E-04	0.000E+00
5	1.400E+06	1.298E-04	0.000E+00
6	9.000E+05	1.028E-04	0.000E+00
7	4.000E+05	5.118E-05	0.000E+00
8	1.000E+05	1.232E-05	0.000E+00
9	1.700E+04	3.837E-06	0.000E+00
10	3.000E+03	3.725E-06	0.000E+00
11	5.500E+02	4.015E-06	0.000E+00
12	1.000E+02	4.293E-06	0.000E+00
13	3.000E+01	4.474E-06	0.000E+00
14	1.000E+01	4.568E-06	0.000E+00
15	3.050E+00	4.558E-06	0.000E+00
16	1.770E+00	4.519E-06	0.000E+00
17	1.300E+00	4.488E-06	0.000E+00
18	1.130E+00	4.466E-06	0.000E+00
19	1.000E+00	4.435E-06	0.000E+00
20	8.000E-01	4.327E-06	0.000E+00
21	4.000E-01	4.198E-06	0.000E+00
22	3.250E-01	4.098E-06	0.000E+00
23	2.250E-01	3.839E-06	0.000E+00
24	1.000E-01	3.675E-06	0.000E+00
25	5.000E-02	3.675E-06	0.000E+00
26	3.000E-02	3.675E-06	0.000E+00
27	1.000E-02	3.675E-06	0.000E+00
28	1.000E+07	8.772E-06	0.000E+00
29	8.000E+06	7.478E-06	0.000E+00
30	6.500E+06	6.375E-06	0.000E+00
31	5.000E+06	5.414E-06	0.000E+00
32	4.000E+06	4.622E-06	2.171E+11
33	3.000E+06	3.960E-06	1.698E+12
34	2.500E+06	3.469E-06	5.472E+13
35	2.000E+06	3.019E-06	6.613E+13
36	1.660E+06	2.628E-06	1.828E+15
37	1.330E+06	2.205E-06	4.494E+15
38	1.000E+06	1.833E-06	8.400E+15
39	8.000E+05	1.523E-06	2.522E+16
40	6.000E+05	1.173E-06	4.250E+16
41	4.000E+05	8.759E-07	0.000E+00
42	3.000E+05	6.306E-07	0.000E+00
43	2.000E+05	3.834E-07	0.000E+00
44	1.000E+05	2.669E-07	0.000E+00
45	5.000E+04	9.347E-07	0.000E+00

* For 24 assemblies

TABLE 7.2-7

FISSION GAS AND VOLATILE NUCLIDES INVENTORY
(Curies/24 Assemblies)

Nuclide	5 Year Decay	10 Year Decay
H-3	7.12E3	5.38E3
Kr-85	7.85E4	5.69E4
Cs-134	3.45E5	6.43E4
Cs-137	1.08E6	9.64E5

References for Section 7.2

1. "ORIGEN2 - Isotope Generation and Depletion Code," CCC-371, Oak Ridge National Laboratory, Oak Ridge, Tenn., January 1987.

2. A.G. Croff, et. al., Revised Uranium - Plutonium Cycle PWR and BWR Models for the ORIGEN Computer Code. ORNL/TM-6051, Oak Ridge National Laboratory, Oak Ridge, Tenn., September 1978.

3. Bucholz, J.A., Scoping Design Analyses for Optimized Shipping Casks Containing 1-, 2-, 3-, 5-, 7-, and 10-Year-Old PWR Spent Fuel, ORNL/CSD/TM-149, Oak Ridge National Laboratory, Oak Ridge, Tenn., January 1983.

4. "Extended Fuel Burnup Demontstration Program Topical Report - Transport Considerations for Transnuclear Casks," DOE/ET 34014-11, Transnuclear, Inc., White Plains, New York, Dec. 1'83

7.3 RADIATION PROTECTION DESIGN FEATURES

7.3.1 Installation Design Features

A description of the installation design features is site specific and will be provided by the applicant. A general description of the installation is covered in Sections 1.2 and 1.3. Generically, there are a number of design features to ensure that exposures are ALARA.

a. There are no radioactive systems other than the storage casks which contain sources as described in Section 7.2

b. The casks are loaded and sealed prior to transfer to the ISFSI.

c. Fuel is not unloaded at the ISFSI.

d. The casks are heavily shielded to minimize dose rates. The shielding design features of the cask are discussed in Section 7.3.2 below.

e. The casks are stored in a controlled area at the ISFSI.

f. No radioactive materials will be discharged during storage.

Design features relevant to Regulatory Guide 8.8 are discussed in Section 7.1.2.

7.3.2 Shielding

7.3.2.1 Shielding Design Features

Shielding for the TN-24 cask is provided mainly by the thick-walled cask body. For neutron shielding, a borated polyester resin compound surrounds the cask body and a polypropylene disk covers the lid and bottom for horizontal storage. Additional shielding is provided by the steel shell surrounding the resin layer and by the steel and copper structure of the basket.

Geometric attenuation, enhanced by attenuation by air and ground, provides additional shielding for distant locations at restricted area and site boundaries. Figure 7.3-1 shows the configuration of shielding in the cask. Table 7.3-1 lists the compositions of the shielding materials.

7.3.2.2 Shielding Analyses

Shielding calculations for the primary gamma source are performed with the QAD-CGGP[1] computer code. Neutron and capture gamma calculations are performed with the SCALE[2] modules XSDRNPM and XSDOSE with the coupled SCALE 27n-18g cross section library.

A single QAD model was used for the primary gamma calculations of the top, bottom and side. This model is shown in Figure 7.3-2.

Four QAD runs are performed, each utilizing one of the four source areas listed in Table 7.2-4: fuel zone, plenum, upper fitting and lower fitting. The sources are uniformly homogenized over the cavity diameter and the appropriate length, as shown in Figure 7.3-2. The fuel basket is also homogenized over the cavity diameter and fuel assembly length and mixed into each source region. The basket material density is reduced by 75% in the top, bottom and plenum source zones to estimate the reduced shielding effectiveness of the basket in the axial direction. The radial resin and aluminum shell are homogenized into a single composition based on the mass of each component. The steel encased polypropylene disk is also homogenized. The materials input for the QAD model is listed in Table 7.3-2.

For the neutron and capture gamma dose on the side of the cask, a cylindrical one-dimensional model is used in XSDRNPM, as shown in Figure 7.3-3. The central fuel region is considered to consist of uranium dioxide. The fuel cladding and steel basket are included in the homogenized fuel region. The fuel region is modeled as a cylinder with the actual cavity diameter. Subsequent regions are

cylindrical shells corresponding to actual dimensions. The source placed uniformly in the fuel region is the source described in Table 7.2-5. The total source in the cylindrical fuel region is the same as the total source in the actual fuel region.

For doses at the ends of the cask, one-dimensional plane geometry XSDRNPM models are used. The fuel region is assumed to consist of uranium dioxide, zircaloy and steel basket, as in the cylindrical model described above. In the top end model the plenum and top end fitting are homogenized with 25% basket material density as used in the QAD model and placed above the fuel zone. A polypropylene/steel slab and a steel layer representing the protective cover are placed over the lid. The bottom end model is similar. Both configurations are shown in Figure 7.3-4. Atom densities of the materials used in the XSDRNPM calculations are listed in Table 7.3-3. A conservative assumption is that the axial distribution of the source is taken as uniform, while in reality, the source will be relatively low near the top and bottom of the fuel region. This is because power shape during operation is non-uniform. The angular fluxes produced by XSDRNPM are processed by XSDOSE to produce dose rates at selected points.

To evaluate doses at long distances from the cask (long by comparison to either radius or height of the cask), a spherical geometry XSDRNPM model is used. This type of model is appropriate because the source region appears to be small and central when viewed from a great distance. This reasoning is confirmed by examination of the analytical solution for dose from a shielded line source of finite height.[3] At large distances, the analytical solution is equivalent to the analytical solution for a point source having the same total source as the line source (line source strength times height of line) and the same thickness of shield. The fuel region of the XSDRNPM model is taken as a sphere of radius such that the volume of the sphere is equal to the volume of the cask cavity. The total primary source contained in the sphere is that listed in Tables 7.2-4 and 7.2-5. Layers of other

materials - resin, steel shells, air - reproduce thicknesses of materials in the actual configuration, as shown in Figure 7.3-5. Appendix 7A contains examples of the input for the computer shielding calculations.

The spherical geometry model does not account for the presence of the ground. At very large distance from a source, characteristic of the distance to the nominal site boundary, the dose should be reduced by a factor of two because of attenuation by the ground[3, 4]. The XSDRNPM model with this correction still is conservative in that attenuation in non-uniform terrain (e.g., hills), natural obstacles (e.g., trees) and man-made structures is neglected. At moderate distances characteristic of the distance to the nominal restricted area boundary, however, the spherical geometry XSDRNPM model should apply without correction because of a balance between attenuation and back-scattering by the ground. Air attenuation is ignored in using XSDOSE to determine the dose rates.

The models described above pertain to an individual storage cask. The actual number of storage casks used and their arrangement will depend on the needs of the individual site. For the purpose of this section, it has been assumed that there will be one hundred casks stored in a ten by ten array.

One hundred casks corresponds to 2400 assemblies. If a single utility were to load a storage area at a rate so as to avoid congestion in a spent fuel pool, it might choose to add casks at a rate corresponding to that at which it loads fresh fuel in the reactor. If this rate is one-third of a core per year, then about three casks per year would be required for a single reactor, about six casks per year for a two-unit station. Thus, by the time the full ten by ten cask array is developed, it is likely that the fuel in the array would be characterized by cooling much longer than the nominal five years assumed in this document. This generic document, in order to provide for a variety of possible scenarios, makes the conservative assumption that the ten by ten array is constructed immediately using fuel cooled five years.

An observer at a distant boundary may view up to nineteen casks directly. One component of total dose at a boundary is obtained by multiplying the dose from a single cask by nineteen. It also is possible for radiation from the top of the other eighty one casks to scatter in air and reach an observer at the boundary. The fraction of radiation released upward is assumed to be the fraction of surface area of the fuel region that faces up, $(2\pi r^2/2\pi rl)$. The total upward source is then treated as a point source for the purpose of calculating the dose at a distant boundary. This assumption is conservative because the directional bias upward is neglected. The calculated scattered dose rate component at large distances from the cask array is the direct dose component (calculated above) increased by the factor:

$$1 + \frac{80.01}{2x366} \quad \frac{100}{19} = 1.57$$

Thus the calculated dose at large distances from a 10x10 array of casks is the dose rate from a single cask (spherical model) times 30. It also is possible, since there is a finite spacing between casks, for a portion of the radiation from the sides of the eighty casks to travel upward and not be intercepted by other casks. The fluxes will be small by comparison with the fluxes at the side of the cask, and may be neglected without introducing significant error, especially in view of the conservative assumptions made. This reasoning is confirmed by examination of the analytical solution for a shielded line source of finite height[3].

As will be seen below, this modeling, when applied, indicates satisfaction of all regulatory requirements for radiation protection by substantial margins. Given the conservative nature of the assumptions made, application to a specific situation at a specific site is likely to lead to a substantial downward revision in dose assessment. Side and end contact dose rates and dose rates at short distances are given in Table 7.3-4.

These dose rates are modest in view of the short duration of the tasks required in handling of the storage casks. Occupational doses are well within the requirements of 10CFR Part 20[5] and are consistent with the 10CFR Part 72[6] ALARA guideline.

Dose rates at long distances for a single cask and for an array of one hundred casks are shown in Figure 7.3-6. It may be observed that the dose rate at the nominal boundary (100 m) of the controlled area is well within the 10CFR Part 20 limit of 2 mrem for continuous exposure for one hour. It is not expected that the operations at the site would lead to individual personnel being at the restricted area boundary on a full working day basis every day for a year. This, of course, is a matter that would be addressed by the particular license applicant's Safety Analysis Report. It, therefore, is not expected that the annual 10CFR20 limit of 500 mrem would be limiting.

The design meets the guidelines of ALARA. Radiation levels at unrestricted and uncontrolled locations, even when evaluated on the basis of conservative assumptions, have been reduced to levels below those required simply to meet regulatory requirements.

7.3.2.3 Experimental Results

A TN-24 prototype cask (TN-24P) has been fabricated and loaded with 24 Westinghouse 15x15 fuel assemblies. The assemblies had about four years cooling time with a burnup of around 30,000 MWD/MTU. Thermal and shielding tests were conducted at INEL on this loaded cask. The results are detailed in EPRI Report NP-5128[7]. The measured contact dose rates (mrem/hr) at mid height radially and at the center of the steel lid and bottom (no polypropylene disks or protective cover) were: 17g, 3n; 52g, 30n and 145g, 90n respectively. At one meter from the surface they became: 10g, 2n; 23g, 12n and 55g, 25n respectively. Although a direct comparison with the calculated values is difficult because of the different fuel parameters, it can be seen that the dose rates around the TN-24 cask are within expected values.

TABLE 7.3-2

MATERIALS INPUT FOR QAD MODEL

ZONE	ELEMENT	DENSITY g/cm^3
Fuel/Basket	Fe	0.907
	Zr	0.334
	U	1.50
Plenum/Basket	Fe	0.356
	Zr	0.372
Top Fitting/Basket	Fe	1.16
Bottom Fitting/Basket	Fe	1.22
Body, Cover, Shell	Fe	7.85
Polypropylene/Steel	C	0.45
	Fe	0.86
Resin/Aluminum	C	0.45
	O	0.53
	Al	0.46

TABLE 7.3-3

MATERIALS INPUT FOR XSDRNPM

ZONE	ELEMENT/ NUCLIDE	LIBRARY NUMBER	DENSITY atom/b.cm
Fuel/Basket	U238	92238	3.66E-3
	U235	92235	1.42E-4
	O	8016	7.59E-3
	Zr	40000	2.20E-3
	Fe	26000	9.97E-3
Plenum/Top	Fe	26000	6.69E-2
Fitting/Basket	Zr	40000	1.65E-3
Bottom Fitting/Basket	Fe	26000	1.31E-2
Body, Cover, Shell	Fe	26000	8.46E-2
Polypropylene/Steel	Fe	26000	9.27E-3
	C	6012	3.41E-2
	H	1001	7.23E-2
Resin/Aluminum	Al	13027	1.03E-2
	C	6012	2.26E-2
	O	8016	2.01E-2
	H	1001	3.89E-2
	B10	5010	1.46E-4

TABLE 7.3-4

TN-24 DOSE RATES AT SHORT DISTANCES

LOCATION	DOSE RATE (mrem/hr)		
	Gamma	Neutron	Total
Radial			
Contact	52.6	4.4	57.0
1 m	28.4	1.7	30.1
2 m	19.2	0.9	20.1
3 m	13.8	0.6	14.4
3.8 m	10.8	0.4	11.2
Top(1)			
Contact	10.5	0.3	10.8
1 m	5.5	0.1	5.6
2.1 m	2.9	0.04	2.9
4.1 m	1.2	0.01	1.2
Top(2)			
Contact	26.3	167	193
Bottom(1)			
Contact	41.8	2.6	44.4
1 m	24.1	1.1	25.2
2.7 m	9.1	0.2	9.3
4.7 m	3.9	0.1	4.0
Bottom(2)			
Contact	62.9	535	598

(1) With polypropylene disc (top and bottom) and protective cover in place.

(2) Without polypropylene discs or protective cover.

FIGURE 7.3-1

TN-24 CASK SHIELDING CONFIGURATION

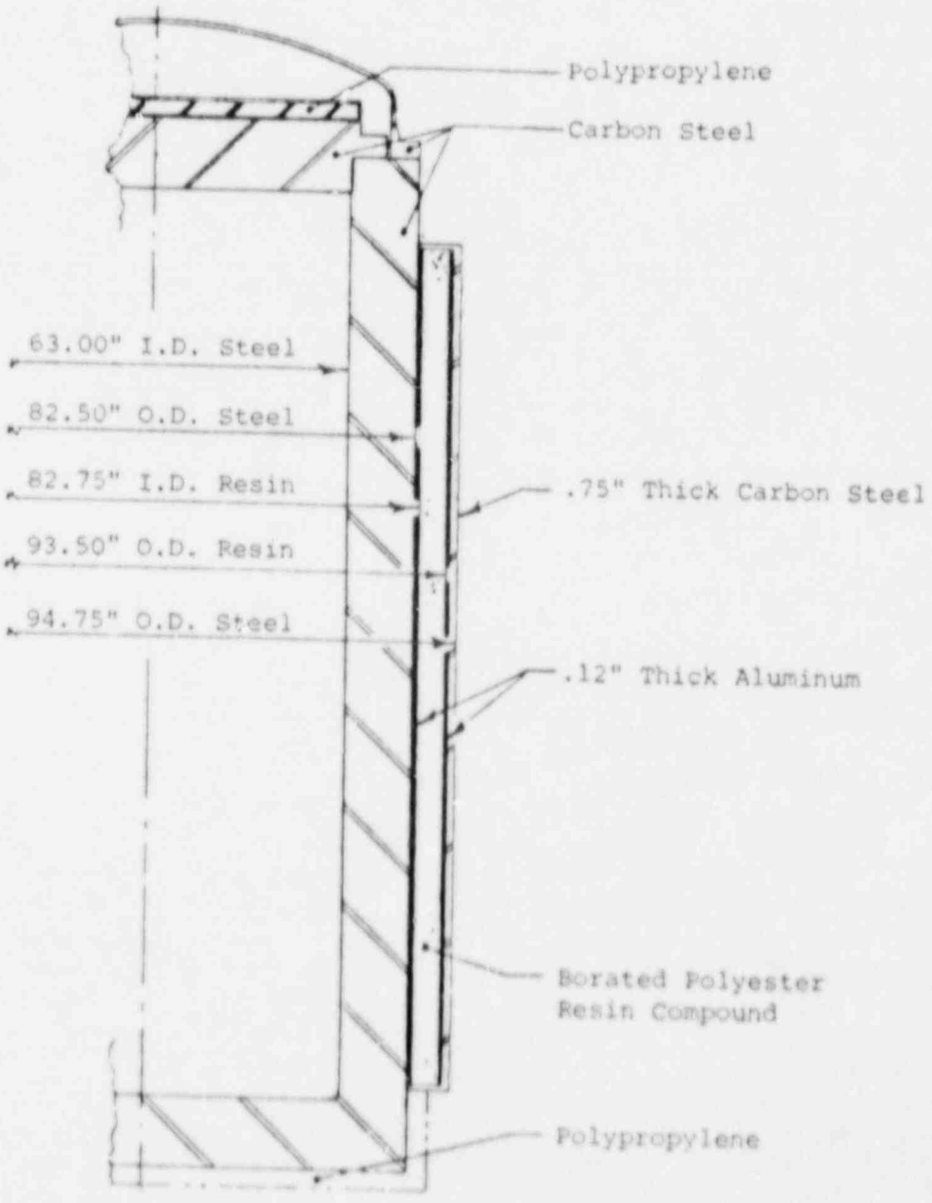

FIGURE 7.3-2

QAD MODEL

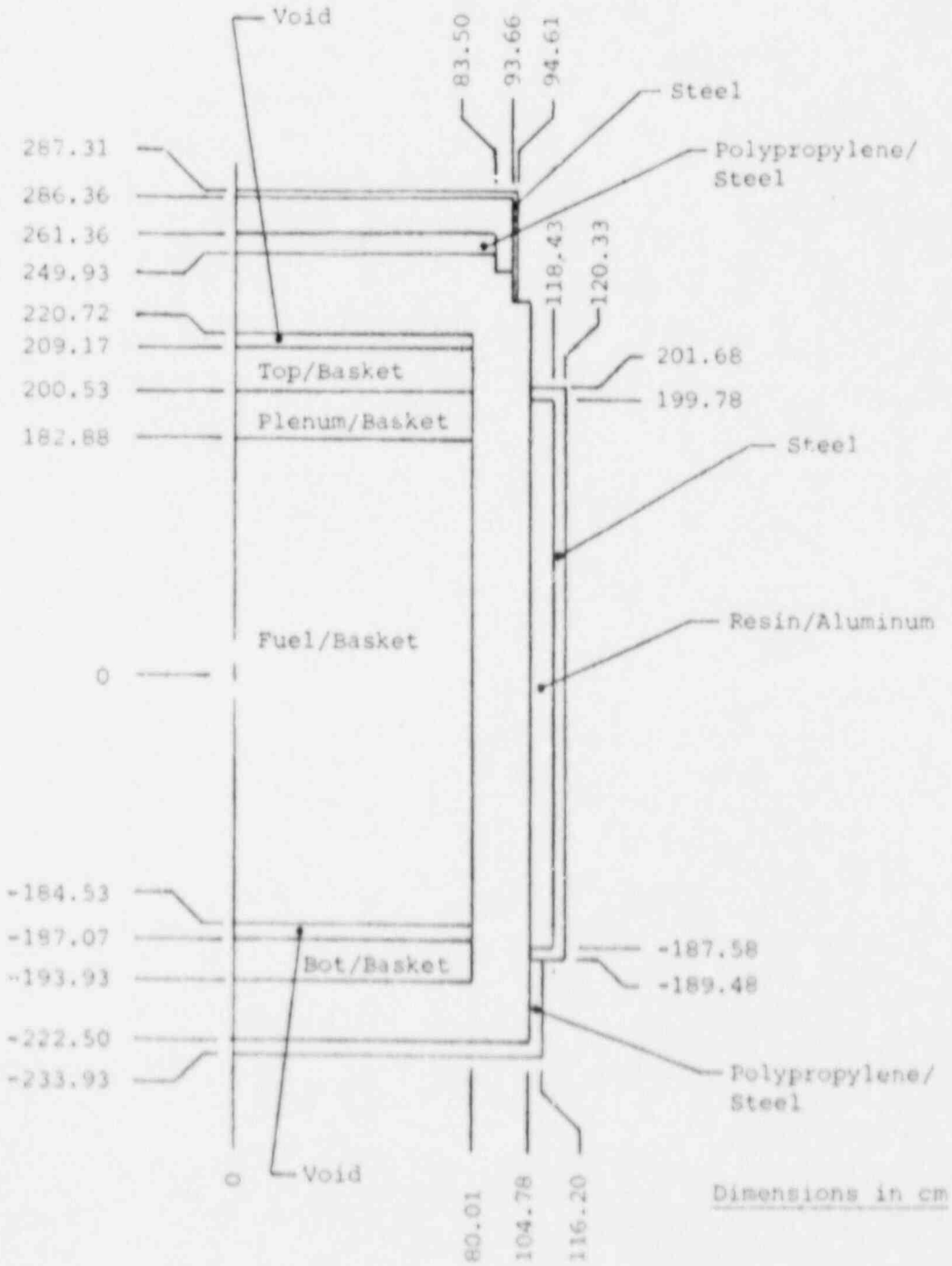

FIGURE 7.3-3

XSDRN-PM RADIAL MODEL

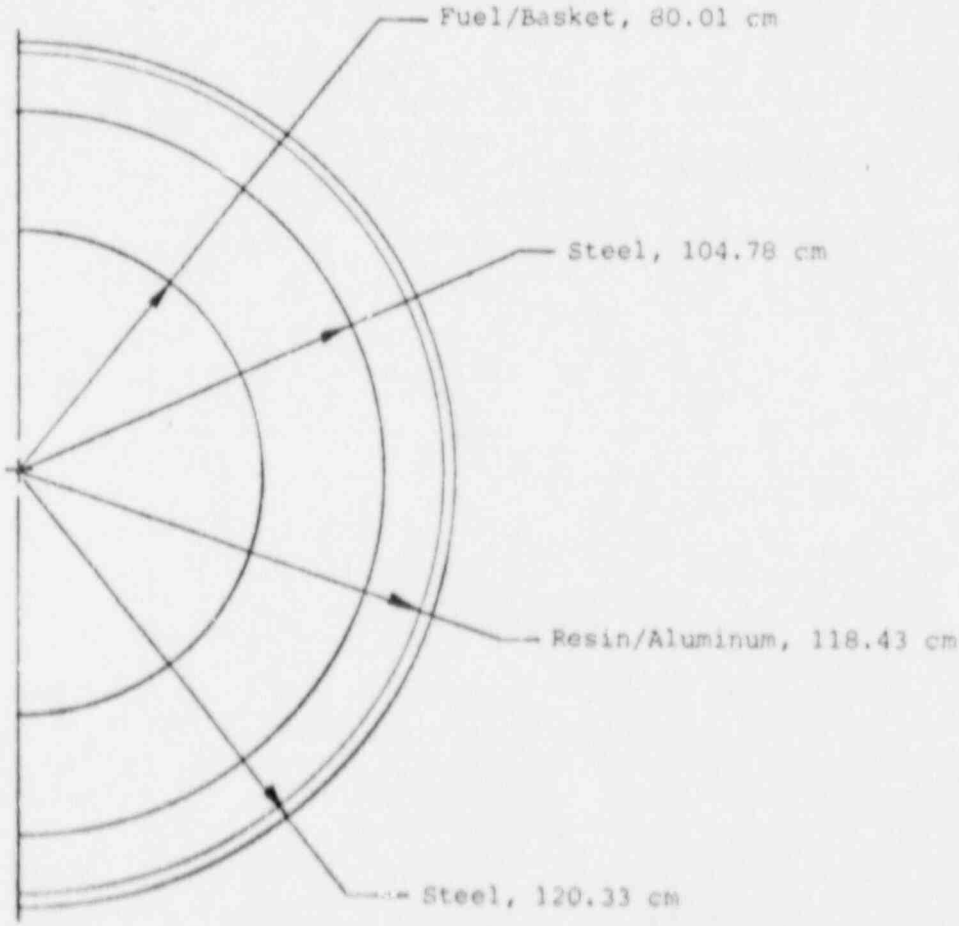

FIGURE 7.3-4

XSDRN-PM AXIAL MODELS

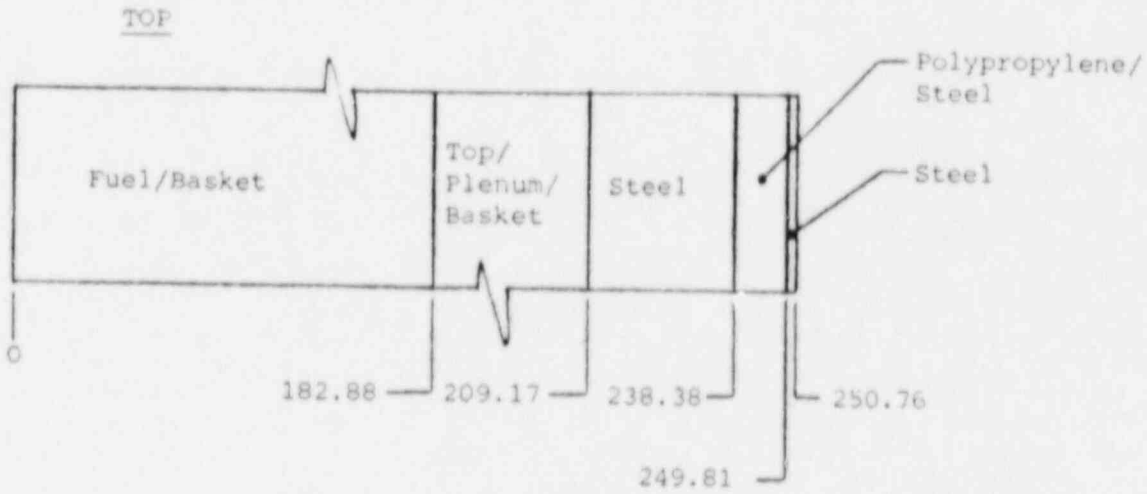

Dimensions in cm

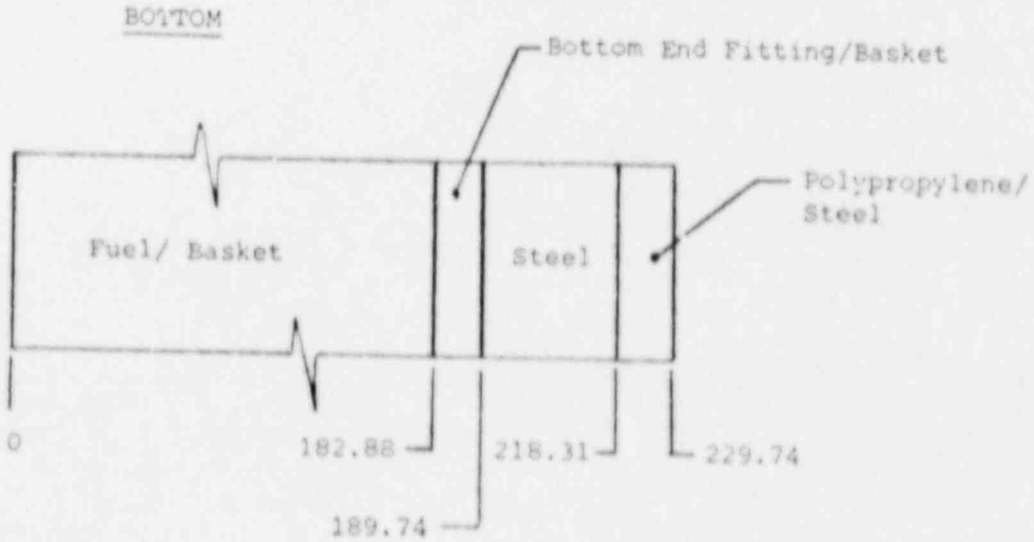

FIGURE 7.3-5

XSDRN-PM SPHERICAL MODEL (LONG DISTANCE)

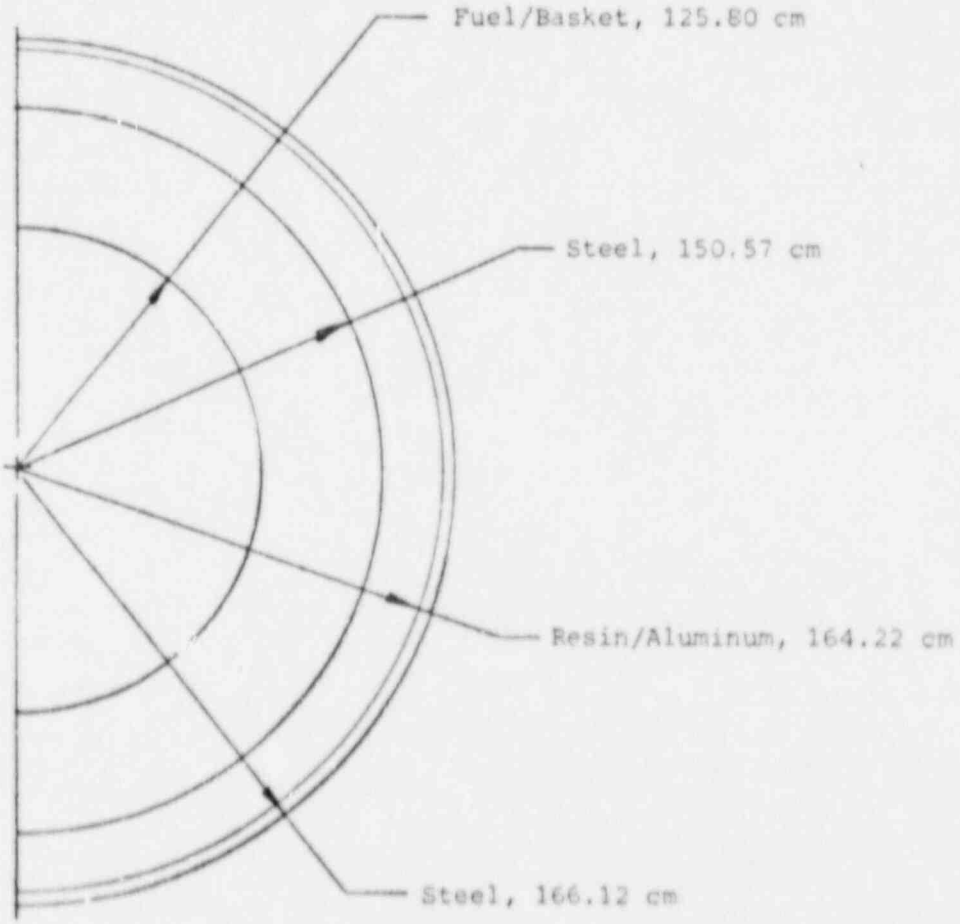

FIGURE 7.3-6

DOSE RATES AT LONG DISTANCES

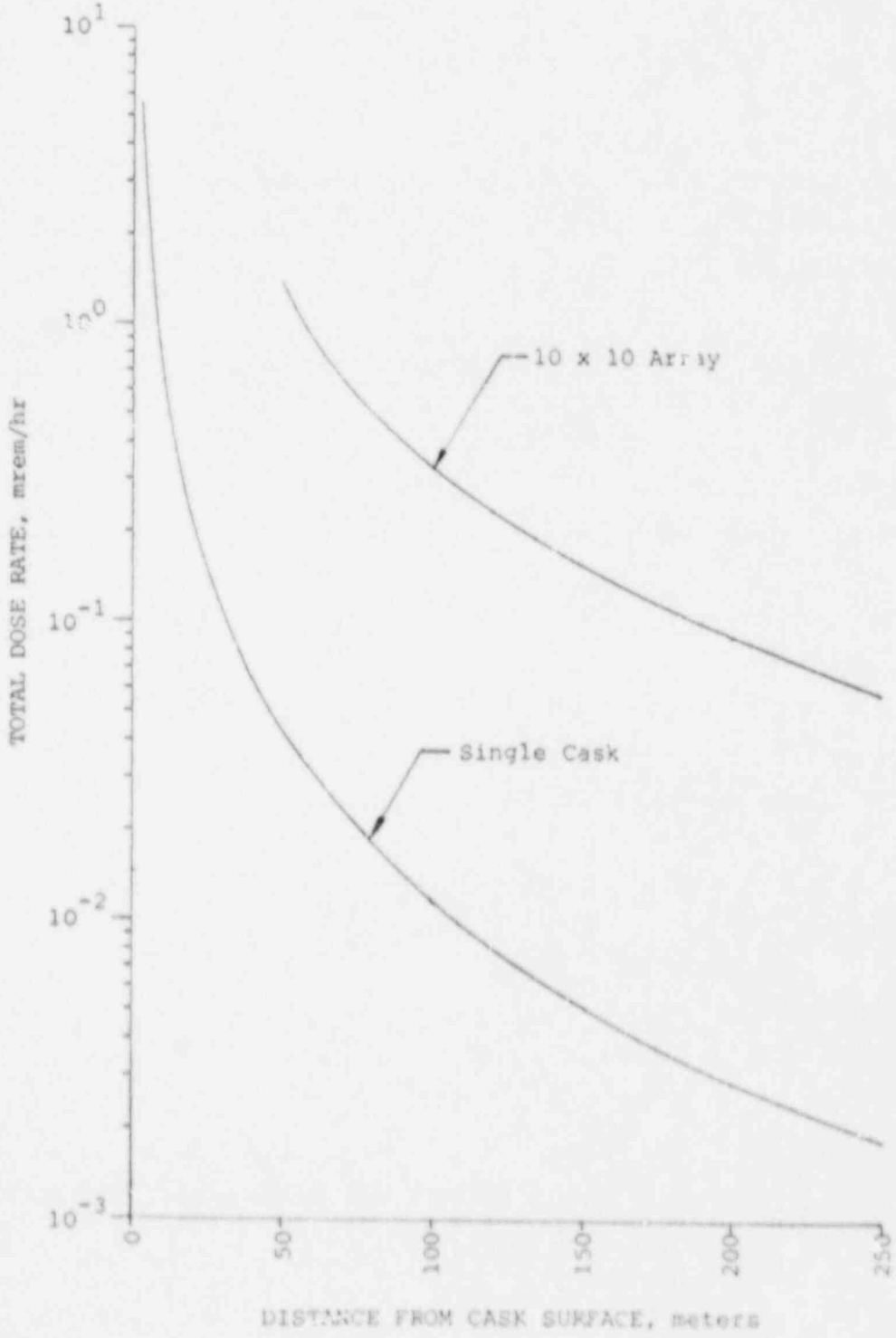

References for Section 7.3

1. "QAD-CGGP - A Combinatorial Geometry Version of QAD-P5A, a Point Kernel Code System for Neutron and Gamma-Ray Shielding Calculations Using the GP Buildup Factor," CCC-493, Oak Ridge National Laboratory, Oak Ridge, Tenn., Sept. 1986.

2. "SCALE: A Modular Code System for Performing Standardized Computer Analyses for Licensing Evaluation," ORNL/NUREG/CR-0200, U.S. Nuclear Regulatory Commission, Revision 3, December 1984.

3. Jaeger, R. G., et. al., Engineering Compendium on Radiation Shielding, Springer-Verlag, New York, 1968.

4. Schaeffer, N. M., Reactor Shielding for Nuclear Engineers, TID-25951, U.S. Atomic Energy Commission, Washington, D.C., 1973.

5. "Standards for Protection Against Radiation", 10CFR Part 20, Rules and Regulations, Title 10, Chapter 1, Code of Federal Regulations - Energy, U.S. Nuclear Regulatory Commission, Washington D.C., Jan 1987.

6. "Licensing Requirements for the Storage of Spent Fuel in an Independent Spent Fuel Storage Installation (ISFSI)", 10CFR Part 72, Rules and Regulations, Title 10, Chapter 1, Code of Federal Regulations - Energy, U.S. Nuclear Regulatory Commission, Washington D.C., Jan 1987.

7. "The TN-24P PWR Spent-Fuel Storage Cask: Testing and Analysis," EPRI NP-5128, Electric Power Research Institute, Palo Alto, California, April 1987.

7.4 ESTIMATED ON-SITE COLLECTIVE DOSE ASSESSMENT

Estimated occupational exposures for cask loading, transport, and emplacement are discussed in Section 3.3.5. Figure 7.3-6 shows the radiation dose rate as a function of distance from a storage array. This figure conservatively assumes a 10x10 array of casks, with each cask containing 24 assemblies cooled for 5 years. Using the conservative data from this figure, the additional dose to personnel at a site boundary greater than 250 meters assuming 2000 hr per year occupancy is less than 114 mrem.

Table 7.4-1 shows the estimated dose due to routine maintenance and possible once in a lifetime repair.

TABLE 7.4-1

MAINTENANCE AND REPAIR OPERATIONS ANNUAL EXPOSURE

Task	Time Required (hr.)	No. of Persons	Dose Rate* (mrem/hr)	Dose (Man-rem/yr)
Visual Surveillance(1)	3	2	30	0.18
Function Testing of Instrumentation(2)	1	2	20	.040
Replace Seals (other than lid) or Transducer(3)	3	3	45	0.41
Replace Protective Cover(3)	3	3	35	0.32

(1) Assumes once a month for 15 minutes each (calculated radial dose rate at 1 meter)

(2) Assumes 2 tests a year 30 minutes each (calculated radial dose rate at 2 meters)

(3) Once in a lifetime repair (measured dose at 1 meter from lid)

*Single Cask.

7.5 HEALTH PHYSICS PROGRAM

Organization and implementation of a health physics program at an ISFSI is the responsibility of the license applicant.

7.6 ESTIMATED OFF-SITE COLLECTIVE DOSE ASSESSMENT

The actual off-site collective dose will be site-specific due to influences of topography, site boundary distance, population density, etc.

Since there are negligible amounts of radioactive effluents expected, only direct radiation plus scattered radiation needs to be considered. From Figure 7.3-6, it can be seen that this radiation is rapidly attenuated at large distances from the cask. The dose rate at 250 meters from a 10 x 10 array of casks is on the order of 0.057 mrem/hr. Assuming 24 hr a day occupancy for 365 days, the annual individual dose would be less than 500 mrem at this distance.

8. ACCIDENT ANALYSIS

The design criteria for the TN-24 storage cask ensure a very rugged and passive confinement structure. Analyses provided in previous sections show that the cask is able to withstand the effects of abnormal operation and credible accidents without impairing its confinement function and without significantly increasing the dose rate beyond the control area.

The simple structure and passive nature of the TN-24 dry storage cask and the simplicity of the storage installation itself allows for minimal handling operations of the cask. This in turn minimizes the possibilities for potential abnormal operations and/or accidents.

The remainder of this chapter will demonstrate the inherent safety of the TN-24 storage cask.

8.1 OFF NORMAL OPERATIONS

After the loaded TN-24 cask is installed at an ISFSI site, no operation is required under normal conditions other than periodic checks of remote pressure monitors and maintenance procedures discussed in Section 4.5. Workers and the general population are protected from radiation exposure by gamma and neutron shielding, prevention of leakage and control of access to the site.

8.1.1 Event

Off-Normal operation at the ISFSI could result from malfunctions of cask components. Two events can be postulated:

a) Seal failure on a cask
b) Malfunction of cask pressure monitoring system.

8.1.1.1 Postulated Cause of the Event

Malfunction of the cask components is not expected during operations at the ISFSI. There are few components that have the possibility of failure due to the relatively simple design and passive nature of the cask.

The seals are checked after cask loading and the choice of corrosion-resistant, "long-life" materials for the seals ensures a very low probability of seal failure. The pressure monitoring instrumentation is also chosen to provide reliable service during operation. Additionally, redundant transducers are provided to ensure a high reliability of this system.

8.1.1.2 Detection of Event

A failure of the seals would be detected by the pressure monitoring (over pressure) system with a remote readout. The operator of an ISFSI may install an alarm or annuciator system to signal the detection of the events.

8.1.1.3 Analysis of Effects and Consequences

The TN-24 cask contains double closure seals to ensure containment. Simultaneous failure of both seals is not considered credible. Thus at least one seal would still provide a containment function during the off-normal event.

Section 3.3.2.2 demonstrates that the interseal pressure will remain above the containment pressure for 20 years. Thus, there is ample time for corrective action to be taken once the monitoring system detects a leak.

The consequences of this event would be minimal, since only the gas in the over pressure system would leak into the cavity or into the area under the protective cover. No leakage of radioactive material would occur. The failure of a pressure transducer is provided for by the use of three transducers in the over pressure tank.

This redundancy ensures reliable operation and negligible consequences from a failure of one transducer.

8.1.1.4 Corrective Action

Corrective action for a seal failure begins with identification of the leaking seal. If it is one that does not require breaking the containment seal, it can easily be replaced at the ISFSI.

If the lid seal is leaking, the cask could be returned to a spent fuel pool and the seal replaced or the protective cover could be replaced at the ISFSI by a containment cover utilizing double metallic seals as described in Section 4.5. The corrective action for a malfunctioning pressure transducer is to simply switch to one of the other three transducers.

8.1.2 Radiological Impact from Off-Normal Operations

The radiological impact from the postulated component failure is negligible beyond the controlled area. Replacement of seals or protective cover will result in limited personnel exposure. This exposure is dependent on the dose rate at the working area, the time involved and the number of personnel required.

An estimate of the exposure for replacing the protective cover is given in Table 7.4-1. The total dose rate is estimated to be 0.32 man-rem.

The radiation exposure associated with instrumentation failure is negligible.

The TN-24 metallic seals, over pressure system and inert cover gas assure the integrity of both the fuel rod cladding and the cask containment for the lifetime of the cask. None of the accident conditions considered in this topical report would compromise the containment. Nonetheless the radiological consequences of a sudden, complete failure of both containment and fuel cladding of a single cask are examined below.

The total inventory of gaseous radionuclides in the design basis fuel is determined to be 645 Ci of tritium and 7114 Ci of Kr85 per MTU using the ORIGEN2[1] computer code. Approximately 10% of this gas[2] is released from the fuel pellets into the fuel rod gaps and plenum. The total gaseous source (Q) which would be released if all cladding on 24 assemblies (0.46 MTU/assy) failed is therefore 712 Ci tritium and 7854 Ci Kr85.

The relative concentrations (x/Q) at 100 m (minimum controlled boundary distance) and 500 m are determined by the method of Reg Guide 1.145[3], Section 1.3.1, assuming stable (Pasquill F) atmospheric conditions and a very slow wind speed of 1 m/s. These conditions provide a high estimate of relative concentration. At 100 m, x/Q = 8.65E-3 s/m^3, and at 500 m, 4.74E-4 s/m^3.

Dose Calculations

Three dose components are calculated following Reg Guide 1.109[4]:

a) Whole body gamma dose from a semi-infinite cloud of Kr85

b) Gamma plus beta dose to skin from a semi-infinite cloud of Kr85

c) Whole body dose to an adult due to inhalation of tritium.

The external dose due to tritium is negligible compared to the inhalation dose, and Kr85 is not considered for inhalation dose because it is a noble gas.

Following Reg Guide 1.109, Regulatory position c.2.e:

Dose = x*DFB*SF

$x = Q*(x/Q)$ = 7854 Ci/y * 8.65E-3 s/m^3
*3.17E4 ypCi/s-Ci
=2.15E6 pCi/m^3 (at 100 m)

SF = 0.5 (Shielding and Occupancy Factor per page 1.109-43 of Reg Guide 1.109)

DFB = 1.61E-5 mrem. m^3/pCi-y
(Reg. Guide 1.109, Table B-1)
Dose = 17 mrem year

Similarly the Kr85 beta plus gamma skin dose and the tritium inhalation dose are calculated according to Regulatory positions c.2.f and c.3.b respectively. The doses at 500 meters are lower by the ratio of relative concentration factors at 500 and 100 meters.

The results are tabulated in Table 8.1-1. They demonstrate that even complete and sudden failure of all fuel cladding and the TN-24 containment will not result in doses in excess of 5 Rem/year limit of 10CFR72.68b at the minimum controlled boundary distance of 100 m.

TABLE 8.1-1

Doses From Complete Containment Failure

Dose, mrem/year

Distance	Kr85(WB)	Kr85(Skin)	H3(WB)
100m	17	2900	246
500m	0.94	160	14

Kr85(WB) = Whole body gamma dose from Kr85

Kr85(Skin) = Gamma plus beta skin dose from Kr85

H3(WB) = Whole body inhalation dose from tritium

References for Section 8.1

1. "ORIGEN2 - Isotope Generation and Depletion Code", CCC-371, Oak Ridge National Laboratory, Oak Ridge, Tenn., Jan 1987.

2. "Extended Fuel Burnup Demonstration Program Topical Report: Transport Considerations for Transnuclear Casks", DOE/ET 34014-11, Transnuclear, Inc., White Plains N.Y. (Dec 1983).8.2 Accidents

3. USNRC Regulatory Guide 1.145, "Atmospheric Dispersion Models for Potential Accident Consequence Assessments at Nuclear Power Plants," Rev 1 (1983).

4. USNRC Regulatory Guide 1.109, "Calculation of Annual Doses to Men From Routine Releases of Reactor Effluents for the Purpose of Evaluating Compliance with 10CFR50, Appendix I," Rev 1 (1977).

8.2 ACCIDENTS

For this section, an accident is defined as any incident that could potentially result in a dose in excess of 25 mrem beyond the controlled area. The potential accidents could result from natural events or man-made events. As shown in the folowing sections, no credible accident will result in direct radiation or release of radioactive materials that will endanger personnel. The analyses and results are covered in detail in Chapters 3, 4 and 5.

8.2.1 Earthquake

8.2.1.1 Cause of Accident

Natural event.

8.2.1.2 Accident Analysis

The postulated earthquake based on the criteria in 10CFR Part 72[1] is discussed in Section 3.2.3. The analysis shows that the distributed stresses on the cask due to the earthquake are less than those due to normal handling. The analysis also shows that the cask will not tip as a result of the postulated earthquake. There are no radiological consequences resulting from the earthquake.

8.2.2 Tornado

8.2.2.1 Cause of Accident

Natural Event.

8.2.2.2 Accident Analysis

The loadings due to the postulated tornado are discussed in Sections 3.2.1.2 and 5.8 of Appendix 4A. The analysis shows that the cask will not tip but may slide due to the postulated tornado winds or missile forces. No radiological consequences will result from the postulated tornado.

8.2.3 Flood

8.2.3.1 Cause of Accident

Natural Event.

8.2.3.2 Accident Analysis

The postulated floods and high water levels are discussed in Section 3.2.2. The analysis presented shows that the cask will withstand the external pressure due to the flood and the velocity of the flowing water will not tip or cause the cask to slide. There are no radiological consequences due to the flood.

8.2.4 Explosion Nearby

8.2.4.1 Cause of Accident

Explosion of material in the vicinity of the cask.

8.2.4.2 Accident Analysis

The cask is designed to withstand 25 psi external pressure. The pressure generated by a credible explosion in the general vicinity of the cask is expected to be only on the order of a few psi. This would not collapse the heavy steel wall, the 0.75 inch thick steel shell surrounding the neutron resin or provide enough lateral load to tip the cask. There would be no radiological consequences as a result of a credible explosion in the vicinity of the cask.

8.2.5 Fire

8.2.5.1 Cause of Accident

Combustible materials will not normally be stored at an ISFSI. Therefore, a credible fire would be very small and of short duration such as that due to a fire or explosion from a vehicle or portable crane. Although a major fire is not credible, the cask was evaluated for the thermal accident as defined in 10CFR Part 71.[2]

8.2.5.2 Accident Analysis

The result of a small credible fire would be a slight increase in temperature near the cask outer surfaces which would be of negligible consequence.

The analysis for the hypothetical thermal accident is described in Section 5.1.3.6. The results of the analysis show that the containment will remain sealed because the metallic seals will withstand the expected temperature and the stresses are well within the required limits. The cavity pressure (Section 3.3.2.2) would remain less than the over pressure system pressure. Although the resin material can be expected to char, it will not completely disappear. However, assuming that all of the hydrogen is driven off, the neutron dose rate would increase by a factor of 30 to about 140 mrem/hr at contact on the side.

8.2.6 Cask Drop

8.2.6.1 Cause of Accident

The cask drop is postulated to occur during handling while the cask is moved onto or off of a transport vehicle.

8.2.6.2 Accident Analysis

Two postulated accidents are evaluated in Section 3.2.11, and Section 5.6 of Appendix 4A. The first one assumes a vertical or near vertical orientation of the cask and the second one assumes that the cask falls off the transport vehicle with a horizontal orientation or at some small angle to the ground. The cask is assumed to fall onto a concrete slab resting on a soil foundation.

The analyses show that the containment vessel will remained sealed. Even if a momentary separation of the seal and sealing surfaces were to occur, any resulting leakage would be from the over pressure chamber into the cavity. The basket compartments will also retain their integrity and the fuel assemblies will remain within their compartments.

The stress levels in the cask are very low for the severe loading conditions assumed.

8.2.7 Cask Tipping

8.2.7.1 Cause of Accident

Tipping of the cask is postulated to occur during handling operations.

8.2.7.2 Accident Analysis

Two tipping accidents were considered in Section 3.2.12 and Section 5.7 of Appendix 4A. The first occurs when the cask is 8 ft above the ground. Although previous analyses showed that an upright cask would not tip due to forces from earthquakes, tornados or floods, this was the second case evaluated.

The results of the evaluation showed that the stresses resulting from the tipping accidents were within allowable limits and no release of cavity gases would occur.

8.2.8 Burial or Insulated Cask

8.2.8.1 Cause of Accident

The cask is assumed to be buried due to an earthquake or insulated by debris caused by a tornado or high winds.

8.2.8.2 Accident Analysis

The analysis for an insulated cask is included in Section 5.1.3.6. The thermal stress induced in the body would be less than the stresses from a major fire. The cavity pressure, assuming 100% fuel failure will not exceed the over pressure system pressure. The cask body (Seal) temperature approaches the maximum temperature limit for the seals of 700°F in about 80 hours. Therefore, corrective action should be taken within 80 hours. As long as such corrective action is taken, the consequences of this accident would be negligible.

References for Section 8.2

1. "Licensing Requirements for the Storage of Spent Fuel in an Independent Spent Fuel Storage Installation (ISFSI)", 10CFR Part 72, Rules and Regulations, Title 10, Chapter 1, Code of Federal Regulations - Energy, U.S. Nuclear Regulatory Commission, Washington D.C., Jan 1987.

2. "Packaging and Transportation of Radioactive Material", 10CFR Part 71, Rules and Regulations, Title 10, Chapter 1, Code of Federal Regulations - Energy, U.S. Nuclear Regulatory Commission, Washington D.C., Jan 1987.

8.3 SITE CHARACTERISTICS AFFECTING SAFETY ANALYSIS

Site specific characteristics which would affect the safety analysis will be identified and addressed by the license applicant.

9. CONDUCT OF OPERATION

Operation of an ISFSI is the responsibility of the license applicant.

10. OPERATING CONTROLS AND LIMITS

10.1 PROPOSED OPERATING CONTROLS AND LIMITS

10.1.1 Contents of Operating Controls and Limits

Operating controls and limits for the TN-24 storage cask include the following:

- cask surface temperature
- cask dose rates
- fuel characteristics
- cask leakage limits
- siting limitations

Table 10.1-1 lists the proposed operating limits.

10.1.2 Bases for Operating Controls and Limits

10.1.2.1 Cask Surface Temperature Limit

The basis for selecting a cask surface temperature limit is to assure that the fuel rod temperature is limited so that the cladding is protected against degradation and gross rupture as specified in 10CFR Part 72.72(h)[1]. Analyses are provided in Section 5.1.3.6.

10.1.2.2 Cask Surface Dose Rate Limit

The basis for specifying a limit for the cask surface dose rate is to assure compliance with the annual dose rates specified in 10CFR Part 72.67 and 10CFR Part 20[2]. Shielding analyses are provided in Section 5.3.2.

10.1.2.3 Cask Leakage Limits

The basis for controlling the cask leakage is the same as in Section 10.1.2.2 above and also to comply with 10CFR Part 72.74(d).

The cask leakage limits are based on the requirement to maintain a positive pressure of helium in the containment and to maintain an over pressure system pressure higher than the containment pressure during the entire 20-year storage life. The analysis is provided in Section 3.3.2. The limit chosen is an order of magnitude less than required.

10.1.2.4 Fuel Characteristics Limit

The bounding spent fuel parameters are given in Tables 3.1-1 and 3.1-2 and summarized below.

- 5 years minimum cooling time
- 35,000 MWD/MTU burnup
- 37.5 MW/MTU specific power
- 3.7 w/o U-235 initial enrichment

10.1.2.5 Siting Limitation

The design earthquake is based on values given in 10CFR Part 72.66(a)(6). The tornado wind parameters are based on Regulatory Guide 1.76[3]. Additional siting limitations for the ISFSI are governed by 10CFR Parts 72.67 and 72.68 concerning radiological protection.

TABLE 10.1-1

Operating Limits Summary

Parameter	Operating Limits
Cask Surface Temperatures	250°F
Cask Surface Dose Rate	60 mrem/hr
Cask Tightness (over all)	1×10^{-6} atm/cc-sec
Max. Decay Heat of Fuel (single cask)	24 kw
Maximum Cladding Temperature	388°C
Siting Limitations	
a. Earthquake	0.25 g horizontal 0.17 g vertical
b. Tornado	360 mph wind speed
c. Radiological Exposure	10CFR 72.67 10CFR 72.68

References for Section 10.1

1. "Licensing Requirements for the Storage of Spent Fuel in an Independent Spent Fuel Storage Installation (ISFSI)", 10CFR Part 72, Rules and Regulations, Title 10, Chapter 1, Code of Federal Regulations - Energy, U.S. Nuclear Regulatory Commission, Washington D.C., Jan 1987.

2. "Standards for Protection Against Radiation", 10CFR Part 20, Rules and Regulations, Title 10, Chapter 1, Code of Federal Regulations - Energy, U.S. Nuclear Regulatory Commission, Washington D.C., Jan 1987.

3. "Design Basis Tornado For Nuclear Power Plants", Regulatory Guide 1.76, U.S. Nuclear Regulatory Commission, Washington D.C., Apr 1974.

10.2 DEVELOPMENT OF OPERATING CONTROLS AND LIMITS

10.2.1 Functional and Operating Limits, Monitoring Instruments, and Limiting Control Settings

This section applies to items listed in Sections 10.1.2.1 through 10.1.2.3 above.

10.2.2 Limiting Conditions for Operations

10.2.2.1 Equipment

The pressure monitoring instrumentation is described in Section 3.3.3.2. Leak testing of the system will be performed after cask loading utilizing a standard helium leak test. Operational function of the monitoring system is discussed in Section 3.3.2.

10.2.2.2 Technical Conditions and Characteristics

- Cask Surface Temperature - The surface temperature of a single cask will be limited to a value of 250°F which assures that the average temperature of the hottest fuel rod will not exceed 388°C.

- Cask Dose Rate - The surface dose rate of the cask will be limited according to the requirements of 10CFR Part 72.67(a)[1] and ALARA principles. The surface dose rate of the TN-24 cask with 24 reference fuel assemblies is less then 60 mrem/hr.

- Fuel Characteristics - Parameters for the spent fuel are established in Section 3.1.

10.2.3 Surveillance Requirements

Cask surveillance to evaluate the dose rate and surface temperature is performed upon arrival of the cask at the ISFSI. Further surveillance is not required for these parameters. Surveillance of the pressure monitoring system is performed by a remote readout device and/or alarm. Direct surveillance is not required. A periodic visual surveillance of the cask is all that may be required.

10.2.4 Design Features

Design features required for safety are controlled through the quality assurance program implemented during design and fabrication.

10.2.5 Administrative Controls

Administrative controls will be site specific and are the responsibility of the license applicant.

10.2.6 Suggested Format for Operating Controls and Limits

Due to the passive nature of the dry storage cask, the operational controls are limited to cask tightness monitoring. Other limits (dose rate, surface temperature, etc.) are evaluated during cask acceptance at the facility.

Leakage Monitoring

1. Title: Cask Leakage Control

2. Specification: See Table 10.1-1.

3. Applicability: Cask double seal system

4. Objective: The purpose of the cask leakage control is to monitor the double seal system for the lid and penetrations and prevent loss of double seal protection.

5. Action: If monitoring indicates leakage of a seal, the seal should be replaced or a containment cover can be placed over the lid.

6. Surveillance Requirement: Leakage testing and functional testing of the monitoring system is performed at the beginning of storage. Periodic maintenance and testing is not required due to the reliability of the redundant monitoring system

References for Section 10.2

1. "Licensing Requirements for the Storage of Spent Fuel in an Independent Spent Fuel Storage Installation (ISFSI)", 10CFR Part 72, Rules and Regulations, Title 10, Chapter 1, Code of Federal Regulations - Energy, U.S. Nuclear Regulatory Commission, Washington D.C., Jan 1987.

11. QUALITY ASSURANCE PROGRAM

Transnuclear, Inc. (TN) has established a Quality Assurance Program for Design, Fabrication, Inspection and Testing of Storage Systems for Spent Fuel and Associated Radioactive Materials (E-9213) in conformance with the requirements of Subpart G of 10CFR72. This QA Program shall be implemented for all activities which are important to safety* for the TN-24.

As required by the QA Program, a specific QA Program Plan shall be established for each TN-24 project. This QA Program Plan shall identify specific project QA requirements, including the identification of items which are important to safety for that project. Table 3.4-1 provides guidance for classification in this regard.

Supplier organizations shall be made aware of the mandatory QA requirements including the applicability of Codes and Standards by identifying such requirements in TN procurement specifications in accordance with TN QA Procedures.

Special processes anticipated for fabrication, inspection and testing of TN-24 dry storage casks are as follows:

a. Welding
b. Heat Treating
c. Non-destructive examination
    - Ultrasonics
    - Radiography
    - Magnetic Particle
    - Liquid Penetrant
d. Surface Coating
e. Cleaning
f. Resin Pouring

* "Important to safety" and "safety related" are used interchangeably in TN documents.